Foaming Novatein Thermoplastic Protein

A thesis

submitted in fulfilment

of the requirements for the degree

of

Doctor of Philosophy in Engineering

at

The University of Waikato

by

CHANELLE ANNE ROSE GAVIN

THE UNIVERSITY OF
WAIKATO
Te Whare Wānanga o Waikato

2019

Abstract

Most plastics are produced from non-renewable and/or non-biodegradable polymers. The negative environmental impact of these has been a strong driver for bioplastic development. Proteins are naturally occurring biopolymers which can be denatured and plasticised to produce thermoplastic materials. Novatein Thermoplastic Protein (NTP) is a patented blend of blood meal (a highly aggregated protein) and processing additives which: reduce hydrogen bonding, break cross links between cysteine residues, disrupt hydrophobic interactions, and facilitate protein unfolding. Water and triethylene glycol (TEG) are added as plasticisers to produce a powder which can be extruded, and subsequently injection moulded.

As Novatein is both bio-derived and biodegradable there is the opportunity for using it as an alternative loose fill packing material. This work aimed to develop an appropriate foaming method and the principles governing it.

Foaming was initially investigated through extrusion which was unsuccessful due to the low speed and pressure drop. However, by using high speed and pressure, Novatein was successfully foamed in an injection moulder under free expansion. Foaming achieved densities between 0.2-0.5 g/cm^3, at temperatures between 160-165°C. The mechanical properties varied with density but compressive strengths between 200 and 600 kPa and elastic moduli between 2.2 and 8 MPa were typical. Increasing temperature further did not improve expansion as the material degraded. The narrow processing window is characteristic of the material's semi-crystalline nature which arises from residual protein secondary structure (α-helices and β-sheets). Although Novatein softens at high temperature, it does not form a typical melt. Processing depends upon the interactions between protein, additives, and plasticisers. Highly plasticised Novatein phase separates into protein rich, protein-plasticiser, and plasticiser rich regions. This results in variable morphology characterised by: unfoamed regions, variable cell sizes and both open and closed cells.

Varying water, urea and TEG impacted the foaming ability; adding urea lowered the extensional viscosity improving foaming while also acting as a blowing agent. Water and TEG reduced the shear viscosity and softening point respectively reducing expansion. Water was expected to improve expansion by acting as a blowing agent, however increasing water and TEG both increased cell size, but delayed stabilisation decreasing expansion.

Following nucleation a bubble grows by diffusion of gas molecules from the surrounding polymer. As these molecules leave, the viscosity increases, controlling bubble growth. Simultaneously, growth causes chain alignment within the surrounding polymer. Through FT-IR, bubbles were shown to appear in regions high in β-sheets. Two mechanisms were proposed; either a bubble nucleates near a β-sheet and grows until it encounters other β-sheet structures or that chain alignment enables hydrogen bonding between the chains, forming these structures. FT-IR also showed a high concentration of TEG at the bubble surface suggesting that nucleation occurred in regions high in water and TEG. The accumulation of TEG at a bubble surface occurs as water (steam) diffuses into the bubble causing expansion, pushing TEG into the surroundings.

Bubble stabilisation is achieved through either a loss plasticiser molecules or a decrease in temperature. In over plasticised blends, water keeps the viscosity in the surrounding polymer low, while increasing TEG reduced the softening point, both allowing more time for gases to diffuse out.

This work developed a suitable foaming method and an understanding of the role of protein secondary structure and rheology for Novatein, which can be foamed despite its high β-sheet content.

Acknowledgments

Firstly, I would like to acknowledge to my supervisors Dr. Mark Lay and Associate Professor Johan Verbeek for their guidance, support, patience and encouragement throughout this project. Thanks to Mark for: many morning coffees at Momento, all our technical discussions, providing perspective through the ups and downs of this journey but most of all for encouraging me to continue onto PhD study to begin with. Johan, thank you for the many hours we have spent discussing the different aspects of this project and material, for challenging me to improve my writing style, and also thank you for always checking in during the stressful times. This experience has given me more opportunities than I could ever have imagined. Mark and Johan I am so blessed to be able to consider you both as my mentors and friends.

To my colleagues, especially Jim Bier and Talia Hicks, I would like to thank you for your friendship, advice and Novatein expertise. Thank you: to Jim for many in-depth technical discussions particularly relating to FT-IR and DMA analysis, and to Talia for sharing her technical knowledge and practical advice. It has been an absolute pleasure to co-author with you both. To everyone in the research group, especially Matt, Jussi, Anu, Safiya, Maria and Sandra, and all the undergraduate students I have worked with, it has been great to share the journey with you. I wish you all the very best for the future and hope our paths cross again.

There are many staff at the University of Waikato that I would like to acknowledge for the opportunities and support they have provided over the years. Firstly, Professor Janis Swan for encouraging my interest in teaching. Thank you Janis, I greatly value those opportunities which have led me to pursue a career in academia. A special thanks to Dr. Graeme Glasgow, it was great working with you. Dr. James Carson, for always having the time to talk when I dropped by, thank you so much for your advice throughout this PhD. Also, Professor Kim Pickering for the research group cake meetings, Mary Dalbeth from the engineering office for all her support, Gwenda Pennington for her advice when I was applying for scholarships, and Cheryl Ward for her assistance with library interloans.

Thank you to all the technical staff who have helped me throughout this project. Particularly, Helen Turner, Brett Nichol and Ivan Bell (from the science store). Also, a big thank you to everyone else in the School of Engineering.

I want to express my gratitude for the financial support I received throughout this project from: the University of Waikato Doctoral Scholarship, the Todd Foundation, the Claude McCarthy Foundation, and funding from the New Zealand Synchrotron Group. Also, a thank you to Sarah Heine and Kate Parker from the Biopolymer Network, for their support of this project. Another thank you to the beamline scientists at the Australian Synchrotron, Dr. Danielle Martin and Dr. Pimm Vongsvivut. Especially, Pimm, for helping set up the ATR and for answering my many questions via email.

Thank you to all my friends for their support. Particularly, Michelle who was always willing to listen and who celebrated even my smallest achievements. Rachael for being my walking buddy whenever I needed to clear my head, and Tim for his friendship. Lastly, Dani and Natalie, for your continuous encouragement, for always making me laugh, and for always somehow having cake on hand when I needed it most.

To my wonderful partner Ben, thank you for always encouraging me to pursue my career aspirations. Also, for participating in/listening to many technical discussions when I just needed to work through my logic out loud. This journey hasn't always been easy, so thank you for your unconditional support. Also, a special thanks to Ben's family especially his parents, Janice and Joe, for their encouragement.

Finally, I would like to acknowledge the love and support I have received from my family. Especially my Mum, Caroline, and my uncle, Eddie. Mum, I cannot thank you enough for always prioritising my education, and for being so supportive and understanding over the last few years. A big thank you to Uncle Eddie as well, for showing me how to always persevere. Thanks to you both for always being my biggest supporters. Last of all, to my Nana, thank you for always believing in me, and for giving me the courage to pursue my academic interests. May perpetual light shine upon you.

Table of Contents

1

Introduction

Introduction

The global demand for polymeric foams in 2015 was 22,000 kilotons (20,000 kilo tonnes) [1] with packaging accounting for 25% (5,000 kilo tonnes). 40% of plastics currently being used for packaging, most are single use [2]. Of these, foams represent the biggest problem due to their lack of biodegradability and the volume they consume when sent to land fill. Global production of biopolymers was only 2050 kilo tonnes in 2017 of which 42.9% are biodegradable, the remainder are just bio-derived [3]. The best foamed packaging alternatives to polystyrene from an environmental stand point are starch and poly-lactic acid (PLA) as they are renewable. However, their manufacture competes with food production and PLA requires commercial composting infrastructure which New Zealand does not have.

Economically plastic products and plastic resins represented 5.1 % of New Zealand's total imports in 2016, equating to 1.82 billion US$ [4]. Most plastics are received in a ready for use condition with commodity plastics accounting for less than 25% of these imports [4]. New Zealand is reliant upon importing plastic products and resins as the country does not manufacture these raw materials [5]. However, the country converted over 250,000 tonnes of polyethylene, polypropylene, polyvinyl chloride, and polyethylene terephthalate to products in 2014 [5].

Single use plastic bags are being phased out in New Zealand with a complete ban, including compostable and biodegradable forms, by mid-2019 [6]. China and Australia stopped accepting plastic material for recycling this year 2018 [7], and strong opposition to using plastic for energy [8] has resulted in an accumulation of 400 tonnes of plastic [9]. Furthermore, it is uncertain if plastics sent overseas for recycling are actually being recycled [7]. Plastics NZ and Packaging NZ support the call to "design out" unnecessary packaging in a recent report by the Sustainable Business Network [10]. It is expected that 1700 workers and 70 companies could be affected by the ban on plastic bags alone [10]. This is a significant proportion of the 300 companies in New Zealand's plastics industry.

One unique bioplastic manufactured in New Zealand is Novatein Thermoplastic Protein (NTP), which is a patented formulation [11] commercialised by Aduro Biopolymers. Novatein® is produced from a co-product of the meat industry, bloodmeal, mixed with chemical denaturants and plasticisers to break bonds within and between protein chains and facilitate chain unfolding, to enable it to be processed like a thermoplastic. Currently, Novatein is injection moulded to produce parts utilised in the meat industry to prevent food contamination from the gastrointestinal track of animals [12]. It is readily compostable under conventional composting conditions [13], it does not require elevated temperatures like PLA or corn starch to compost, and it is renderable along with the offal into meat meal.

This work examines the ability of Novatein to foam to expand its potential market into foam packaging. Foaming this material is a complex process and requires knowledge of thermoplastic foaming principles, thermoplastic processing and protein behaviour.

Thermoplastic foaming is a three stage process consisting of ***bubble nucleation***, ***growth*** and ***stabilisation*** [14]:

Nucleation occurs when an accumulation of gas is unable to return to an equilibrium state through methods such as diffusion when a change in the surrounding conditions occurs. The gas will then form a spherical bubble as a means to restore equilibrium [15]. Homogenous nucleation occurs when gas evolves from a system where no gas cavities existed previously. The alterative, heterogeneous nucleation is more common and occurs when additives, such as talc, are used to provide a surface for nucleation thereby lowering the activation energy [16]. In polymers there is also the possibly of pseudo classical nucleation where a bubble nucleates from the gas (free volume) between polymer chains or through shear induced nucleation.

Irrespective of the nucleation mechanism, once nucleated ***cell growth*** occurs through diffusion of the excess gas from the polymer. Bubble growth is influenced by many factors but the gas concentration, foaming temperature and the viscosity of the polymer are critical [17]. The bubble will cease to grow

when the gas in the surrounding polymer has been depleted. In order to provide gas for bubble growth chemical (e.g. azodicarbonamide and sodium bicarbonate) or physical blowing (N_2, CO_2, H_2O and alkanes) agents are commonly used. As the gas in the surrounding polymer is depleted an increase in the viscosity of the surrounding polymer occurs which assists with preventing cell coalescence and bubble rupture.

Stabilisation of the bubble structure is the final step and must take place before the gas within the bubble exceeds the polymers ability to withstand its growth, leading to cell rupture. Stabilisation is related to the glass transition temperature (T_g) and in order to stablise the material the temperature is often decreased to bring the material to below the T_g causing the structure to solidify [17]. Alternatively in materials processed near their T_g the loss of plasticiser may be sufficient to elevate the T_g of the polymer also achieving stabilisation.

The foaming window is different for semi crystalline and amorphous polymers due to their different softening behaviour. To have flow, the material must be above its T_g (associated with chain movement of the amorphous phase) and some materials are processed above their melt temperature (associated with melting of the lamellae and spherulites in semi-crystalline polymers) [18]. Both the T_g and melt temperatures can be measured through dynamic mechanical analysis (DMA) and differential scanning calorimetry (DSC). The degree of crystallinity can also be determined by DSC or through X-ray diffraction (XRD).

Thermoplastic processing such as extrusion is typically influenced by rheology as the material experiences shear or extensional flow. Many polymers demonstrate shear thinning behaviour which is also temperature dependent [18]. Extensional forces are important during foaming and strain hardening of the material is a desirable property which usually arises from physical entanglements/branching [19]. Finally the polymer will also experience a decrease in viscosity in comparison to the neat polymer through the incorporation of a blowing agent. The blowing agent-polymer mixture should ideally be kept supersaturated prior to the die so that nucleation and growth only occur once the pressure is released [20].

Thermoplastic proteins are different in their structure and function compared to conventional polymers. Protein thermoplastics can be considered semi-crystalline but their crystallinity arises from the protein secondary structure (α-helices and β-sheets) and the amorphous component is more strictly speaking disordered (β-turns and random coils) [21, 22]. These materials still demonstrate a thermal transition analogous to those detected in traditional polymers [23, 24] and in the case of Novatein demonstrate shear thinning behaviour [25].

Novatein is processable above its glass transition temperature (120 °C) but does not form a traditional melt and requires shear to enable processing. It also has a low melt strength compared to other polymers and can be easily broken following extrusion. The semi-crystalline nature of this material and the tendency of the protein to denature and crosslink at high temperature reduces the processing window for this material. Novatein also has a high extensional viscosity [25] which will impact bubble growth. The influence of the plasticisers added (water, urea and triethylene glycol) in foaming is unknown and these may be lost during foaming affecting foam production.

The unique nature of this material provides a challenge for foaming. This may explain why few foamed protein thermoplastics exist. Foamed product from zein and gluten have used batch processing [26] but soy is the only other reported protein thermoplastic which has been foamed through extrusion or foam injection moulding [27-29]. The food industry has also investigated the mechanism behind protein elasticity for gluten which has been linked to its secondary structure [30, 31]. All of the proteins listed above have a lower content of β-sheets than bloodmeal and the presence of this rigid structure expected to have implications for foaming with higher β-sheet content linked to collapsed zein foams [32]. This highlights the influence of protein secondary structure on foaming and the need to consider this.

1.1 Thesis Objectives

This study combines the principles outlined above to the foaming behaviour of Novatein. The specific objectives of this thesis are:

1. Develop a reliable foaming method by investigating combinations of Novatein with nucleating and blowing agents and other polymers.
2. Characterise and relate the morphology and mechanical properties of the foams to assess suitability for packaging applications.
3. Evaluate the role of protein secondary structure and of blowing agents during foaming of a protein thermoplastic
4. Examine the role of shear and extensional rheology in this system and its influence on foaming ability.

1.2 Thesis Structure

This thesis is structured into two parts: 1. Introduction and scoping 2. Factors affecting foaming. A diagram of the thesis structure is provided in Figure 1, which illustrates how each chapter contributes to the thesis objectives.

Part 1: Introduction and Scoping

The thesis begins with a review of protein foams (Chapter 2). This considers the use of proteins in a wide variety of foaming methods and provides an overview of the factors which affect both batch and foam extrusion methods. This review focuses specifically on studies which have foamed thermoplastic proteins or thermoplastic protein blends, providing a background to the experimental work.

Chapter 3 consists of two short conference articles which outline the technical challenges faced during the scoping work. The first article outlines attempts to foam Novatein and Novatein blended with linear low density polyethylene (LLDPE) through extrusion. The blend was considered in an effort to reduce the viscosity of Novatein and provide melt strength.

The second article examines foaming through free expansion by using an injection moulder and withholding the nozzle from the mould to maximise

pressure drop. Novatein, Novatein – LLDPE and another blend (Novatein with low density polyethylene) were foamed using water and sodium bicarbonate as blowing agents.

The use of free expansion in the injection moulder proved promising for foaming pure Novatein which is the focus of Chapter 4. In this chapter, the foaming window for this material is investigated which proved to be very narrow. This study examines the resulting foam morphology and mechanical properties and considers the applicability of the Gibson and Ashby models for the mechanical properties of open and closed cell foams.

Part 2: Factors affecting Foaming of Protein Thermoplastics

Foaming of Novatein was thought to be linked to several factors including: protein secondary structure, thermomechanical behaviour and rheology. This forms the focus for the second part of the thesis which begins with a small review of methods used to obtain structural information for protein thermoplastics.

Fourier transform infrared (FT-IR) analysis is often used to determine protein secondary structure. However, other techniques do exist which may be more suitable depending upon sample type. Chapter 5, discusses the use of circular dichroism, Raman spectroscopy, X-ray crystallography (wide and small angle X-ray diffraction), nuclear magnetic resonance (NMR) and FT-IR are discussed. Particular attention is paid to the protein sample state and methods and limitations of data interpretation as not all methods can be applied to protein thermoplastics. Of all methods FT-IR is the most versatile and simplistic for determining protein secondary structure in the solid state.

Blood meal is also only one possible processing route for waste blood. Chapter 6 discusses the application of FT-IR to blood meal and blood fractions (red blood cells, haemoglobin, plasma and bovine serum albumin). The analysis of these fractions will inform the understanding and processing of Novatein and the thermal behaviour of these fractions was investigated through differential scanning calorimetry (DSC), dynamic mechanical analysis (DMA), X-ray diffraction (XRD) and thermogravimetric analysis.

In Chapter 7, similar techniques to those used in Chapter 6 are applied to evaluate what changes have occurred within the material after foaming. The behaviour of blood meal, pre-processed NTP (PNTP) and extruded NTP (ENTP) have been previously studied but are included to establish relative changes in a foaming context and to overcome variability in the protein feed stock. FT-IR is first applied to foamed samples here to examine changes in secondary structure and plasticisation.

Chapter 8 continues to build on the mechanism of how protein thermoplastics physically foam by examining foamed samples produced at different temperatures and therefore at different expansion ratios. This study uses FT-IR in attenuated total reflectance (ATR) mode using globar and synchrotron light.

Novatein rheology is examined in Chapter 9 in light of variable plasticiser and blowing agent content. This material does not form a traditional melt and the viscosity can only be measured using capillary rheology. The role of shear and extensional rheology are addressed in detail and supported by DMA. These results have been linked with foam expansion and final protein secondary structure.

The final chapter (Chapter 10) contains a summary of the conclusions reached by this work. It aims to ingrate the conclusions reached in each study and to build an overall view of the aspects which need to be considered when foaming a protein thermoplastic. The chapter concludes with recommendations for future work.

Thesis Overview

This work aims to develop a method for foaming Novatein and to examine the factors affecting foaming.

Thesis Objectives

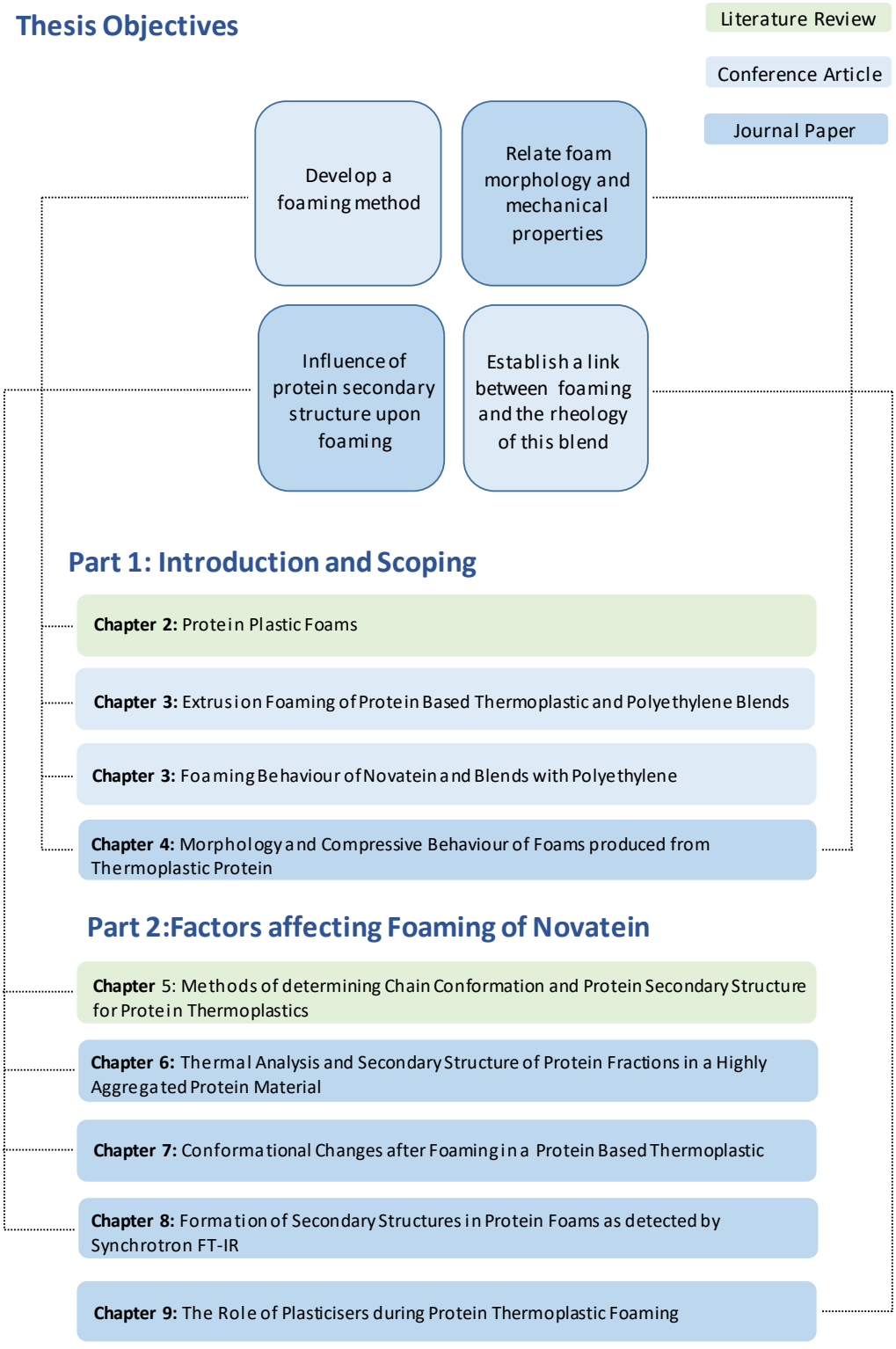

Figure 1: Thesis overview showing how each chapter links with the overall thesis objectives.

1. GlobeNewswire. *Global Polymer Foam Market Analysis 2015-2018 & and Segment Forecasts 2018-2024*. 2018; Available from: https://globenewswire.com/news-release/2018/11/07/1646715/0/en/Global-Polymer-Foam-Market-Analysis-2015-2018-and-Segment-Forecasts-2018-2024.html.
2. Harris, C. *Recycling is not enough to get rid of plastic waste: report*. 2018; Available from: https://www.stuff.co.nz/business/better-business/109024756/recycling-is-not-enough-to-get-rid-of-plastic-waste-report.
3. European Bioplastics. *Bioplastics market data*. Available from: https://www.european-bioplastics.org/market/.
4. Alexander Simoes. *New Zealand*. 2018; Available from: https://atlas.media.mit.edu/en/profile/country/nzl/.
5. Plastic NZ - New Zealands Industry Association. *New Zealand Industry - General Statistics*. 2018; Available from: http://www.plastics.org.nz/doing-business-in-nz/new-zealand-industry/general-statistics.
6. Woolf, A.-L. *New Zealand to ban single-use plastic bags*. 2018; Available from: https://www.stuff.co.nz/environment/106160806/new-zealand-to-ban-singleuse-plastic-bags.
7. Woolf, A.-L. *Kiwis' recycling is piling up in Malaysia and being burnt in secret, environmentalists say*. 2018; Available from: https://www.stuff.co.nz/environment/109100190/kiwis-recycling-is-piling-up-in-malaysia-and-being-burnt-in-secret-environmentalists-say.
8. Woolf, A.-L. *Is it time to consider burning New Zealand's plastic waste?* 2018; Available from: https://www.stuff.co.nz/environment/109052484/is-it-time-to-consider-burning-new-zealands-plastic-waste.
9. Woolf, A.-L. *New Zealand's plastic stockpile is at 400 tonnes and could be going mouldy*. 2018; Available from: https://www.stuff.co.nz/environment/108978268/new-zealands-plastic-stockpile-is-at-400-tonnes-and-could-be-going-mouldy.
10. Harris, C. *Plastics industry calls for time to restructure itself*. 2018 December 3rd; Available from: https://www.stuff.co.nz/national/109047433/-.
11. Pickering, K.L., et al., *Plastics material*. 2012, Novatein Limited: USA.
12. Verbeek, C.J.R., *Closing the loop, adding value.* The Chemical Engineer, 2015(884): p. 34-36.
13. Verbeek, C.J.R., T. Hicks, and A. Langdon, *Biodegradation of Bloodmeal-Based Thermoplastics in Green-Waste Composting.* Journal of Polymers and the Environment, 2012. **20**(1): p. 53-62.
14. Lee, S.T., *History and trends of polymeric foams: From process/product to performance/regulation*, in *Polymeric Foams: Technology and Developments in Regulation, Process and Products*, S.T. Lee and D. Scholz, Editors. 2009, CRC Press: Boca Raton. FL. p. 1-40.
15. Lee, S.T., C.B. Park, and N.S. Ramesh, *Introduction to polymeric foams*, in *Polymeric Foams: Science and Technology*, S.T. Lee, C.B. Park, and N.S. Ramesh, Editors. 2007, CRC Press: Boca Raton, FL.
16. Wong, A. and C.B. Park, *Fundamental Mechanisms of Cell Nucleation in Plastic Foam Processing* in *Foam extrusion: principles and practice*, S.-T. Lee and C.B. Park, Editors. 2014, CRC press
17. Lee, S.T., C.B. Park, and N.S. Ramesh, *Foaming fundamentals*, in *Polymeric Foams: Science and Technology*. 2007, CRC Press: Boca Raton, FL.
18. Chung, C.I., *Extrusion of polymers: theory and practice*. 2011, Munich; Cincinnati: Hanser Publishers.

19. Gendron, R. and L.E. Daigneault, *Rheology of Thermoplastic Foam Extrusion Process*, in *Foam extrusion: principles and practice*, S.T. Lee and C.B. Park, Editors. 2014, Taylor & Francis: Boca Raton.
20. Michaeli, W., et al., *Foam Extrusion Using Carbon Dioxide as a Blowing Agent*, in *Polymeric Foams: Technology and Developments in Regulation, Process and Products*, S.T. Lee and D. Scholz, Editors. 2009, CRC Press: Boca Raton. FL. p. 92-96.
21. Bier, J.M., C.J.R. Verbeek, and M.C. Lay, *Using synchrotron FTIR spectroscopy to determine secondary structure changes and distribution in thermoplastic protein.* Journal of Applied Polymer Science, 2013. **130**(1): p. 359-369.
22. Bier, J.M., C.J.R. Verbeek, and M.C. Lay, *Thermally resolved synchrotron FT-IR microscopy of structural changes in bloodmeal-based thermoplastics.* Journal of thermal analysis and calorimetry, 2014. **115**(1): p. 433-441.
23. Bier, J.M., C.J. Verbeek, and M.C. Lay, *Thermal transitions and structural relaxations in protein‐based thermoplastics.* Macromolecular Materials and Engineering, 2014. **299**(5): p. 524-539.
24. Bier, J.M., C.J.R. Verbeek, and M.C. Lay, *Identifying transition temperatures in bloodmeal-based thermoplastics using material pocket DMTA.* Journal of thermal analysis and calorimetry, 2013. **112**(3): p. 1303-1315.
25. Uitto, J.M., C.J.R. Verbeek, and C. Bengoechea, *Shear and extensional viscosity of a thermally aggregated protein-based thermoplastic polymer.* Submitted to Journal of Materials Science, 2018.
26. Salerno, A., et al., *Thermoplastic foams from zein and gelatin.* International Polymer Processing 2007. **22**(5): p. 480-488.
27. Jane, J.L. and S. Wang, *Soy protein-based thermoplastic composition for preparing molded articles*, U.P. Office, Editor. June 1996: USA.
28. Mungara, P., J.W. Zhang, and J. Jane, *Extrusion processing of soy protein-based foam.* Polymeric Preprints, 1998. **39**(2): p. 148-149.
29. Zhang, J., P. Mungara, and J. Jane, *Mechanical and thermal properties of extruded soy protein sheets.* Polymer, 2001. **42**(6): p. 2569-2578.
30. Belton, P., *Mini review: on the elasticity of wheat gluten.* Journal of Cereal Science, 1999. **29**(2): p. 103-107.
31. Wellner, N., et al., *Changes in protein secondary structure during gluten deformation studied by dynamic Fourier transform infrared spectroscopy.* Biomacromolecules, 2005. **6**(1): p. 255-261.
32. Marrazzo, C., E. Di Maio, and S. Iannace, *Foaming of synthetic and natural biodegradable polymers.* Journal of Cellular Plastics, 2007. **43**(2): p. 123-133.

Introduction
&
Scoping Work

Part 1

2

Protein Plastic Foams

A book chapter

by

C. Gavin, M.C. Lay, C.J.R Verbeek and A. Walallavita

Published in

Advances in Physiochemical Properties of Biopolymers, Part 2

Overview:

Chapter 2 reviewed methods of producing protein plastic foams including batch and extrusion foaming. It aimed to provide an overview of work done in the field and to outline the factors which affect polymeric foaming and how these may relate to foaming protein thermoplastics.

This chapter relates to the development of a foaming method (Objective 1), by outlining the relevant behaviour which must be considered for continuous foaming. This background understanding informs the rest of this work.

Contribution:

As first author for this publication the PhD candidate prepared the first draft of the manuscript, excluding the batch foaming section. Under the supervisors' guidance and with the assistance of the co-authors the manuscript was revised and edited.

Permission:

CHAPTER 9

Protein Plastic Foams

Chanelle Gavin, Mark C. Lay*, Casparus J.R. Verbeek* and **Anuradha Walallavita**

School of Engineering, Faculty of Science and Engineering, University of Waikato, Hamilton, New Zealand

Abstract: The development of protein-based biopolymers has been driven by the increasing global demand for polymer products, the need for sustainable practice within this industry and the availability of low cost by-products, such as high protein content meals. The continuing development of new and existing protein-based biopolymers will enable these materials to help supplement the increasing global demand for polymer products and to develop new markets with their niche applications. To date various compositions of protein-based biopolymers have been successfully used to produce injection moulded articles, films and foams. Biopolymers typically display poor foaming behavior and commonly produce foams with irregular morphology and high densities. Protein-based biopolymers are no exception, therefore it is important to fully understand how the foaming mechanisms of bubble nucleation, growth and stabilization are affected by the inherently different properties of these materials.

This chapter aims to review the production of stable protein-based foams for use in applications such as cushioning, insulation and packaging through a variety of methods. The review specifically focuses on the production of protein-based foams through thermosetting, the emerging role of proteins as a renewable substitute in polyurethane production and the application of thermoplastic foam technologies to protein-based thermoplastics, with an emphasis on batch and extrusion foaming methods. The similarities and differences between the production of traditional foams and those produced from proteins are highlighted here. Discussion of foam morphologies, properties and processing conditions is also included. Overall, this chapter intends to provide the reader with a greater understanding of the existing research and the current challenges associated with the production of protein-based thermoplastic and thermoset foams.

Keywords: Batch foaming, Extrusion foaming, Polyurethane foams, Protein biopolymers, Protein foams, Thermoplastic proteins, Thermoset foams.

* **Corresponding authors Mark C. Lay and Casparus J.R. Verbeek:** School of Engineering, Faculty of Science and Engineering, University of Waikato, Hamilton, New Zealand; Tel: +64 7 856 2889; E-mails: mark.lay@waikato.ac.nz, johan.verbeek@waikato.ac.nz

Martin Masuelli & Denis Renard (Eds.)

INTRODUCTION

This review examines the application of protein-based biopolymers to the polymer foam industry and discusses potential manufacturing methods for stable protein-based foams intended for use as packaging, insulation or cushioning. Until now, reviews regarding protein foaming have typically been limited to those relevant to the food industry with very little emphasis on their application to or use in thermoset or thermoplastic foams [1]. However with increasing interest in thermoplastic proteins for producing injection molded articles and films it is only logical that the industry also begins to assess the foaming ability of these materials on a wider scale.

The development of protein-based foams with similar or enhanced properties in comparison to their traditional polymer counterparts creates an entirely new market at the intersection of the polymer foam industry and the growing biopolymers sector. Recent reports regarding the polymer processing sector show that the global demand for polymer foam products is increasing, such that by 2019 it is predicted that the sector will generate 25 million tons of material. This represents an increase in production of nearly 32% on the 2013 figures, when the industry totaled 19 million tons (equivalent to $USD 87 billion) [2]. The majority of materials consumed by this sector are non-renewable and/or non-biodegradable including polyurethane, polystyrene and polyolefin materials such as polypropylene and polyethylene [2].

Traditional polymeric materials are being supplemented, and to some extent replaced, by biopolymers to address issues regarding the sustainability of this industry. The leading biopolymers are currently starch and PLA, however the use of protein-based biopolymers is also increasing, especially within the US [3]. Combined, this sector is expected to generate $USD 3.67 billion in revenue in 2018 [4, 5]. Unfortunately, the economics relating to the proportion of these materials which are foamed are as yet unpublished, hence the exact size and value of this market is unknown. Furthermore, a number of barriers exist for these and other biopolymer foams including consumer acceptance, poor thermal stability and the associated difficulty and cost of manufacture [6].

In general, the production of foamed polymeric products involves the introduction of a gaseous phase to the polymer system through chemical blowing agents (CBA) or physical blowing agents (PBA), the expansion or evolution of this gas due to changes in physical parameters such as pressure or temperature and the subsequent solidification of the resulting structure (usually by temperature changes or crosslinking) before the cells rupture or collapse due to condensation of the gaseous phase [7, 8]. Following stabilization the blowing agent is

eventually replaced by air as the gaseous species exchange across the cellular matrix (Fig. **1**). This phenomenon has been extensively studied and reviewed with respect to polyurethane, polystyrene, polypropylene and polyethylene foams where the behavior of these materials can be predicted relatively well in relation to physical foaming behavior; however the foaming mechanisms of bubble nucleation, growth and stabilization are yet to be fully understood.

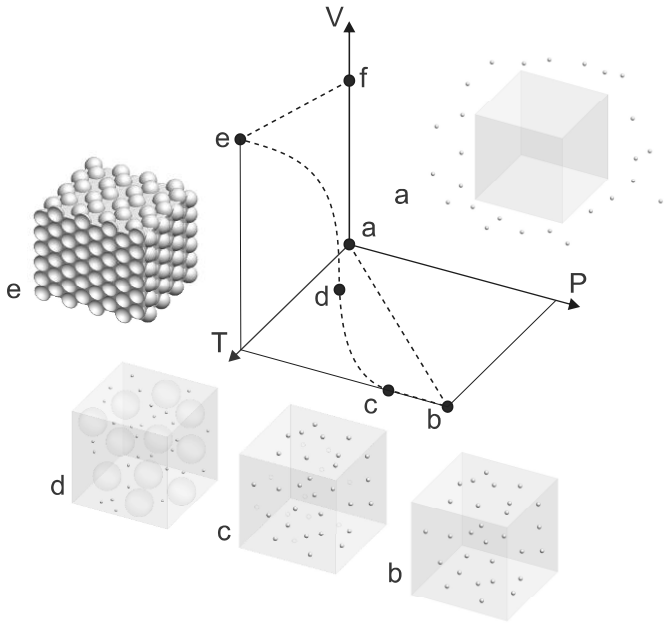

Fig. (1). Polymeric foaming process represented using a pressure, volume, and temperature diagram [7], with each stage shown by a letter and picture. The polymer and gas (**A**) is heated and pressurised to saturate the polymer (**B**), which is then depressurised so the gas changes phase and nucleates in the polymer (**C**), and as pressure drops, the remaining gas diffuses into the bubbles and the bubbles grow (**D**), until the final expanded foam is produced (**E**), and cooled (**F**).

Furthermore, the behavior of protein based biopolymers is still being characterized in relation to their structure, reactivity and processing ability. These are all related to their primary structure (amino acid sequence) and secondary structure (α-helices and β-sheets). Research is limited regarding the behavior of proteins within foaming systems. The properties of these materials, including poor rheological properties, low solubility of blowing agents and diffusion behaviour, severely hinder the foaming process. Consequently foamed biopolymers typically demonstrate non-uniform morphology and high density [6].

To date, efforts have been made to foam proteins through thermosetting methods

based on existing knowledge of the crosslinking behavior of casein and formaldehyde (although the possibility of using glutaraldehyde has also been noted) [9]. Aldehydes can react with the amine group from lysine and amino acids with side chains including cysteine, tyrosine, histidine, tryptophan, and arginine (Fig. **2**). Cereal and animal-based proteins are typically high in these amino acids, which enables good crosslinking. In comparison, glutaraldehyde is more selective reacting with lysine, cysteine, histidine, and tyrosine residues only [10]. Reaction with either crosslinking agent reduces the proportion of hydrophilic amino acids in protein blends and consequently these materials display lower water absorption capacities, thereby improving the properties of the resulting foams.

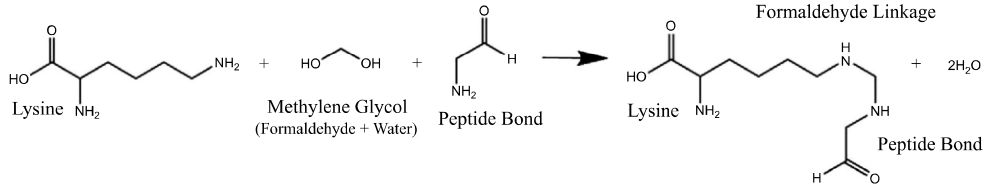

Fig. (2). Protein formaldehyde reaction chemistry [11]. Reproduced with permission, see note[1].

Proteins are also finding applications in polyurethane products in an effort to reduce production costs and increase the renewable fraction. Proteins are naturally reactive with these systems and the reactions are self-catalytic in water blown systems demonstrating how the unique chemistry of protein biopolymers, *i.e.* the presence of amide groups, can benefit this part of the market as well.

The increased interest in the production of value-added thermoplastic materials from waste animal and plant proteins has led to investigations regarding their extrudability, injection moulding capacity, film forming ability and recently their foaming ability. These protein based biopolymers have great potential to replace traditional thermoplastic materials in applications such as packaging as they can remain biodegradable after processing.

To enable thermoplastic processing, most proteins need to be blended with denaturants and plasticisers to disrupt protein bonding, lower the glass transition temperature (T_g) and enable chain mobility. A variety of proteins have been successfully utilized to produce thermoplastics although only a small proportion of these have been foamed *via* thermoplastic methods, which will be discussed in depth in this review.

This chapter will review the production and properties of thermoset protein foams, the role these protein biopolymers have in polyurethane systems, the production of thermoplastic proteins and thermoplastic foaming. The application

of these materials to these techniques is discussed by drawing on existing knowledge of these systems and protein behavior in general. This review includes an overview of the efforts to foam both plant and animal proteins including: zein, gluten, collagen, myofibrillar and bloodmeal and how these materials differ from traditional thermoplastic materials with respect to their physiochemistry. The underlying principles governing the foaming phenomenon are also briefly discussed including bubble nucleation, growth and stabilization. Attention is given to the factors which govern the foaming ability of these materials such as crystallinity, glass transition temperature, molecular weight distribution and the melt behavior including shear viscosity, extensional rheology, melt strength, surface tension and strain hardening behavior.

PROTEINS AND THEIR SOURCES

Proteins are genetically encoded molecules found in living organisms where they perform vital structural or functional roles. However, these molecules find secondary applications within the plastics industry. Proteins which have been identified as possible plastic feedstocks include: animal proteins, milk (casein and whey), collagen, gelatin, keratin, egg white, myofibrillar and bloodmeal; and plant and cereal sources. While the structure of animal proteins is very diverse, as they carry out a wide range of biological functions, the proteins found in plants can be described as more or less analogous to each other with most acting as storage proteins. For example, zein is the major prolamine protein in corn/maize while kafirin is analogous, performing the same function in sorghum. Other plant proteins which have been recognised as potential feedstocks include wheat gluten, soy, sunflower, barley and peanut proteins.

Proteins are long chains of amino acids, a fraction of which are folded into structured regions containing α-helices, β-sheets and β-strands while the rest remains amorphous. Their structure is held together by hydrogen bonds, hydrophobic interactions, covalent bonds, ionic interactions and van der Waals forces. Some proteins can be readily incorporated into foams, for example native/soluble proteins can be mixed in solution and mechanically whipped or aerated to produce foams which can be set by a combination of cooking and drying. The available amide groups on native proteins and peptides can also enable them to react with isocyanates to produce polyurethane foams.

Other proteins can be manipulated to behave like thermoplastic protein by adding plasticisers and denaturants which reduce the existing bonding within and between polymer chains to reduce their glass transition temperature (dried proteins have glass transition temperatures >180°C). Sodium sulphite or sodium bisulphite break cysteine-cysteine covalent bonds between chains [12], while

compounds like urea and sodium dodecyl sulphate disrupt hydrogen bonding and hydrophobic interactions respectively [13]. Plasticisers also disrupt hydrogen bonding and increase the free volume between chains allowing greater mobility [13].

Typical plasticisers include glycerol, triethylene glycol, water and other compounds which contain large proportions of hydroxyl groups [13]. This treatment is required to enable these materials to be extruded below their thermal degradation temperature. However these materials can still crosslink during processing leading to excessive pressure and torque in some cases [12]. Thermoplastic proteins have been produced from bloodmeal [14 - 18], gelatin [19, 20], keratin [21, 22], soy [23 - 26], kafirin [27], and zein [20, 27 - 30].

The feasibility of incorporating these molecules into protein-based thermoplastics is dependent upon a combination of the cost and continuity of supply of the proteins and their processability. These heteropolymers each display unique biochemistry which enables them to perform their primary role. Their structure and function of these molecules has been extensively reviewed elsewhere, although only briefly for application in bioplastics. Due to the large amount of available literature on these materials the structures, sources and function of these molecules will not be reviewed here; instead their application shall be the focus.

THERMOSET PROTEIN-BASED FOAMS

Protein foams (*e.g.* from whey or egg white) can be produced through thermosetting methods where the foamed structure is stabilized by crosslinking the protein chains by heating (*e.g.* meringue/pavlova) or chemical reagents (typically aldehydes).

In the food industry protein foaming is usually conducted by mechanical mixing (whipping) of a protein in a liquid phase to incorporate the air phase [31]. The resulting foam is dependent upon the physical-chemical properties of the solution such as viscosity, surface tension, and surface elasticity [32]. This is dependent on: (i) aggregation properties, protein-protein interactions, (ii) hydration properties, protein-water interactions and (iii) interfacial properties, such as surface tension [33].

Solidified whey protein foams have been produced from whey mixed with NaCl, Na_2CO_3 and water by high speed mechanical whipping and baking in an oven at 160°C for 40-50 minutes [33]. Whey foam blends with starch, gluten, and soy protein have also been produced. Such products are of interest to the food industry as whey has a high nutritional value and reasonable cost [34]. However whey protein is seldomly used alone in applications other than food because it is brittle

and has limited mechanical strength. These properties can be improved by blending whey with cross linking agents, plasticizers or other polymers such as alginate [35].

The compressive and flexural strength of hot moulded starch-based foams have been improved by adding gluten and zein proteins [36] while adding palm oil provides water resistance. Foamed combinations of sunflower protein, cassava starch and cellulose fibres have also been produced with densities of 0.45-0.51 g/cm^3 [37].

Thermoset plastic foams have also been produced *via* chemical reaction through mechanical mixing of a solution of egg albumin, 37% formaldehyde (cross linking agent) and camphor (waxy plasticizer). Once mixed the material was microwaved for 4-10 minutes to cure and partially dry the resulting foam. The foams had densities between 0.18-0.39 g/cm^3, a porosity of 77-79% and thermal conductivities between 0.06-0.065 W/mK, with little dependence of the thermal conductivity on foam density [38]. Blends with higher water content resulted in a softer material which was more elastic. Increasing the formaldehyde content gave a more rigid foam and camphor acted as an external plasticiser which resulted in more elastic and softer foams. An optimal formulation was 4 g camphor, 30 g water, and 8 g formaldehyde to 15 g of albumin protein, and a curing time of four minutes. Adding glycerol enabled foams to retain their elasticity over the course of two months [38]. Foam flexibility was temperature dependent for glycerol containing foams but not for foams produced without this plasticizer [39].

PROTEINS INCORPORATED INTO POLYURETHANE FOAMS

Polyurethane foams require different processing technologies and have different cell morphologies compared to thermoplastic foams and other thermosets previously described. In general, polyurethane foams contain mainly polyurethane chains with some polyurea blocks and foaming is strongly linked to surface tension effects. Foam formation is governed by the reaction (Fig. **3**) between a diisocyanate and a diol to form a urethane linkage [40]. Carbon dioxide is evolved as a blowing agent through the reaction of water (1-4%) with the diisocyanate monomer. Amide groups on both terminals of the monomer also react with diisocyanate monomers to form urea linkages. Recently, research has been conducted to incorporate protein isolates, concentrates and meals into polyurethane foams due to the availability of reactive amino acid groups which can reduce production costs and give unique morphologies. To date, protein products have been successfully incorporated into both flexible [40, 41] and rigid polyurethane products [42, 43].

Flexible polyurethane foams have been produced with soy protein isolate (SPI),

concentrate (SPC) or defatted soy flower (DFS) in concentrations between 0-30 wt% with varying purity (50-90%) [41]. These proteins were mixed with glycerol/propylene oxide polyether triol, a tertiary amine as catalyst, a surfactant, triethnolamine as a crosslinking agent and water (to evolve CO_2 as a blowing agent). Polymeric methylene-4,4'-diphenyldiisocyanate (pMDI) was used as the isocyanate component and the foam was allowed to rise for one hour at room temperature and cured at 25°C for one week.

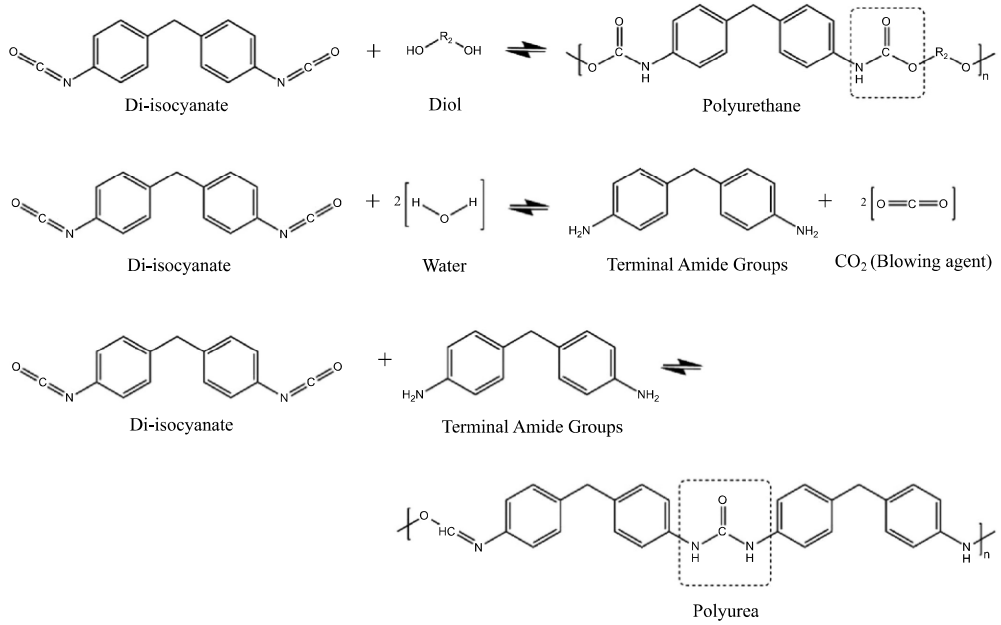

Fig. (3). Polyurethane reaction chemistry [8].

Foam density increased with higher contents of soy protein products. Foams containing DFS had a greater expansion ratio than those containing SPI or SPC due to the lower availability of active hydrogen atoms in DFS for reaction with the isocyanate. Foams containing up to 20% SPI demonstrated a higher compressive strength before reaching a plateau. This plateau was due to the protein reacting with all of the available isocyanate, resulting in a lower level of isocyanate available to evolve carbon dioxide and the excess protein weakened the foam structure. Furthermore, all foams containing soy protein products in this study showed greater resilience in comparison to polyurethane, suggesting that these may be suitable for packaging or cushioning applications [41].

A similar study produced polyurethane foams containing SPI, soy fiber and corn starch with toluene di-isocyanate (TDI) and demonstrated that using protein rather

than carbohydrates (starch) produced foams with better properties [40]. At lower amounts of additives (10%), foams containing SPI had a greater resilience compared to the other two formulations at the same level. At 20 wt% all formulations displayed similar resilience while 30% resulted in higher resilience for the soy based foams (SPI and soy fibre) than corn starch.

SPI and soybean meal (SM) have also been used to produce rigid polyurethane foams [43]. This was achieved by blending polyol (PEG-400), catalyst (DABCO), foam stabiliser (L-6865), water, crosslinker (triethanolamine) and protein (SM or SPI in either an activated or non-activated state). Polymeric isocyanate (PAPI-200) was then added and the mixture stirred before curing at room temperature for 30 minutes and aged at 35°C for 24 hours [43]. Up to 30% activated SM gave rigid foams with better thermal and mechanical properties than foams with SPI. Activation of the soybean meal *via* alkali treatment and sulphur bonding reduction increased availability of reactive protein groups to react with isocyanate, increasing foam density. Fibres in SM gave a more compact structure causing higher foam densities (67.6 kg/m^3 at 30 wt% SM) compared to foams with SPI (65.3 kg/m^3) [43].

The compressive strength of foams increased with increasing SM and SPI and foams containing activated fractions demonstrated higher compressive strength (348 and 262 kPa respectively at 30 wt%) than those which were not activated (242 and 221 kPa respectively) [43]. The polysaccharide and fibre fractions in SM (absent in SPI) may have helped increase compressive strength. Activated SM and SPI gave foams with smaller cell sizes, resulting in lower thermal conductivities, 0.0265 W/mK for activated SM at 30 wt% compared to 0.0312 W/mK for inactivated SM. SM based foams had lower thermal conductivities than those with SPI [43].

Similar thermal conductivities were achieved by another study which used soy flours (SF). SF has a protein content of 50-53% compared to 46% for SM from the previous study. Polyurethane foams containing SF were prepared in a similar manner. Typical thermal conductivities for these foams with 30% SF with the same blowing agent concentration were between 0.0263-0.0266 W/mK [42]. Densities for 30% SF polyurethane foams were 43.3-38.0 kg/m^3 which is lower than those from SM. Compressive strengths were also reported and ranged from 247-265 kPa which is comparable to the non-activated (native) SM polyurethane foams previously described.

A study investigated the use of algal protein, a co-product of the biofuels industry, with polyurethane. The algal proteins were first extracted, hydrolysed and the soluble peptides and amino acids retained for freeze drying. The freeze dried

material was then reacted with diamine and ethylene carbonate to produce the necessary polyol structure required for producing polyurethane. The algae polyol was then combined at a concentration of 5% with the other polyols, surfactant, water and isocyanate to produce the polyurethane foam. The algal polyols were high in hydroxyl content and very compatible with other polyols. The polymerisation process was self-catalytic and gave a rigid polyurethane foam which was less flammable than traditional polyurethane foams [44]. The resulting cellular structure was irregular open cell pores with a cell size of 0.6 ± 0.23 mm. Compared to the reference foam from commercial polyols, there was no change in core density (53 kg/m^3) but there was a decrease in resiliency, tensile strength, elongation and compressive strength when algal polyol was incorporated.

A review of the applications for a natural silk protein called sericin suggests that this protein may also behave favourably in polyurethane systems. A large number of Japanese patents are cited for the incorporation of sericin into polyurethane foams [45], however there is little available literature on these foaming systems.

THERMOPLASTIC FOAMING PRINCIPLES

The mechanisms which define foaming of thermoplastic polymers are bubble nucleation, growth and stabilisation and have been reviewed at length elsewhere for traditional systems. However, to briefly summarise, the creation of a foamed product is dependent upon the development of gas bubbles within a liquid/melt or softened phase. These bubbles must grow and stabilise to result in a permanent cellular product [46 - 48]. These processes are thermodynamically controlled and polymer must exhibit suitable rheology to successfully produce a cell structure [8].

Initial bubble formation is referred to as cell nucleation. From a thermodynamic perspective, the evolution of gas bubbles within a polymer melt requires instabilities, *i.e.* the presence of a driving force [8]. During bubble nucleation the decrease in the free energy of the system which occurs with the development of the gaseous phase (molecules have a lower Gibb's free energy when present as a distinct phase rather than as individual molecules) provides this driver [49]. Later, as the cells grow to reach a stable state, there is a corresponding increase in Gibb's free energy as new interfaces are formed [47]. Overall, the free energy of the system is said to increase during the foaming process.

Polymer melts can be described as either homogenous or heterogenous which affects the nucleation mechanism. Self-nucleation occurs when a homogenous melt (the primary phase) develops gas bubbles (a secondary phase) without external assistance. In reality, self-nucleation is very seldomly achieved as such a process would encounter a large activation energy barrier. However, should a

number of dissolved gas molecules cluster together, it is theoretically possible [47, 48]. Polymer melts typically contain additives (usually talc 1-3%) or impurities resulting in an inhomogeneous system to which homogenous nucleation theory cannot be directly applied. The presence of these particles and cavities reduces the activation energy required to achieve a stable nucleus, therefore foaming more commonly occurs *via* this mechanism [47 - 50]. The efficiency of the nucleating agent depends on the type and shape of the nucleating particles as well as the interfacial tension between the polymer and nucleating agent [50].

Once nucleated, cells grow as gas continues to diffuse from the polymer into the cells. Growth ceases when the cells are stabilized (through cooling) or when they rupture (*i.e.* the polymer is unable to contain the gas). Bubble coalescence and rupture will continue to occur simultaneously with bubble growth. A permanent cellular product will only result if the cell structure can be stabilised. Typically, a foamed structure becomes stabilised through the cooling process which raises the viscosity of the polymer melt. Eventually, the expansion ceases and the cellular structure appears to stabilize when the polymer has cooled sufficiently to return to a solid state [51].

FACTORS WHICH AFFECT THERMOPLASTIC FOAMING

Excluding processing conditions, the foaming ability of biopolymers and proteins is similar to that of traditional polymers. Factors which affect foaming include: solubility and diffusivity of the gaseous phase, melt rheology, melt strength and strain hardening behaviour, all of which can be related to the crystallinity of the material. The relationship between these effects are well established with traditional polymers and can easily be manipulated. An improvement of foaming ability has been linked to the introduction of branching, or through increasing the molecular weight distribution in traditional systems [6]. This section aims to discuss the material properties which affect foaming ability in relation to foaming in general and to highlight the factors which are more important in batch and extrusion foaming respectively before these methods are discussed in depth.

Crystallinity and Thermal Transitions in Polymers and Proteins

Polymers are described as either amorphous, semi-crystalline or crystalline depending upon the degree of ordered structures they contain. For traditional polymers, crystallinity is defined by the proportion of ordered regions called lamellae made by regular folding of the polymer chain. The subsequent production of spherulites from these lamellae results in larger crystalline structures which can reach up to several millimetres in size [15, 52]. In protein thermoplastics, the semi-crystalline nature of these materials is determined by the

secondary structure of the proteins and the relative proportion of α-helices and β-sheets in comparison to less structured regions such as random coils. The crystalline regions within protein polymers are smaller than those observed in traditional polymers, approximately 10 nm in size, but have been shown to dictate the processing temperature of protein thermoplastics and the ability of these materials to form stable products [15, 53].

During processing, ordered regions are disrupted through the addition of heat which enables the production of a melt. At the melting temperature (T_m) complete disruption of these ordered structures occurs in the case of traditional polymers. The semi-crystalline nature and the transitional behaviour of protein-based polymers has been extensively reviewed in comparison to the responses demonstrated by traditional polymers [15].

Dry proteins typically display glass transition temperatures which are close to their degradation temperature. This is overcome when denaturants and plasticisers are added to lower the T_g. A denaturing temperature (T_d) is typically observed in protein biopolymers which is often very similar to the representative melt temperature observed in semi-crystalline polymers.

Above the T_d protein polymers will either unfold to a less ordered conformation associated with the partial dissociation of these ordered structures (α-helices and β-sheets) or the increased temperature can induce the production of these ordered regions, mainly β-sheets, known as aggregation. For protein polymers these transitions can be poorly defined, occurring over a broad temperature range, and depend upon the degree of hydrogen bonding, electrostatic forces and hydrophobic interactions which exist within the protein. Therefore, these transitions are protein dependent.

It is important to emphasize the production of a protein thermoplastic melt does not necessarily indicate the complete disruption of α-helices and β-sheet conformations to an amorphous phase (unlike traditional thermoplastics) and in some cases may promote the formation of β-sheets [15]. However, mechanical shear may result in a reduction or dispersion of these crystalline regions, enabling a thermoplastic melt. The crystallinity of a protein-based thermoplastic affects the melt, the corresponding rheological properties and its behaviour with respect to solubility and diffusivity of gases. The stabilisation of foams will also be effected by the ability of these materials to recreate these ordered regions on cooling to freeze the resulting foam structure.

Solubility and Diffusivity

Foaming relies on the introduction and retention of a gaseous phase within a

polymer matrix. The solubility and diffusivity of gases strongly influences the foaming ability of these materials. Gases can be incorporated through the use of either physical blowing agents (PBA) or chemical blowing agents (CBA). Common PBAs used to include chlorofluorocarbons (CFC), hydrochloro-fluorocarbons (HCFC), and hydrocarbons such as pentane and butane. However, there has been a recent migration towards more environmentally benign agents such as CO_2, O_2 and N_2. Azodicarbonamide, sodium bicarbonate or sodium bicarbonate/citric acid systems are examples of CBAs where gases are evolved by heating to decompose the CBA.

Factors which affect solubility and diffusivity within polymer systems have been reported as the phase of the polymer (molten or glassy), the structure and degree of crosslinking, crystallinity of the polymer and type, concentration and behaviour of plasticisers and fillers. An excellent review [54] defines the relationship between solubility and diffusivity of gases within polymers for foaming. The production of a fine cell homogenous foam is produced by the complete dissolution of the gaseous phase while partial dissolution results in a heterogeneous foam structure.

Normally, the solubility of a gas can be improved by increasing pressure and decreasing temperature. However, CO_2 or N_2 in a polymeric systems does not necessarily behave as expected. For example, the solubility of CO_2 has been observed to decrease with an increase in temperature while N_2 displays an increase in solubility with temperature in polystyrene. Consequently they are often used as a blend during batch foaming, for example 75% vol. N_2 and 25% vol. CO_2 for zein proteins [6].

The crystallinity of the polymer dictates the gas its solubility and diffusivity as the crystalline regions oppose the movement of absorbed gas within the amorphous phase. Additional factors, which have been noted as affecting the properties of semi-crystalline polymers, include orientation of the crystalline phase, chain stretching and free volume changes. It is also believed that these crystalline regions can promote nucleation by acting as heterogenous nucleating agents.

Adsorption and absorption of gaseous molecules is greatly influenced by the temperature of the polymer system in relation to its glass transition temperature. When $T>T_g$ the amorphous regions of the polymer or protein system become fluid although motion is still restricted by the crystalline phase (if present) if $T<T_m$. The solubility of the gaseous phase in the polymer matrix is similar to that of gas into a viscous fluid. When $T<T_g$ the polymer remains glassy with limited chain mobility. When gases are taken up they become trapped within polymer chains and physically disrupt the bonding between the polymer chains. In this case the

free volume of the polymer is increased and the absorbed gas has a temporary plasticising effect. During this process the solubility of these gases into the solid phase is governed by surface adsorption rates. High solubility of a gas within a polymer results in more blowing agent which benefits nucleation and cell growth.

The uptake of gases within a solid matrix is a controlling factor in batch foaming. During this process, plasticisation of the solid matrix can occur which provides the system with sufficient mobility to enable foaming. The resulting cellular structure is solidified by the loss of this plasticisation as the gaseous phase moves out of the polymer and into the bubble resulting in an increase in polymer viscosity.

In extrusion systems where a fluid melt is produced, the melt experiences additional plasticisation by the introduction of a gas phase from PBA or CBA. This decreases the viscosity of the polymer melt, reducing the melt pressure with respect to the internal bubble pressure, favouring faster bubble growth. The solidification of the foamed structure once again corresponds to a change in polymer viscosity. Once the melt has exited the extruder and depressurises, the gas migrates into the nucleated bubbles resulting in cell growth, and the material expands. The melt also cools which induces crystallisation and increases the viscosity slowing cell growth, and solidifies the foam structure.

Diffusivity of gas within a polymeric material is dictated by the polymer chain mobility, packing, crystallinity and degree of crosslinking, which are temperature dependent. The diffusion rate is dependent on the gas concentration gradient which decreases as the material approaches saturation. The presence of side chains in a polymer decreases packing resulting in a more amorphous structure, increasing diffusivity. An increase in the crosslinking within a polymer decreases diffusivity and solubility of the gas [54].

High diffusivity of gases within a polymer is ideal for nucleation but has a detrimental effect on bubble growth. High diffusivity results in greater nucleation as the gas leaves the polymer/BA phase quickly, giving a finer cellular structure, but during bubble growth, the gas can escape from the bubble and material easily, reducing bubble size. Diffusivity is particularly important in extrusion processes as the material has a short time before it cools. Gas diffusivity can be manipulated by controlling polymer viscosity and crystallinity by adjusting temperature, enabling bubble size and cell density to be controlled.

The solubility and diffusivity of gases within traditional polymers is well defined and gases with a variety of phases (subcritical, supercritical and gaseous) have been used. Gas solubility and diffusivity in protein-based thermoplastics is not widely reported, but will depend on the blowing agent, denaturants and

plasticisers used. For example proteins have been selected for film and coating applications due to their low oxygen permeabilities, but protein films have high water vapour permeabilities [55].

Viscoelastic Behavior and Melt Rheology in Foaming

Polymers and proteins have defined thermal transitions where they change from a solid to a melt. The ability of polymers to foam is closely related to their temperature dependent viscoelastic behaviour which is a controlling factor in both batch and extrusion foaming systems. Foaming behaviour is greatly influenced by viscosity and is related to melt strength, extensional viscosity and the ability to display strain hardening. The mechanisms which control foaming are linked to the amorphous and semi-crystalline nature of these materials and the presence of side chains.

As previously described, bubble growth during foaming is directly linked to the viscosity of the polymer and the pressure difference between the bubble and the matrix. As such, polymer viscosity is a controlling factor for foaming and influences nucleation and stabilisation as well. Ideally viscosity of the polymer is low during the nucleation phase to enable high nucleation rates. It should then increase during bubble growth to restrain bubble growth.

This is commonly achieved through loss of the gaseous phase from the polymer melt or a decrease in temperature to produce high viscosities which stabilise the foam structure in amorphous polymers. If the viscosity of the polymer is too low and the melt strength is poor, the cells are prone to rupture and collapse. In materials with chain branching, *e.g.* polypropylene, strain hardening occurs which can be used to overcome low melt strength [56]. For semi-crystalline polymers the stabilisation effects are also related to crystallization of the material in addition to the factors listed above.

Many attempts have been made to describe the required rheological properties for foaming in relation to melt strength and extensional viscosity. Extensional viscosity is described as being the factor which allows two materials with the same shear viscosity to behave differently in extensional flow. Extensional flows are experienced by polymers in processes such as such as fiber spinning, film blowing and extrusion foaming [57]. The relationship between extensional viscosity and foaming ability is better defined by transient behaviour, as during foaming deformation occurs within a limited timeframe.

Extensional viscosity can be determined from Rheotens curves if there is optical monitoring of the extrudate size, however the results are qualitative. Therefore, the Rheotens method is more commonly used to determine melt strength [57]. The

melt strength is defined as the maximum tensile strength required to break the strand extruded through a capillary with a gradual increase in haul off speed. Sufficient melt strength is required for foaming in addition to extensional viscosity.

Strain Hardening

The correlation between melt strength, melt elasticity and strain hardening has been reviewed in depth for polyolefin materials, which are favoured in many applications due to their toughness, flexibility and chemical resistance. For foam extrusion, polyethylene (PE) has typically been favoured over polypropylene due to cost, thermal and chemical stability and processability (PE has a wide foaming window). Polypropylene foams demonstrate high stiffness and can be used static load bearing applications. However, their manufacture is limited as they demonstrate low melt strength and little elasticity. Consequently the cells within polypropylene foams rupture easily as the cell walls are not able to withstand the extensional forces which occur during foaming.

The melt strength of PP can be improved by introducing long-chain branches which restrict the movement of polymer chains under strain and introduce strain hardening effects, stabilising the bubbles during growth and reducing cell coalescence and rupture. An increase in the long chain branching (LCB) content of PP resulted in lower and broader DSC melting peaks, a reduction in crystallinity, and increased zero-shear and elongational viscosities. This resulted in lower foam densities with well-developed and uniform foam structures compared to unbranched PP [58]. Another study looking at blends of linear PP with LCB PP found that increasing LCB PP content past 50% had little effect on the degree of foaming because elongational viscosity of 100% LCB PP was similar to 50% linear PP:50% LCB PP blends [59].

The extensional viscosity of proteins and thermoplastics thereof have been linked to the secondary structure of the proteins for zein and kafirin under film blowing conditions. The film blowing process requires good melt deformability and elongational properties which is similar to the properties required for foaming. Two studies have been conducted to correlate the molecular structure, rheological behaviour and film blowing abilities of these proteins. Zein-based materials containing a high proportion of α-helical structures produced the best blown films, with the highest extensional viscosity, best strain hardening behaviour and haul of force. It was concluded that the change in extensional behaviour could be contributed to the relative content of α-helical to β-sheets [53].

Another study examined film formation from kafirin protein, where it was found that heat treatments promoted β-sheets formation which reduced film forming

ability. Freeze-dried material contained the highest proportion of α-helical structures. The higher strain and tensile strength films produced from freeze-dried kafirin is a result of not only the greater ratio of α-helical structures to β-sheets and other protein conformations but also their homogenous distribution and the ability of native-like structures to pack together more efficiently than denatured and aggregated proteins [55].

The correlation between secondary structure and foaming ability has been discussed for the foaming ability of zein proteins. Plasticised zein protein (75% zein: 25% PEG400) has been shown to depend heavily on the concentration of β-sheets within the original zein protein. During this study zein was obtained from the same producer and extracted using the same technique, however FTIR analysis detected differences in the secondary structure of the zein protein. This suggests that variability within protein supplies such as small changes in growth conditions, extraction or protein aging may influence foaming results. The foaming ability of these zein proteins was once again linked to the ratio of α-helical to β-sheet content. The governing conformation was linked to the β-sheet content which influenced how deformable the plasticised material was. Zein with a higher concentration of β-sheets resulted in a collapsed foam under batch foaming conditions which was contributed to the material being unable to withstand deformation during foaming. In comparison the zein a lower β-sheet content resulted in a far more deformable material and a fine cell low density foam [6].

BATCH FOAMING

An effective method for producing cellular foams is the batch foaming technique, also known as the autoclave method. Batch foaming can produce microcellular foams, structures with cell sizes smaller than 10 μm and cell population density greater than 10^9 cells.cm^{-3} [60].

Microcellular foams are attractive because the material's bulk density is reduced while possessing high impact strength, toughness, stiffness-to-weight ratio, low thermal conductivity as well as low weight and cost [61].

There are two approaches to batch foaming. The first is the ***temperature soak*** method where the polymer at room or low temperature is placed in a high-pressure gas environment which forces the gas to diffuse into the polymer matrix. The vessel is depressurised and material transferred to a mould or water bath and heated past the glass transition temperature, resulting in the gas nucleating and forming micro-bubbles. Subsequently, the material is cooled resulting in a stable foam.

The second approach is the ***pressure quench*** method where the material is heated in an autoclave past its glass transition temperature and exposed to gas at high pressure, resulting in the gas diffusing into the material. The pressure is released resulting in the gas forming micro-bubbles in the polymer, and the temperature lowered resulting in a stable foam. Fig. **4-A** shows a typical set-up of a supercritical batch foaming system [62].

The setup consists of an autoclave which is temperature controlled by circulating oil heated/cooled by a cryo-thermostat. The CO_2 is supplied by a CO_2 cylinder connected to a gas booster. Pressure and temperature are monitored and computer controlled. For batch foaming, cell morphology, size and number can be manipulated by controlling pressure, temperature, gas type, saturation time, nucleating agents and depressurisation rate. Polymer crystallinity, viscosity, and melt strength also influences cell size, density and the resulting foam mechanical properties.

Gas Absorption

Gas absorption can be measured directly by change in weight of the material or indirectly by measuring foam density after the material has been foamed. Absorption will depend on gas pressure, absorption time, gas solubility, and diffusion rate.

Gas diffusion rate and solubility will be dependent on gas and material type, decrease with increasing polymer viscosity (which decreases with increasing temperature) and crystallinity (which is dependent on the melting temperature of the crystalline regions and whether or not absorption is carried out above the melting temperature of the crystalline regions).

Doourdiani, *et al.*, were able to manipulate the crystallinity of HDPE, PB, PP and PET by heating them above the melting temperature and cooling them at different rates following compression moulding into a film. Slow cooling rates induced high crystallinity while cold water quenching on the material gave the lowest crystallinity. CO_2 solubility was halved and diffusivity decreased by 5% for PP and up to 100 fold for PET when crystallinity was increased from 45% to 69% for PP and 36-58% for PET [65]. Increasing gas pressure will increase gas absorption and polymer swelling and decrease in foam cell size. PLA (grades 3001D, 8051D and 4060D) showed an increase in swelling ratio of 1.04 to 1.16-1.20 when CO_2 gas pressure was increased from 6 to 22 MPa (at 190^{o}C), while gas solubility increased from 0.04 to 0.14 g/g [66].

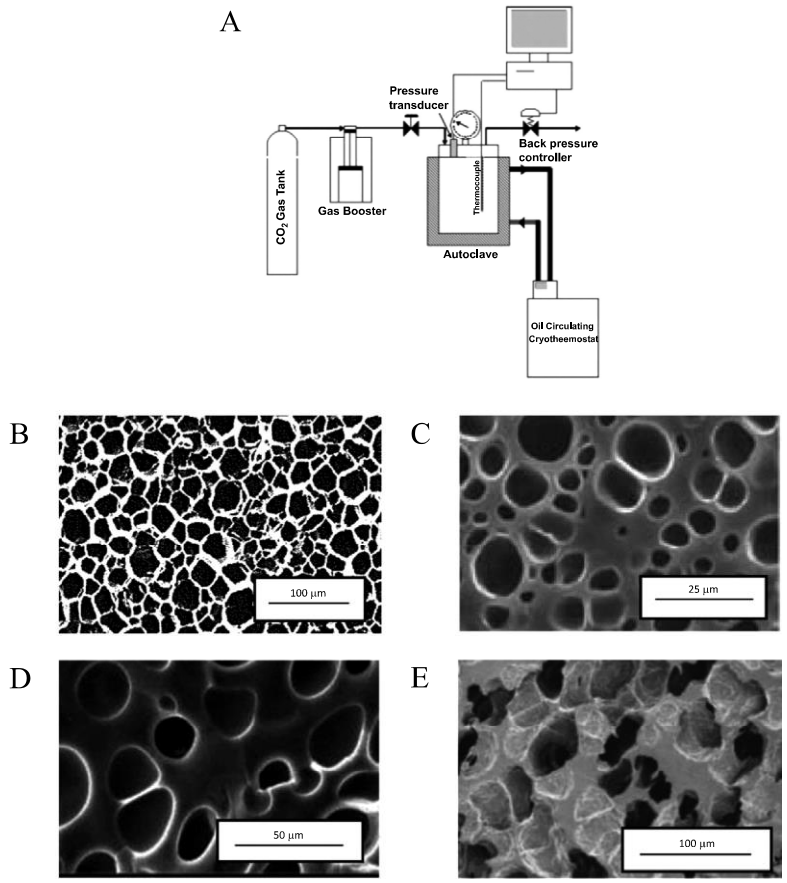

Fig. (4). A: Typical batch foaming system [62] **B:** SEM image of TPZ (Thermoplastic Zein) foamed with N_2-CO_2 80-20 vol%, P_{sat} = 180 bar, T_f =79°C [20] **C:** SEM image of TPZ (Thermoplastic Zein) foamed with N_2-CO_2 80-20 vol%, P_{sat} = 170 bar, T_f =55°C [63] **D:** SEM image of TPG (Thermoplastic Gluten) foamed with CO_2, P_{sat} =85 bar, T_f =100°C [19] **E:** SEM image of NTP/PLA blend foamed with supercritical CO_2, P_{sat} = 200 bar, T_f =55°C [64]. Images reproduced with permission, see note[2].

Aionicesei *et al.* showed similar results for poly(L-lactide), PLLA (42 kDa, semi-crystalline) and poly(D, L-lactide-co-glycolide) PLGA (72 kDa, 50:50 D and L-lactide, amorphous) where CO_2 solubility doubled or tripled when CO_2 pressure was increased from 10-30 MPa. PLLA had almost twice the CO_2 solubility of PLGA (0.75 g/g compared to 0.4 g/g for PLGA at 30 MPa), but both had similar diffusion coefficients, probably due PLLA being semi-crystalline and a lower molecular weight, while PLGA is amorphous, but a larger molecular weight [67]. Similarly, CO_2 solubility in polymethyl methacrylate (PMMA) increased from 0.08 g/g at 15 MPa to 0.24 g/g at 25 MPa [68]. LLDPE showed a foam density of

0.27 g/cm^3 when saturated with N_2 at 12 MPa compared to 0.17 g/cm^3 at 20 MPa [69]. Polystyrene showed a decrease in average cell size with increased CO_2 pressure from 440 μm at 7.5 MPa to 40 μm at 10 MPa when foamed at 80°C [56].

Increasing gas absorption time will increase the amount of gas adsorbed in the matrix up until it reaches saturation, which will decrease foam density. This behaviour is also linked to diffusion rate which is dependent on the polymer, gas and temperature. Higher temperatures will reduce polymer viscosity and increase diffusivity, reducing saturation time. For example, LDPE at 125°C saturated with N_2 took longer to reach saturation (8 min at 12 MPa) than LDPE at 135°C (5 min), while LLDPE at 119°C took 10 min and 8 min at 135°C [69].

Foaming

Extent of foaming will depend on the amount of gas absorbed (see previous section), temperature and pressure at which the material is foamed, depressurisation rate, and polymer melt strength, viscosity and elasticity. These effects on foaming can be measured by foam density, cell density, cell size and cell size distribution.

Kwon and Bae showed higher CO_2 gas solubility (manipulated by ranging CO_2 pressure between 15-25 MPa) in PMMA will result in greater cell density and lower cell mean diameter when the material is foamed [68].

A higher foaming temperature will generally reduce foam density, but this will be polymer dependent. For example LLDPE foamed at 123°C had a foam density of 0.08 g/cm^3 compared to 0.17 g/cm^3 at 119°C, while LDPE showed little difference in foam density when foamed at 125°C and 135°C [69]. The foaming temperature window will depend on the melt strength of the polymer, which is dependent on polymer viscosity and temperature. Higher viscosities will slow bubble growth, while high foaming temperatures will reduce viscosity and increase gas diffusion and bubble growth [56, 70]. As the bubble grows, and the matrix stretches around it, the matrix will undergo strain hardening as previously described, which will slow bubble growth. If bubble growth is too fast for the polymer, it will result in collapsed bubbles. For example LLDPE foamed at temperatures greater than 123°C resulted in collapsed bubbles, whereas LDPE, which has a greater melt strength than LLDPE, had a broad foaming window of 105 to 160°C, and cell size and morphology was largely independent of temperature tested [69]. LLDPE foamed at lower temperatures and showed more irregular cell morphology due to the presence of crystalline regions in the polymer melt.

Polymer viscosity and melt strength can be increased by grafting long chain branches (LCB) onto the polymer back bone, or extending chain length. Grafting

LCB onto polystyrene resulted in a narrower cell size distribution and smaller average cell diameters, and higher cell densities (2 wt% LCB grafted PS gave a 100 fold increase in cell density compared to ungrafted PS foamed with CO_2 at 10 MPa and 110°C). Cell size and distribution increased with increasing foaming temperature (0-19 μm at 70°C to 70-230 μm at 110°C), while the effect of chain branching on cell density was more pronounced for the higher foaming temperatures (80-110°C) [56].

Increased depressurisation rate increases cell nucleation, resulting in higher cell densities and lower cell size [61]. Bimodal foams, *i.e.* foams with two discrete cell size distributions, can be generated by using two step depressurisation after the polymer has been saturated with gas. These have the advantage of having a low thermal conductivity and low weight from the larger average cell size while retaining the high mechanical strength imparted by the microcellular foam. Bimodal foams were produced from PS saturated with CO_2 at 20 MPa and 100°C and depressurised to 15 MPa, held for a period of time, and then depressurised to ambient pressure. Increasing holding time from 0 to 60 min increased the average cell diameter from 4 μm to 22 μm and reduced cell density from $8x10^8$ cells per cm^3 to ~ $1x10^6$ cells per cm3 [61].

Dorourdiani *et al.*, showed that HDPE, PB, PP and PET with increased crystallinities (see previous section) had quite different foam morphologies. Samples with lower crystallinities had a more regular cell structure and smaller cell size, while samples with the higher crystallinities were more difficult to foam only exhibiting foam structures in a few localised regions in the polymer. This was partly due to lower gas solubility and diffusivity at higher crystallinities, but Dorourdiani *et al.* also speculated that CO_2 acted to plasticise the polymer, resulting in easier foaming at lower crystallinities and higher CO_2 concentrations in the matrix [65]

Liao *et al.* manipulated the crystallinities of unbranched and branched PP by heating it to 180°C, exposing it to CO_2 at 14 MPa for 4 hours, cooling it to 130°C at holding at that temperature for different periods of time before depressurising. Longer holding times for unbranched and branched PP resulted in increased crystallinities (observed by measuring the spherulite size and density) and consequently smaller cell sizes and larger cell densities. Reducing holding time resulted in ellipsoid shaped cells, while the longer holding times gave more spherical cells [70]. Unfortunately their foaming windows for unbranched and branched PP were quite different so a direct comparison between using the same conditions for the two types was not possible.

EXAMPLES OF BATCH FOAMED PROTEINS

There are only a few examples of successfully batch foamed proteins using the autoclave method. These used zein, gelatin and bloodmeal (which was blended with PLA).

Salerno *et al.* [20] foamed protein based discs cut from hot-pressed gelatin with 20 wt% glycerol and zein with 25 wt% PEG 400 (Fig. **4-B**). They explored varying the gas composition using a mixture of N_2 and CO_2, saturation pressures between 6-18 MPa at 70°C, foaming temperatures between 50-140°C, and pressure drop rates of 25 and 70 MPa/s. The best foams from zein were obtained using 80% N_2 and 20% CO_2 at 18 MPa at 70°C, with a foam density of 0.1 g/cm^3 and average cell size of 32 μm. At lower foaming temperatures (44°C), the cells were smaller (14 μm) with thicker walls with a foam density of 0.65 g/cm^3, due to the increased viscosity of the material, while higher temperatures (100°C) resulted in apparent cell shrinkage (15 mm) due to gas diffusion through the cell walls. Gelatin foam densities were between 0.5 to 0.7 g/cm^3 and cell sizes ranged between 3 to 25 mm when foamed at 44-120°C, but temperatures above this resulted in browning and loss of glycerol.

Olivierio *et al.* [63] found adding acid or alkali derived lignin to zein thermoplastics was detrimental to foaming (using similar conditions to Salerno *et al.*), and were only able to produce microcellular foams (Fig. **4-C**) with addition of lignin up to 1% by weight. Olivierio *et al.* [19] also foamed hot pressed gelatin (with 20% glycerol)/poly(butylene succinate) discs (Fig. **4-D**) using CO_2 at 6.5-8.5 MPa at 100 and 120°C and foaming temperatures between 75-100°C. Gelatin was immiscible in PBS and *vice versa*, but the presence of PBS reduced the cell size compared to plasticised gelatin foams which was between 15-40 μm.

Trujillo-de Santiago *et al.* [30] produced foams from zein (plasticised with PEG 400), starch (with urea and formaldehyde (UF) and sorbital and glycerol (SG), a blend of starch and zein (with UF and SG), and blue maize (SG)). The materials were saturated with CO_2 at 15 MPa and 70°C, and foamed at temperatures between 75 to 140°C. Foamed zein increased eight fold in volume, followed by starch (UF) which increased in volume by six times. Starch (SG), the zein/starch blend, and blue maize showed only a slight increase in volume and the morphology appeared to be fractures in the material rather than regular cells.

Walallavita *et al.* [64] blended Novatein® thermoplastic (NTP) (a bloodmeal protein based bioplastic) with PLA (Ingeo™ 4060D, fully amorphous) at NTP concentrations between 5-60 wt%. Extruded rods were saturated with CO_2 at 6 MPa, transferred to a hot water bath and heated to 70°C. Rods were also foamed

by saturating them with CO_2 at 20 MPa at 50°C, followed by depressurisation. Expansion ratio decreased with increased NTP content (Fig. **4-E**).

FOAM EXTRUSION

Extrusion foaming is highly economical due to the continuous nature of this operation. Foam extrusion can be carried out in any of the common extruder configurations: twin screw extruders (TSE), single screw extruders (SSE) or tandem lines [71], but the equipment must produce a sufficient melt temperature to decompose the blowing agent, the pressure of the melt must be kept high to prevent gas dissolution and the back pressure in the hopper must be controllable to ensure consistent results [71]. Each of the extruder configurations has unique advantages and disadvantages and are typically optimised for a particular polymer/blowing agent system through a trial-and-error approach. Specialised extruders have been designed for foaming applications, although to do so the behaviour of the material and the subsequent interaction of the blowing agent with this material must be well defined. Typically, the extruder contains several zones along the barrel where temperature, pitch, element type can be varied to better control melt properties and pressure (Fig. **5-A**).

The polymeric material is melted and blended with any CBAs within the first zone, the material is then mixed and PBAs can be added. As a general rule of thumb the feed zone within a foaming system must be lower than the initial decomposition temperature of the CBA if it is added with the feed [71]. The material is extruded across the remaining zones, where changes in temperature further alter the rheology of the material to enable foaming such that when the material reaches the die nucleation and bubble growth can occur [72].

Until then the gaseous phase remains dissolved within the polymer melt due to pressure within the barrel. Within these systems foaming occurs under free expansion (atmospheric pressure) unlike foaming conducted *via* injection moulding were the limited volume of the mould dictates the pressure experienced by the expanding melt. Once the material has exited the die, the material must solidify quickly before the gaseous phase causes excessive cell rupture or collapse.

The operating parameters such as screw speed, extrusion temperature, die size and the configuration of the screw elements all influence the properties of the resulting foams such as cell size, cell density, expansion ratio and radial expansion ratio. There are a limited number of examples of extrusion foaming of thermoplastic proteins, as such parameter optimisation has yet to be presented for foaming thermoplastic proteins and these are expected to be highly protein dependent. Therefore, the influence that these parameters have are described in

relation to traditional polyolefin foaming and biopolymers such as starch and PLA.

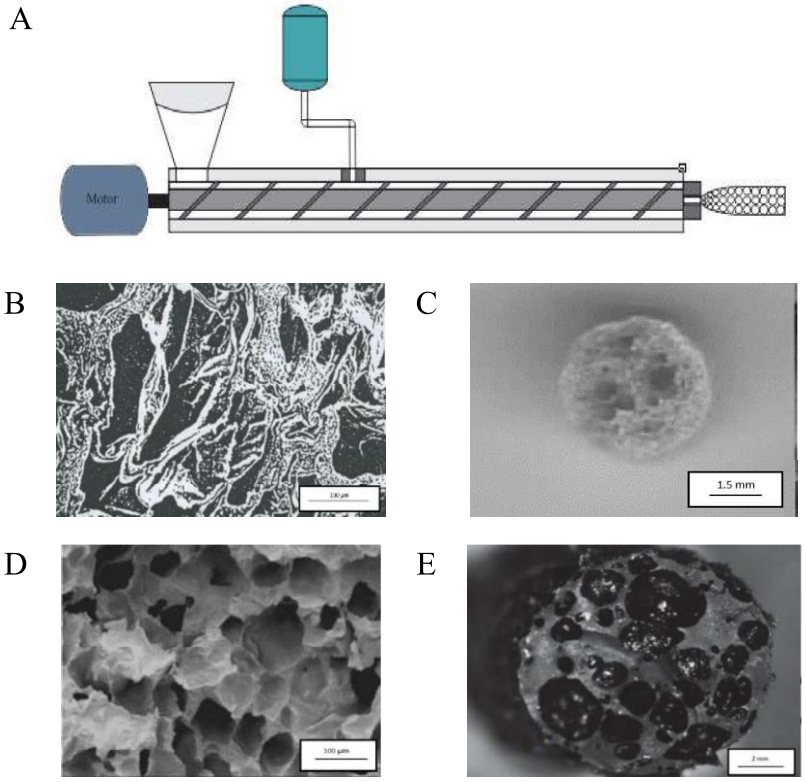

Fig. (5). A: diagram of a foam extruder with PBA capability, **B**: SEM image of Thermoplastic Soy foamed at 150-160°C [73], **C:** Image of 70% Zein 30% Pearl Millet Flour, Screw Speed 80 RPM, Die Size 2 mm [74], **D.** SEM image of PLA/SPC, 2 phr CBA, Screw Speed 60 RPM, Die Size 1 mm [23], **E.** Image of NTP/PE---MAH/LLDPE Foam, Steam Blown, Screw Speed 150 RPM, Die Size 10 mm [75]. Images reproduced with permission see note[3].

During extrusion foaming the behaviour of all thermoplastics are relatively similar therefore it is expected that thermoplastic protein foams will display similar responses to changes in extrusion speed, die size, CBA, PBA and nucleating agent content.

Foam extrusion behaviour of polyethylene and polypropylene is well defined and has been reviewed extensively [7, 51, 76, 77]. One review outlines the behaviour of polyolefins within extrusion foaming using linear low density polyethylene (LDPE) and polypropylene (PP) as examples. Sodium bicarbonate and citric acid

was used as a blowing agent. The material was extruded through a single screw extruder, 19 mm in diameter with a length/diameter (L/D) ratio of 25. The extruded foam was then submerged in a water bath to stabilise the foam structure [78]. This particular study discusses a comprehensive set of process variables including melt temperature, cooling water temperature, and blowing agent content on the resulting cell size and distribution. Material characteristics such as molecular weight, structure, melt viscosity and melt tension was also investigated.

The foaming ability of these materials was shown to be directly correlated with the molecular weight of the polymer. Higher molecular weights resulted in smaller cells and lower overall expansion due to the increase in polymer viscosity. The highest foaming ability was demonstrated for polypropylenes with a molecular weight of 231,000 (degree of foaming: 98%) and for LDPE with a similar molecular weight (degree of foaming: 65%). Melt tension was observed to be the governing factor which dictated the differences in foaming ability of the PP when compared to LDPE [78]. PP has a lower melt strength than PE hence lower degree of foaming was observed in PE systems, as an increase in melt tension restrains the bubble growth and results in smaller cells and a corresponding decrease in the foam expansion.

The effect of melt temperature on extrusion foaming was determined between 180-240°C for PP and LDPE. Foaming was observed to increase for both polyolefins with increasing melt temperature from 180-240°C due to a reduction in viscosity. Changes in blowing agent content (sodium bicarbonate/citric acid blend) in polypropylene systems resulted in a decrease in cell size as more gas was generated with greater nucleation rates. An addition of 5 wt% of these CBAs resulted in a degree of foaming of approximately 98%, while 2 wt% achieved 45%.

Stabilisation of the foam structure *via* cooling is also particularly important. In polypropylene systems, the degree of foaming observed was directly linked to the cooling temperature. Highest degrees of foaming were observed when the cooling temperature was lowered to 0-20°C in comparison to a melt temperature of 200°C. While a reduction in foaming degree was evident at higher cooling temperatures >30°C with the lowest foaming degree of 38% observed when the cooling temperature was only 65°C. This emphasizes the stabilising effect which higher cooling rates can have on foamed extrudates. Despite the greater solidification of the extrudate surface with lower temperature no change in cell size was observed.

Extrusion foaming has also been applied to amorphous PLA with azodicarbonamide (azo) as the blowing agent. A single screw extruder with an

L/D of 25 with five temperature zones of 138, 193, 232, 177, 149°C from feeder to die was used. Optimal CBA content for PLA was 0.8% which gave foam densities of 0.55 g/cm^3 compared to LDPE, which was 2% and a foam density of 0.45 g/cm^3. CBA content above and below this gave higher foam densities, which could be explained by phase separation occurring during extrusion resulting in lower amounts of gas within the polymer melt thereby decreasing expansion. A corresponding increase in rod diameter was observed with small quantities of CBA but degassing occurred at the die for blends with increased CBA content [79].

Extrusion foaming has also been used to produce starch based products for loose fill applications. Starch alone is high hydrophilic in nature which is detrimental to the physical and mechanical properties of the foam because it will readily absorb water in a humid environment. Therefore, starch is either modified before extrusion or blended with materials like polystyrene. The water which is incorporated with the starch typically acts as the blowing agent. For a 70% starch 30% polystyrene blend the optimum water content was 18% which gave a radial expansion ratio of 28-29 at processing temperatures of 140 and 160°C respectively, with large cells of up to 1 mm. Increasing water content further plasticised the material so its melt viscosity was too low to sustain foaming and the cell walls lacked the strength to contain the expanding bubbles [80]. Addition of talc, a nucleating agent and filler, reduced the radial expansion ratio and overall expansion ratio of these foams, but increased cell density from 24 cells/cm^2 to 342 cells/cm^2 at 3% talc to a blend with 20% moisture content (MC), narrowed cell size distribution, but increased bulk density from 14.6 to 17.7 kg/m^3 and made the foam more brittle. For foams containing talc, an optimal composition was found to be 18% MC, 1% talc and an extrusion temperature of 160°C [80].

THERMOPLASTIC PROTEIN EXTRUSION FOAMING

Previous reviews of foam extrusion of proteins have typically discussed the necessity of blending proteins with carbohydrates, flours or PLA, and there are very few examples of foamed unblended thermoplastic proteins [1, 76]. In this section four examples of protein foam extrusion will be discussed. These studies have all been conducted with the final product intended for packaging applications. The first is a true thermoplastic protein foam produced from soy protein, the second and third studies examine the foaming ability of blends of zein protein with pearl millet flour and soy protein concentrate - PLA blends. The final study investigated blends of Novatein® Thermoplastic Protein, a thermoplastic derived from bloodmeal with linear low density polyethylene.

Thermoplastic SPI was prepared by extruding SPI, water, glycerol and salts

($CaCl_2$, sodium tripolyphosphate (STP), and $ZnSO_4$) in a co-rotating twin screw extruder and granulated. This was foamed using a CBA in a single screw extruder equipped with a six inch flat sheet die at 150-160°C. The resulting foams had a density of 0.4-0.6 g/cm^3 (Fig. **5-B**). Blends which were heavily plasticised had a lower Young's modulus while those with lower levels of glycerol addition produced a rigid foam structure [73]. Using STP resulted in a more processable and consolidated thermoplastic material, possibly due to disruption of ionic bonding between or within protein chains, but a higher foam density (0.62 g/cm^3). Adding $CaCl_2$, or $ZnSO_4$ increased Young's modulus, possibly due to Ca^{2+} and Zn^{2+} ions crosslinking negatively charged groups on the proteins. Adding $CaCl_2$ gave lower densities (0.53 g/cm^3), higher tensile strength (3.56 MPa) and elongation at break (24.1%) compared to adding $ZnSO_4$ (0.58 g/cm^3, 3.03 MPa and 21.19% respectively). All foams showed similar elongational to break despite the increase in tensile modulus which was due to a similar degree of crosslinking.

Zein protein (70-75%) can be combined with pearl millet flour (25-30%), derived from cereal crops, to produce foams [74]. The composition of pearl millet flour can vary significantly depending upon growing conditions, however, the material typically contains 8.5-19.5% protein, and 63.1-78.5% starch. The foamed blends contained 4.6 g water, 20 g polyethylene glycol (PEG-400) and 3.0 g ammonium bicarbonate per 100 g of zein/flour. Foaming was conducted using a compact extruder with a 1.5-2.0 mm die, screw speeds between 20 and 150 rpm with a temperature profile from hopper to die of 65, 105, 95, 80°C. A foam expansion ratio of 2-3.2 was achieved with a decrease in moisture content from 12% to 6.5%. Zein formed a continuous matrix while the pearl millet remained as discrete particles (Fig. **5-C**). The average cell size was 5 μm although the cell distribution observed was broad and foam density ranged from 0.35-0.5 g/cm^3. The elastic modulus of these foams under compression was 25-50 MPa.

Another study investigated the ability of polylactic acid (PLA) and soy protein concentrate (SPC) to foam (Fig. **5-D**) through twin screw extrusion using poly(2-ethyl-2-oxazoline) as a compatibiliser [23]. The material was foamed in a secondary extrusion step following compounding with a CBA (4-methylbenzen--1-sulfonohydrazide with 5% $CaCO_3$ for nucleation) and co-compatibliser of polymeric methylene diphenyl diiscocynate (pMDI). PLA/SPC blends were prepared using a co-rotating twin screw extruder with a screw diameter of 18 mm and an L/D of 40 with a screw speed of 150 RPM. The temperature profile was 90, 120, 140, 150, 160, 160, 155°C from hopper to die. The blends also contained a compatibiliser (PEOX, 3 phr), and citroflex A-4 (6 parts per hundred parts resin) and glycolube WP2200 (2 phr) as a plasticiser. Extrusion foaming was conducted using a screw speed of 60 RPM, die size of 1 mm and with a variable die temperature of 115-160°C. Cell rupture was a problem during extrusion and

SP/PLA blends displayed severe degradation at higher processing temperatures.

Gas from the CBA lowered melt viscosity enabling lower extrusion temperatures to be used. Adding pMDI as an interfacial modifier promoted cross linking between the hydroxyl groups of PLA and the amine groups of SPC which resulted in a higher viscosity. Cell densities in foams without pMDI decreased with increasing foaming temperature but increased by 1.7-1.8 times when pMDI was added. For foams without pMDI, the cell density increased with increasing CBA content up to 0.5-2 phr, after which cell density decreased. With pMDI, cell density was higher overall, possibly due to a decrease in nucleation activation energy through a heterogenous nucleation mechanism, but decreased with increasing CBA content. CBA content and extrusion temperature affected the pressure drop by altering viscosity. The material without pDMI had its lowest bulk density (0.53 g/cm^3) when extruded through a die at 140°C while blends wih pMDI displayed the lowest bulk densities (0.77 g/cm^3) at 150°C with 2 phr CBA.

In other research, expansion ratios of 1.85 and less were observed for an extrusion foamed blend of a thermoplastic bloodmeal (Novatein®) and linear low density polyethylene (LLDPE) in the presence of polyethylene grafted maleic anhydride (Fig. **5-E**) as a compatibiliser (PE-g-MAH) [75]. Foaming was conducted by adding Novatein® granules to LLDPE and PE-g-MAH in the hopper of a twin screw extruder. Sodium bicarbonate was used as the blowing agent and the material subjected to an extrusion profile of 70,100,100,110,120°C feeder to die. The die size was 10 mm.

As the proportion of NTP was increased the foaming ability reduced until consolidation of the extrudate was lost. A blend of 50% NTP, 10% PE-g-MAH and 40% LLDPE without additional blowing agent resulted in a bulk density of 0.58 g/cm^3. The addition of compatibliser at 6, 8 and 10% had no effect on the foam expansion ratio. Increasing the die temperature from 120 to 140°C resulted in a decrease in radial expansion ratio from 1.37 to 1 and the extrudate surface appeared to be more degraded. Addition of sodium bicarbonate as a blowing agent resulted in a very fine cellular structure while the bulk density remained constant, and the final material was more flexible than foams without the blowing agent.

Foam extrusion cooking is an analogous technique to extrusion foaming and is highly relevant to extrusion foaming processes involving proteins in particular. Extrusion foam cooking is common for starch/carbohydrate based snack foods and whey or soy protein are commonly added to improve the nutritional value of the snack food [81, 82]. Examples of research using foam extrusion cooking are listed in Table **1**, and two examples are discussed below.

Table 1. Extrusion cooking of protein foams. Carb-carbohydrate SPC- soy protein concentrate, SWS- sweet whey solids, WPC- whey protein concentrate, WPI- whey protein isolate. TS- twin screw, SS- single screw. ER – expansion ratio, EI- expansion index.

Blend Properties								Extrusion Conditions		Foam Properties			
Protein	**Protein Purity (%)**	**Protein Added (wt. %)**	**Max Protein (%)**	**Carb**	**Protein in Carb Phase (%)**	**Carb Added (wt. %)**	**Total Protein (%)**	**Screw Type**	**Screw Speed**	**ER**	**EI**	**Radial ER**	**Ref**
Acid Casein	88.5	50	44.25	Potato Starch	0.02	50	44.35	SS	80	-		3.98-4.96	[83]
Casein Casinate	92	25	23	Corn Meal	9.0	75	29.75	TS	300	-	5.5	-	[84]
Cow Pea	27	100	27	Sorghum Meal	8.5	0	27	TS	200	2.0-5.4		-	[85]
Soy Bean Protein	51.5	50	25.75	Potato Starch	0.02	50	25.85	SS	100	-		1.93-2.70	[83]
SPC	71	50	35.5	Corn starch	-	-	35.5	TS	230-300	3.5-5.2		-	[86]
SPC	-	-	30	Corn Meal	-	-	-	TS	250	-		-	[87]
SPC	64.7	14.00	9.0	Corn Meal	6.5	64.15	13.16	TS	300	-		-	[88]
SPI	-	-	30	Corn Meal	-	-	-	TS	250	-		-	[87]
SPI/SPC	89.3/ 64.7	8.70/ 4.0	10.36	Corn Meal	6.5	66.25	14.66	TS	300	-		-	[88]
SWS	12.9	50	6.45	Potato Flour	8	50	10.45	TS	300		1.0-2.2	-	[89]
SWS	12.9	50	6.45	Rice Flour	5.7	50	9.3	TS	300		0.7-2.8	-	[89]
SWS	12.9	50	6.45	Corn	5.6	50	9.25	TS	300		0.6-2.3	-	[89]
WPC	58.3	25	14.58	Potato Starch	0.02	75	14.59	SS	80	-		3.05-3.45	[83]
WPC	80	-	40	Corn Starch	-	-	40	TS	200	4-26		-	[90]
WPC	80-86	30	25.80	Corn Starch	-	-	25.80	TS	140	-		5.43-10.9	[91]
WPC	34.9	50	17.45	Potato Flour	8	50	21.45	TS	300		1.2-2.2	-	[89]
WPC	34.9	50	17.45	Rice Flour	5.7	50	20.3	TS	300		0.8-2.8	-	[89]
WPC	34.9	50	17.45	Corn	5.6	50	20.25	TS	300		0.5-2.3	-	[89]
WPC	80	25	20	Corn meal	-	-	20	TS	300	-		-	[92]
WPC	78.7	25	19.68	Corn Meal	9.0	75	26.43	TS	300	-	5.2	-	[84]

(Table 1) contd.....

Blend Properties								Extrusion Conditions		Foam Properties			
Protein	**Protein Purity (%)**	**Protein Added (wt. %)**	**Max Protein (%)**	**Carb**	**Protein in Carb Phase (%)**	**Carb Added (wt. %)**	**Total Protein (%)**	**Screw Type**	**Screw Speed**	**ER**	**EI**	**Radial ER**	**Ref**
WPC	70.2	7.5	5.27	Pearl Millet Flour	10.50	92.50	14.98	TS	350	-	4.34	-	[82]
WPC	34	15	5.1	Corn starch	-	-	5.1	-	-	-		-	[93]
WPI	93.3	35	32.66	Corn Meal	7.2	65	37.34	TS	800	4.5-9		-	[94]
WPI	93.6	25	23.4	Corn Meal	9.0	75	30.15	TS	300	-	4.5	-	[84]
WPI	92	18	16.56	Corn starch	-	-	16.56	TS	300	-		-	[81]

Typical production conditions for expanded products for protein carbohydrate blends use a twin screw extruder operating around 300 RPM. Die sizes are typically limited to 3-3.2 mm in size and typical processing temperatures are between 70-150°C with lower feed zone temperatures of 30°C occurring in some systems (Table **1**). Moisture content, protein type, protein purity and the composition of the carbohydrate phase all affect the mechanical and physical properties of the resulting foams.

When foaming WPI and corn starch blends, an increase in the water content, which acts as a plasticiser and blowing agent, reduced the required specific mechanical energy from 315-359 kJ/kg at 23% moisture content to 274-314 kJ/kg for 27% moisture [81].

At the higher moisture content (27%) expansion ratio and radial expansion ratio was reduced as the melt no longer had the required melt strength to sustain the foamed structure. Increased water content in the blend was observed to reduce cell size from 1.06-2.94 mm at 23% MC to 1.00-2.05 mm at 27% MC. Foam hardness decreased with increasing whey protein up to 12% whey, due to the gelling properties of whey [81].

In another study, addition of soy protein concentrate to starch with high amylose content increased foam mechanical strength. Crushing force measured by a texture analyser increased from 10 N at 0% SPC to 42 N at 20% SPC. Increasing SPC further resulted in a lower crush strength than the control foam, probably due to protein agglomeration due to heat and shear, as well as reducing water available to starch to gelatinise during extrusion [86].

CONCLUSION

Protein based foams present a new and exciting area for research. They provide a means to reduce dependence on fossil fuels, and decrease the environmental impact of non-biodegradable foams. Proteins can be sourced from a wide variety of plant or animal products or wastes, reducing the impact on food supply.

Foaming is a trade-off between manipulating polymer properties for increasing gas solubility to reduce foam density and increase cell nucleation, diffusivity which needs to be high initially for nucleation and low later on to reduce bubble coalescence and prevent gas loss while the polymer is cooling. Solubility will depend on polymer properties such as crystallinity and gas type and gas pressure, while diffusivity is dependent on polymer viscosity which is dependent on crystallinity, polymer type and chain branching, and melt temperature. Bubble formation is also dependent on melt strength, *i.e.* the ability of the material to contain the bubble, which is dependent on the same properties as for polymer viscosity.

The main challenges to be overcome with protein based foams are:

1. Controlling protein-protein interactions so that they can extruded or batch foamed at temperatures lower than the protein degradation temperature using combination of denaturants, reducing agents and plasticisers to reduce hydrophobic interactions, hydrogen bonding, and cysteine-cysteine bonds, as well as increasing free volume between chains to increase chain mobility. Protein-protein interactions are dictated by the amino-acid sequence of the proteins, the secondary structures that they form, and environment they are in, so a potential area of future research is manipulating protein amino acid sequence to produce plastics with desired properties.
2. Dried denatured proteins are rich in β-sheets, and will form more β-sheets when exposed to heat, which results in a highly crystalline, brittle material with low melt strength and extremely high extensional viscosity which is detrimental to producing foams. Furthermore, protein based thermoplastics need mechanical shear as well as heat to form a melt, which provides a challenge for batch foaming, while for extrusion foaming, mechanical shear is provided by the extruder. Proteins such as zein with a high α-helical content have been successfully used to produce foams and films.
3. Proteins have poor gas solubility and high gas diffusion properties, which results in low foam cell densities and high bulk densities compared to conventional foams. A combination of CO_2 and N_2 gas as a blowing agent has been successfully used for zein and gelatin in batch foams, while water or chemical blowing agents serve for extruded zein, soy and bloodmeal protein

foams. Blending proteins with starch or other polymeric materials such as PLA is another way of improving gas solubility and diffusion properties.

The main proteins to be successfully foamed are zein, gelatin, soy and bloodmeal. Whey has been used as an additive in food foams where the main material is starch. As research progresses and new proteins tried, we expect to see more successful protein based foams in the future.

NOTES

[1] Reproduced from J.A.Kiernan 'Formaldehyde, formalin, paraformaldehyde and glutaraldehyde: What they are and what they do', Microscopy Today, v.1: 8-12, Fig. **2**, 2000, copyright Cambridge University Press, with permission.

[2] **A.** Reprinted from The Journal of Supercritical Fluids, 58/1, Y.-M Corre, A. Maazouz, J. Duchet, and J. Reignier, "Batch foaming of chain extended PLA with supercritical CO_2: Influence of the rheological properties and the process parameters on the cellular structure,", Page No. 177-188, Copyright (2011), with permission from Elsevier. **B.** Reproduced with permission from the journal International Polymer Processing, IPP, Vol.22, 2007, pp 480-488, by A. Salerno, M. Oliviero, E. Di Maio and S. Iannace, © Carl Hanser Verlag GmbH & Co.KG, Muenchen. **C.** Reproduced with permission M. Oliviero, L. Verdolotti, I. Nedi, F. Docimo, E. Di Maio, and S. Iannace, "Effect of two kinds of lignins, alkaline lignin and sodium lignosulfonate, on the foamability of thermoplastic zein–based bionanocomposites", 48 (6), pp. 516-525, copyright © 2012 by the authors. Reprinted by permission of SAGE Publications, Ltd. **D.** Reproduced with permission, from B. Liu, L. Jian, and J. Zhang, "Extrusion foaming of Poly (lactic acid)/Soy protein concentrate blends", Macromolecular Materials and Engineering, Wiley. Copyright ©2011 WILEY-VCH Verlag GmbH & Co. KGaA, Weinheim. **E.** Reproduced from A. Walallavita, C. J. R. Verbeek, and M. C. Lay, "Blending Novatein Thermoplastic Protein with PLA for carbon dioxide assisted batch foaming," In: Proceedings of PPS-31: The 31st International Conference of the Polymer Processing Society–Conference Papers, Jeju Island, South Korea, 2015., with the permission of AIP Publishing (http://dx.doi.org/10.1063/1.4942311)

[3] **B.** Image reproduced with permission from the authors: P. Mungara, J. W. Zhang, and J. Jane. **C.** Image reproduced from "Development and characterization of extruded biodegradable foams based on zein and pearl millet flour" with permission from the authors. **D.** Reproduced with permission from Wiley, from M. Olivero, L. Sorrentino, L. Cafiero, B. Galzerano, A. Sorrentino, and S.

Iannace, “Foaming behaviour of bio based blends based on thermoplastic gelatin and poly(butylene succinate)”, Journal of Applied Polymer Science, Wiley. © Wiley periodicals, Inc. J. Appl. Polym. Sci. 2015, 132, 42704. **E.** Reproduced from C. Gavin, M. C. Lay, and C. J. R. Verbeek, “Extrusion foaming of protein-based thermoplastic and polyethylene blends,” In: Proceedings of PPS-31: The 31st International Conference of the Polymer Processing Society–Conference Papers, Jeju Island, South Korea, 2015., with the permission of AIP Publishing (http://dx.doi.org/10.1063/1.4942308)

CONFLICT OF INTEREST

The author (editor) declares no conflict of interest, financial or otherwise.

ACKNOWLEDGEMENTS

Declared none.

REFERENCES

[1] G. Mensitieri, E. Di Maio, G.G. Buonocore, I. Nedi, M. Oliviero, L. Sansone, and S. Iannace, "Processing and shelf life issues of selected food packaging materials and structures from renewable resources", *Trends Food Sci. Technol.,* vol. 22, no. 2–3, pp. 72-80, March 2011. [http://dx.doi.org/10.1016/j.tifs.2010.10.001]

[2] Smithers Rapra, *Polymer Foams Market Expected to Consume 25.3 Million Tonnes by 2019,* 2014. Available at: http://www.smithersrapra.com/news/ 2014/may/polymer-foam-market-to-consume-25-3-million-tonnes Accessed: 2nd Aug. 2015

[3] Freedonia Group Inc, *US Natural Polymer Demand (2002-2012),* 2008. Available at: http://www.plasticsnews.com/article/20081208/FYI/312089989/us-natural-polymer-demand-2002-12 Accessed: 2nd Aug. 2015

[4] MarketsandMarkets.com, *Bioplastics & Biopolymers Market by Type (Bio PET, Bio PE, PLA, PHA, Bio PBS, Starch Blends, and Regenerated Cellulose), by Application (Packaging, Bottles, Fibers, Agriculture, Automotive, and Others) & by Geography – Trends & Forecasts to 2018,* 2014. Available at: http://www.marketsandmarkets.com/Market-Reports/biopolymers-bioplastics-market-88795240.html Accessed: 2nd Aug. 2015

[5] *The Biopolymers Market is Expected to Generate Global Revenue of 3.67 Billion US Dollars By 2018,* 2014. Available at: http://milksci.unizar.es/bioquimica/temas/azucares/disacaridos.html

[6] C. Marrazzo, E. Di Maio, and S. Iannace, "Foaming of synthetic and natural biodegradable polymers", *J. Cell. Plast.,* vol. 43, no. 2, pp. 123-133, 2007. [http://dx.doi.org/10.1177/0021955X06073214]

[7] S.T. Lee, C.B. Park, and N.S. Ramesh, "Introduction to polymeric foams", In: *Polymeric Foams: Science and Technology. ,* S.T. Lee, C.B. Park, N.S. Ramesh, Eds., 1st ed CRC Press: Boca Raton, FL, 2007.

[8] S.T. Lee, "History and trends of polymeric foams: From process/product to performance/regulation", In: *Polymeric Foams: Technology and Developments in Regulation, Process and Products. ,* S.T. Lee, D. Scholz, Eds., 1st ed CRC Press: Boca Raton, FL, 2009, pp. 1-40.

[9] S. Park, D. Bae, and K. Rhee, "Soy protein biopolymers cross-linked with glutaraldehyde," ", *J. Am. Oil Chem. Soc.,* vol. 77, no. 8, pp. 879-884, 2000. [http://dx.doi.org/10.1007/s11746-000-0140-3]

[10] J.M. Raquez, M. Deléglise, M.F. Lacrampe, and P. Krawczak, "Thermosetting (bio)materials derived from renewable resources: A critical review", *Prog. Polym. Sci.,* vol. 35, no. 4, pp. 487-509, 2010. [http://dx.doi.org/10.1016/j.progpolymsci.2010.01.001]

[11] J.A. Kiernan, "Formaldehyde, formalin, paraformaldehyde and glutaraldehyde: what they are and what they do", *Micros. Today,* vol. 1, no. 5, pp. 8-12, 2000.

[12] C.J. Verbeek, and L.E. van den Berg, "Extrusion processing and properties of protein-based thermoplastics", *Macromol. Mater. Eng.,* vol. 295, no. 1, pp. 10-21, 2010. [http://dx.doi.org/10.1002/mame.200900167]

[13] C.J. Verbeek, and J.M. Bier, "Synthesis and characterization of thermoplastic agro-polymers", In: *A Handbook of Applied Biopolymer Technology: Synthesis, Degradation and Applications.* , S.K. Sharma, A. Mudhoo, Eds., 1st ed Royal Society of Chemistry, 2011. [http://dx.doi.org/10.1039/9781849733458-00197]

[14] J.M. Bier, *"The Eco-Profile of Thermoplastic Protein Derived from Bloodmeal"*, Masters Thesis, University of Waikato, New Zealand, 2010.

[15] J.M. Bier, C.J. Verbeek, and M.C. Lay, "Thermal transitions and structural relaxations in protein-based thermoplastics", *Macromol. Mater. Eng.,* vol. 299, no. 5, pp. 524-539, 2014. [http://dx.doi.org/10.1002/mame.201300248]

[16] J.M. Bier, C.J. Verbeek, and M.C. Lay, "Thermal and mechanical properties of bloodmeal-based thermoplastics plasticized with tri(ethylene glycol)", *Macromol. Mater. Eng.,* vol. 299, no. 1, pp. 85-95, 2013. [http://dx.doi.org/10.1002/mame.201200460]

[17] J.M. Bier, C.J. Verbeek, and M.C. Lay, "Using synchrotron FTIR spectroscopy to determine secondary structure changes and distribution in thermoplastic protein", *J. Appl. Polym. Sci.,* vol. 130, no. 1, pp. 359-369, 2013. [http://dx.doi.org/10.1002/app.39134]

[18] J.M. Bier, C.J. Verbeek, and M.C. Lay, "Thermally resolved synchrotron FT-IR microscopy of structural changes in bloodmeal-based thermoplastics", *J. Therm. Anal. Calorim.,* vol. 115, no. 1, pp. 433-441, 2014. [http://dx.doi.org/10.1007/s10973-013-3340-8]

[19] M. Oliviero, L. Sorrentino, L. Cafiero, B. Galzerano, A. Sorrentino, and S. Iannace, "Foaming behavior of biobased blends based on thermoplastic gelatin and poly(butylene succinate)", *J. Appl. Polym. Sci.,* vol. 132, no. 48, pp. 1-9, 2015. [http://dx.doi.org/10.1002/app.42704] [PMID: 25866416]

[20] A. Salerno, M. Oliviero, E. Di Maio, and S. Iannace, "Thermoplastic foams from zein and gelatin", *Int. Polym. Process.,* vol. 22, no. 5, pp. 480-488, 2007. [http://dx.doi.org/10.3139/217.2065]

[21] J.R. Barone, W.F. Schmidt, and N. Gregoire, "Extrusion of feather keratin", *J. Appl. Polym. Sci.,* vol. 100, no. 2, pp. 1432-1442, 2006. [http://dx.doi.org/10.1002/app.23501]

[22] J.R. Barone, W.F. Schmidt, and C.F. Liebner, "Thermally processed keratin films", *J. Appl. Polym. Sci.,* vol. 97, no. 4, pp. 1644-1651, 2005. [http://dx.doi.org/10.1002/app.21901]

[23] B. Liu, L. Jiang, and J. Zhang, "Extrusion foaming of poly (lactic acid)/soy protein concentrate blends", *Macromol. Mater. Eng.,* vol. 296, no. 9, pp. 835-842, 2011. [http://dx.doi.org/10.1002/mame.201000449]

[24] P. Guerrero, and K. de la Caba, "Thermal and mechanical properties of soy protein films processed at different pH by compression", *J. Food Eng.,* vol. 100, no. 2, pp. 261-269, 2010. [http://dx.doi.org/10.1016/j.jfoodeng.2010.04.008]

[25] J.L. Jane, and S. Wang, Soy protein-based thermoplastic composition for preparing molded articles, 1996.U.S. Patent 5523293

[26] J. Zhang, P. Mungara, and J. Jane, "Mechanical and thermal properties of extruded soy protein sheets", *Polymer (Guildf.),* vol. 42, no. 6, pp. 2569-2578, 2001.
[http://dx.doi.org/10.1016/S0032-3861(00)00624-8]

[27] E. Di Maio, R. Mali, and S. Iannace, "Investigation of thermoplasticity of zein and kafirin proteins: Mixing process and mechanical properties", *J. Polym. Environ.,* vol. 18, no. 4, pp. 626-633, 2010.
[http://dx.doi.org/10.1007/s10924-010-0224-x]

[28] D.J. Sessa, G.W. Selling, J.L. Willett, and D.E. Palmquist, "Viscosity control of zein processing with sodium dodecyl sulfate", *Ind. Crops Prod.,* vol. 23, no. 1, pp. 15-22, 2006.
[http://dx.doi.org/10.1016/j.indcrop.2005.02.001]

[29] L. Verdolotti, M. Oliviero, M. Lavorgna, V. Iozzino, D. Larobina, and S. Iannace, "Bio-hybrid foams by silsesquioxanes cross-linked thermoplastic zein films", *J. Cell. Plast.,* vol. 51, no. 1, pp. 75-87, 2015.
[http://dx.doi.org/10.1177/0021955X14529138]

[30] G. Trujillo-de Santiago, C. Rojas-de Gante, S. García-Lara, L. Verdolotti, E. Di Maio, and S. Iannace, "Thermoplastic processing of blue maize and white sorghum flours to produce bioplastics", *J. Polym. Environ.,* vol. 23, no. 1, pp. 72-82, 2015.
[http://dx.doi.org/10.1007/s10924-014-0708-1]

[31] S.H. Richert, "Physical-chemical properties of whey protein foams", *J. Agric. Food Chem.,* vol. 27, no. 4, pp. 665-668, 1979.
[http://dx.doi.org/10.1021/jf60224a036]

[32] K.G. Marinova, E.S. Basheva, B. Nenova, M. Temelska, A.Y. Mirarefi, B. Campbell, and I.B. Ivanov, "Physico-chemical factors controlling the foamability and foam stability of milk proteins: Sodium caseinate and whey protein concentrates", *Food Hydrocoll.,* vol. 23, no. 7, pp. 1864-1876, 2009.
[http://dx.doi.org/10.1016/j.foodhyd.2009.03.003]

[33] D. Gammariello, J. Laverse, V. Lampignano, A.L. Incoronato, and M.A. Del Nobile, "Effect of compositional formulation on texture and microstructural of whey protein foam", *Food Res. Int.,* vol. 53, no. 1, pp. 496-501, 2013.
[http://dx.doi.org/10.1016/j.foodres.2013.05.023]

[34] J. Leman, T. Dołgań, M. Smoczyński, and Z. Dziuba, "Fractal characteristics of microstructure of beta-lactoglobulin preparations and their emulsifying properties", *Food Sci. Technol. (Campinas.),* vol. 8, no. 3, p. 29, 2005.

[35] H-B. Chen, Y-Z. Wang, and D.A. Schiraldi, "Foam-like materials based on whey protein isolate", *Eur. Polym. J.,* vol. 49, no. 10, pp. 3387-3391, 2013.
[http://dx.doi.org/10.1016/j.eurpolymj.2013.07.019]

[36] N. Kaisangsri, O. Kerdchoechuen, and N. Laohakunjit, "Characterization of cassava starch based foam blended with plant proteins, kraft fiber, and palm oil", *Carbohydr. Polym.,* vol. 110, no. 1, pp. 70-77, 2014.
[http://dx.doi.org/10.1016/j.carbpol.2014.03.067] [PMID: 24906730]

[37] P.R. Salgado, V.C. Schmidt, S.E. Ortiz, A.N. Mauri, and J.B. Laurindo, "Biodegradable foams based on cassava starch, sunflower proteins and cellulose fibers obtained by a baking process", *J. Food Eng.,* vol. 85, no. 3, pp. 435-443, 2008.
[http://dx.doi.org/10.1016/j.jfoodeng.2007.08.005]

[38] X. Li, A. Pizzi, M. Cangemi, P. Navarrete, C. Segovia, V. Fierro, and A. Celzard, "Insulation rigid and elastic foams based on albumin", *Ind. Crops Prod.,* vol. 37, no. 1, pp. 149-154, 2012.
[http://dx.doi.org/10.1016/j.indcrop.2011.11.030]

[39] X. Li, A. Pizzi, M. Cangemi, V. Fierro, and A. Celzard, "Flexible natural tannin-based and protein-

based biosourced foams", *Ind. Crops Prod.,* vol. 37, no. 1, pp. 389-393, 2012.
[http://dx.doi.org/10.1016/j.indcrop.2011.12.037]

[40] Y. Lin, and F. Hsieh, "Water-blown flexible polyurethane foam extended with biomass materials", *J. Appl. Polym. Sci.,* vol. 65, no. 4, pp. 695-703, 1997.
[http://dx.doi.org/10.1002/(SICI)1097-4628(19970725)65:4<695::AID-APP8>3.0.CO;2-F]

[41] S.K. Park, and N. Hettiarachchy, "Physical and mechanical properties of soy protein-based plastic foams", *J. Am. Oil Chem. Soc.,* vol. 76, no. 10, pp. 1201-1205, 1999.
[http://dx.doi.org/10.1007/s11746-999-0094-3]

[42] L.C. Chang, Y. Xue, and F.H. Hsieh, "Comparative study of physical properties of water-blown rigid polyurethane foams extended with commercial soy flours", *J. Appl. Polym. Sci.,* vol. 80, no. 1, pp. 10-19, 2001.
[http://dx.doi.org/10.1002/1097-4628(20010404)80:1<10::AID-APP1068>3.0.CO;2-Y]

[43] Y. Mu, X. Wan, Z. Han, Y. Peng, and S. Zhong, "Rigid polyurethane foams based on activated soybean meal", *J. Appl. Polym. Sci.,* vol. 124, no. 5, pp. 4331-4338, 2012.
[http://dx.doi.org/10.1002/app.35612]

[44] S. Kumar, E. Hablot, J.L. Moscoso, W. Obeid, P.G. Hatcher, B.M. DuQuette, D. Graiver, R. Narayan, and V. Balan, "Polyurethanes preparation using proteins obtained from microalgae," ", *J. Mater. Sci.,* vol. 49, no. 22, pp. 7824-7833, 2014.
[http://dx.doi.org/10.1007/s10853-014-8493-8]

[45] Y-Q. Zhang, "Applications of natural silk protein sericin in biomaterials", *Biotechnol. Adv.,* vol. 20, no. 2, pp. 91-100, 2002.
[http://dx.doi.org/10.1016/S0734-9750(02)00003-4] [PMID: 14538058]

[46] R. Elshereef, J. Vlachopoulos, and A. Elkamel, "Comparison and analysis of bubble growth and foam formation models", *Eng. Comput.,* vol. 27, no. 3, pp. 387-408, 2010.
[http://dx.doi.org/10.1108/02644401011029943]

[47] N.S. Ramesh, "Fundamentals of bubble nucleation and growth in polymers", In: *Polymeric Materials: Mechanisms and Materials. ,* S.T. Lee, N.S. Ramesh, Eds., 1st ed CRC Press Boca Raton: FL, 2004.
[http://dx.doi.org/10.1201/9780203506141.ch3]

[48] J. Wang, *"Rheology of Foaming Polymers and its influence on Microcellular Processing"*, PhD Thesis, University of Toronto, Canada, 2009.

[49] V. Kumar, *"Process Synthesis for Manufacturing Microcellular Thermoplastic Parts: A Case Study in Axiomatic Design"*, PhD Thesis, Massachusetts Institute of Technology, US, 1988.

[50] D.R. Uhlmann, and B. Chalmers, "The energetic of nucleation", *Ind. Eng. Chem. Res.,* vol. 57, no. 9, pp. 19-31, 1965.
[http://dx.doi.org/10.1021/ie50669a006]

[51] S.T. Lee, C.B. Park, and N.S. Ramesh, "Foaming fundamentals", In: *Polymeric Foams: Science and Technology.* 1st ed CRC Press: Boca Raton, FL, 2007.

[52] N.G. McCrum, C. Buckley, and C.B. Bucknall, *Principles of Polymer Engineering.* Oxford University Press, 1997.

[53] M. Oliviero, E. Di Maio, and S. Iannace, "Effect of molecular structure on film blowing ability of thermoplastic zein," ", *J. Appl. Polym. Sci.,* vol. 115, no. 1, pp. 277-287, 2010.
[http://dx.doi.org/10.1002/app.31116]

[54] A.V. Nawaby, and Z. Zhang, "Solubility and diffusivity", In: *Thermoplastic Foam Processing: Principles and Development. ,* S.T. Lee, Ed., 1st ed CRC Press: Boca Raton, 2004.

[55] C. Gao, J. Taylor, N. Wellner, Y.B. Byaruhanga, M.L. Parker, E.N. Mills, and P.S. Belton, "Effect of preparation conditions on protein secondary structure and biofilm formation of kafirin", *J. Agric. Food Chem.,* vol. 53, no. 2, pp. 306-312, 2005.

[http://dx.doi.org/10.1021/jf0492666] [PMID: 15656666]

[56] R. Liao, W. Yu, and C. Zhou, "Rheological control in foaming polymeric materials: I. Amorphous polymers", *Polymer (Guildf.),* vol. 51, no. 2, pp. 568-580, 2010. [http://dx.doi.org/10.1016/j.polymer.2009.11.063]

[57] R. Gendron, "Rheological behavior relevant to extrusion foaming", In: *Thermoplastic Foam Processing: Principles and Development.* , S.T. Lee, Ed., 1st ed CRC Press: Boca Raton, 2005.

[58] G. Nam, J. Yoo, and J. Lee, "Effect of long-chain branches of polypropylene on rheological properties and foam-extrusion performances", *J. Appl. Polym. Sci.,* vol. 96, no. 5, pp. 1793-1800, 2005. [http://dx.doi.org/10.1002/app.21619]

[59] H. Münstedt, and F.R. Schwarzl, *Deformation and Flow of Polymeric Materials.* Springer: Berlin, 2014. [Germany]

[60] D.F. Baldwin, C.B. Park, and N.P. Suh, "A microcellular processing study of poly(ethylene terephthalate) in the amorphous and semicrystalline states. Part I: Microcellular nucleation", *Polym. Eng. Sci.,* vol. 36, no. 11, pp. 1437-1445, 1996. [http://dx.doi.org/10.1002/pen.10538]

[61] J-B. Bao, T. Liu, L. Zhao, and G-H. Hu, "A two-step depressurization batch process for the formation of bi-modal cell structure polystyrene foams using $scCO_2$", *J. Supercrit. Fluids,* vol. 55, no. 3, pp. 1104-1114, 2011. [http://dx.doi.org/10.1016/j.supflu.2010.09.032]

[62] Y-M. Corre, A. Maazouz, J. Duchet, and J. Reignier, "Batch foaming of chain extended PLA with supercritical CO_2: Influence of the rheological properties and the process parameters on the cellular structure", *J. Supercrit. Fluids,* vol. 58, no. 1, pp. 177-188, 2011. [http://dx.doi.org/10.1016/j.supflu.2011.03.006]

[63] M. Oliviero, L. Verdolotti, I. Nedi, F. Docimo, E. Di Maio, and S. Iannace, "Effect of two kinds of lignins, alkaline lignin and sodium lignosulfonate, on the foamability of thermoplastic zein-based bionanocomposites", *J. Cell Plast.,* vol. 48, no. 6, pp. 516-525, 2012. [http://dx.doi.org/10.1177/0021955X12460043]

[64] A. Walallavita, C.J. Verbeek, and M.C. Lay, "Blending novatein thermoplastic protein with pla for carbon dioxide assisted batch foaming", *Proceedings of PPS-31: The 31st International Conference of the Polymer Processing Society–Conference Papers,* 2015 Jeju Island, South Korea

[65] S. Doroudiani, C.B. Park, and M.T. Kortschot, "Effect of the crystallinity and morphology on the microcellular foam structure of semicrystalline polymers", *Polym. Eng. Sci.,* vol. 36, no. 21, pp. 2645-2662, 1996. [http://dx.doi.org/10.1002/pen.10664]

[66] S.H. Mahmood, M. Keshtkar, and C.B. Park, "Determination of carbon dioxide solubility in polylactide acid with accurate PVT properties", *J. Chem. Thermodyn.,* vol. 70, pp. 13-23, 2014. [http://dx.doi.org/10.1016/j.jct.2013.10.019]

[67] E. Aionicesei, M. Škerget, and Ž. Knez, "Measurement of CO_2 solubility and diffusivity in poly(l-lactide) and poly(d,l-lactide-co-glycolide) by magnetic suspension balance", *J. Supercrit. Fluids,* vol. 47, no. 2, pp. 296-301, 2008. [http://dx.doi.org/10.1016/j.supflu.2008.07.011]

[68] Y-K. Kwon, and H-K. Bae, "Production of microcellular foam plastics by supercritical carbon dioxide", *Korean J. Chem. Eng.,* vol. 24, no. 1, pp. 127-132, 2007. [http://dx.doi.org/10.1007/s11814-007-5022-3]

[69] C. Yu, Y. Wang, B. Wu, and W. Li, "A direct method for evaluating polymer foamability", *Polym. Test.,* vol. 30, pp. 118-123, 2011. [http://dx.doi.org/10.1016/j.polymertesting.2010.11.001]

[70] R. Liao, W. Yu, and C. Zhou, "Rheological control in foaming polymeric materials: II. Semi-

crystalline polymers", *Polymer (Guildf.),* vol. 51, pp. 6334-6345, 2010. [http://dx.doi.org/10.1016/j.polymer.2010.11.001]

[71] D. Scholz, "Development of endothermic chemical foaming/nucleation agents and it processes", In: *Polymeric Foams: Technology and Developments in Regulation, Process, and Products.* , S.T. Lee, D. Scholz, Eds., 1st ed CRC Press USA, 2009, pp. 42-65.

[72] W. Ernst, J.r. Oblotzki, and H. Potente, "Description of the foaming process during the extrusion of foams based on renewable resources", *J. Cell. Plast.,* vol. 42, no. 3, pp. 241-253, 2006. [http://dx.doi.org/10.1177/0021955X06063513]

[73] P. Mungara, J.W. Zhang, and J. Jane, "Extrusion processing of soy protein-based foam", *Polymer Prepr.,* vol. 39, no. 2, pp. 148-149, 1998.

[74] M. Filli, M. Sjoqvist, C. Ohgren, M. Stading, and M. Rigdahl, "Development and characterization of extruded biodegradable foams based on zein and pearl millet flour", *Annu. Trans. NRS,* vol. 19, 2011.

[75] C. Gavin, M.C. Lay, and C.J. Verbeek, "Extrusion foaming of protein-based thermoplastic and polyethylene blends", *Proceedings of PPS-31: The 31st International Conference of the Polymer Processing Society–Conference Papers,* 2015 Jeju Island, South Korea

[76] S.T. Lee, and C.B. Park, *Foam Extrusion: Principles and Practice.* 2nd ed Taylor & Francis: Boca Raton, 2014. [http://dx.doi.org/10.1201/b16784]

[77] S.T. Lee, C.B. Park, and N.S. Ramesh, "General foam process technologies", In: *Polymeric Foams: Science and Technology.* , S.T. Lee, C.B. Park, N.S. Ramesh, Eds., 1st ed CRC Press: Boca Raton, FL, 2007.

[78] C.H. Lee, K-J. Lee, H.G. Jeong, and S.W. Kim, "Growth of gas bubbles in the foam extrusion process", *Adv. Polym. Technol.,* vol. 19, no. 2, pp. 97-112, 2000. [http://dx.doi.org/10.1002/(SICI)1098-2329(200022)19:2<97::AID-ADV3>3.0.CO;2-B]

[79] S. Lee, L. Kareko, and J. Jun, "Study of thermoplastic PLA foam extrusion", *J. Cell. Plast.,* vol. 44, no. 4, pp. 293-305, 2008. [http://dx.doi.org/10.1177/0021955X08088859]

[80] H.A. Pushpadass, G.S. Babu, R.W. Weber, and M.A. Hanna, "Extrusion of starch-based loose-fill packaging foams: effects of temperature, moisture and talc on physical properties", *Packag. Technol. Sci.,* vol. 21, no. 3, pp. 171-183, 2008. [http://dx.doi.org/10.1002/pts.809]

[81] E. Cheng, S. Alavi, T. Pearson, and R. Agbisit, "Mechanical–acoustic and sensory evaluations of cornstarch–whey protein isolate extrudates", *J. Texture Stud.,* vol. 38, no. 4, pp. 473-498, 2007. [http://dx.doi.org/10.1111/j.1745-4603.2007.00109.x]

[82] D.N. Yadav, T. Anand, Navnidhi, and A.K. Singh, "Co-extrusion of pearl millet-whey protein concentrate for expanded snacks", *Int. J. Food Sci. Technol.,* vol. 49, no. 3, pp. 840-846, 2014. [http://dx.doi.org/10.1111/ijfs.12373]

[83] M. Włodarczyk-Stasiak, and J. Jamroz, "Analysis of sorption properties of starch–protein extrudates with the use of water vapour", *J. Food Eng.,* vol. 85, no. 4, pp. 580-589, 2008. [http://dx.doi.org/10.1016/j.jfoodeng.2007.08.019]

[84] C. Onwulata, R. Konstance, P. Smith, and V. Holsinger, "Co-extrusion of dietary fiber and milk proteins in expanded corn products", *LWT-Food Sci. Technol. (Campinas.),* vol. 34, no. 7, pp. 424-429, 2001.

[85] L.A. Pelembe, C. Erasmus, and J.R. Taylor, "Development of a protein-rich composite sorghum–cowpea instant porridge by extrusion cooking process", *LWT - Food Sci. Technol. (Campinas.),* vol. 35, no. 2, pp. 120-127, 2002.

[86] L-J. Zhu, R. Shukri, N.J. de Mesa-Stonestreet, S. Alavi, H. Dogan, and Y-C. Shi, "Mechanical and

microstructural properties of soy protein–high amylose corn starch extrudates in relation to physiochemical changes of starch during extrusion", *J. Food Eng.,* vol. 100, no. 2, pp. 232-238, 2010. [http://dx.doi.org/10.1016/j.jfoodeng.2010.04.004]

[87] J. Faller, B. Klein, and J. Faller, "Acceptability of extruded corn snacks as affected by inclusion of soy protein", *J. Food Sci.,* vol. 64, no. 1, pp. 185-188, 1999. [http://dx.doi.org/10.1111/j.1365-2621.1999.tb09888.x]

[88] R.P. Konstance, C.I. Onwulata, P.W. Smith, D. Lu, M.H. Tunick, E.D. Strange, and V.H. Holsinger, "Nutrient-based corn and soy products by twin-screw extrusion", *J. Food Sci.,* vol. 63, no. 5, pp. 864-868, 1998. [http://dx.doi.org/10.1111/j.1365-2621.1998.tb17915.x]

[89] C.I. Onwulata, P.W. Smith, R.P. Konstance, and V.H. Holsinger, "Incorporation of whey products in extruded corn, potato or rice snacks", *Food Res. Int.,* vol. 34, no. 8, pp. 679-687, 2001. [http://dx.doi.org/10.1016/S0963-9969(01)00088-6]

[90] K.E. Allen, C.E. Carpenter, and M.K. Walsh, "Influence of protein level and starch type on an extrusion-expanded whey product", *Int. J. Food Sci. Technol.,* vol. 42, no. 8, pp. 953-960, 2007. [http://dx.doi.org/10.1111/j.1365-2621.2006.01316.x]

[91] F.P. Matthey, and M.A. Hanna, "Physical and functional properties of twin-screw extruded whey protein concentrate–corn starch blends", *LWT - Food Sci. Technol. (Campinas.),* vol. 30, no. 4, pp. 359-366, 1997.

[92] C.I. Onwulata, and R.P. Konstance, "Extruded corn meal and whey protein concentrate: Effect of particle size", *J. Food Process. Preserv.,* vol. 30, no. 4, pp. 475-487, 2006. [http://dx.doi.org/10.1111/j.1745-4549.2005.00082.x]

[93] A.M. Trater, S. Alavi, and S.S. Rizvi, "Use of non-invasive X-ray microtomography for characterizing microstructure of extruded biopolymer foams", *Food Res. Int.,* vol. 38, no. 6, pp. 709-719, 2005. [http://dx.doi.org/10.1016/j.foodres.2005.01.006]

[94] C.I. Onwulata, R.P. Konstance, J.G. Phillips, and P.M. Tomasula, "Temperature profiling: Solution to problems of co-extrusion with whey proteins", *J. Food Process. Preserv.,* vol. 27, no. 5, pp. 337-350, 2003. [http://dx.doi.org/10.1111/j.1745-4549.2003.tb00521.x]

3

Scoping Work

Conference papers

By

C. Gavin, M.C. Lay and C.J.R Verbeek

Published by

American Institute of Physics (AIP) Conference Proceedings

Extrusion foaming of protein-based thermoplastic and polyethylene blends

Overview:

To improve the melt strength and to lower the viscosity Novatein was blended with linear low density polyethylene (LLDPE) and compatibilised with polyethylene grafted Maleic Anhydride (PE-g-MaH) and extrusion foamed. In this study sodium bicarbonate was evaluated as a possible blowing agent and the effect of extrusion temperature was evaluated. Expansion was poor due to gas escaping through the extruder feed hoper.

This presents some of the early scoping work which was conducted during the development of a foaming method (Objective 1).

Contribution:

As first author for this publication the PhD candidate conducted all experimental work, data analysis and prepared the first draft of this manuscript. Under guidance from the supervisors the manuscript was revised and edited.

Permission:

Extrusion Foaming of Protein-Based Thermoplastic and Polyethylene Blends

Chanelle Gavin[a], Mark C. Lay[a*] and Casparus J.R. Verbeek[a]

[a]*University of Waikato, Knighton Road, Hamilton, New Zealand*

chanellegavin@gmail.com, mclay@waikato.ac.nz, jverbeek@waikato.ac.nz

Abstract. Currently the extrusion foamability of Novatein® Thermoplastic Protein (NTP) is being investigated at the University of Waikato in collaboration with the Biopolymer Network Ltd (NZ). NTP has been developed from bloodmeal (>86 wt% protein), a co-product of the meat industry, by adding denaturants and plasticisers (tri-ethylene glycol and water) allowing it to be extruded and injection moulded. NTP alone does not readily foam when sodium bicarbonate is used as a chemical blowing agent as its extensional viscosity is too high.

The thermoplastic properties of NTP were modified by blending it with different weight fractions of linear low density polyethylene (LLDPE) and polyethylene grafted maleic anhydride (PE-g-MAH) compatibiliser. Extrusion foaming was conducted in two ways, firstly using the existing water content in the material as the blowing agent and secondly by adding sodium bicarbonate. When processed in a twin screw extruder (L/D 25 and 10 mm die) the material readily expanded due to the internal moisture content alone, with a conditioned expansion ratio of up to 1.85 ± 0.13. Cell structure was non-uniform exhibiting a broad range cell sizes at various stages of formation with some coalescence. The cell size reduced through the addition of sodium bicarbonate, overall more cells were observed and the structure was more uniform, however ruptured cells were also visible on the extrudate skin. Increasing die temperature and introducing water cooling reduced cell size, but the increased die temperature resulted in surface degradation.

Keywords: Foam extrusion, Biodegradable polymers, Polyethylene, Compatibilised blends
PACS: 82.35.Pq, 83.80.TC, 83.80.Iz, 81.20.Hy

INTRODUCTION

Foamed products are produced by using a dissolved gas, or decomposing a blowing agent, within a molten polymer matrix to form bubbles. The desired density, foam structure and cell size can be achieved through manipulating processing conditions such as temperature, cooling rate, pressure, type and concentration of nucleating and blowing agents, and polymer type and grade. Foamed polymers are versatile and can be tailored to suit particular applications such as packaging, insulation, impact attenuation, and bead fillers.

Foamed products can be produced by expanding polymer beads in moulds, injection moulding and foam extrusion. Foam extrusion is a continuous method using single or twin-screw extruders where the desired foamed properties are achieved by manipulating extrusion feed rate, screw speed and temperature profile. This has been applied to polystyrene, polyvinylchloride, polypropylene, polyvinyl alcohol and polyethylene. Single screw extruders are typically used due to lower capital cost and operational simplicity; however they require a long screw length with an L/D (length over diameter ratio) > 38. In comparison, twin-screw extruders require an L/D ratio of around 25, demonstrate good controllability, high shear, mixing and heat transfer, and are therefore the preferred design; although they are limited in their cooling capacity and incur higher capital cost [1].

Using bio-derived, renewable and bio-degradable materials such as thermoplastic starch (TPS) and PLA for foamed products is becoming more popular. A relatively new protein-based material is Novatein® Thermoplastic Protein (NTP). This is derived from bloodmeal, a by-product of the meat processing industry, which contains aggregated haemoglobin and serum proteins. NTP has been used to produce injection moulded products such as renderable meat-processing aids and weed mat pegs. Extruded and granulated NTP contains 25-26 wt% water which acts as a plasticizer reducing the viscosity and the glass transition temperature, but which could also be used as a blowing agent for foaming.

While NTP can be extruded and injection moulded, its extensional viscosity is currently too high for film production and foam formation. One method of reducing NTP's extensional viscosity is by blending it with other

Proceedings of PPS-31
AIP Conf. Proc. 1713, 100003-1–100003-5; doi: 10.1063/1.4942308

polymers. Previous work successfully blended NTP with linear low density polyethylene (LLDPE) and (PE-g-MAH) maleic anhydride grafted polyethylene [2]. While LLDPE is not biodegradable, other work has suggested that blending it with thermoplastic starch (TPS), may promote breakdown of the LLDPE phase provided that it is finely dispersed [3]. Protein-based examples of extrusion foaming typically use compatibilised blends with either polyethylene or polylactic acid. Extrusion foaming of soy protein concentrate has been achieve through twin screw extrusion with PLA in the presence of poly(2-ethyl-2-oxazoline) as a compatibiliser [4]. While Zein protein has been foamed with pearl millet flour by utilizing production of steam during the extrusion process [5].

This work investigated the extrusion foaming ability of NTP/LLDPE compatibilised blends using the water content in NTP and sodium bicarbonate as blowing agents.

MATERIALS AND METHODS

Pre-extruded Novatein® Thermoplastic Protein (PNTP) was prepared via batch blending of bloodmeal, denaturants and plasticisers [6] shown in TABLE 1. A mixture of sodium sulphite (SS), sodium dodecyl sulphate (SDS) and urea in water was made by heating at 50ºC until dissolved. This solution was added to the sieved bloodmeal and mixed for five minutes before triethylene glycol was introduced followed by another four minutes of mixing. The PNTP was then stored in a zip lock plastic bag, at 4 ºC, until extrusion.

TABLE 1: Pre-extruded NTP composition

Reagent	Source	Grade	Weight (g)
Bloodmeal (< 710 µm)	Wallace Corporation Limited, NZ	Agricultural	300
Water	Produced on-site	Distilled	120
Sodium Sulfite	Merck, Germany	Analytical	9
Sodium Do-decyl Sulfate	Merck, Germany	Synthesis	9
Urea	Ballance Agri-Nutrients, NZ	Agricultural	30
Triethylene Glycol	Merck, Germany	Industrial	60

PNTP was extruded with a ThermoPrism TSE-16-TC Twin Screw Extruder (TSE) with an L/D ratio of 25 and die size of 10 mm. A screw speed of 150 RPM was used across a temperature profile of 70, 100, 100, 100, 120 °C from feeder to die, and the feed rate was adjusted to maintain a relative torque of 35-40%. The extruded Novatein® Thermoplastic Protein (NTP) was then granulated by a Castin Machinery Tri-blade granulator using a 4 mm screen.

Cotene 3901 linear low density polyethylene (LLDPE) was mixed with NTP and polyethylene grafted maleic anhydride (PE-g-MAH) in 200 g batches in the extruder hopper for the foam extrusion trials (TABLE 2). Cotene is a specialty powder supplied by J.R. Courtenay (NZ) with a melt flow index (MFI) of 4.0 g/10 min and annealed density of 0.905 g/cm³. PE-g-MAH was supplied by Sigma Aldrich (CAS 9006-26-2).

TABLE 2: Summary of extrusion foaming blends and conditions trialed.

Trial	Effect	PE-g-MAH Content (wt %)	Die Temp ( )	Cooling Type (Air/Water)	Sodium Bicarbonate (pph)
1	NTP/PE Composition	10	120	Air	0
2	PE-g-MAH Content	8	120	Air	0
3	PE-g-MAH Content	6	120	Air	0
4	Die Temperature	10	140	Air	0
5	Water Cooling	10	120	Water	0
6	Water Cooling	10	140	Water	0
7	Sodium Bicarbonate Content	10	120	Water	2
8	Sodium Bicarbonate Content	10	140	Water	2
9	Sodium Bicarbonate Content	10	120	Water	4
10	Sodium Bicarbonate Content	10	140	Water	4

Foam extrusion was conducted using the same equipment and conditions for NTP, except the die temperature was set to 120 or 140ºC (TABLE 2). A relative torque of 50-60% was maintained, while the mass flowrate, feed rate, pressure and temperature profile were recorded. Specific mechanical energy (SME) was calculated in kJ/kg [7]. The foamed extrudate was either air cooled or submerged in a water bath for one minute, at approximately 18-23°C. For all trials dry extrudate samples were retained for moisture analysis by oven drying at 100ºC until constant weight. The extrusion samples produced with water cooling retained excess water once removed from the water bath, which was removed by oven drying at 100ºC.

Sample diameters and lengths for radial expansion and density were measured for both unconditioned and conditioned samples (following one week in a humidity chamber at 50% RH and 23ºC). The diameter was measured at three independent points along each of the sample rods and at each of these points two diameter values were taken to account for non-uniform expansion. These six values were then averaged and used to determine the radial expansion ratio (E_r) and cross sectional area (CSA). Sample length was multiplied by CSA to obtain sample volume. The sample mass was then divided by sample volume to obtain sample density (ρ_f) in g/cm³ as per ASTM D1662 [8]. The overall expansion ratio (E_f) was calculated by dividing the unfoamed material density (ρ_0) by the density of the foamed material (ρ_f). The expected unfoamed density of the given compositions was determined using a weighted average of the density of the individual components. The density for the compatibiliser was assumed to be equal to that of the LLDPE, 0.905 g/cm³ and a density of 1.2 g/cm³ was used for NTP.

To investigate the internal structure of the extruded rods, samples were immersed in liquid nitrogen for 10-15 seconds before snapping. The foam cellular structure on the fracture surfaces was visualized using a Wild M38 stereo microscope equipped with a Nikon digital camera for image capture.

RESULTS AND DISCUSSION

The Effect of Composition – NTP:LLDPE Ratio and Compatibiliser Content

Blends containing 50-65% NTP foamed readily although the cell size and distribution was non-uniform and the cells asymmetrical (FIGURE 1). Between 70-80% NTP, the extrudate contained fewer but larger cells with more irregular boundaries, while compositions containing 85-90% NTP produced a brittle extrudate with no cells. Foamed product density increased with increasing NTP content while expansion ratios, extrudate diameters and radial expansion ratios decreased (FIGURE 2). The lowest density achieved was 0.58 ± 0.04 g/cm³ for the 50% NTP composition, which corresponds to an expansion ratio of 1.85 ± 0.13. A decrease in the extrudate diameter and radial expansion ratio was observed with increasing NTP, especially for blends containing greater than 75% NTP.

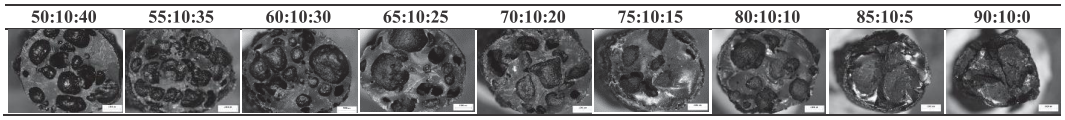

FIGURE 1: Fracture surfaces of NTP/LLDPE foams containing 10 wt% PE-g-MAH, arranged from left to right in increasing NTP content. Compositions above each picture are NTP: PE-g-MAH: LLDPE. Cell sizes range from 0.5 to 4 mm

The specific mechanical energy required to extrusion foam the above blends increased with increasing NTP content until consolidation was lost at 90% NTP. Loss of consolidation was unexpected as 100% NTP can be extruded again and consolidates easily. Consolidation problems were also observed for the 85% NTP composition, suggesting that the high ratio of compatibiliser to LLDPE is responsible. Therefore the effect of 10, 8 and 6% PE-g-MAH content on foaming and consolidation were also investigated.

Decreasing the proportion of compatibiliser within the blends resulted in a glassy extrudate surface with a more chaotic foam structure (FIGURE 3). All blends consolidated during extrusion foaming with 10, 8 and 6% compatibiliser and there was little difference in the overall foam expansion and the radial expansion ratios (although foams compatibilised with 6% PE-g-MAH did exhibit a small increase in both types of expansion, their averages fell within variation of the 10% case). Also, the extrudate skin for samples containing lower compatibiliser content appeared to be more prone to tearing from cell rupture during cooling. As there was no significant benefit in reducing compatibiliser content, the remainder of the trials were conducted using 10% PE-g-MAH.

The Effect of Die Temperature, Water Cooling and Additional Blowing Agent

Increasing the die temperature from 120 to 140 for air-cooled samples resulted in a thinner extrudate with a larger number of non-uniform cells (FIGURE 4). The change in die temperature reduced the conditioned radial expansion ratio for a 50:10:40 blend from 1.37 ± 0.18 (conditioned) at 120ºC to below 1 for 140 ºC (FIGURE 5), while the overall foam expansion ratio remained constant. This suggests expansion was longitudinal at 140ºC rather than radial, due to the blend being more fluid and stretching under its own weight. The extrudate skin also appeared highly degraded and torn due to cell rupture and collapse.

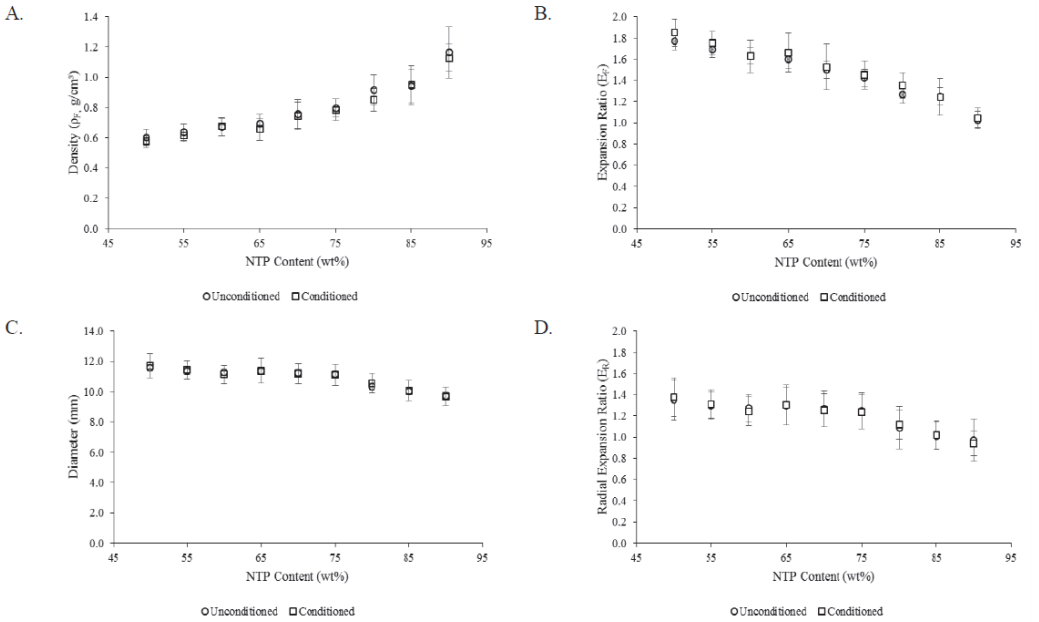

FIGURE 2: The effect of blend composition on unconditioned and conditioned samples for: A. Foam density, B. Expansion ratio, C. Extrudate diameter, D. Radial expansion ratio. Error bars represent standard deviation.

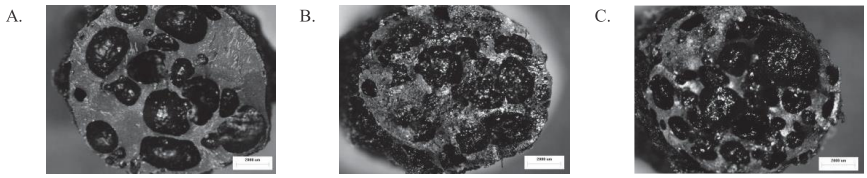

FIGURE 3: Variation in foam structure for 50 wt% NTP with A. 10, B. 8 and C. 6 wt% compatibiliser. The remainder is LLDPE.

Die temp	Air cooled 0 pph sodium bicarbonate	Water cooled 0 pph sodium bicarbonate	Water cooled 2 pph sodium bicarbonate	Water cooled 4 pph sodium bicarbonate
120°C	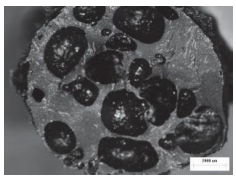	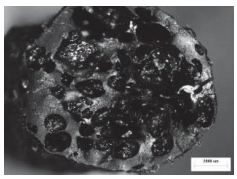	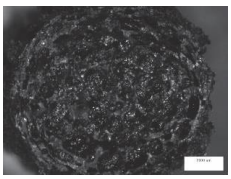	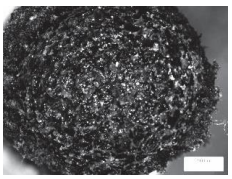
140°C	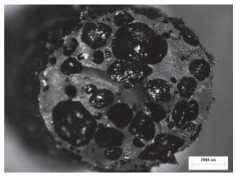	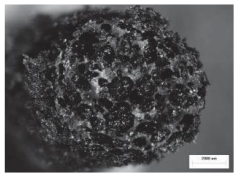	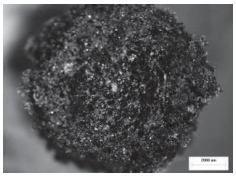	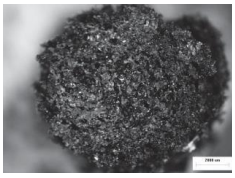

FIGURE 4: Effect of die temperature, cooling and blowing agent for the 50:10:40 blend on cell structure.

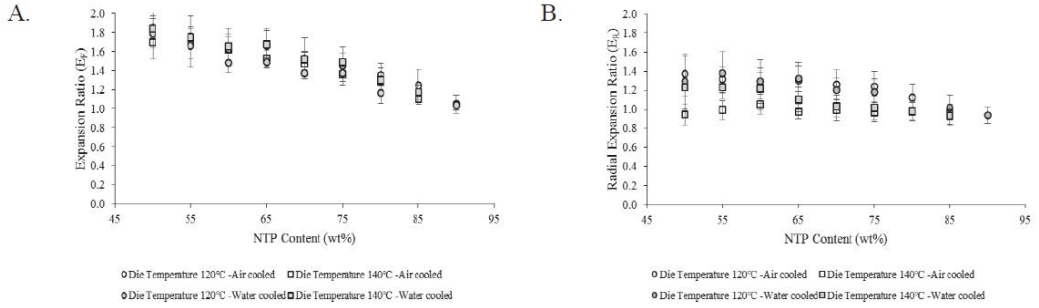

FIGURE 5: Effect of die temperature on A. foam expansion ratio and B. radial expansion ratio. Error bars represent standard deviation.

Water cooled samples contained a larger number of smaller cells which were not completely enclosed compared to air cooled samples (FIGURE 4). While no change in sample density was observed with water cooling, radial expansion ratio increased for the water cooled 140℃ case for compositions containing between 50-60% NTP, suggesting that the material contracts in length, as cells develop when submerged in a water bath. Despite water cooling, the extrudate skin remained coarse and can most likely be attributed to the degradation of the NTP phase.

Adding 2 pph and 4 pph sodium bicarbonate to the 50:10:40 system produced a very fine cell structure with no large regions of unfoamed material. However sample density increased slightly compared to those without sodium bicarbonate. The resulting material was also more flexible than samples without sodium bicarbonate.

CONCLUSIONS

An extruded foam was successfully produced by blending NTP with LLDPE and PE-g-MAH using the internal moisture content from the protein phase as a blowing agent. Increasing LLDPE reduced foam density and increased the expansion ratio. The amount of PE-g-MAH trialed had no observable effect on foam expansion and radial expansion ratio. Increasing the die extrusion temperature and introducing water cooling resulted in a larger number of smaller cells although there was no corresponding decrease in density, and the higher temperature resulted in a degraded extrudate skin. Adding sodium bicarbonate as a blowing agent resulted in a finer cellular structure, but with a slight increase in foam density.

ACKNOWLEDGEMENTS

The authors would like to acknowledge the contributions of the Biopolymer Network Ltd (BPN) and Aduro Biopolymers (Novatein® commercialization), and the funding received from the New Zealand Ministry of Business, Innovation and Employment (BPLY1302 contract). Also thanks to Mr. Andrew Taylor who assisted in collecting these results and Dr. Jim Bier for sharing his expert knowledge of NTP.

REFERENCES

1. Thiele, W.C. and C. Martin, *Extrusion Equipment for Foam Processing*, in *Foam extrusion: Principles and Practice*, S.T. Lee and C.B. Park, Editors. 2014, Taylor & Francis: Boca Raton.
2. Marsilla, K.I.K. and C.J.R. Verbeek, *Properties of Bloodmeal/Linear Low-density Polyethylene Blends Compatibilized with Maleic Anhydride Grafted Polyethylene.* Journal of Applied Polymer Science, 2013. **130**(3): p. 1890-1897.
3. Vieyra, H., M.A. Aguilar Méndez, and E. San Martín Martínez, *Study of biodegradation evolution during composting of polyethylene–starch blends using scanning electron microscopy.* Journal of Applied Polymer Science, 2013. **127**(2).
4. Liu, B., L. Jiang, and J. Zhang, *Extrusion Foaming of Poly (lactic acid)/Soy Protein Concentrate Blends.* Macromolecular Materials and Engineering, 2011. **296**(9): p. 835-842.
5. Filli, M., et al., *Development and Characterization of Extruded Biodegradable Foams based on Zein and Pearl Millet Flour.* Annual Transactions of the Nordic Rheology Society, 2011. **19**.
6. Pickering, K.L., et al., *Plastics material*. 2010, Google Patents.
7. Lay, M.C., C.J.R. Verbeek, and G. Ahuja, *Effect of bloodmeal hydrolysate on bloodmeal-based thermoplastic mechanical properties*, in *2014 CHEMECA Conference*. 2014: Perth, Western Australia.
8. ASTM Standard D1622/D1622M, *Standard Test Method for Apparent Density of Rigid Cellular Plastics*. 2014, ASTM International: West Conshohocken, PA.

Foaming behaviour of Novatein and blends with polyethylene compatibilised by maleic anhydride

Overview:

To lower the melt viscosity Novatein, Novatein – LLDPE and another blend (Novatein with Low Density Polyethylene) were foamed under free expansion in an injection moulder by withholding the nozzle from the mould. The LDPE blend was added to assess whether foaming could be improved by incorporating chain branching. The injection moulder prevented excessive gas loss and improved the pressure drop and pressure drop rate aiding foaming.

This presents some of the early scoping work which was conducted during the development of a foaming method (Objective 1).

Contribution:

As first author for this publication the PhD candidate conducted all experimental work, data analysis and prepared the first draft of this manuscript. Under guidance from the supervisors the manuscript was revised and edited

Permission:

Foaming Behavior of Novatein and Blends with Polyethylene Compatibilised by Maleic Anhydride

Chanelle Gavin[a#], Mark C. Lay[a*] and Casparus J.R. Verbeek[a$]

[a]*University of Waikato, Knighton Road, Hamilton, New Zealand*
[#]*chanellegavin@gmail.com*
[*]*mclay@waikato.ac.nz* , [$]*jverbeek@waikato.ac.nz*

Abstract. Novatein® thermoplastic protein (NTP), a bloodmeal based thermoplastic, was successfully foamed without blowing agent or blending with other polymers using a BOY-35A injection moulder in free expansion mode. Previously, only soy protein has been successfully continuously foamed and zein and gluten batch foamed without blending or rheological modification. The greatest expansion ratio for NTP was 4.4 at 165ºC. Blending NTP with compatibilised LLDPE and LDPE and adding blowing agent reduced expansion ratios. The foams exhibited a fibrous nature, with cell structures similar to those reported in literature for extrusion foamed thermoplastic soy protein isolate. SEM pictures suggested a possible role of either sodium sulphite, sodium dodecyl sulphate or sodium sulphate as a nucleating agent as particulates were found on the cell surfaces. Triethylene glycol and urea were thought to contribute to NTP foaming, along with water present in NTP, with two or more acting as the blowing agent.

Keywords: Free Expansion Foaming, Single Screw, Protein Bio-polymer, Polyethylene, Compatibilised Blend
PACS: 82.35.Pq, 83.80.TC, 83.80.Iz, 81.20.Hy

INTRODUCTION

The waste disposal problems of using non-biodegradable foamed polymeric materials in short-term/limited-life applications such as packaging has resulted in increased use of biodegradable, bio-derived and protein based thermoplastics. One potential biodegradable, protein based thermoplastic is Novatein® Thermoplastic Protein (NTP), developed from bloodmeal by the University of Waikato and Aduro Biopolymers, New Zealand. Bloodmeal is plasticized by adding urea, sodium sulphite, sodium dodecyl sulphate, water and triethylene glycol, and extruded to produce a consolidated thermoplastic with similar mechanical properties to linear low density polyethylene.

Only a small number of thermoplastic proteins have been successfully foamed using extrusion. Examples include soy protein isolate which was successfully foamed into sheets at 150-160°C [1], blends of pearl millet flour and zein (30:70) foamed at 105°C [2], and blends of soy protein concentrate and polylactic acid (PLA) at 150-160°C [3]. In all cases, an additional chemical blowing agent was employed to promote foaming. In comparison, injection foaming is usually conducted into a mould and either a short shot or core pull is used to enable the required expansion. Injection foaming has been applied to a wide range of biopolymers including PLA, PHBV, PBAT and starch [4], however it has only been applied to one other protein thermoplastic (soy) [5].

Previously, the extrusion foaming ability of NTP blended with compatibilised linear low density polyethylene (LLDPE) was investigated using the internal moisture content and sodium bicarbonate as the blowing agent [6]. Two twin screw extruders were used with 10 mm diameter dies. Expansion ratios of < 2 were observed and foam morphology consisted of large irregular closed cells up to 2 mm in size. A foaming grade LDPE was also tried with NTP. While the material was expected to foam better when compared to using LLDPE, because of its different melt flow index and strain hardening behavior, no difference in foaming ability of the blends was observed at 120ºC. The low expansion ratios were attributed to the significant losses of blowing agent through the feed hopper and to gases escaping through the unconsolidated material at the die.

To prevent the loss of gases and improve foaming, this work explored the use of a single screw BOY 35A injection moulder in free expansion mode for extrusion foaming. The foaming ability of NTP, LDPE, LLDPE and 50:50 blends was explored over a temperature range of 150-165ºC. The materials, blends and resulting foams were characterized by examining cell morphology and expansion ratios.

Proceedings of PPS-32
AIP Conf. Proc. 1914, 060002-1–060002-5; https://doi.org/10.1063/1.5016722
Published by AIP Publishing. 978-0-7354-1606-2/$30.00

MATERIALS AND METHODS

Pre-extruded NTP (PNTP) was prepared in a Labtech bench scale high speed mixer at 1400 RPM by blending bloodmeal with a denaturing solution and triethylene glycol as a plasticizer. The denaturating solution was prepared by dissolving sodium sulphite (SS), sodium dodecyl sulphate (SDS) and urea in water by heating and agitation (**TABLE 1**). This solution was added to the bloodmeal in the high speed mixer in two stages with two minutes of mixing between additions. The plasticizer component was then added in the same manner. The PNTP was then stored overnight at 4 °C in a zip lock bag until extrusion.

TABLE 1: Pre-extruded NTP composition

	Reagent	Source	Grade	Weight (g)
Protein Source	Bloodmeal (< 710 µm)	Wallace Corporation Limited, NZ	Agricultural	1500
Denaturing Solution	Water	Produced on-site	Distilled	600
	Sodium Sulphite	Merck, Germany	Analytical	45
	Sodium Do-decyl Sulphate	Merck, Germany	Synthesis	45
	Urea	Ballance Agri-Nutrients, NZ	Agricultural	150
Plasticiser	Triethylene Glycol	Merck, Germany	Industrial	300

Consolidated NTP was produced by extruding PNTP using a Labtech Scientific Twin Screw Extruder across a temperature profile from feed to die of 70,100,100,110,120°C. This extruder has an L/D ratio of 40, 26 mm diameter screws and was operated at a torque of 55-60%. The extruded material (ENTP) was then granulated to a size of less than 4 mm using a tri-blade granulator from Castin Machinery (NZ).

The ENTP and the polyethylene phase (either LLDPE or LDPE) was then extruded with polyethylene grafted maleic anhydride (PE-g-MAH) compatibiliser (10 % on a weight basis). Cotene 3901 (Elastochem, NZ) with a melt flow index (MFI) of 4.0 g/10 min and annealed density of 0.905 g/cm³ was used for LLDPE. LDPE used was Lotrene FD0274 (MFI of 2.4 g/10 min) commonly used for foamed polyethylene products. This material was supplied by Interplas Agencies Limited via Nulon Limited, Auckland, New Zealand. PE-g-MAH was supplied by Sigma Aldrich (CAS 9006-26-2).

Following the second extrusion the material was granulated to less than 4 mm for foaming in the BOY 35A injection moulder. The single screw has a diameter of 24 mm and an L/D ratio of 22. The machine was operated by withholding the die from the mould to enable free expansion of the material.

The foaming behavior of NTP, LDPE, a 50:10:40 blend of NTP: PE-g-MAH:LDPE blend, LLDPE and a 50:10:40 LLDPE blend was investigated in this study with respect to temperature and sodium bicarbonate content (**TABLE 2**). Temperature profiles of 100, 125, X, 135 and 125 °C from feed to die were investigated for foaming where temperature X was set to either 150, 155, 160 or 165 °C

TABLE 2: Summary of extrusion foaming blends, compatibiliser and blowing agent content.

Trial	Material	PE-g-MAH Content (wt %)	Sodium Bicarbonate (pph)
1	NTP	0	0
2	NTP	0	2
3	NTP	0	4
4	NTP: PE-g-MAH: LDPE 50:10:40	10	0
5	NTP: PE-g-MAH: LDPE 50:10:40	10	2
6	NTP: PE-g-MAH: LDPE 50:10:40	10	4
7	LDPE	0	0
8	LDPE	0	2
9	LDPE	0	4
10	NTP: PE-g-MAH: LLDPE 50:10:40	10	0
11	NTP: PE-g-MAH: LLDPE 50:10:40	10	2
12	NTP: PE-g-MAH: LLDPE 50:10:40	10	4
13	LLDPE	0	0
14	LLDPE	0	2
15	LLDPE	0	4

The density and expansion ratio of the material was measured after foaming. Density was determined by measuring a sample block with vernier calipers and weighing the material. The sample mass was then divided by sample volume to obtain sample density (ρ_f) in g/cm³. The expansion ratio (ER) was determined relative to the unfoamed material density (ρ_0). The expected unfoamed density of the given compositions was determined using a weighted average of

the density of the individual components. The density for the compatibiliser was assumed to be equal to that of the LLDPE (0.905 g/cm^3) and a density of 1.2 g/cm^3 was used for NTP.

Cell morphology was observed at low magnification with a Wild M38 optical microscope and at high magnification using a Hitachi S-4700 scanning electron microscope. Samples were first dried at 70°C over 48 hours, then sputter coated with platinum before imaging using an acceleration voltage of 20 kV.

RESULTS AND DISCUSSION

NTP and NTP/PE blends were successfully foamed using extrusion foaming using the BOY35A injection moulder. It was generally observed that expansion ratio increased as the melt temperature increased, with the exception of PE (which was very hard and difficult to cut for analysis), with a processing temperature of 165°C giving the greatest expansion ratio for NTP (4.4). At greater temperatures the material was too fluid to retain the gases and was spitting from the die.

While 165°C is close to the protein degradation temperature for NTP, processing at just 10-15°C lower (150°C) resulted in little to no expansion. LDPE and LLDPE did not foam without a blowing agent, and blends of NTP with PE showed lower expansion ratios than 100% NTP. NTP blended with LDPE at 165°C had an expansion ratio of 3 while NTP blended with LLDPE had an expansion ratio of 2.5. Adding 2 pph blowing agent resulted in a finer cell structure but lower expansion ratio for NTP of 3.91, and 4 pph blowing agent gave an expansion ratio of 2.53 and the material looked highly degraded. Adding blowing to the blends also reduced expansion ratios from to 3 to 2.35 for LDPE blends at 4 pph while the expansion ratio did not change for LLDPE and remained at 2.5. Adding blowing agent to LDPE and LLDPE did result in some foaming (**FIGURE 2**), but expansion ratios were unable to be obtained, because the samples were not sufficiently foamed to be able to be cut and measured.

Based on the above observations, NTP can be foamed (**FIGURE 1A)** using the internal moisture content and possibly urea and triethylene glycol, which are likely to flash off with the water. NTP does not need to be blended or have a blowing agent added. Blending NTP with PE required a second extrusion step which reduced the amount of water present for foaming by about 6%. In addition, the amount of water present was lower because the amount of NTP was lower in the blends overall. Adding the blowing agent resulted smaller cells due to increased bubble nucleation, but resulted in lower expansion ratios.

The resulting NTP foam appeared fibrous on a macro scale and the cell morphology was not completely uniform (**FIGURE 1B**). In 100% NTP foams, distinct regions of large and small cells were observed. Thin walls were associated with highly foamed areas with small cells while the larger cells are often surrounded by a region of unfoamed material. The addition of 2 pph blowing agent modified the morphology such that a smaller more uniform cell structure was observed. However, the addition of blowing agent did not result in greater expansion. SEM images of NTP with 2 pph sodium bicarbonate revealed a series of cells which were more defined in their cell boundary, but larger than those small cells observed in NTP alone. The material directly surrounding these cells is clearly devoid of smaller cells and many of the cells are elliptical in shape, most likely due to the direction of material flow during foaming. However at higher magnifications very thin cell walls are visible suggesting that the overall expansion of this material can be improved further.

For pure LDPE, as sodium bicarbonate content increased the number of visible cells also increased, as expected. Their size however remains very similar. A similar trend was observed for LLDPE with blowing agent although there appears to be more cell coalescence occurring, with localized regions of cells with very thin walls for one or two regions of the cell perimeter with the rest surrounded by unfoamed material. Overall, a more cellular structure was observed for LDPE as opposed to LLDPE.

The NTP:PE blends also developed cells which increased in number and decreased in size with increased blowing agent. The cellular structure of these blends is chaotic with a wide distribution of cell sizes in both cases. However, a more defined cellular structure is observed for NTP:LDPE blends as opposed to NTP:LLDPE blends and once again the cells have thinner wall structures. SEM images at higher magnification showed some very thin wall structures which could almost be described as open cell. However the cells appear to be open only on the surface with no fibrous crosslinked structure below (complete walls visible). This is most likely due to cell rupture which occurred when a vacuum was pulled on the sample for SEM analysis.

SEM analysis at high magnification also revealed a possible nucleating agent in embedded in the walls of the cells (**FIGURE 1C**). Elemental analysis of these particles indicated sodium, sulphur and oxygen was present. This is most likely residual sodium sulphite or sodium dodecyl sulphate which did not dissolve fully during mixing. Alternatively sodium sulphate is formed when sodium sulphite oxidizes and sodium sulphate peaks have previously been noted in powder x-ray diffraction and Fourier transform infra-red analysis of NTP.

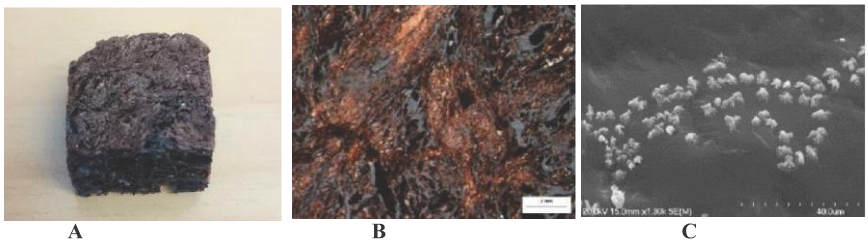

A B C

FIGURE 1: A. Block of NTP foam **B.** Cell structure by optical microscopy x6.4, **C.** SEM image of particles present in cell wall on which elemental identification was conducted.

	Blowing Agent Content – Sodium Bicarbonate		
Material/Blend	**0 pph**	**2 pph**	**4 pph**
NTP Crude	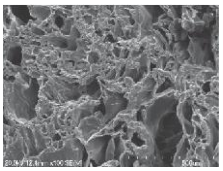 **4.4**	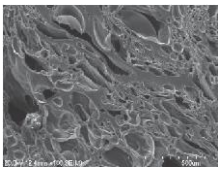 **3.9**	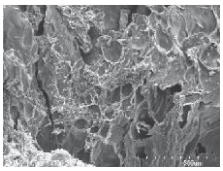 **2.4**
50:10:40 LDPE	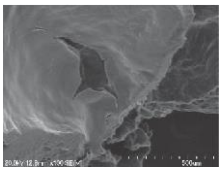 **3.0**	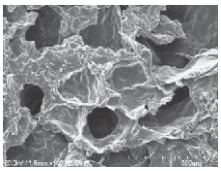 **2.7**	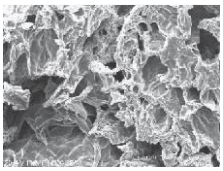 **2.4**
LDPE ER-N/A	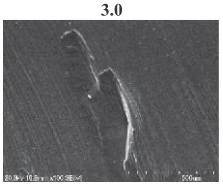	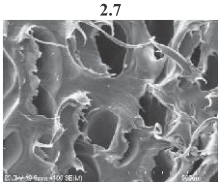	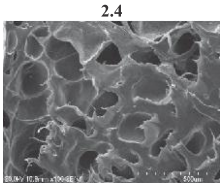
50:10:40 LLDPE	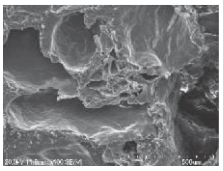 **2.5**	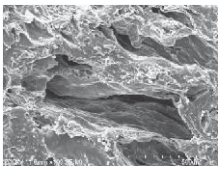 **2.2**	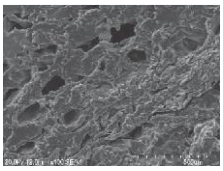 **2.5**
LLDPE (ER-N/A)		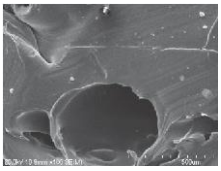	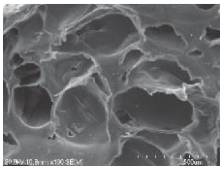

FIGURE 2: Comparison of observed cellular morphology for foams produced at 165°C. Images are at x150 magnification. Expansion Ratios (ER) are shown below images

An ammonia smell was noticed when foaming NTP and NTP containing blends. Like sodium bicarbonate urea is capable of thermally decomposing to form gaseous reaction products. For sodium bicarbonate water and CO_2 are direct products [7], and although urea can thermally decomposes to ammonia, it is more likely to undergo a hydrolysis reaction due to the presence of water and heat and will produce NH_3 and CO_2 [8]. Likewise, both sodium bicarbonate and urea could potentially react with exposed R groups on the protein chain (carboxylic) to evolve the same gaseous products [8], explaining the ammonia smell observed.

The greatest expansion ratio was observed for 100% NTP, this sample contained no added sodium bicarbonate as a blowing agent and therefore would have resulted in the lowest CO_2 evolution by any mechanism. As sodium bicarbonate content increased in any blend containing NTP the expansion ratio decreased, suggesting that an increased ability to generate CO_2 was not beneficial and may be linked to the ratio of gaseous NH_3 to CO_2 where low CO_2 is favored (if these species are not just a by-product of this method). CO_2 is known to be an excellent blowing agent for PLA in both batch and continuous systems [4], while batch foaming of thermoplastic zein and gelatin determined that N_2 or high N_2/low CO_2 mixtures were preferable for these two proteins [9]. The rapid reduction in pressure at the die may also result in a flashing of water and TEG (dictated by vapour –liquid equilibrium).

Future work will determine which component of the system is the primary blowing agent in the case of NTP and NTP – bicarbonate blends. This will be determined by examining the amount of urea lost from the system, the moisture of the resulting products and the loss of TEG through phase–equilibria and changes in mechanical properties of these foams. The effect of other processing variables such as injection pressure, injection speed, cycle time, shot size and back pressure will also be investigated to further improve the expansion ratio of NTP foams.

CONCLUSIONS

NTP was successfully foamed without blowing agent or blending using a BOY-35A injection moulder, one of the few proteins for which foaming has been successful without blending or rheological modification. The greatest expansion ratio for NTP was 4.4 at 165ºC. Blending with LLDPE and LDPE and adding blowing agent reduced expansion ratios. Foam morphology appeared fibrous with a mixture large and small cells. SEM pictures suggest a possible role of sodium sulphite, sodium dodecyl sulphate or sodium sulphate as a nucleating agent. Future work will investigate the role of internal water, urea, and TEG in NTP foaming.

ACKNOWLEDGEMENTS

The authors would like to acknowledge the contributions of the Biopolymer Network Ltd (BPN) and Aduro Biopolymers (Novatein® commercialization), and the funding received from the New Zealand Ministry of Business, Innovation and Employment (BPLY1302 contract). Also Dr. Jim Bier for practical help with the injection moulder.

REFERENCES

1. Mungara, P., J. Zhang, and J. Jane, *Extrusion processing of soy protein-based foam.* Polymer Preprints, 1998. **39**(2): p. 148-149.
2. Filli, M., et al., *Development and Characterization of Extruded Biodegradable Foams based on Zein and Pearl Millet Flour.* Annual Transactions of the Nordic Rheology Society, 2011. **19**.
3. Liu, B., L. Jiang, and J. Zhang, *Extrusion Foaming of Poly (lactic acid)/Soy Protein Concentrate Blends.* Macromolecular Materials and Engineering, 2011. **296**(9): p. 835-842.
4. Jeon, B., et al., *Microcellular foam processing of biodegradable polymers—review.* International Journal of Precision Engineering and Manufacturing, 2013. **14**(4): p. 679-690.
5. Jane, J.L. and S. Wang, *Soy Protein-Based Thermoplastic Composition for Preparing Molded Articles*, U.P. Office, Editor. 1996, Iowa State University Research Foundation, Inc" Ames, Iowa: US.
6. Gavin, C., M.C. Lay, and C.J. Verbeek. *Extrusion foaming of protein-based thermoplastic and polyethylene blends*. in *Proceedings of PPS-31: The 31st International Conference of the Polymer Processing Society–Conference Papers*. 2016. AIP Publishing.
7. Janković, B., *Kinetic analysis of isothermal decomposition process of sodium bicarbonate using the weibull probability function-estimation of density distribution functions of the apparent activation energies.* Metallurgical and Materials Transactions B: Process Metallurgy and Materials Processing Science, 2009. **40**(5): p. 712-726.
8. Brooks, B., et al., *Apparatus for quantitatively converting urea to ammonia on demand*. 2004.
9. Sessa, D.J., et al., *Viscosity control of zein processing with sodium dodecyl sulfate.* Industrial Crops and Products, 2006. **23**(1): p. 15-22.

4

Morphology and Compressive Behaviour of Foams Produced from Thermoplastic Protein

A journal article

by

C. Gavin, C.J.R Verbeek and M.C. Lay

Published in

The Journal of Materials Science

Overview:

Foaming is often dependent upon foaming temperature. This work aims to assess the effect of temperature during foaming of Novatein, to establish the maximum expansion ratio and to evaluate the compressive properties of the resulting foams.

This chapter presents the improved foaming method and resulting mechanical properties of Novatein foams. It therefore relates to the development of a foaming method (Objective 1) and to understanding the relationship between foam morphology and mechanical properties (Objective 2).

Contribution:

As first author for this publication the PhD candidate conducted all experimental work, data analysis and prepared the first draft of this manuscript. Under guidance from the supervisors the manuscript was revised and edited.

Morphology and Compressive Behaviour of Foams produced from Thermoplastic Protein

Chanelle Gavin[a]*, Casparus J.R. Verbeek[a], and Mark C. Lay[a]

[a]School of Engineering, Faculty of Science and Engineering, University of Waikato, Knighton Road, Hamilton, 3420, New Zealand

chanellegavin@gmail.com, verbeek@waikato.ac.nz, mclay@waikato.ac.nz

Abstract

Novatein® is a patented thermoplastic biopolymer produced from denatured haemoglobin and serum albumin proteins, in blood meal. This material is biodegradable after processing, and when foamed could provide an alternative to expanded polystyrene and polyurethane for short term applications such as packaging. This study aims to investigate the effect of processing temperature on foam density and morphology and how these properties effect compression behaviour. Unconstrained rapid expansion produced a range of foam densities, 0.28-0.45 g/cm^3, which were strongly dependant on temperature. The foams had compressive strengths between 200 to 600 kPa and an elastic moduli between 2.2-8 MPa. Under compression, high density foams behaved like traditional plastic foams, while at low density they behaved more elastomeric. Models for open and closed cells successfully predicted the compression modulus and strength in the linear elastic region. The foams demonstrated a mixed mode morphology (open and closed cells) and an irregular distribution of cells, which explained the deviation from the models.

Introduction

Novatein® is a patented thermoplastic biopolymer produced from blood meal, water, urea, denaturants and plasticizer [1,2]. This material is biodegradable after processing and is a promising alternative to polymeric foams for short term applications such as packaging. Other biopolymers which have been considered as replacements for foamed petrochemical polymers include: poly-lactic acid (PLA) [3-5], starch [6-10], poly-hydroxyalkanoates (PHA) [11,12], polyhydroxybutyrate (PHBV) [13,14], polycaprolatones [15,16], and some protein thermoplastics (and their blends) [17-20].

Factor such as pressure, temperature and viscosity [21] govern bubble nucleation and growth [22,23] due to their influence on gas solubility and diffusivity [24], and chain movement. Specifically, increasing temperature increases gas solubility, diffusivity, and volatility, while simultaneously decreasing viscosity, surface tension, and density and affecting cell size distribution and shape until the polymer is not viscous enough to retain the bubbles [25,26]. The influence of processing temperature and pressure on foam expansion, morphology and compressive behavior is well understood for traditional polymers, and has been studied for polylactic acid (PLA) [27] and starch [8] foams. These effects however are not well established for protein foams as there are only a few studies of thermoplastic proteins which have not been blended with other biopolymers to facilitate foaming. Comparing these studies is further complicated by the different foaming methods used.

The effect of temperature during the batch foaming of thermoplastic Zein and Gelatin has been examined by Salerno et al. For thermoplastic Zein at constant pressure and pressure drop rate (PDR), they determined that foaming temperature affected foam density (0.1-0.65 g/cm^3) and cell size (~45 μm) and that there was an optimum temperature region 70-80 °C after which the cells shrunk. Similar results were observed for thermoplastic gelatin. Foams with densities of 0.55- 0.70 g/cm^3 were produced at higher foaming temperatures (100-140 °C) with an average cell size of less than 20 μm. In comparison sheets of soy protein foams with densities between 0.4-0.6 g/cm^3 have been produced via extrusion at 150-160°C [17]. This material can also be foamed into a mold at temperatures between 120-160 °C resulting in moulded articles with densities between 0.1-0.5 g/cm^3. The resulting compressive strength is between 140-300 kPa with a modulus of 1.7-4.6 MPa [20]. To the authors knowledge there are very few studies which assess the effect of temperature on the foaming ability and foam morphology for protein based foams, produced by any method, which also examine their compression behavior

Typical thermoplastics demonstrate either elastomeric or plastic behaviour under compression where a region of linear elasticity is observed followed by a plateau of either elastic buckling or plastic yielding before densification. Polyurethane and polyethylene foams are typically elastomeric, polymethacrylimid foams deforms plastically and starch foams exhibit brittle failure under compression [28]. Each type of behavior is due to differences in the energy absorbing mechanism and whether or not the foam consists of open or closed cells. The linear elastic deformation is due to the edges of open cells bending and face stretching in closed cells, whereas elastic buckling or plastic yielding is due to cell collapse. If the foam is elastomeric and predominately open celled, they will collapse by bending at almost constant load, resulting in a long plateau in comparison to closed cells where the contribution of the gases within the cells results in a slightly positive gradient in this region. For this case the edges of the cells buckle while the corners remain rigid. In comparison, plastic collapse is preceded by yielding where the edges are considered to be rigid, hinging at the corners [28].

Biopolymer foams have comparable mechanical properties to traditional foams [3]. Compressive modulus for both EPS and EPLA at similar densities is between 3-6 MPa while compressive strength is 80 – 150 kPa. The compressive properties of these materials increases with foam density. This relationship has been extensively modelled, by the most widely applicable is the Gibson and Ashby model. This model considers the mechanical properties to be a combination of the matrix's properties, foam density, the ratio of open vs. closed cells, and the amount of solid material within the wall structures [28]. The main limitation of this model is that it does not account for cell size or shape. Other models such as Mills and Liu [29] do so, but are most successful for foams with uniform cell size and shape. The Christensen and Lo model has also been applied to polyurethane foams but requires knowledge of the polymer viscoelastic properties and Poisson's ratio [30-32]. Finite element analysis has also been used to analyze foams and can provide a better understanding of the behaviour of the foam under compression but requires either a uniform cell structure or a model of the real foam structure [33].

Novatein® has been recently processed into a foamed product with a wide range of densities, cell morphologies and cell sizes during initial scoping work. This study is unique as it is a combined assessment of processing conditions, foam morphology and compressive behavior for a thermoplastic protein foam. It aims to identify the behavior of these foams under compression and how they differ to

classical behavior of petrochemical polymers, as predicted by the Gibson and Ashby model.

Methodology

Materials

Novatein Thermoplastic Protein (NTP) granules were provided by Aduro Biopolymers, New Zealand. It is a patented blend, produced by combining a protein source (blood meal) with an aqueous solution containing water, sodium sulphite, sodium dodecyl sulphate, urea and triethylene glycol as a plasticizer [1].

This specific formulation, Novatein crude, contains approximately 40 parts water, 10 parts urea and 20 parts triethylene glycol per 100 grams of blood meal. The water and urea used in production have the potential to act as blowing agents and previous scoping experiments showed that no additional blowing agents were required to foam this material.

Foaming

Foaming is greatly affected by temperature, pressure, ejection rate, and residence time. Many of these factors are dependent on each other. The rate of pressure drop is related to ejection speed, while temperature effects the rate of plasticisation, and consequently the residence time of the material in the barrel. This study primarily focused on the effect of processing temperature when foaming.

Foamed Novatein was produced under free expansion through a capillary nozzle 2.5 mm in diameter and 25 mm in length. This was conducted using a BOY 35A injection moulder by withholding the nozzle from the mould, to maximize the pressure drop when the material was ejected (Figure 1). As a result, moulding parameters including mould temperature and cooling time could be ignored.

Scoping experiments established a range of ejection speeds (120-150 mm/s), and cycle times (60-90 seconds) that enabled foaming. Cycle time, in this case, is not determined by the residence time in the mould. Instead, it combines the time taken to plasticise the material at 150 rpm, while the screw moves back, and the residence time of the material in the barrel prior to ejection (holding time).

For this study ejection speed was set to 50 mm/s to create the greatest rate of pressure drop rate (otherwise referred to as pressure gradient), and the total cycle time was approximately 90 seconds to mitigate any variability in plasticisation time (approx. 20 seconds). The feed zone remained constant at 100°C to prevent bridging and irregular feeding. The shot size, 90 mm, experienced a pressure drop of 13 MPa at the die and a corresponding pressure gradient of approximately 24 MPa/s. No back pressure was applied to the system.

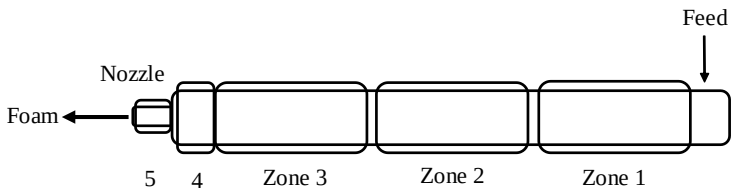

Figure 1: Heating zones of the BOY 35-A injection moulder.

Experimental Design

From scoping studies, foaming was achieved when the material was heated above 150 °C which is 20°C above normal processing temperatures for injection moulding Novatein. It was also observed that increasing temperatures improved the expansion of this material.

The current study was conducted in two parts. In the first part, a constant temperature in zones 2-5 (Table 1) was used, while the second examined the effect of decreasing the temperature in zone 2. As plasticisation took approximately 20 seconds to occur, the material resided in this zone for a long time, which may affect expansion by altering the properties of the melt, and blowing agent evolution. These profiles were selected as the plinth and nozzle (zones 4 and 5 respectively) and are not independently cooled making it difficult to maintain lower temperatures due to heat transfer from the adjacent zone.

Table 1: Temperature profiles used.

Trial	Part A	Part B	
	zone 2-5	zone 2	zone 3-5
1	150		
2	155		
3	160		
4	165		
5	170		
6		130	155
7		130	160
8		130	165
9		145	155
10		145	160
11		145	165

The resulting foams were characterised by determining density, cell morphology and compressive behaviour. Further investigation of mechanical behaviour and changes to the matrix were determined using dynamic mechanical analysis.

Foam Characterisation

The foams were cut into blocks approximately 25 x 25 x 20 mm^3 to characterise density and expansion ratio. Following conditioning at 23 °C and 50% relative humidity for two weeks, the average density was determined using 10 blocks. The volume of each block was measured using Vernier callipers and each sample was weighed. The density (g/cm^3) was calculated and the expansion ratio was based on the unfoamed density of Novatein (1.2 g/cm^3).

Cell morphology of the resulting foams was examined at both low and high magnification. Optical microscopy was used to observe the cellular structure at 6.4 and 16 times magnification, while scanning electron microscopy was used to observe higher magnifications of between 35 and 1000 times. Low magnification images were taken using a Wild M38 microscope (Wild Heerburgg, Switzerland) equipped with image capture capabilities through a Nikon Digital Sight Camera. High magnification images were produced through the use of platinum sputter coated samples on a Hitachi S-4700 SEM with an acceleration voltage of 20 kV.

Compression Analysis

Conditioned foamed blocks were compression tested on a Lloyd tensile tester between two compression plates. Samples were orientated such that the greatest surface area was in contact with the compression plate to minimise buckling effects. A 1 kN load cell was used and the deformation rate set to 2.5 ± 0.1 mm/min. Deformation of the material was carried out until 25% of the initial sample height had been compressed according to ASTM standard D1621. Compression strength and elastic modulus were calculated using the method outlined in the standard for a material which did not display yielding. Compressive strength was determined by extending back the

steep linear region of the load deformation curve, then finding the corresponding load after adding 10% deformation and dividing by the sample height. Elastic modulus (Pa) was calculated according to load (N) x height (m) divided by area (m^2) x deformation (m) using the slope of the linear elastic region. Blocks of polyurethane (Eco Pour Foam) and polystyrene (Waikato Sheet Plastics), both with relative densities of 0.03, were also tested as reference materials. The compressive strength for this material was 183 kPa while that of polystyrene was 125-130 kPa.

Repeated compression tests were conducted (to 25% deformation, using the same procedure as outlined above) after letting the Novatein Foams recover for five minutes between testing. Foam height was measured upon the removal of the load and prior to the next test. The repeated compression tests were conducted five times or until densification of the foamed product was observed.

Dynamic Mechanical Analysis

To measure the behaviour of the matrix after foaming, powder pocket DMA analysis was conducted in a single cantilever configuration using a PerkinElmer DMA 8000 equipped with a temperature controlled furnace which was regulated by Pyrius software. Conditioned powdered samples (approximately 50 mg) were crimped in stainless steel pockets, heated to 25°C and allowed to equilibrate. The temperature was then increased at a rate of 2 °C/min up to 150 °C. Multi-frequency data was collected between 0.1-30.0 Hz with a dynamic displacement of 0.05 mm.

Whole foams were also analysed using the single cantilever configuration following conditioning. Samples were cut from the bulk foam, with the approximate dimensions of 25 mm x 7 mm x 4mm. Tests were performed with a displacement of 0.01 mm at a frequency of 1 Hz. Loss modulus and storage modulus were characterised for temperatures between 25-150 °C. The foams were also tested isothermally at 25 °C under the same conditions for 120 mins, equating to 7200 cycles.

Results and Discussion

Establishing a Processing Window

Foaming depends upon the nature or the polymer (amorphous vs. semi crystalline) and the rheology of the melt; including melt strength and viscosity. Novatein is a biopolymer made from denatured protein, which demonstrates shear thinning behaviour similar to LDPE. As temperature increases the apparent viscosity has been shown to decrease [34] and more moisture loss occurs. As a thermoplastic, this material still retains α-helical and β-sheets structures which constrain chain movement [35]. Novatein therefore behaves similarly to a semi-crystalline polymer when foamed between its glass transition temperature and melting point.

Initial scoping experiments showed that pressure gradient, cycle time and temperature affected foam expansion. Pressure gradient (MPa/s) is dependent on ejection speed. For Novatein, the best expansion was achieved when the ejection speed was high (40-50 mm/s), this maximised the pressure gradient, which in turn, aided nucleation [36]. The pressure gradient remained constant (24 MPa/s), irrespective of temperature when the ejection speed was high. However for lower ejection speeds, with the same shot size, the pressure gradient was less when the temperature of the material was higher, i.e. more molten. Consequently the pressure gradient varied with temperature and while the material was still capable of foaming, expansion was noticeably less.

Cycle time (plasticisation time and hold time combined) also affected foam expansion. For initial trials holding time was short to minimise protein

degradation. It was observed that plasticisation time varied greatly for different temperatures and appeared to dictate foaming i.e. the longer the material took to plasticise the more expanded the product. To minimise this effect on foam expansion a longer holding period was used to mitigate these effects by making the total residence time of the material in the barrel approximately constant, 90 seconds. Longer cycle times overall, also increased the expansion of the foam. Therefore, foaming of this material was carried under free expansion with an ejection speed of 50 mm/s, pressure gradient of 24 MPa/s and a cycle time of 90 seconds to investigate the effect of temperature.

Effect of Temperature

Two temperature studies were performed: the first used constant temperatures across the zones between 150-170°C while the second investigated the effect of lowering the temperature in zone 2. Altering this temperature was expected to change the properties of the melt and amount of blowing agent evolved, which usually results in an optimal foaming temperature. If the processing temperature is too low, the viscosity remains high and the rate of blowing agent evolution is too slow for effective foaming. While increasing the temperature excessively, to lower viscosity or to increase blowing agent evolution (water evaporation), will cause protein degradation. .

From these experiments, in Part A, a temperature range for foaming was established between 155-165°C. These temperatures are above the normal processing temperature for solid Novatein articles (130°C) and resulted in foams with an irregular appearance and a lighter colour than solid Novatein (Figure 2). Foaming at 155 °C produced a foam with a density of 0.41 g/cm^3 while 160 °C lowered the foam density to 0.32 g/cm^3 (Figure 2). Further increasing the temperature to 165 °C resulted in foams with densities as low as 0.25 g/cm^3, equating to an expansion ratio of approximately 5. Processing at temperatures higher than reported here was difficult due to protein degradation and loss of material from the die. The second experiment (Part B) showed that zone 2 had a minimal effect on expansion, suggesting that higher temperatures later in the barrel dictated foaming.

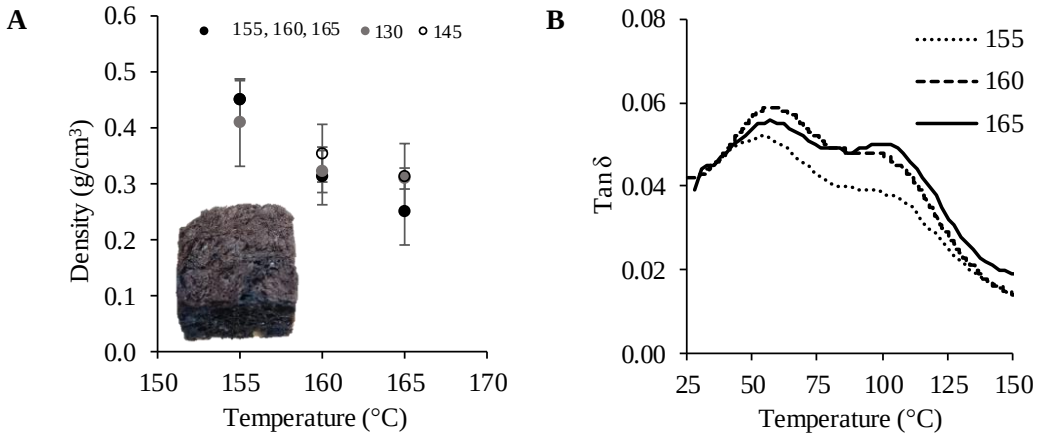

Figure 2 A Foam density vs. foaming temperatures with representative images of foamed blocks of Novatein. **B** Material transitions identified by DMA analysis of powdered samples.

Table 2: Density and expansion ratios of NTP foams in a conditioned state. Density reported in g/cm^3, with standard deviation reported in brackets and expansion ratio (ER).

Trial	Density	ER
1	Insufficent foaming	
2	0.45 (0.04)	2.68 (0.24)
3	0.31 (0.05)	3.90 (0.59)
4	0.25 (0.06)	5.05 (1.25)
5	Material degraded	
6	0.41 (0.08)	3.03 (0.58)
7	0.32 (0.09)	3.93 (0.95)
8	0.31 (0.04)	3.93 (0.58)
9	0.45 (0.06)	2.70 (0.32)
10	0.35 (0.12)	3.69 (1.16)
11	0.31 (0.04)	5.05 (1.25)

While water was the main blowing agent which flashed as the material exited the die, an ammonia smell was also detected during processing. This was either as a result of urea hydrolysis or the protein itself. Urea hydrolysis occurs within the same temperature range, and the residence time of 90 seconds would provide time for urea to convert to ammonia and carbon dioxide. The role of urea within this foaming system will be the subject of a further investigation and was not heavily focused on here.

While the foaming temperature had a significant effect on foam density, no changes were observed in the transition temperatures of the conditioned matrix, as determined by DMA analysis (Figure 2). Irrespective of foaming temperature the matrix demonstrated a glass transition at 55°C and another transition at 110 °C, relating to movement of amorphous chains still constrained by crystalline regions. This analysis establishes that the properties of the matrix can be considered comparable for all foams.

Cell Morphology

All the foams showed a mixture of foamed and solid Novatein regions with both open and closed cells (Figure 3) and a range of sizes from <10 μm up to 4 mm in diameter. The majority of cells were smaller than 0.2 mm^2 (500 μm diameter). Higher foaming temperatures promoted a greater number of larger cells leading to greater foam expansion. For all samples the cell size distribution appeared bimodal with the majority of cells around either 100 μm in diameter or less than 30 μm (Figure 4). The bimodal distribution of cell sizes arises from nucleation continuing throughout the foaming process, provided gases are still available. Their smaller size can be attributed to gas depletion or the reduced time they have to expand before stabilization. The increased cell size at higher temperatures is most likely a combined effect of a reduction in gas density and potentially a greater rate of cell coalescences at higher temperatures. The irregular distribution of the cells observed and the non-uniformity of the foam is most likely due to the semi-crystalline nature of Novatein which is not disrupted fully in the polymer melt. This promotes heterogeneous nucleation and constrains bubbles in some regions of the material preventing a uniform foam forming.

The cells are also elongated due to the shear experienced during manufacture. This effect is more evident at high foaming temperatures where there is more cells of a higher aspect ratio. These elongated structures may be linked to rapid stabilization of the foam upon exiting the die, due to a rapid loss of water (flashing). This would result in insufficient time for the cells to reach a spherical equilibrium conformation. While these foams have elongated cells on a microscopic level they are randomly oriented within the foam, therefore the foam is unlikely to have anisotropic properties. Irregular foam structures have been previously observed for foams produced by continuous methods, including soy protein isolate, zein and millet flour and soy with PLA [17,37,38].

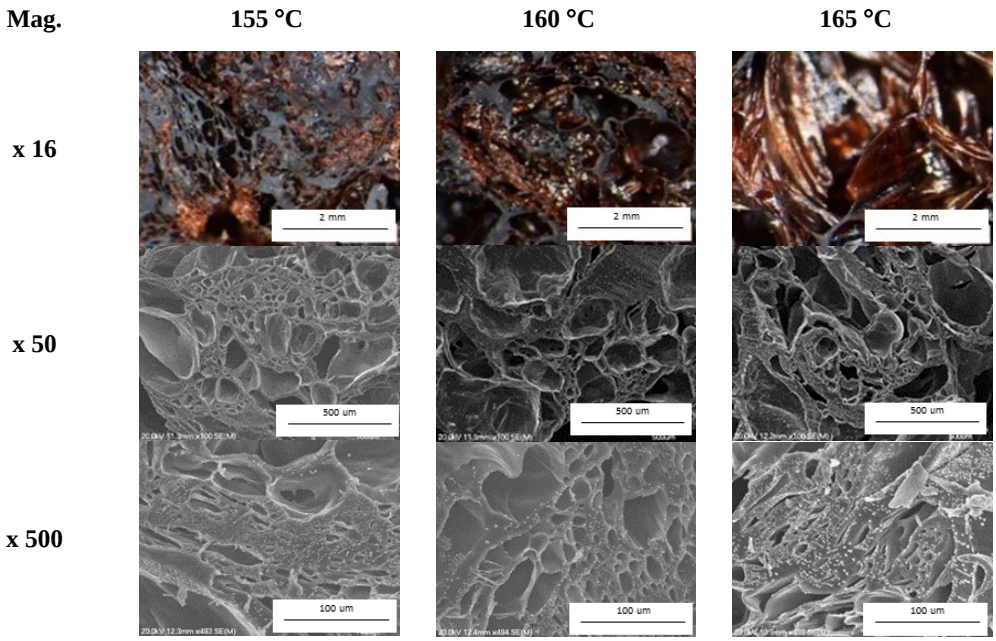

Figure 3: Foam morphology by temperature at both low and high magnification.

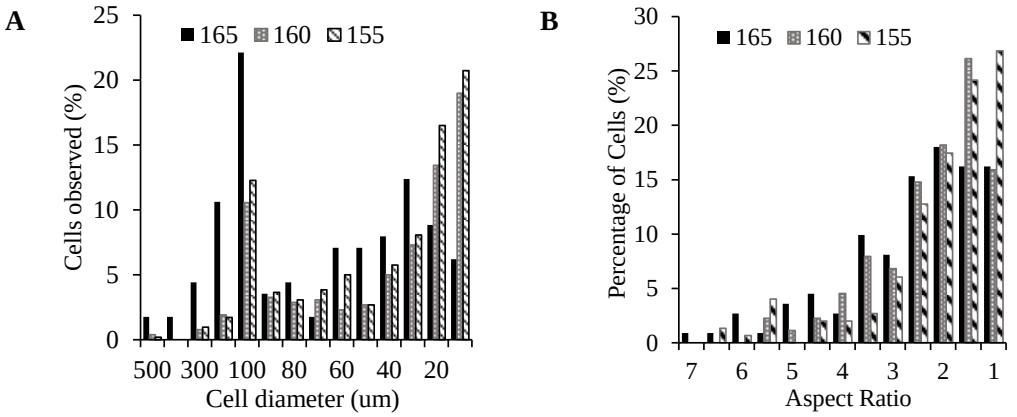

Figure 4: Cell diameter and cell aspect ratio as a percentage of observed cells.

Compression Behaviour

Under compression, polymeric foams demonstrate linear elasticity (at small deformations), a clear plateau (once the linear elastic limit has been exceeded), and eventually densification. Their behaviour can be broadly classified as either plastic or elastomeric depending upon their performance under load and whether they demonstrate a yield point (Figure 5A). Yielding can be observed in plastic foams as a local maxima prior to the plateau region however at low densities this become less distinct and compression curves appear closer to elastomeric in nature [28]. In reality many foams demonstrate intermediate behaviour depending upon compression rate, temperature and foam morphology [39].

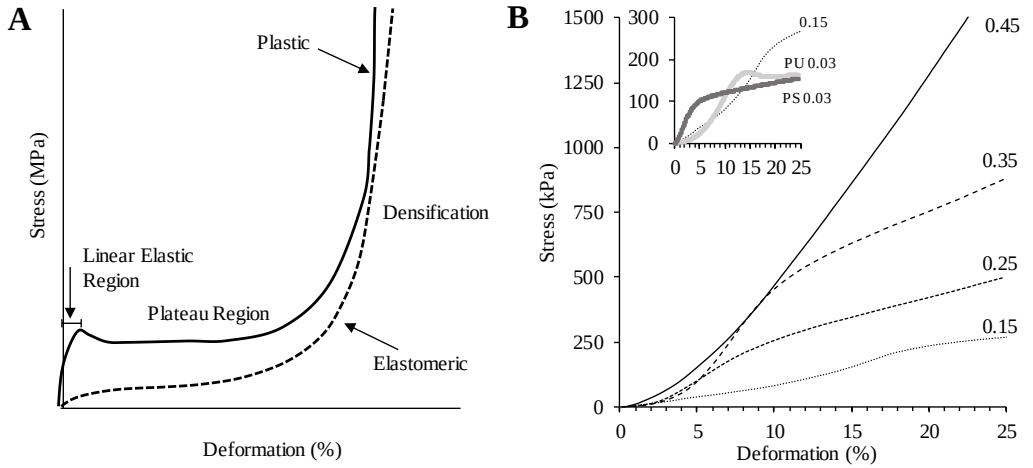

Figure 5: A. Examples of compression curves for plastic and elastomeric foams [26]. **B.** Stress vs. deformation for Novatein foams under compression and the effect of relative density. Polystyrene and polyurethane reference samples shown as insert.

Despite the lack of a clear yield point under compression (Figure 5B), Novatein foams behaved more like a low density rigid plastic foam than an elastomeric foam according to the two criteria outlined by Gibson and Ashby [28]. The first criteria is an inequality which identifies when a foam will experience elastic collapse (cell edge bending and stretching of the faces of closed cells) prior to the onset of plastic collapse (the struts of the cell yield and the membranes collapse). By definition elastomeric foams always meet this condition. For Novatein foams, this inequality (Equation 1) was never satisfied between the relative densities of 0.15 and 0.45 confirming that the foams demonstrated plastic behavior only.

$$0.05E_s\left(\frac{\rho}{\rho_s}\right)^2 < 0.3\,\sigma_{y,s}\left(\frac{\rho}{\rho_s}\right)^{3/2} \qquad (1)$$

Where: E_s is the elastic modulus of the solid (250 MPa), $\sigma_{y,s}$ the yield strength of the solid (4-7 MPa), ρ is the density of the foam (g/cm^3), and ρ_s is the density of the unfoamed solid (g/cm^3).

According to the second criteria the onset of densification occurs much earlier for elastomeric foams (relative density of 0.3) than plastic foams (0.5). Novatein foams with a relative density of 0.35 still demonstrated a steep plateau (Figure 5B) while foams of 0.45 appeared to have densified immediately. If the foams were elastomeric in nature, Novatein foams with a relative density above 0.3 should show densification behavior, which they do not. Therefore this criteria supports the conclusion that low density Novatein foams are not elastomeric and demonstrate plastic behaviour. Plastic behavior is more desirable for energy absorbing applications such as foaming and may enable the foam to be compressed multiple times before failure.

Effect of Relative Density

The shape of the compression curve also changes with relative density for lower density foams (Figure 5B) and the elastic modulus and compressive strength of the foams is affected accordingly. Novatein foams with low relatively densities (0.15) have a longer linear elastic region at low stress, as the relatively density increases the length of the linear elastic region shortens and the material increases in strength. When the relatively density reaches 0.45, the material does not demonstrate a plateau within 25% deformation and appears to immediately densify. At this point the material behaves less like a foam and more like a solid (a solid containing voids). Similar changes in

compression behaviour with relative density have been observed in polyurethane foams [32].

Low density polyurethane and polystyrene samples have also been included for comparison. The polystyrene sample quickly exceeds the linear elastic zone (at less than 5% deformation), with a flat plateau region while the polyurethane sample had a longer elastic region and a slightly inclined plateau. The behaviour of Novatein foams appears to shift between the two samples and their behaviours with relative density. Novatein foams with a relative density of 0.15 are similar in nature to the polyurethane sample, however at higher densities this behaviour becomes more similar to the polystyrene in comparison. While the density of Novatein foams is higher than polystyrene or polyurethane foams, these results suggest that foams can be manufactured for specific applications with desirable mechanical properties.

General Compressive Properties

Foams were conditioned prior to testing in accordance with ASTM standards to mitigate the effect of water which can alter the properties of biopolymers. As a result of conditioning, water was lost from the thermoplastic material (which acts as a plasticiser) and the matrix became more rigid in nature. The conditioned foams demonstrated elastic moduli between 1.3 - 3.8 MPa (Figure 6A) and compressive strengths between 200 – 600 kPa (Figure 6B). Greater values of compressive strength or elastic moduli correlated with higher foam densities. The rate of change in compressive strength vs relative density is steeper than for other foams reported in literature, for example PU and PVC. Likewise, the rate of change in the compressive modulus is also greater. However, the relative density of PU and PVC foams is an order of magnitude less than that of Novatein foams which may explain why these properties change at a greater rate.

The best comparison for the performance of these protein foams is foams made from thermoplastic soy protein isolate. These foams have been produced through a similar method and their densities ranged between 0.1 - 0.5 g/cm^3 [20]. The compressive strength of these foams was reported to be between 140 - 300 kPa, with a compression modulus of 1.7 - 4.6 MPa, which is very similar to Novatein foams and is comparable to other biopolymers.

Modelling Compressive Behaviour

The compressive properties of Novatein foams were modelled using the Gibson and Ashby's model as it was the best suited to the morphology of these foams which included un-foamed regions, a mixture of open and closed cells, a bimodal cell size distribution and elongated cells. For the purpose of modelling, the elastic modulus of the solid was set at 250 MPa and the yield strength of the solid was 8 MPa, based on previous work on Novatein [40]. Through non-linear regression, the parameters for the open and closed cell models for the elastic modulus were determined (Table 3). The predicted elastic modulus as a function of relative density is shown in Figure 6A. The closed cell model provided a slightly better fit, based upon sum of squared errors which matches the observed foam morphology.

The closed cell model for the linear elastic region (Equation 3) includes the open cell model (Equation 2) as the first term as well as a contribution factor, ϕ (the fraction of material in the cell edges). For the case presented here, the gas related term has been ignored for the closed cell model as many of the cells have incomplete cell walls and the pressure difference is expected to be small. Furthermore, all the foams were mixed mode containing both open and closed cells, suggesting that ϕ is not zero.

Table 3: Fitted model parameters where SSE is the sum of square errors. E is the elastic modulus of the foam (MPa), E_s is the elastic modulus of the matrix (MPa), σ the compressive strength of the foam (MPa), $\sigma_{y,s}$ the yield strength of the solid (MPa), ρ_s is the density of the unfoamed solid (g/cm^3) and ρ is the density of the foam (g/cm^3), and C_1, C_1', C_2 and C_2' are empirical coefficients.

			Elastic modulus			
Model			**C_1**	**C_1'**	**ϕ**	**SSE**
Open Celled	$\frac{E}{E_s} = C_1\left(\frac{\rho}{\rho_s}\right)^2$	(2)	0.2	-	-	25.0
Closed Celled	$\frac{E}{E_s} = C_1\phi^2\left(\frac{\rho}{\rho_s}\right)^2 + C_1'(1-\phi)\left(\frac{\rho}{\rho_s}\right)$	(3)	0.255	0.09	0.7	19.00
			Compressive strength			
Model			**C_2**	**C_2'**	**σ_s**	**ϕ**	**SSE**
Open Celled	$\frac{\sigma}{\sigma_{y,s}} = C_2\left(\phi\frac{\rho}{\rho_s}\right)^{\frac{3}{2}}$	(4)	0.54	-	8	-	0.188
Closed Celled	$\frac{\sigma}{\sigma_{y,s}} = C_2\left(\phi\frac{\rho}{\rho_s}\right)^{\frac{3}{2}} + C_2'(1-\phi)\frac{\rho}{\rho_s}$	(5)	0.57	1	5.7	0.7	0.105

The compressive strength was also modelled for both open and closed cells (Figure 6B). The closed cell model and open cell model both appeared to fit the data reasonably well. For the closed cell model, the fraction $\phi = 0.7$, was determined by modelling the linear elastic region and had a marginally lower sum of squared errors.

One of the limitations of these models is that they do not account for how the cells are arranged in the foam, the average cell size or the corresponding wall thickness. Therefore, foams of similar density can have very different morphologies, which affects their load bearing capacity and explains the variability observed in the experimental data. This effect is seen for foams with the same relative density (0.25), which have slight variation in their compressive properties. A foam of comparable density could appear more rigid (higher elastic modulus) if there are a few very thick struts amongst the foamed material. Likewise, a lower stiffness and compressive strength may occur if the foam was contained more open cells. The goodness of fit for both these models is therefore reasonable.

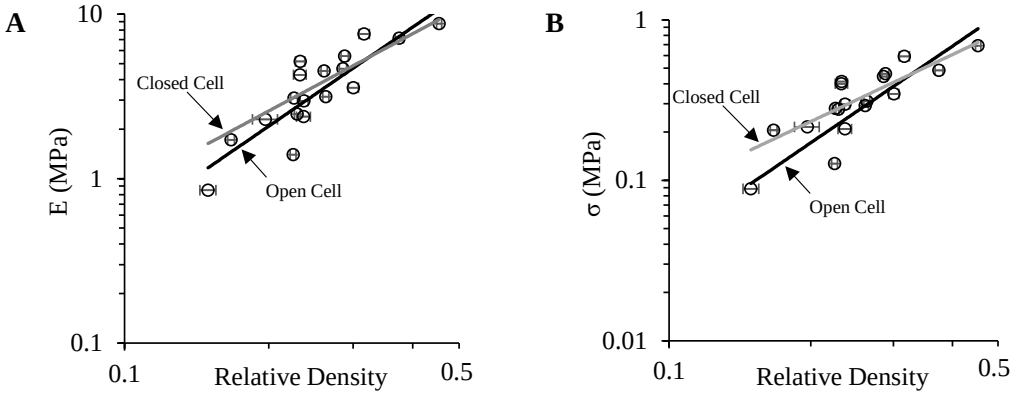

Figure 6: A Elastic modulus with open and closed cell models shown. **B** Compressive strength with open and closed cell models shown.

The models have also been noted to fail for very low or very high density foams (relative densities of 0.04 and 0.3 in rigid plastic foams). This is due to elastic collapse commonly preceding plastic collapse at very low densities and the inaccuracy associated with modelling foams as a regular arrangement of cubic cells [28]. At relative densities above 0.3, modelling the foam as a series of struts is no longer appropriate and the material should be considered as a solid containing voids.

These models are best suited to foams which have a regular arrangement of either open or closed cells. For irregular foams, with both open and closed cells such as Novatein, the behaviour could be closer to one of the two extremes or in-between, depending upon the contribution of the wall structures. In this case, the closed cell models appear to be the most appropriate fit indicating that the cell walls/faces, contribute to the compressive strength and elastic modulus

Cyclic Compression

Some polymeric foams demonstrate recovery after repeated compression allowing them to be cyclically loaded upwards of 100 times across their useful life. After repeated compression, Novatein foams regained the majority of their height within five minutes after compression (93-97%, Table 4) however, they did not always regain their compressive strength (Figure 7). Typically these foams could withstand two to three compression cycles before losing integrity. Figure 7A and C show the behaviour of a high and low density foam which have been repeatedly compressed. The figure includes the initial compression test, the result after five cycle and the cycle which demonstrated intermediate behaviour.

For the high density foam, cycles 1 and 2 were identical, however, a change in the shape of the compression curve was observed by the third cycle. This behaviour was reflected in the height of these samples (Figure 7B). The foam recovered most of its height between cycle 1 and 2 (97%) but then decreased at a steeper rate than the low density foam (Figure 7D, Table 4). The difference between the two samples was that the low density foam demonstrated intermediate behaviour earlier (by the second cycle) which was also reflected in the height recovery. Initially, between cycles 1 and 2 for the low density foam, the sample only recovered 93.5%, however for the following cycles, height recovery decreased a further 4.5%. I.e. the change is less, and all the damage done to the low density foam occurred in the first cycle. However, overall this change in behaviour is probably more significant for the higher density foams as the compressive strength of the low density foam is a third of the high density sample.

This is consistent with other plastic foams where non-recoverable deformation of the cell edges (plastic deformation/ yielding) and cell faces occurs such that compressive loads cannot be supported. Effectively the number of load supporting cell walls is reduced with each cycle and limits the applications of these foams to short lived applications.

Similar results have been observed for other cyclic loading of thermoplastic wheat gluten foams containing carbon nanotubes [41], which took a similar number of cycles to densify. Denser foams retained their ability to be repeatedly compressed longer than low density foams. This could be explained by higher density foams having a mixture of thicker cell walls or regions of unfoamed Novatein which continue to provide support after the rupture of finer walled cells. Low density foams have a larger cell size and thinner walls which are broken during the first compression of the foam.

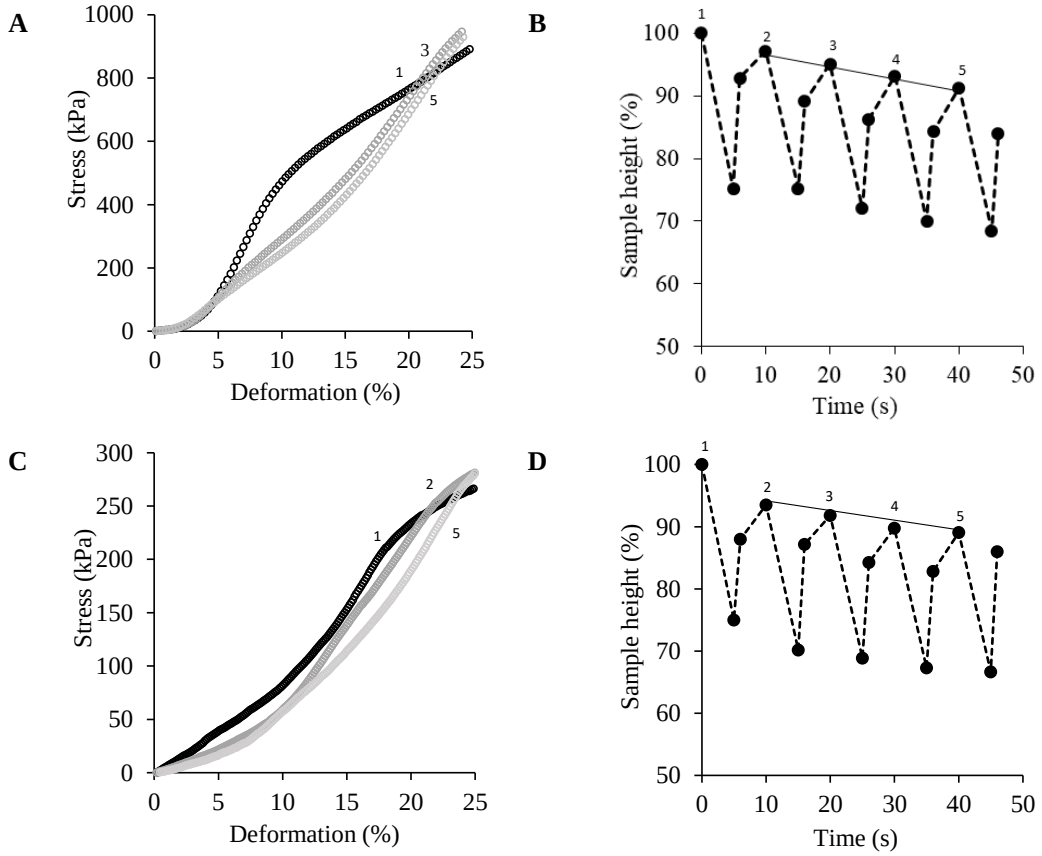

Figure 7: Repeated compression tests (**A** and **C**) and recovery (**B** and **D**). **A** and **B**: High relative density foam 0.35, **C** and **D**: Low relative density foam 0.15.

Table 4: Height recovery properties of Novatein foams by relative density.

	Repeat 1		Repeat 4		
Relative density	**Immediate recovery (6 mins)**	**End of the recovery time (10 mins)**	**Immediate recovery (36 mins)**	**End of the recovery time (40 mins)**	**Slope between points 2-5**
0.45	92.0 %	95.9 %	90.9 %	93.3 %	-0.087
0.35	92.8 %	97.1 %	84.3 %	91.3 %	-0.193
0.25	91.6 %	97.2 %	85.3 %	92.3 %	-0.163
0.15	88.0 %	93.5 %	82.8 %	89.0 %	-0.153

Dynamic mechanical analysis confirmed that, similar to other foams, modulus increased with increasing density (Figure 8A) [32,42]. There is also evidence of a thermal transition at about 105 °C, where the drop in storage modulus correlates with the end of the second transition observed using powder pocket analysis (Figure 2B). Below this temperature the storage modulus was relatively constant, except for the lowest density sample, where the onset of the drop in modulus corresponded to the first transition observed using powder pocket analysis. It was thought that this was due to their thinner wall structures, which were more affected by changes in temperature. Above 105 °C, only the highest density foams retained some stiffness, similar to unfoamed Novatein [43]. It was concluded that the rapid drop in modulus for low density foams was as a result of softening, not as a result of melting, as no evidence of this was observed in the morphology of the material after heating (Figure 8B).

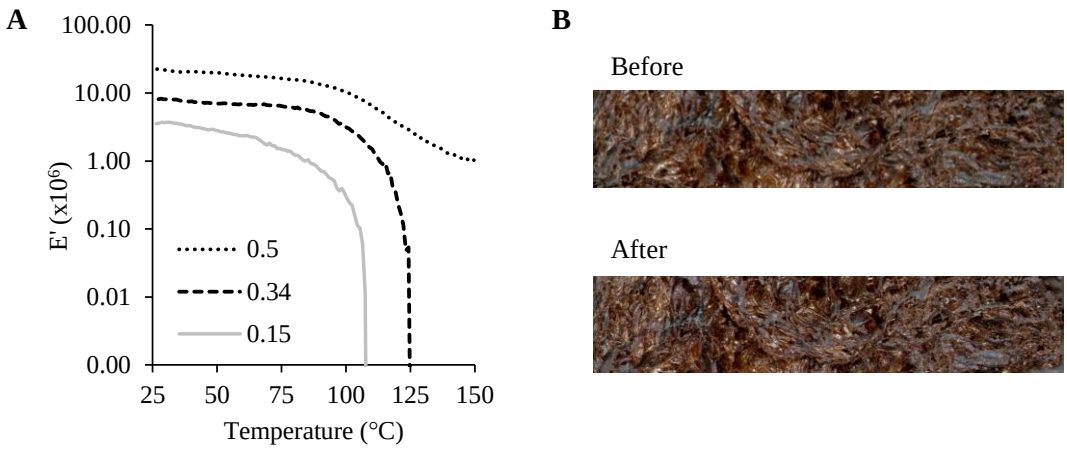

Figure 8: A Storage modulus of foamed bars during thermal scan. **B** Images of foam surface before (top) and after (bottom) thermal scan.

Conclusions

Novatein can be foamed only within a narrow temperature range, where higher temperatures produced lower density foams consisting of larger and more elongated cells. Matrix properties were unaffected by any plasticizer loss during foaming, showing a constant T_g, irrespective of density, however, low density foams did soften more severely at high temperature.

Foam morphology and density strongly affected compression behaviour, with low density foams being more elastomeric, while denser foams behaved more like a plastic foam. Low density foams experienced most damage during the first cycle under cyclic compression, while higher density foams could be compressed two to three times before densification, with each cycle causing new damage and a decrease in recovery. Models for open and closed cells successfully predicted the compression modulus and strength in the linear elastic region. The foams demonstrated a mixed mode morphology (open and closed cells) and an irregular distribution of cells, which explained the deviation from the models.

Lower density foams may provide a competitive alternative for foam packing material, however, the implication of these results is that the foams will be best used in a once-off or applications with a short useful life.

Acknowledgements

The authors would like to acknowledge the contributions of the Biopolymer Network Ltd (BPN), Aduro Biopolymers (Novatein® commercialization), and the funding received from the New Zealand Ministry of Business, Innovation and Employment (BPLY1302 contract).

References

[1] Pickering KL, Verbeek CJR, Viljoen C, Van Den Berg LE (2012) Plastics material. USA Patent US 20100234515 A1,

[2] Verbeek CJR, van den Berg LE (2010) Extrusion processing and properties of protein-based thermoplastics. Macromol Mater Eng 295 (1):10-21.

[3] Parker K, Garancher J-P, Shah S, Fernyhough A (2011) Expanded polylactic acid-an eco-friendly alternative to polystyrene foam. J Cell Plast 47 (3):233-243.

[4] Nofar M, Park CB (2014) Poly (lactic acid) foaming. Prog Polym Sci 39 (10):1721-1741.

[5] Garancher J-P, Fernyhough A (2012) Crystallinity effects in polylactic acid-based foams. J Cell Plast 48 (5):387-397.

[6] Kaisangsri N, Kerdchoechuen O, Laohakunjit N (2014) Characterization of cassava starch based foam blended with plant proteins, kraft fiber, and palm oil. Carbohydr Polym 110 (1):70-77.

[7] Mariam I, Cho KY, Rizvi SSH (2008) Thermal properties of starch-based biodegradable foams produced using supercritical fluid extrusion (SCFX). Int J Food Prop 11 (2):415-426.

[8] Pushpadass HA, Babu GS, Weber RW, Hanna MA (2008) Extrusion of starch-based loose-fill packaging foams: effects of temperature, moisture and talc on physical properties. Packag Technol Sci 21 (3):171-183.

[9] Salgado PR, Schmidt VC, Ortiz SEM, Mauri AN, Laurindo JB (2008) Biodegradable foams based on cassava starch, sunflower proteins and cellulose fibers obtained by a baking process. J Food Eng 85 (3):435-443.

[10] Tatarka PD, Cunningham RL (1998) Properties of protective loose-fill foams. J Appl Polym Sci 67 (7):1157-1176.

[11] Schwier C, Krishnaswamy R (2010) Polyhydroxyalkanoates (PHA) bioplastic packaging materials. Report, Metabolix Inc, Cambridge, MA,

[12] Dix SE, Anderson JR, Lindenfelzer ME (Nov 2013) Method of forming polymeric foam and related foam articles. USA Patent 20130303645,

[13] Szegda D, Tarverdi K, Duangphet S, Song J (2014) Extrusion foaming of PHBV. J Cell Plast 50 (2):145-162.

[14] Richards E, Rizvi R, Chow A, Naguib H (2008) Biodegradable composite foams of PLA and PHBV using subcritical CO_2. J Polym Environ 16 (4):258-266.

[15] Di Maio E, Mensitieri G, Iannace S, Nicolais L, Li W, Flumerfelt R (2005) Structure optimization of polycaprolactone foams by using mixtures of CO_2 and N_2 as blowing agents. Polym Eng Sci 45 (3):432-441.

[16] Salerno A, Di Maio E, Iannace S, Netti P (2011) Solid-state supercritical CO_2 foaming of PCL and PCL-HA nano-composite: effect of composition, thermal history and foaming process on foam pore structure. J Supercrit Fluids 58 (1):158-167.

[17] Mungara P, Zhang JW, Jane J (1998) Extrusion processing of soy protein-based foam. Polym Prepr 39 (2):148-149.

[18] Walallavita A, Verbeek CJR, Lay MC (2015) Blending novatein thermoplastic protein with pla for carbon dioxide assisted batch foaming. Paper presented at the The 31st International Conference of the Polymer Processing Society, Jeju Island, South Korea,,

[19] Gavin C, Lay MC, Verbeek CJR (2015) Extrusion foaming of protein-based thermoplastic and polyethylene blends. Paper presented at the The 31st International Conference of the Polymer Processing Society–Conference Papers, Jeju Island, South Korea,

[20] Jane J-l, Zhang SS (1998) Soy protein-based thermoplastic composition for foamed articles. USA Patent 5710190A,

[21] Gendron R (2005) Rheological behavior relevant to extrusion foaming. In: Thermoplastic Foam Processing: Principles and Development. Polymeric Foams, 1st edn. CRC Press, Boca Raton,

[22] Ramesh NS (2004) Fundamentals of bubble nucleation and growth in polymers. In: Lee ST, Ramesh NS (eds) Polymeric Materials: Mechanisms and Materials. 1st edn. CRC Press Boca Raton, FL, pp 81 - 119

[23] Saengow C, Giacomin AJ, Wú X, Kolitawong C, Aumnate C, Mix AW (2016) Bubble growth from first principles. Can J Chem Eng 94 (8):1560-1575.

[24] Nawaby AV, Zhang Z (2004) Solubility and diffusivity. In: Gendron R (ed) Thermoplastic Foam Processing: Principles and Development. Polymeric Foams, 1st edn. CRC Press, Boca Raton,

[25] Lee ST, Park CB (2014) Foam Extrusion: Principles and Practice.

vol Book, Whole, 2nd edn. Taylor & Francis, Boca Raton

[26] Michaeli W, Cramer A, Florez L (2009) Process and Process Analysis of Foam Injection Molding with Physical Blowing Agents. In: Lee ST, Scholz D (eds) Polymeric Foams: Technology and Developments in Regulation, Process and Products. Polymeric Foams Series CRC Press, Boca Raton. FL, pp 102-120

[27] Lee S, Kareko L, Jun J (2008) Study of thermoplastic PLA foam extrusion. 44 (4):293-305.

[28] Gibson LJ, Ashby MF (1997) Cellular solids: structure and properties, vol 2nd. vol Book, Whole. Cambridge University Press, Cambridge; New York

[29] Mills NJ, Zhu HX (1999) The high strain compression of closed-cell polymer foams. J Mech Ph Solids 47 (3):669-695.

[30] Chen L, Rende D, Schadler LS, Ozisik R (2013) Polymer nanocomposite foams. J Mater Chem A 1 (12):3837-3850.

[31] Christensen R (1986) Mechanics of low density materials. J Mech Phys Solids 34 (6):563-578.

[32] Saint-Michel F, Chazeau L, Cavaillé J-Y, Chabert E (2006) Mechanical properties of high density polyurethane foams: I. Effect of the density. Compos Sci Technol 66 (15):2700-2708.

[33] Zhu HX, Hobdell JR, Windle AH (2000) Effects of cell irregularity on the elastic properties of open-cell foams. Acta Mater 48 (20):4893-4900.

[34] Mohan VB (2010) Rheology and Processing of Novatein Thermoplastic Protein. University of Waikato, Hamilton, New Zealand

[35] Bier JM, Verbeek CJ, Lay MC (2014) Thermal transitions and structural relaxations in protein-based thermoplastics. Macromol Mater Eng 299 (5):524-539.

[36] Park CB, Baldwin DF, Suh NP (1995) Effect of the pressure drop rate on cell nucleation in continuous processing of microcellular polymers. Polym Eng Sci 35 (5):432-440.

[37] Filli M, Sjoqvist M, Ohgren C, Stading M, Rigdahl M (2011) Development and characterization of extruded biodegradable foams based on zein and pearl millet flour. Annu Trans NRS 19:1-7.

[38] Liu B, Jiang L, Zhang J (2011) Extrusion foaming of poly (lactic acid)/soy protein concentrate blends. Macromol Mater Eng 296 (9):835-842.

[39] Kuncir EJ, Wirta RW, Golbranson FL (1990) Load-bearing characteristics of polyethylene foam: an examination of structural and compression properties. J Rehabil Res Dev 27 (3):229.

[40] Bier JM, Verbeek CJR, Lay MC (2013) Thermal and mechanical properties of bloodmeal-based thermoplastics plasticized with tri(ethylene glycol). Macromol Mater Eng 299 (1):85-95.

[41] Wu Q, Sundborg H, Andersson RL, Peuvot K, Guex L, Nilsson F, Hedenqvist MS, Olsson RT (2017) Conductive biofoams of wheat gluten containing carbon nanotubes, carbon black or reduced graphene oxide. RSC Adv 7 (30):18260-18269.

[42] Rodríguez-Pérez M, Rodríguez-Llorente S, De Saja J (1997) Dynamic mechanical properties of polyolefin foams studied by DMA techniques. Polym Eng Sci 37 (6):959-965.

[43] Bier JM, Verbeek CJR, Lay MC (2013) Identifying transition temperatures in bloodmeal-based thermoplastics using material pocket DMTA. J Therm Anal Calorim 112 (3):1303-1315.

Factors Affecting Foaming

Part 2

5

Methods of Determining Chain Conformation and Protein Secondary Structure for Protein Thermoplastics

A literature review

Methods of Determining Chain Conformation and Protein Secondary Structure for Protein Thermoplastics

Abstract

Protein thermoplastics are materials derived from protein feed stocks which are converted to thermoplastics using chemical denaturants and plasticisers. Like conventional polymers, protein chain conformation will have implications for extrusion and injection moulding. Processing requires some disruption of the protein secondary structure, however residual secondary structures will still influence the ability of these materials to be used in certain applications such as film blowing and foaming.

In this review techniques commonly used to determine protein secondary structure are discussed. The review specifically focuses on X-ray crystallography, nuclear magnetic resonance (NMR), circular dichroism (CD), Fourier transform infrared (FT-IR) and Raman spectroscopy. While these methods are commonly used for determining protein structures, using them to analyse protein thermoplastics is challenging. However, they still provide insight for structural changes incurred from grafting, plasticisation and heat treatment. Where possible alternative uses of these techniques have been included.

The primary challenge of the above techniques is that in many cases they rely upon the protein being soluble. FT-IR and Raman spectroscopy are therefore the most appropriate methods due to their ability to analyse solid state materials, although care should be taken to ensure no interference occurs from additives when conducting protein secondary structure determination (PSSD). Many methods are available for PSSD for either Raman or IR spectra, which are outlined here. Ultimately irrespective of PSSD method used, these techniques can be used for estimating relative changes in protein thermoplastic materials.

Introduction

Proteins are naturally occurring biopolymers which can be turned into thermoplastics by extrusion and subsequently injection moulding. During the process protein structure is disrupted through the use of chemical denaturants and plasticisers. The remaining structure has implications for processing analogous to the effect of chain conformation in polymers. During thermal processing protein chains denature, unravel and align with flow providing an opportunity for these chains to rearrange and form new bonds [1]. Therefore reliable methods for determining the secondary structure of the protein and the changes which occur following blending, extrusion and any subsequent processing are critical for understanding their impact on processing and resulting thermoplastic properties.

The secondary structure of proteins has been studied extensively as well as their response to heat treatment and stress. Techniques commonly used to determine the secondary structure include circular dichroism (CD) [2-4], nuclear magnetic resonance (NMR) [5-8], X-ray crystallography [9, 10], Fourier transform infrared (FT-IR) [11, 12], and Raman spectroscopy [13-15]. However, these may not all be applicable to assessing the conformational changes which occur during bioplastic production where the material is in a solid state and often not soluble.

This review will provide the reader with an overview of how each of these techniques provides information on protein secondary structure and/or the structure of a protein thermoplastic and, the difficulties associated with sample preparation and data analysis. It focuses upon the use of FT-IR, the most commonly used technique and highlights some of the advantages and disadvantages of this method.

Protein Structure

Proteins consists of primary, secondary, tertiary, and quaternary structures. Primary structure is the sequence of amino acids in the protein prior to folding, while secondary structure refers to the formation of α-helices, β-sheets, random coils and β-turns (Figure 1) which occur through hydrogen bonding and is the focus of most spectroscopy techniques. These arrange to form the

tertiary structure and multiple proteins group together to form quaternary structures. The formation of these structures is influenced by the amino acid sequence. Alanine, leucine, methionine, glutamine and glutamic acid, arginine and lysine promote α-helices, while isoleucine, phenylalanine, tryptophan, valine, tyrosine, threonine and cysteine promote β-sheets [16].

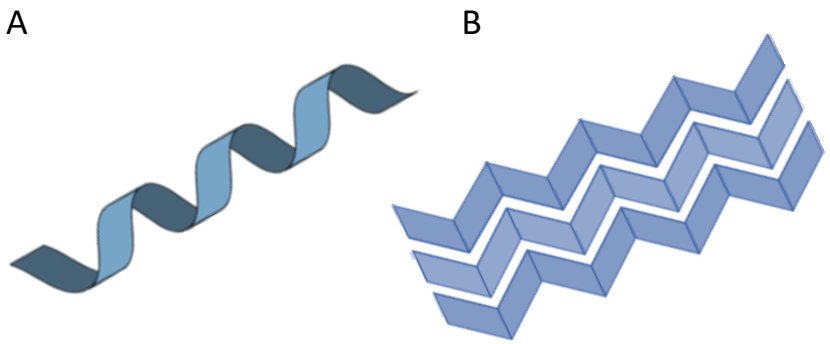

Figure 1: Common protein secondary structures. A. α-helices and B. β-sheets

5.1 X-ray Crystallography and X-ray based Techniques

NMR and X-ray crystallography techniques are useful when high resolution (nm scale) detail is required for protein conformation [10]. While these methods are the two most common for structural determination in proteins [10], in applications where high resolution information is not required (bioplastics) it is difficult to justify their application as they are very time intensive.

X-ray crystallography requires a highly ordered protein crystal to form from solution to achieve a diffraction pattern that can be used to determine protein structure. X-ray crystallography studies are usually used as the bench mark when defining the structure of a protein, although this method relies heavily upon the crystallised structure being representative of the protein in its native state. Establishing the correct conditions for crystallisation to occur is time consuming and requires further refinement of these conditions in order to achieve a good X-ray diffraction pattern [10]. In many cases it is difficult to crystallise proteins which have been glycosylated or contain flexible structures [9] and this method is not suitable for impure protein fractions.

Most bioplastics consist of more than one protein or protein subunit in a highly denatured state, therefore achieving a highly ordered crystal for protein secondary structure determination is impossible. However this does not prohibit other X-ray based techniques including powder X-ray diffraction such as wide angle (WAXS) and small angle (SAXS) X-ray scattering providing valuable information such as crystallinity and protein chain alignment.

X-ray diffraction has been used to show how glycerol affects the crystallinity of soy protein isolate and agar films [17] where adding glycerol led to a more amorphous film structure. In another study the differences between zein and thermoplastic zein following the addition of 25 wt% polyethylene glycol were analysed. Plasticisation resulted in a reduction of the ratio of two characteristic peaks at 9.5 and 20° 2θ compared to unplasticised material (Figure 2). This was attributed to the plasticiser disrupting inter-helix packing (9.5°) but not intra-helical packing (20°) within zein [18].

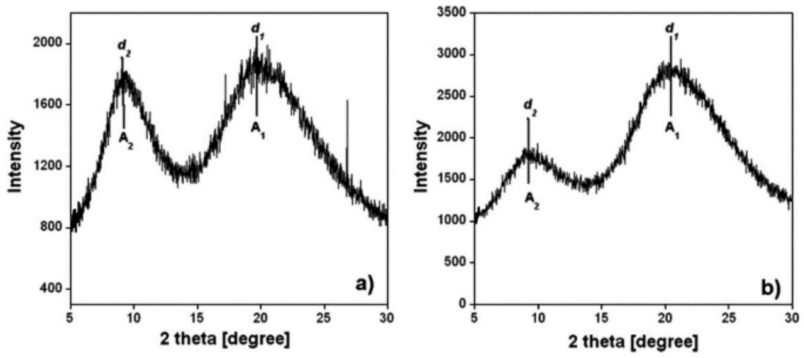

Figure 2: X-ray patterns of zein powder (a) and thermoplastic zein (b). [18]

Similar results to the above were observed in silk fibroin membranes [19]. In this case silk contains a high proportion of β-sheets and the peak at 20° was assigned to β-sheet structures. XRD is unable to distinguish between bonding in an α-helical configuration or β-sheet configuration so this technique is limited for proteins which contain a mixture of structural motifs. However it is commonly accepted that the peak at 9.5° relates to inter structure packing d-spacing (9.5 Å) and the other peak at 20 ° is intramolecular packing (4.5 Å) for both structures [19]

WAXS was used to examine structural changes in wheat gluten (WG) where widening of the second peak (intramolecular bonding) was observed with increasing urea content. At higher urea content the peak at 4.5 Å shifted to 4.2 Å, a smaller packing distance which suggested the urea unfolded the protein enabling aggregation to occur resulting in a more highly packed structure [20]. SAXS was used to study changes to the hexagonal closed packed structure with urea addition both perpendicular to and with extrusion direction. Urea swelled the structure with an increase in inter-domain distance (Figure 3), behaving like an internal plasticiser rather than an external one like glycerol [20].

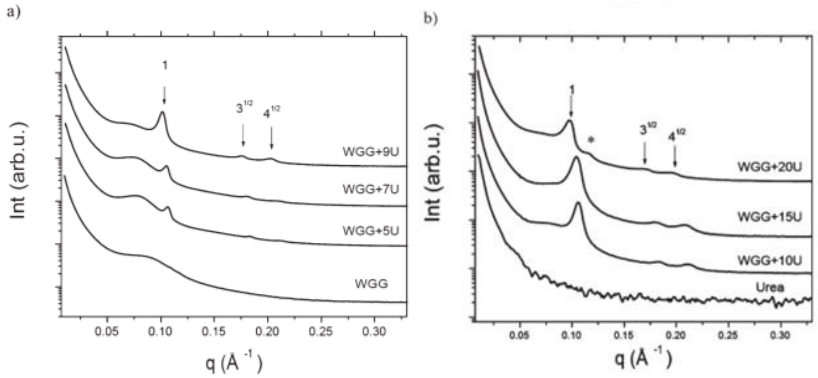

Figure 3: SAXS curves from WG films without and with urea with the X-ray beam perpendicular to the film plane [20].

In the same study SAXS also showed wheat gluten (containing urea) denatured at 55 °C where the HCP structure was disrupted, seen as a loss of peak intensity at 0.1 Å $^{-1}$ (reciprocal d-spacing). WGG films without urea did show a HCP structure although the peak was much broader in nature. Upon heating the peak shifted to lower q values indicating a more tightly bound structure.

SAXS is also useful for observing intercalation when protein systems are blended with other components such as clay in bionanocomposites. When clay was added to thermoplastic zein (TPZ) at 5 and 10% by weight the peak corresponding to the clay basal spacing shifted to a lower angle indicating that the basal spacing increased, showing it been intercalated by the protein [21].

WAXS and SAXS have also been used to observe the differences in structure of zein-oleic acid in cast and stretched resin dough films [22]. Adding oleic acid increased the a-helix diameter compared to zein, but no helix orientation was

observed for cast and stretched films, which was unexpected as chains normally align in the direction of pull.

5.2 Nuclear Magnetic Resonance

NMR applies high magnetic fields to a molecule causing alignment of the magnetic moments (or spins) of individual nuclei to the magnetic field direction. Radio waves are then passed through the material which shift the nuclei into a different state. Each nuclei will respond to a different frequency of radio waves which is characteristic of the atom and its environment [6]. As the molecules return to their original state they emit a small electromagnetic wave which is measured by the spectrometer.

The information gathered from NMR is useful in determining the structure of small molecules but in reality the determination of an unknown structure from NMR is very difficult [7]. Also the interpretation of an NMR spectra into a protein secondary structure is convoluted and time intensive as it requires the chemical shifts to first be assigned to particular residues [8]. This method has not widely been applied and works best for low molecular weight molecules [5] less than 15 kDa [23]. This technique will not be further described here as it would be difficult to apply to protein thermoplastics which consist of very large macromolecules (e.g. zein up to 45 kDa, wheat glutenin 250 kDa, and soy 180 kDa) [1] and, whose structure is significantly altered during protein extraction (e.g. zein) or processing (crosslinking and aggregation). However, some success has been reported for estimating the secondary structure of silk biomaterials produced from glycerol using solid state NMR [24].

Aside from protein secondary structure NMR can provide other information relevant to protein thermoplastics. For soybean protein extruded with water, proton NMR has been capable of observing the distribution of water within the resulting material [25] (Figure 4).

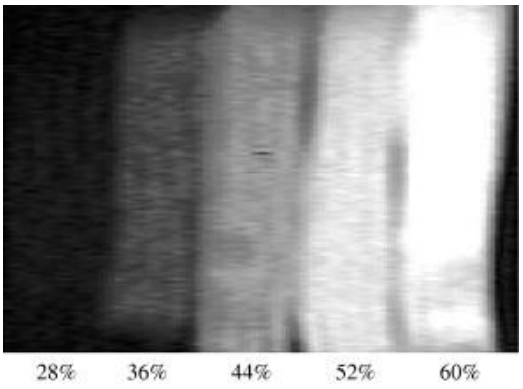

Figure 4: Proton density images of TSP extruded at 150 °C cooking temperature and 28%, 36%, 44%, 52% and 60% moisture content.[25].

NMR has also been used to confirm structural changes in chicken feathers arising from cyanoethylation where modified and unmodified feathers were later blended with glycerol and compression moulded. In this case the NMR spectra added very little to this study as the cyanoethylation was also confirmed by FT-IR [4]. Cyanoethylation reduces the glass transition of the chicken feather protein, such that the feathers melt during compression moulding to form a transparent material.

The combined use of NMR and FT-IR in the previous study is not unique. Together they have also been used to confirm grafting of acrylates onto soy proteins. This modification with methyl, ethyl, butyl acrylates and methacrylates enabled the functional soy protein isolate to be compression moulded without further additives [26].

5.3 Circular Dichroism

Circular dichroism (CD) analyses the interaction of chromophores with polarized light. It is used to study proteins in solution and is mainly used for structural studies of native proteins in biological environments [3, 27]. However, it can also detect conformational changes due to pH or temperature.

The principle of this technique is explained well by Kelly, Jess and Price [27]. This method uses a plane of polarised light, consisting of two circularly polarised components L (anticlockwise rotation) and R (clockwise rotation). This circularly polarised light is created when two linear polarised sources exist at a 90 degree angle to one another and are out of phase by 90 degrees.

Upon interaction with an optically active structure (chromophore) a difference in absorption between the L and R components will occur causing the radiation to appear elliptically polarised when they recombine [27]. A chromophore is said to be an optically active molecule with its activity arising from either intrinsic chirality, covalently linked to a chiral centre or it exists in an asymmetric environment due to the 3D structure of the molecule. In proteins the optically active groups are the amide bonds within the peptide backbone and the aromatic side chains [3].

Most CD instruments operate in a mode called modulation, where the incoming radiation is switched between L and R components. This is achieved by alternating the electric field in the modulator through which the plane of polarised light passes. The difference in the absorbance of the L and R components is typically reported in terms of ellipicity (θ) where $\theta = \tan^{-1}(b/a)$ where a) and b) describe the major and minor axis of the resulting ellipse. $\theta = 32.98\ \Delta A$ (Figure 5).

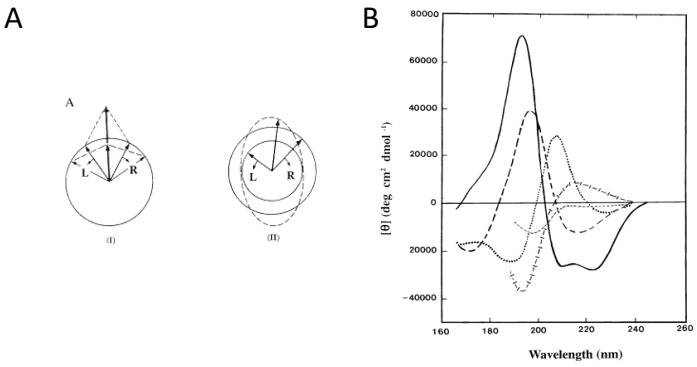

Figure 5: A. Origin of the CD effect. (A) the left (L) and right (R) circularly polarised components of plane polarised radiation: (I) the two components have the same amplitude and when combined generate plane polarised radiation (II). The components are of different magnitudes and the resultant (dashed line) is elliptically polarised. (B) Far UV CD spectra associated with various types of secondary structure. Solid line α-helix; long dashed line, anti-parallel β-sheet; dotted line, type I β-turn; cross dashed line, extended 31 – helix or poly(Pro) II helix; short dashed line, irregular structure both reproduced from [27]

CD is predominantly a solution technique but there are solid state CD techniques to analyse single crystals, pellets, materials in potassium bromide and films [2]. While solid state CD is reasonably new it overcomes some of the problems of CD in solution:

- The need for a highly pure sample (greater than 95%) as determined by HPLC, mass spectroscopy or gel electrophoresis
- Potential contamination from other optically active molecules including nucleotides, and buffers [3].
- The need to consider buffer and protein concentration [3] for signal strength.

Most methods of secondary structure determination rely upon datasets comprising of the CD spectra of proteins where their secondary structures have been established by X-ray crystallography.

Methods of extracting structural information include: multilinear regression (G&F, LINCOMB, MLR), singular value decomposition, ridge regression (CONTIN), convex constraint analysis (CCA), neural network (K2D), and self consistent methods (SELCON) [3, 27]. These methods are quite complex and will not be further discussed as they are outside the scope of this review.

5.3.1 How Secondary Structure Changes are Observed in Circular Dichroism

CD is able to give quantitative estimates of secondary structure by examining regions below 240 nm for the peptide bond, 260-320 nm for aromatic side chains and weak bands at 260 nm for disulphide bonds [8]. CD can identify α-helices, distorted α-helices, regular β-strand, distorted β-strand, β-turns and disordered structures [28]. Antiparallel β-sheets have negative bands at 218 nm and positive bands at 195 nm. Disordered proteins have low peaks at 210 nm and negative bands at 195 nm. CD is also able to identify the poly-L-proline II (PII) helix found in collagen and some short globular proteins [3]. All amino acids are optically active except glycine [29].

Khrapunov (2009) outlined limitations of CD for protein secondary structure determination [30]. These were the poor quality of reference crystallographic

structures in some CD databases, the inconsistency of protein quality used in solution and crystallographic studies, and the intrinsic variation between instruments which has not been accounted for [30].

As CD is predominantly a soluble protein technique it has not been extensively used to characterise protein thermoplastics. It can however be used to characterise soluble proteins as feed stocks or the soluble fraction of a solid material. This has been applied to the production of whey protein isolate extrudates. When extruded at 75°C the material was observed to denature and through extrusion at 100°C the structure became mainly random coils [31]. This is the opposite of what thermal treatment does to other proteins where they tend to experience protein aggregation and crosslinking.

In another extrusion system CD has been used to assess structural changes in zein which was passed through an extruder multiple times. Using the magnitude of the peaks at 208 nm (α-helices) and 222 nm (β-sheets) it was shown that these structures increase after a first pass through the extruder, however after three passes a loss of structure occurred [32]. The authors take care to point out that this technique only analyses the soluble fraction after each extrusion and that this analysis relies upon protein structure being unaltered by the process to make them soluble.

Lastly CD has also been used to confirm modification of zein by γ-irradiation. CD measurements showed that with increasing radiation dose the α-helical and β-sheet content decreased in favour of β-turns and other structures [33]. In addition to these structural changes irradiating zein improved the water barrier properties of zein films.

5.4 Fourier Transform Infrared Analysis (FT-IR)

The benefits of FT-IR include sample type diversity (solids and liquids primarily), and the small amounts of sample required, down to 10 μg and a short step time (1 μs) for analysis [11].

FT-IR works by the excitation of vibrational motions in the molecule of interest. This typically occurs when the frequency of the IR light and the vibration are equal. According to Andreas Barth [11] IR is sensitive to inter and intra

molecular bonding as the strength and polarity of the bond affect the probability of absorption. A typical IR spectra is reported against the inversed wave number (cm^{-1}) (Figure 6). This is used as it is proportional to the energy associated with that transition. Raman is the other vibrational spectroscopy technique which is commonly used, however Raman spectra is a report of scattering by measuring the difference in incident and scattered radiation [8].

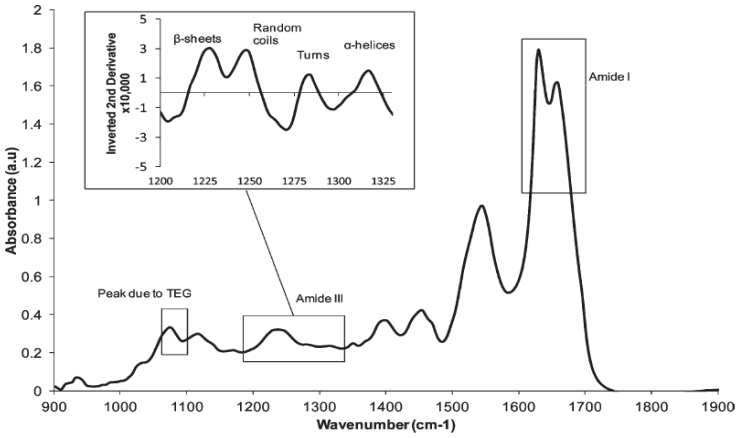

Figure 6: Example spectra of Extruded Novatein (derived from blood meal) from a single 5 µm spot on a mapped grid [34].

The physical mechanism through with FT-IR works involves beam splitting such that when the FT-IR beam passes through the sample it is recombined with light which bypassed the sample. Constructive and destructive interference occurs depending upon the path length of each beam. By altering the distance of the movable mirror the light intensity will change resulting in an interferogram. This is then converted to an IR spectra through a Fourier transform [11].

5.4.1 How Secondary Structure Changes are Observed in FT-IR

In an IR spectrum certain regions are associated with protein structures. The most commonly known regions are Amide I (1700-1600 cm^{-1}), Amide II (1510 and 1580 cm^{-1}) and Amide III (1330-1180 cm^{-1}) although other regions including Amide A (3225 and 3280 cm^{-1}), Amide B (3100 cm^{-1}) and Amide IV-VII also exist [8, 35]. The Amide bands I-III are associated with particular types of protein bonding. The Amide I consists of 80% $C = O$ bonding, therefore the Amide I measures the behaviour of the protein backbone. The Amide II is

influenced by N − H bonding (60%) and C-N stretching (40%) and the Amide III by N − H bonding (30%) and C-N stretching (40%) [8].

Within these bands individual wave numbers or ranges have been assigned to certain secondary structures. Protein secondary structure determinaton (PSSD) is most commonly carried out using the Amide I (1700-1600 cm^{-1}) region using the peak assignments outlined in Table 1. However Murayama and Tomida [36] discuss the challenges of using the Amide I region for PSSD and highlight the tendency for imperfect assignment of protein bands and the deconvolution of the spectra into the component bands as particular challenges (this will be discussed later). Li, Zhang and Ma [37] also highlight the interference of water with the Amide I band . Deuterated water can be used to overcome this interference although care must be taken as this shifts the location of the Amide regions to lower wave numbers [38].

Table 1: Peak assignments in Amide I in solution

Conformation	Wave number
α-helix	1650-1657
Antiparallel β-sheet	1612-1640
	1670-1690
Parallel β-sheet	1626-1640
Turn	1655-1675
	1680-1696
Unordered	1640-1651

5.4.2 Use of Amide III Region during Structural Studies of Proteins

Cai and Singh [39] argue that PSSD using the Amide III band may be better than the Amide I as it avoids water interferences. Band assignments for this region are reported below (Table 2).

Table 2: Peak assignments in Amide III [40].

Conformation	Wave number
α-helix	1330-1295
β-turns	1295-1270
Random coils	1270-1250
β-sheet	1250-1220

5.4.3 FT-IR Sample Preparation, Measurement and Interpretation

FT-IR is capable of working with both solid and liquid samples in multiple modes. This review will cover the use of transmission, attenuated total reflectance and synchrotron vs. globar light sources. It focuses mainly on the application of IR to solids in the dry state.

Transmission mode is the traditional method of IR spectroscopy. In transmission the IR beam passes through the material which is commonly embedded in a KBr disk or compressed between two IR transparent windows [12]. Attention must be paid to the Amide regions, while collecting the spectra as it can become saturated if the sample concentration is too high in the KBr disk or the sample is too thick between the IR transparent windows.

Attenuated total reflectance (ATR FT-IR) is more complicated and depends upon the refractive index of the crystal and the material. The ATR crystal is made from an IR transparent material such as ZnSe, diamond, silicon or germanium [12]. The configuration is such that at a critical angle an evanescent wave is formed which propagates into the material between 0.5-2 μm. The absorbance spectrum is therefore a subtraction of the signal from the IR light and what is reflected.

One of the main benefits of ATR is that it does not require complicated mounting procedures. The method is still highly sensitive for detecting changes in protein conformation and has found application in plastics and identifying protein based materials. ATR has been used to identify the difference between true tortoiseshell and horn and their imitations. Paris, Lecomte and Coupry [41] used ATR to study the protein configuration in the Amide I region and PSSD was conducted using the second derivative and peak fitting method. ATR has also been used to study conformational changes in

bread dough using the Amide III region from a globar source [39]. Peaks were identified using the second derivative whose intensity was shown to change during mixing with an increase in the peak intensity for α-helices, β-turns and β-sheets and a decrease in intensity for random coils. In this study only one peak was studied for each conformation as the second derivative only demonstrated four main peaks with a fifth observed around 1305 cm^{-1} which was unassigned but likely to be α-helices. Similar changes have also been observed in gluten when heated. Georget and Belton [42] used the Amide I region of spectra obtained through ATR mode to investigate the effect of heat and water content on gluten. Above 40°C significant changes to the protein structure occurred (exact changes not specified), which were not permanent at low moisture contents. When heated to 85°C with a water content of 47%, these changes became less reversible.

In many cases lab scale IR machines (globar light sources) are sufficient to provide adequate signal for secondary structure determination but the signal to noise ratio must always be considered. The Amide I is most commonly used for PSSD from these sources as the Amide III can experience noise. Achieving a spectrum in the Amide III for secondary structure analysis can be challenging and may require using Synchrotron light which is 1000 times brighter. Another benefit of Synchrotron light is the ability to spatially map samples similar to IR microscopy. This technique has been very widely applied with one particular study investigating the structure of feed protein sources including feather, wheat, oat and barley [43].

5.4.4 Estimates of Protein Secondary Structure by FTIR

One of the challenges with FT-IR analysis is the deconvolution of the spectra to enable the relative proportions of each structure to be obtained. Popular methods include Fourier self-deconvolution (FSD) and the second derivative method with peak fitting (Figure 7). However, these methods do not necessarily provide the same result. The two methods are compared by Dong [35] for determining the structure of β-lactoglobulin where FSD gave 50.6% β-sheets, 10.5% α-helices 20.4% β-turns and 18.5% unordered structures [35], while the second derivative method gave 54.5% β-sheets, 9.4% α-helices, 19.2%

β-turns and 16.9% unordered. Dong reports that both of these methods agree with X-crystallography analysis which reports 53 % β-sheets and 7% α-helix [35].

Attempts to deconvolution of a spectra using FSD requires two parameters: the half bandwidth (FWHH) and enhancement factor (k). Altering either of these alters the deconvolution result including the total number of bands observed and their position as well as generating artefacts (Figure 7B) [35]. The advantage of the second derivative method is that there is no need to choose values for k and FWHH (Figure 7A) and the peak intensity of the second derivative is related to the original intensity [35].

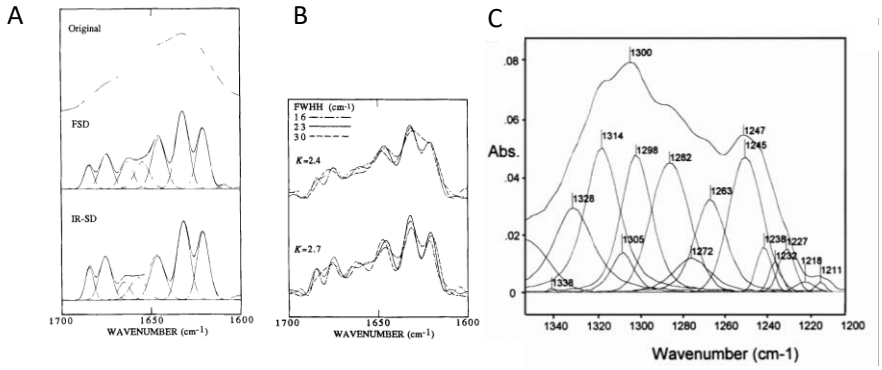

Figure 7: A. The original, Fourier self-deconvoluted and inverted second derivative spectra of β-lactoglobulin. Top: the original spectrum, middle: the curve fitted FSD spectrum (half bandwidth 23cm-1, K 2.7, Bottom: curve fitted inverted second derivative spectrum. B. Effects of input parameter variation on the Amide I spectrum of β-lactoglobulin by FSD. A and B reproduced from [35]. C. Deconvolution of BSA spectrum in the Amide III region from [40].

Multiple peaks have been observed during deconvolution of the Amide III region for recombinant human albumin with 8-9 Gaussian curves fitted to the region (k=2.7) [44] and bovine serum albumin has had up to 11 assigned to peak structures (Figure 7C) from spectra obtained using bench top ATR (k=2.0) [40]. Deconvolution of the Amide I area can overestimate structures if the absorptions corresponding to tyrosine, phenylalanine, glutamine, arginine and lysine are not corrected for [45].

Using the second derivative and inverted peak heights to identify protein structures has been applied to gluten [46] and blood meal [34]. The

advantages of this method include removing the need for baselining which may not be constant in mapped samples (discussed later) and an improvement in resolution of overlapping spectral bands. Narrow peaks will however demonstrate a higher intensity which may not be representative, noise may be introduced through side lobes on either side of the main peak [9] and the peaks need to be sufficiently resolved for the method to work [47].

Statistical methods also exist for PSSD which use the secondary structure of known proteins to assist with fitting [8, 12].

5.4.5 Examples of IR Used with Bioplastics for Secondary Structure

FT-IR has been used to determine the secondary structure of different zein powders. Oliverio, Maio and Iannace [18] highlighted the natural variation in protein feed stocks with the peak area associated with α-helices varying from 145 to 230, while the peak position also varied within a 5 cm^{-1} range. More importantly their work showed a consistent reduction in β-sheet content for thermoplastic zein. A greater proportion of α-helices to β-sheets reduced the elongational viscosity of the blend improving processabilty of these materials into films.

Wheat gluten formulations containing urea were shown to be more processable during sheet extrusion [48]. FT-IR analysis concluded that native gluten has a peak maximum in the Amide I region at 1644 cm^{-1} correlating to random coils. Following dough production the peak for α-helices is most prominent and after extrusion the β-sheet peak is most pronounced. Extrudates containing urea have a pronounced peak between 1630-1620 cm^{-1} identified by the authors to be β-sheets, but it could also be urea interference as that also contains the same C=O structure as those used in the Amide I region for PSSD.

Structural changes in feather keratin, egg albumin, wheat gluten and lactalbumin mixed with glycerol and pressed into films has been studied by ATR. PSSD was conducted through deconvolution of the Amide I through Gaussian peaks and showed that the protein conformation was more likely to

change if the protein contained a low amount of cysteine and were more polar overall [49].

FT-IR has also been used to examine other changes in bioplastics which can be examined from the same spectra making the technique very powerful. For example FT-IR has been used to study the role of acetamide (CH_3CONH_2) in soy protein plastics. Acetamide is similar to urea, however it has a CH_3 whereas urea has another NH_2 group, and therefore gives a peak within the Amide I region. Liu and Zhang studied the effect that acetamide had on the Amide I region in KBr. They noted that compression moulded soy protein isolate had a peak at 1652 cm^{-1} which was shifted to 1660 cm^{-1} when acetamide was added indicating bonding between the C=O of the protein and the NH_2 of the acetamide [50].

In another study when soy protein was mixed with ethylene glycol and compression moulded, ATR showed a decrease in two peaks at 1040 cm^{-1} and 1084 cm^{-1} indicating intermolecular hydrogen bonding between the carbonyl and N-H groups of the soy protein isolate and the hydroxyl groups on ethylene glycol [51].

ATR with FSD has been used to study the effect of the extraction method on kafirin during extraction and drying. Two main peaks were observed in the IR spectra at 1620 (α-helices) and 1650 cm^{-1} (β-sheets) in the Amide I region. The authors of this study noted that there was the potential for overlapping peaks from random coils and α-helices during peak assignment meaning that these could not be sufficiently resolved for PSSD [52]. Thermal drying increased β-sheets relative to α-helices compared to freeze drying. due to protein aggregation [49]

5.4.6 Application of FT-IR to Blood Meal Protein and Novatein Thermoplastic

FT-IR has been used to study structural changes in Novatein which contains blood meal, water and urea. Urea and water interfere in the Amide I region preventing its use for PSSD. The Amide III region combined with the second derivative peak height method was used for PSSD where four peaks were

assigned to α-helices, β-sheets, β-turns and random coils. Relative proportions of these structures have been determined by using ratios based upon relative peak heights. The origin of this method is outlined in [34].

The spatial distribution of ordered and disordered structures in blood meal, pre-processed, extruded, injection moulded and conditioned Novatein has been studied using Synchrotron FT-IR in transmission mode [34]. Blood meal was estimated to contain 24% α-helices, 35% β-sheets and 41% disordered structures (turns and random coils combined) [34]. During extrusion and injection moulding, heat exposure increased the proportion of β-sheet compared to pre-processed Novatein [34]. The spatial distribution of triethylene glycol (TEG) (Figure 8A) was also examined using the total area under the peak at 1040-1090 cm^{-1} (C-O-H bonding in TEG) [34]. Heating freeze dried pre-processed NTP to 50, 70, 90, 110 and 130 °C increased β-sheets content while decreasing disordered structures (Figure 8B), with an increase in α-helices and β-sheet clusters [53]. Heating also induces TEG migration further increasing β-sheet structures [54].

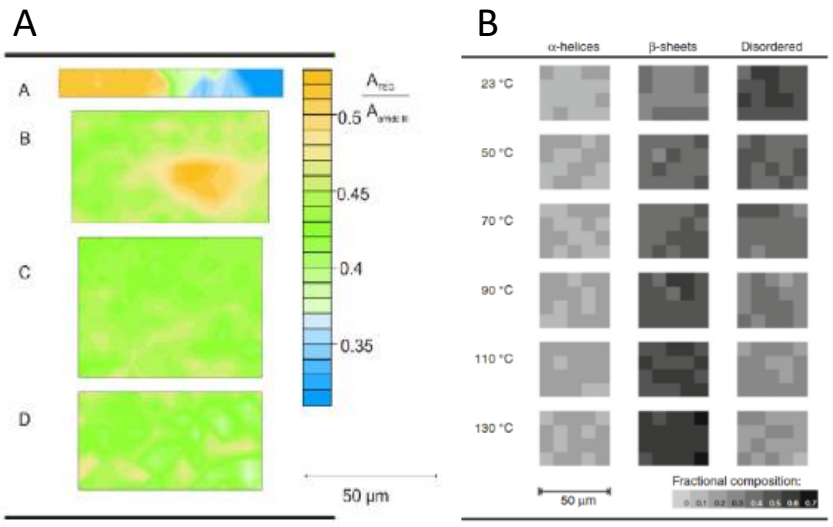

Figure 8: A. Ratio of Peak area for TEG relative to Amide III in A) Blood meal, B) Pre-processed NTP, C) extruded NTP, D) Conditioned NTP from [34]. B. Effect of temperature on the secondary structure of PNTP, from [53].

Spatially resolved Synchrotron FT-IR has also been used to examine differences in blood meal and blood meal decoloured with peracetic acid (PAA) [16]. The differences in structure between the perimeter and core of blood meal and decoloured blood meal particles were examined (Figure 9A). Blood

meal was heterogeneous with structures randomly distributed but decoloured blood meal had lower β-sheets at the surface. The effect of sodium dodecyl sulphate [55] and triethylene glycol on chain mobility has also been examined for decoloured blood meal materials [56]. SDS and TEG homogenized secondary structure distribution, SDS increased α-helices and decreased β-sheets and β-turns, while SDS and TEG combined reduced α -helices and β-sheets and increased random coils [55].

The primary alcohol group (C-O-H) to Amide III ratio is an effective tool for examining the effect of polyol plasticisers (glycerol, ethylene glycol, propylene glycol and TEG) on their distribution in Novatein. In this case FT-IR was used to assess phase distribution and secondary structure which showed the creation of more random structures upon the addition of TEG [57].

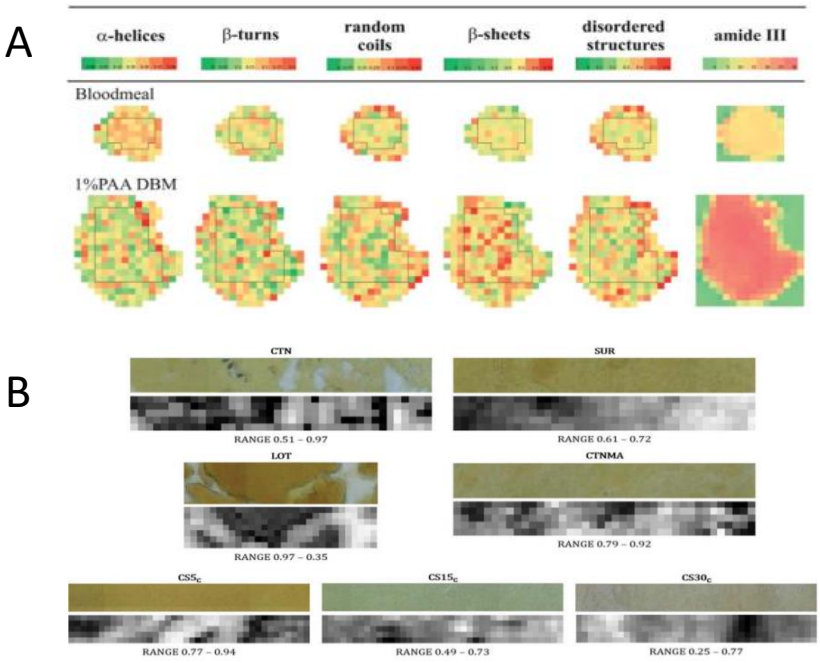

Figure 9: A. Fractional composition of protein secondary structures for blood meal and decoloured blood meal produced through a 1% peracetic acid solution [16, 58]. B. Maps showing phase distribution of Novatein and polyehtylene, from [59].

FT-IR also informed the fracture mechanics of Novatein and polyethylene (PE) blends where filaments were observed on the fracture surface. The proportions of Novatein and PE were determined using peaks outside the Amide III area within the 3800-2800 cm^{-1} region. Once the proportion of the

PE phase had been established (Figure 9B), a characteristic spectra normalised to the relative amount was subtracted from the combined spectra to provide the corrected Novatein spectra for a particular point. Secondary structure analysis was then performed as previously outlined [59].

5.5 Raman Spectroscopy

Raman spectroscopy provides information on protein secondary and tertiary structure relative to model compounds including amino acids and peptides [14]. This method involves using a single monochromatic light source (laser) to irradiate a sample. Interaction with the sample scatters a small amount of light that has a corresponding frequency shift according to the vibration in the molecule it interacts with. As the frequency of the laser is known the frequency shift can be back calculated to give a Raman spectrum [13, 15]. The Amide I and Amide III bands are strong in Raman spectroscopy while the Amide I and Amide II bands are strong in FT-IR [38]. Amide I occurs within the 1630-1690 cm^{-1} region while Amide III is in the 1225-1275 cm^{-1} region (Table 3). Deconvolution of the spectrum is conducted using the same methods as described for IR above. Water does not interfere with the Raman spectra which is an issue for FT-IR [60], but protein fluorescence can be a challenge [13]. Resonance Raman spectroscopy is used to study chromophore vibrations such as heme within porphyrins [15] which can be collected on the same spectrometer (but not discussed in this review).

Table 3: Peak assignments in Amide I in Raman Spectroscopy

Conformation	Amide I	Amide III
Anti-parallel β pleated sheet	1670	1235
α-helix	1655	1310-1275 (debatable)
Disordered structures	1665	1245

5.5.1 Protein Studies by Raman Spectroscopy.

Raman spectroscopy has been used to study the secondary structure of four silk proteins through deconvolution of the Amide I region through the curve fitting method. In addition to the limits outlined above two extra component bands were assigned at 1684 and 1698 cm^{-1} to β-turn structures [61]. It has also been used to assess the behaviour of keratin, sodium sulphite and glycerol

blends that were extruded. Raman spectroscopy was used to infer that β-sheet structures were disrupted through the addition of sodium sulphite [62].

A review by Tursan and Kokini concluded that while Raman has been extensively used to study zein, secondary structure determination is difficult as information can be lost due to fluorescence and the need for subjective baseline correction [63].

Finally, Raman spectroscopy has been performed for blood meal but not used to assess protein secondary structure [64]. Achieving a good signal from blood meal is challenging as it contains heme which fluoresces but it is possible with the spectra shown below (Figure 10).

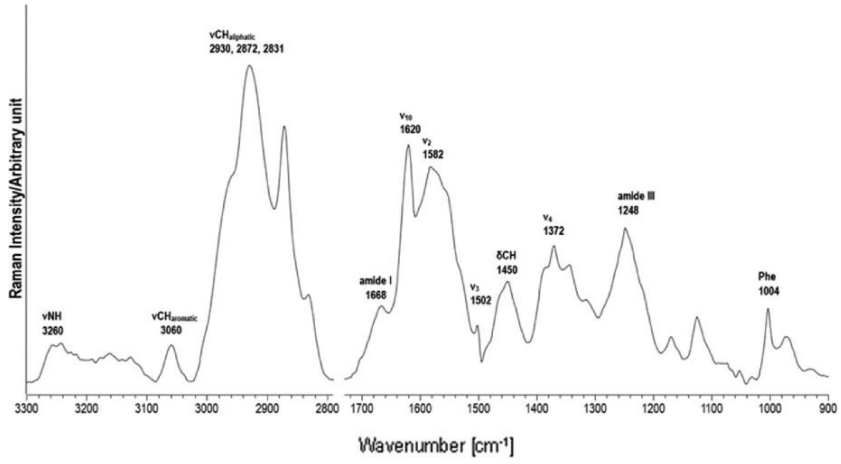

Figure 10: Raman spectroscopy of blood meal, from [64].

Conclusion

The application of traditional techniques for investigating protein structure is limited in protein thermoplastics. The insolubility and the disruption of the native structure of proteins through thermoplastic processing limits the application of circular dichroism, X-ray crystallography and NMR. Raman and Fourier transform infrared are more suitable techniques.

While FT- IR has been more widely used, no method of spectra deconvolution for secondary structure determination is perfect. Peak position is often determined by second derivative to minimise artefacts produced by Fourier self-deconvolution, however the fit of Gaussian peaks, centred at the peak positions identified is still subject to how the spectra is baselined. The use of

the second derivative height method is far less subjective and has been shown to provide a good indication of the relative changes in Novatein. FT-IR can also provide information on protein additives and blends within the same spectra making it a very powerful technique but care must be taken that these components such as urea, triethylene glycol and water do not interfere with structure determination.

References

1. Hernandez-Izquierdo, V. and J. Krochta, *Thermoplastic processing of proteins for film formation—a review.* Journal of food science, 2008. **73**(2): p. R30-R39.
2. Castiglioni, E., P. Biscarini, and S. Abbate, *Experimental aspects of solid state circular dichroism.* Chirality, 2009. **21**(1E): p. E28-E36.
3. Greenfield, N.J., *Methods to estimate the conformation of proteins and polypeptides from circular dichroism data.* Analytical biochemistry, 1996. **235**(1): p. 1-10.
4. Reddy, N., et al., *Thermoplastic films from cyanoethylated chicken feathers.* Materials Science and Engineering: C, 2011. **31**(8): p. 1706-1710.
5. Cavalli, A., et al., *Protein structure determination from NMR chemical shifts.* Proceedings of the National Academy of Sciences, 2007. **104**(23): p. 9615-9620.
6. Kwan, A.H., et al., *Macromolecular NMR spectroscopy for the non-spectroscopist.* The FEBS journal, 2011. **278**(5): p. 687-703.
7. Manolikas, T., T. Herrmann, and B.H. Meier, *Protein structure determination from 13C spin-diffusion solid-state NMR spectroscopy.* Journal of the American Chemical Society, 2008. **130**(12): p. 3959-3966.
8. Pelton, J.T. and L.R. McLean, *Spectroscopic methods for analysis of protein secondary structure.* Analytical biochemistry, 2000. **277**(2): p. 167-176.
9. Smyth, M. and J. Martin, *x Ray crystallography.* Molecular Pathology, 2000. **53**(1): p. 8.
10. Yee, A.A., et al., *NMR and X-ray crystallography, complementary tools in structural proteomics of small proteins.* Journal of the American Chemical Society, 2005. **127**(47): p. 16512-16517.
11. Barth, A., *Infrared spectroscopy of proteins.* Biochimica et Biophysica Acta (BBA)-Bioenergetics, 2007. **1767**(9): p. 1073-1101.
12. Glassford, S.E., B. Byrne, and S.G. Kazarian, *Recent applications of ATR FTIR spectroscopy and imaging to proteins.* Biochimica et Biophysica Acta (BBA)-Proteins and Proteomics, 2013. **1834**(12): p. 2849-2858.
13. Callender, R. and H. Deng, *Nonresonance Raman difference spectroscopy: a general probe of protein structure, ligand binding, enzymatic catalysis, and the structures of other biomacromolecules.* Annual review of biophysics and biomolecular structure, 1994. **23**(1): p. 215-245.
14. Herrero, A.M., *Raman spectroscopy a promising technique for quality assessment of meat and fish: A review.* Food Chemistry, 2008. **107**(4): p. 1642-1651.
15. Spiro, T.G. and B.P. Gaber, *Laser Raman scattering as a probe of protein structure.* Annual review of biochemistry, 1977. **46**(1): p. 553-570.
16. Hicks, T.M., *Oxidative Decolouring of Bloodmeal Using Peracetic Acid*. 2015, University of Waikato.
17. Tian, H., et al., *Microstructure and mechanical properties of soy protein/agar blend films: Effect of composition and processing methods.* Journal of Food Engineering, 2011. **107**(1): p. 21-26.
18. Oliviero, M., E. Di Maio, and S. Iannace, *Effect of molecular structure on film blowing ability of thermoplastic zein.* J. Appl. Polym. Sci., 2010. **115**(1): p. 277-287.
19. Weska, R.F., et al., *Effect of freezing methods on the properties of lyophilized porous silk fibroin membranes.* Materials Research, 2009. **12**(2): p. 233-237.
20. Kuktaite, R., et al., *Changes in the hierarchical protein polymer structure: urea and temperature effects on wheat gluten films.* RSC Advances, 2012. **2**(31): p. 11908-11914.

21. Nedi, I., E. Di Maio, and S. Iannace, *The role of protein–plasticizer–clay interactions on processing and properties of thermoplastic zein bionanocomposites.* Journal of Applied Polymer Science, 2012. **125**(S2): p. E314-E323.
22. Lai, H.M., P. Geil, and G. Padua, *X-ray diffraction characterization of the structure of zein–Oleic acid films.* Journal of applied polymer science, 1999. **71**(8): p. 1267-1281.
23. Wüthrich, K., *Protein structure determination in solution by NMR spectroscopy.* Journal of Biological Chemistry, 1990. **265**(36): p. 22059-22062.
24. Brown, J.E., et al., *Thermal and Structural Properties of Silk Biomaterials Plasticized by Glycerol.* Biomacromolecules, 2016. **17**(12): p. 3911-3921.
25. Chen, F.L., Y.M. Wei, and B. Zhang, *Characterization of water state and distribution in textured soybean protein using DSC and NMR.* Journal of food engineering, 2010. **100**(3): p. 522-526.
26. Shi, Z., et al., *Grafting soyprotein isolates with various methacrylates for thermoplastic applications.* Industrial Crops and Products, 2014. **60**: p. 168-176.
27. Kelly, S.M., T.J. Jess, and N.C. Price, *How to study proteins by circular dichroism.* Biochimica et Biophysica Acta (BBA) - Proteins and Proteomics, 2005. **1751**(2): p. 119-139.
28. Sreerama, N., S.Y. Venyaminov, and R.W. Woody, *Estimation of the number of α-helical and β-strand segments in proteins using circular dichroism spectroscopy.* Protein Science, 1999. **8**(2): p. 370-380.
29. Hammann, F. and M. Schmid, *Determination and Quantification of Molecular Interactions in Protein Films: A Review.* Materials, 2014. **7**(12): p. 7975.
30. Khrapunov, S., *Circular dichroism spectroscopy has intrinsic limitations for protein secondary structure analysis.* Analytical biochemistry, 2009. **389**(2): p. 174-176.
31. Qi, P.X. and C.I. Onwulata, *Physical properties, molecular structures, and protein quality of texturized whey protein isolate: Effect of extrusion moisture content1.* Journal of Dairy Science, 2011. **94**(5): p. 2231-2244.
32. Selling, G.W. and K.D. Utt, *Effect of multiple extrusion passes on zein.* Polymer Degradation and Stability, 2013. **98**(1): p. 184-189.
33. Soliman, E.A., M.S. Mohy Eldin, and M. Furuta, *Biodegradable Zein-Based Films: Influence of γ-Irradiation on Structural and Functional Properties.* Journal of Agricultural and Food Chemistry, 2009. **57**(6): p. 2529-2535.
34. Bier, J.M., C.J.R. Verbeek, and M.C. Lay, *Using synchrotron FTIR spectroscopy to determine secondary structure changes and distribution in thermoplastic protein.* Journal of Applied Polymer Science, 2013. **130**(1): p. 359-369.
35. Dong, A., et al., *Infrared spectroscopic studies of lyophilization-and temperature-induced protein aggregation.* Journal of pharmaceutical sciences, 1995. **84**(4): p. 415-424.
36. Murayama, K. and M. Tomida, *Heat-Induced Secondary Structure and Conformation Change of Bovine Serum Albumin Investigated by Fourier Transform Infrared Spectroscopy.* Biochemistry, 2004. **43**(36): p. 11526-11532.
37. Li, D., Hong Zhang, & Gang Ma., *Secondary structure investigation of bovine serum albumin (BSA) by Fourier transform infrared (FTIR) spectroscopy in the amide III region.* European Journal of Chemistry 2014. **5**(2): p. 287-290.
38. Yada, R., R. Jackman, and S. Nakai, *Secondary structure prediction and determination of proteins—a review.* Chemical Biology & Drug Design, 1988. **31**(1): p. 98-108.

39. Kaddour, A.A., M. Mondet, and B. Cuq, *Description of Chemical Changes Implied During Bread Dough Mixing by FT-ATR Mid-Infrared Spectroscopy.* Cereal chemistry, 2008. **85**(5): p. 673-678.
40. Cai, S. and B.R. Singh, *Identification of β-turn and random coil amide III infrared bands for secondary structure estimation of proteins.* Biophysical Chemistry, 1999. **80**(1): p. 7-20.
41. Paris, C., S. Lecomte, and C. Coupry, *ATR-FTIR spectroscopy as a way to identify natural protein-based materials, tortoiseshell and horn, from their protein-based imitation, galalith.* Spectrochimica Acta Part A: Molecular and Biomolecular Spectroscopy, 2005. **62**(1-3): p. 532-538.
42. Georget, D.M. and P.S. Belton, *Effects of temperature and water content on the secondary structure of wheat gluten studied by FTIR spectroscopy.* Biomacromolecules, 2006. **7**(2): p. 469-475.
43. Yu, P., et al., *Using Synchrotron-Based FTIR Microspectroscopy To Reveal Chemical Features of Feather Protein Secondary Structure: Comparison with Other Feed Protein Sources.* Journal of Agricultural and Food Chemistry, 2004. **52**(24): p. 7353-7361.
44. Costantino, H.R., et al., *Fourier-transform infrared spectroscopic investigation of protein stability in the lyophilized form.* Biochimica et Biophysica Acta (BBA) - Protein Structure and Molecular Enzymology, 1995. **1253**(1): p. 69-74.
45. Jackson, M. and H.H. Mantsch, *The use and misuse of FTIR spectroscopy in the determination of protein structure.* Critical reviews in biochemistry and molecular biology, 1995. **30**(2): p. 95-120.
46. Seabourn, B.W., et al., *Determination of Secondary Structural Changes in Gluten Proteins during Mixing Using Fourier Transform Horizontal Attenuated Total Reflectance Spectroscopy.* Journal of Agricultural and Food Chemistry, 2008. **56**(11): p. 4236-4243.
47. Zhang, J. and Y.-B. Yan, *Probing conformational changes of proteins by quantitative second-derivative infrared spectroscopy.* Analytical biochemistry, 2005. **340**(1): p. 89-98.
48. Türe, H., et al., *Protein network structure and properties of wheat gluten extrudates using a novel solvent-free approach with urea as a combined denaturant and plasticiser.* Soft Matter, 2011. **7**(19): p. 9416-9423.
49. Athamneh, A.I., et al., *Conformational changes and molecular mobility in plasticized proteins.* Biomacromolecules, 2008. **9**(11): p. 3181-3187.
50. Liu, D. and L. Zhang, *Structure and Properties of Soy Protein Plastics Plasticized with Acetamide.* Macromolecular Materials and Engineering, 2006. **291**(7): p. 820-828.
51. Wu, Q. and L. Zhang, *Properties and structure of soy protein isolate– ethylene glycol sheets obtained by compression molding.* Industrial & engineering chemistry research, 2001. **40**(8): p. 1879-1883.
52. Gao, C., et al., *Effect of preparation conditions on protein secondary structure and biofilm formation of kafirin.* J. Agric. Food Chem., 2005. **53**(2): p. 306-312.
53. Bier, J.M., C.J.R. Verbeek, and M.C. Lay, *Thermally resolved synchrotron FT-IR microscopy of structural changes in bloodmeal-based thermoplastics.* Journal of thermal analysis and calorimetry, 2014. **115**(1): p. 433-441.
54. Bier, J.M., C.J.R. Verbeek, and M.C. Lay, *Plasticizer migration in bloodmeal-based thermoplastics.* Journal of Applied Polymer Science, 2014. **131**(4).
55. Hicks, T.M., et al., *The effect of SDS and TEG on chain mobility and secondary structure of decolored bloodmeal.* Macromolecular Materials and Engineering, 2015. **300**(3): p. 328-339.
56. Hicks, T.M., et al., *Changes in hydrogen bonding in protein plasticized with triethylene glycol.* Journal of Applied Polymer Science, 2015. **132**(26).

57. Uitto, J.M. and C.J. Verbeek, *Phase separation of plasticizers in thermally aggregated protein-based thermoplastics.* Advances in Polymer Technology, 2018.
58. Hicks, T., et al., *Effect of oxidative treatment on the secondary structure of decoloured bloodmeal.* RSC Advances, 2014. **4**(59): p. 31201-31209.
59. Smith, M.J. and C.J. Verbeek, *Structural changes and energy absorption mechanisms during fracture of thermoplastic protein blends using synchrotron FTIR.* Polymer Engineering & Science, 2018.
60. Benevides, J.M., S.A. Overman, and G.J. Thomas, *Raman spectroscopy of proteins.* Current protocols in protein science, 2004: p. 17.8. 1-17.8. 35.
61. Lefèvre, T., M.-E. Rousseau, and M. Pézolet, *Protein Secondary Structure and Orientation in Silk as Revealed by Raman Spectromicroscopy.* Biophysical Journal, 2007. **92**(8): p. 2885-2895.
62. Barone, J.R., W.F. Schmidt, and N. Gregoire, *Extrusion of feather keratin.* J. Appl. Polym. Sci., 2006. **100**(2): p. 1432-1442.
63. Turasan, H. and J.L. Kokini, *Advances in Understanding the Molecular Structures and Functionalities of Biodegradable Zein-Based Materials Using Spectroscopic Techniques: A Review.* Biomacromolecules, 2017. **18**(2): p. 331-354.
64. Yunta, F., et al., *Blood Meal-Based Compound. Good Choice as Iron Fertilizer for Organic Farming.* Journal of Agricultural and Food Chemistry, 2013. **61**(17): p. 3995-4003.

Permissions

Figure 2: Reproduced from Effect of molecular structure on film blowing ability of thermoplastic zein. originally published in the Journal of Applied Polymer Science, Vol. 115, 277–287 (2010) ©2009 Wiley Periodicals, Inc. Reproduced with permission from John Wiley and Sons

Figure 3: Reproduced from Changes in the hierarchical protein polymer structure: urea and temperature effects on wheat gluten films. RSC Advances, 2012. 2(31): p. 11908-11914. © The Royal Society of Chemistry 2012. Reproduced with permission.

Figure 4: Reproduced from Characterization of water state and distribution in textured soybean protein using DSC and NMR. Journal of food engineering, 2010. 100(3): p. 522-526 Copyright (2010) © Elsevier. Reproduced with permission.

Figure 5 A & B: Reproduced from How to study proteins by circular dichroism. Biochimica et Biophysica Acta (BBA) - Proteins and Proteomics, 2005. 1751(2): p. 119-139. Copyright (2005) Elsevier. Reproduced with permission

Figure 6: Reproduced from Using synchrotron FTIR spectroscopy to determine secondary structure changes and distribution in thermoplastic protein originally published in the Journal of Applied Polymer Science, ©2013 Wiley Periodicals, Inc. Reproduced with permission from John Wiley and Sons

Figure 7 A & B: Reprinted with permission from Infrared spectroscopic studies of lyophilization ‐ and temperature ‐ induced protein aggregation. Journal of pharmaceutical sciences, 1995. 84(4): p. 415-424. © Elsevier.

Figure 7 C: Reprinted with permission from Cai, S. and B.R. Singh, Identification of β-turn and random coil amide III infrared bands for secondary structure estimation of proteins. Biophysical Chemistry, 1999. 80(1): p. 7-20. Copyright (1999) Elsevier.

Figure 8 A: Reproduced from Using synchrotron FTIR spectroscopy to determine secondary structure changes and distribution in thermoplastic

protein originally published in the Journal of Applied Polymer Science, ©2013 Wiley Periodicals, Inc. Reproduced with permission from John Wiley and Sons.

Figure 8 B: Reproduced from Thermally resolved synchrotron FT-IR microscopy of structural changes in bloodmeal-based thermoplastics. originally published in the Journal of Thermal Analysis and Calorimetry with permission of Springer © 2013 Akade´miai Kiado´, Budapest, Hungary 2013

Figure 9 A: Reproduced from Effect of oxidative treatment on the secondary structure of decoloured bloodmeal. RSC Advances, 2014. 4(59): p. 31201-31209. © The Royal Society of Chemistry 2012. Reproduced with permission.

Figure 9 B: Reproduced from Structural changes and energy absorption mechanisms during fracture of thermoplastic protein blends using synchrotron FTIR originally published in the Polymer Engineering & Science ©2017 Wiley Periodicals, Inc. Reproduced with permission from John Wiley and Sons

Figure 10: Reprinted with permission from Blood Meal-Based Compound. Good Choice as Iron Fertilizer for Organic Farming. Journal of Agricultural and Food Chemistry, 2013. 61(17): p. 3995-4003.Copyright (2013) American Chemical Society.

6

Thermal Analysis and Secondary Structure of Protein Fractions in a Highly Aggregated Protein Material

A journal article

by

C. Gavin, C.J.R Verbeek, M.C. Lay, J.M. Bier & T. M. Hicks

Published in

The Journal of Polymer Testing

Overview:

Blood meal can either be considered to be influenced by the individual proteins within blood or as its own unique polymer. Blood meal and therefore Novatein has been viewed as a unique polymer in most previous work and this will have implications for foaming if true. This paper therefore aims to verify that blood meal is a highly aggregated protein that cannot be considered the sum of its individual components unlike soy and corn gluten meal.

This work relates to objective three by establishing how Novatein should be viewed as a material.

Contribution:

As an author for this publication the PhD candidate prepared the first draft of this manuscript. Experimental work was conducted in collaboration with the co-authors but analysed and formatted by the PhD candidate. The PhD candidate also assisted with the collection of the spectra at the Australian Synchrotron. Under guidance from the supervisors and the co-authors the manuscript was revised and edited.

Permission:

Reproduced from Thermal Analysis and Secondary Structure of Protein Fractions in a Highly Aggregated Protein Material. Published in the Journal of Polymer Testing.

Polymer Testing 77 (2019) 105876

Contents lists available at ScienceDirect

Polymer Testing

journal homepage: www.elsevier.com/locate/polytest

Thermal analysis and secondary structure of protein fractions in a highly aggregated protein material

Chanelle Gavin[a,*], Casparus J.R. Verbeek[b], Mark C. Lay[a], James M. Bier[c], Talia M. Hicks[d]

[a] School of Engineering, Faculty of Science and Engineering, University of Waikato, Knighton Road, Hamilton, New Zealand
[b] Mechanical Engineering, Faculty of Engineering, The University of Auckland, Auckland, 1142, New Zealand
[c] Aduro Biopolymers LP, Vickery Street, Te Rapa, Hamilton, 3200, New Zealand
[d] AgResearch, Meat Quality, Food & Bio-based Products, Ruakura, Hamilton, 3214, New Zealand

ARTICLE INFO

Keywords:
Protein thermoplastic
Thermal analysis
Protein secondary structure

ABSTRACT

Thermal analysis can generally be applied to protein-based thermoplastics although standard protein analysis techniques are not always possible to assess chain architecture. Blood (17% protein) from the meat industry can be fractionated or dried to blood meal, which can be converted to a thermoplastic called Novatein. The objective of this paper was to use a consistent methodology to compare different protein fractions from blood to that of blood meal, as well as the plastic produced from it, and how these changes relate to processing. Thermal properties were similar between protein fractions, but there were differences in chain conformation between blood meal, the haem containing fractions (red blood cells and spray dried haemoglobin) and the non-haem fractions (plasma and serum albumin). Blood meal is therefore best considered a single polymer, rather than the sum of its individual fractions. Thermoplastic processing reduces protein aggregation, and this phenomenon is more important than the behaviour of any of the individual proteins.

1. Introduction

Techniques which are routinely used in the assessment of conventional polymers can often be used to investigate protein-based materials. Thermal analysis techniques such as dynamic mechanical analysis (DMA), differential scanning calorimetry (DSC) and thermogravimetric analysis (TGA), can all be applied to protein-based materials to investigate polymer mobility and stability [1–4]. Similarly, techniques such as FT-IR and Raman spectroscopy, as well as X-ray diffraction (XRD) are often used to examine chain architecture and other chemical changes [5–8]. However, other techniques typically used to assess the size and structure of proteins, such as chromatography, mass spectrometry, gel electrophoresis and circular dichroism, require the protein to be in solution [9], and are often of limited use since some protein-based materials cannot be solubilised in an appropriate solvent [10]. Further, although solid state NMR can be used for assessing protein structure, it produces a complex spectrum, which is difficult to interpret [11], especially when more than one protein is present. As a consequence, there are limited techniques which can be used to assess protein-based materials during development, instead requiring a thorough understanding of the properties of the feedstock from which it is derived.

The protein-based material of interest here is Novatein®, a patented bioplastic produced from blood meal. Blood meal is produced by steam coagulation, dewatering and thermal drying whole animal blood [1,5], giving rise to a powder containing 80–100 wt% protein. This is an aggressive method which leads to extensive denaturation and aggregation and subsequently produces a material almost insoluble in water or any other solvent, severely limiting potential analysis techniques. It has a glass transition temperature above 200 °C, around which thermal degradation also occurs [12]. To enable processing below the degradation temperature, it is mixed with a blend of additives to disrupt protein-protein interactions, hydrate the protein chains, and to plasticise the blend. The resulting material has a vastly different thermal behaviour, with a drastically reduced glass transition temperature allowing the mixture to be extruded at 120 °C [13]. Foaming is a new area of research for Novatein which may be significantly affected by the molecular structure and crystallinity of the material, which can influence the rheology of the system and in conventional polymers nucleation [14]. Understanding the nature of Novatein and whether it is influenced by the individual proteins it consists of will inform processing.

Whole blood consists of 80.9% water, 17.3% protein, 0.23% fat, 0.07% carbohydrate and 0.62% minerals [15], with the protein fraction

* Corresponding author.
E-mail addresses: chanelle.gavin@waikato.ac.nz (C. Gavin), johan.verbeek@auckland.ac.nz (C.J.R. Verbeek), mclay@waikato.ac.nz (M.C. Lay), jim@adurobiopolymers.com (J.M. Bier), talia.hicks@agresearch.co.nz (T.M. Hicks).

https://doi.org/10.1016/j.polymertesting.2019.04.023
Received 12 December 2018; Received in revised form 17 April 2019; Accepted 20 April 2019
Available online 22 April 2019

consisting of 3.61% albumin, 0.51% α-globulins, 0.53% β-globulins, 0.63% γ-globulins, 0.6% fibrinogen and 10.3% haemoglobin [16]. Whole blood can be separated into two fractions; 67 wt% plasma and the remainder is cellular matter [16]. Separation is most commonly achieved by centrifugation and/or clotting. Plasma is produced when un-clotted blood is separated and contains 6–8 wt% protein on a wet basis, consisting of albumin, globulins and fibrinogen. Upon dehydration plasma contains 7% moisture, 80% protein, 7.9% minerals and 1% fat [15]. Blood serum is differentiated from plasma due to the removal of the fibrinogen component and some globulins, by adding a clotting agent [16] or through the use of the Cohn method [17]. The cellular fraction consists of erythrocytes (RBC), leukocytes (WBC) and platelets. The erythrocyte fraction contains haemoglobin and is sometimes dried to produce a product referred to as haemoglobin, although it is more correctly referred to as dried red blood cells. Alternatively, the haemoglobin can be extracted from the red blood cells through haemolysis which is achieved using either mechanical (centrifugation), chemical methods or osmotic shock to break the cell walls.

In a mixture of proteins, the individual fractions can often be distinguished from one another using thermal analysis, such as glutelin and zein in corn gluten meal [2] and various glutenins in wheat [4]. Soy also shows two distinct glass transition temperatures associated with the 11s and 7s sub-fractions [3]. This would suggest that blood meal also may be able to be considered as the sum of the behaviour of its components (haemoglobin and plasma proteins) which could be used to inform processing strategies. This paper demonstrates the use of thermal analysis (DMA, DSC), fast protein liquid chromatrography (FPLC), as well as FT-IR and XRD to analyse the differences between multiple protein fractions of bovine blood. DMA examines viscoelastic properties as a function of temperature and transitions are either observed as a decrease in the loss modulus or a peak in tan δ. Identification of these have been extensively reviewed for protein thermoplastics [1]. DSC measures changes in heat flow for a sample and a reference and is useful to detect protein denaturing [18,19] and an endothermic event commonly associated with physical ageing of protein [18,20]. The T_g is determined by a second heating scan [18]. FPLC provides insights into the protein size before and after different processing steps. On the other hand, FT-IR and XRD are used to determine the complex folding behaviour of proteins. Certain amino acids/amino acid sequences have a propensity to form specific secondary structures such as α-helices, β-turns, β-sheets and random coils [5], each of which may have a different influence on material properties and processing.

Identifying thermal transitions using DMA and DSC in dry proteins and protein thermoplastics is more difficult than for traditional polymers. Dry proteins do not show a clear melting peak and transitions are usually assigned to local chain movement, side chain movement and movement within a side chain [1]. The system becomes even more complicated once plasticised through the addition of water and polyols, a common combination for protein thermoplastics, as phase separation can arise when secondary plasticisation occurs [21]. DMA can also provide an indication of the nature of the thermal event (α- or β-transition) by examining its frequency response as not all transitions follow the same frequency dependence [22].

The complex folding of proteins is very sensitive to the surrounding environment including pH, salts, oxidation state and hydration and can also change during separation and drying [23]. FT-IR is a useful way to assess these changes by examining the Amide I (1600-1700 cm^{-1}) or Amide III (1180–1330 cm^{-1}) region of the spectra. Determining secondary structure from the Amide I is usually conducted using Fourier self deconvolution (FSD) or through curve fitting of Gaussian peaks [24]. However, both these methods require subjective baseline correction. Alternatively, the inverted second derivative of the Amide I or III region can be used, provided a sufficient signal to noise ratio is achieved (often much improved using a synchrotron source).

Previous studies of blood meal have shown that it contains a high β-sheet content, attributed to thermal aggregation during drying (Table 1) [5]. The secondary structure of a protein is highly dependent upon the hydration state and in their native state, the fractions of blood meal (haemoglobin and plasma) are initially highly α-helical, although there is some discrepancy in the proportion using different techniques and separation processes (Table 1). Knowing the aggressive nature of blood meal production, it can be expected that protein chains are highly denatured, accompanied by a change in secondary structure. Heat induced changes have been observed in bovine serum albumin above 40 °C with the unfolding of α-helices at 52–60 °C. Above 60 °C β-aggregation occurs and FT-IR confirmed a reduction in α-helices and increase in intermolecular β-sheets [7]. Wolkers and Oldnehof also examined the effect of temperature on the secondary structure of porcine red blood cells and observed that above 40 °C the same changes occurred [25].

Secondary structure has been shown to influence the processing of protein. A large ratio of α-helices to β-sheets were desired for zein during film or foam production [6,8]. There is also a link between these structures and elasticity, e.g. during bread production a conversion of β-turns to β-sheets occurs at low strain rates consistent with the loop and train method [26]. Dynamic FT-IR has shown that this change is reversible highlighting that this is a mechanism for energy storage [27].

Thermal analysis and secondary structure determination can reveal changes that occur when blood meal is converted into a protein-based plastic. The objective of this paper was to build on the understanding of these changes by using a consistent methodology to compare different protein fractions from blood to that of blood meal, as well as the plastic produced from it and how these changes relate to processing protein-based materials. Blood meal, Novatein prior to (PNTP) and after extrusion (ENTP) have previously been characterised by DMA and Synchrotron FT-IR [1,12,24], but were re-evaluated and prepared as outlined in a recent work on producing thermoplastic foam [32] for direct comparison with blood protein fractions using a consistent processing technique.

2. Materials and methods

The secondary structure and thermal behaviour of blood meal was compared to individual protein fractions from blood, from sources which were either spray dried (SD) or freeze-dried (FD). The fractions included red blood cell concentrate (RBCC, FD), bovine serum albumin (BSA, FD) and plasma (FD). Haemoglobin (SD) and coagulated, mechanically dewatered blood were also included to examine the effect of drying.

Blood meal and coagulate were obtained from Wallace Corporation, Waitoa, New Zealand. Red blood cell concentrate and plasma were supplied by ANZCO, New Zealand. Spray dried haemoglobin from American Protein Corporation, United States. Invitrogen BSA, Cohn Fraction V was purchased from Sigma Aldrich. All protein fractions were commercial grade purity except BSA which was analytical grade > 90% pure.

PNTP, as analysed in this work, was prepared by dissolving the following additives on a parts per hundred blood meal basis (pph_{BM}): 3 pph_{BM} sodium sulfite (Merck, Germany), 3 pph_{BM} sodium doceyl sulfate (Merck, Germany), 10 pph_{BM} urea (Balance Agri-Nutrients, New Zealand) dissolved in 40 pph_{BM} distilled water. Once this solution was mixed with dry blood meal, 20 pph_{BM} triethylene glycol (Merck, Germany) was blended in. ENTP was produced by extruding this PNTP with previously described extrusion conditions [32].

The thermal transitions and stability of these protein sources was examined using dynamic mechanical analysis, differential scanning calorimetry and thermal gravimetric analysis. Information about their structure was obtained through fast protein liquid chromatography, X-ray diffraction and Fourier transform infrared analysis. A list of abbreviations used during this study is presented in Table 2.

Table 1
Secondary structure of proteins found in blood fractions.

Protein	Method	State	α-helices	β-turns	Random coils	β-sheets	Reference
Blood meal	FT-IR	Thermally dried	19	15	20	46	[5]
Haemoglobin	XRD	Crystallised	87	8	7	–	[28]
	FT-IR	In buffer	78	10		12	[29]
BSA	XRD	Crystallised	68		15	17	[30]
	FT-IR	In solution	53	4	16	14	[30]
	FT-IR	Freeze dried	48	8	4	25	[30]
Human blood							
	FT-IR	Solution	58	0	42	0	[31]
	FT-IR	Freeze dried	30		55	5	[31]
	FT-IR	Spray dried	30	0	16	16	[31]

Table 2
Table of Nomenclature for this study.

Material	Abbreviation
Blood meal	BM
Red blood cell concentrate	RBCC
Spray dried haemoglobin	SDH
Bovine serum albumin	BSA
Plasma	Plasma
Novatein – Pre-processed, produced from blood meal	PNTP
Novatein – Extruded, produced from PNTP	ENTP

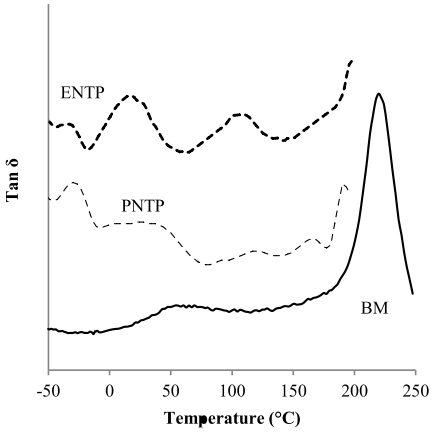

Fig. 1. DMA behaviour of blood meal, pre-processed Novatein thermoplastic protein (PNTP) and extruded Novatein thermoplastic protein (ENTP).

2.1. Dynamic mechanical analysis

Powder pocket DMA was conducted in a single cantilever configuration in a PerkinElmer DMA 8000. The DMA was equipped with a temperature controlled furnace which was cooled with liquid nitrogen. 50 mg of protein sample was crimped into stainless steel powder pocket and cooled to −135 °C. Multi-frequency analysis was conducted at 0.1, 0.3, 1, 3, 10, and 30 Hz during the heating scan. For blood meal, samples were scanned to 250 °C, but analysis stopped at 180 °C, above which excessive degradation occurs. A dynamic displacement of 0.05 mm was used with a heating rate of 2.0 °C/min.

2.2. Differential scanning calorimetry (DSC)

For DSC analysis, between 5 and 10 mg of powdered samples were analysed in sealed aluminium pans using a PerkinElmer DSC 8500. A heat, cool, heat cycle from −50 °C to 140 °C was conducted under nitrogen purge (20 mL/min) at 50 °C/min. A high scanning speed of 50 °C/min was used for DSC analysis as the PerkinElmer DSC 8500 is a hyper DSC which detects weak transitions better at faster scanning rates. Slow scanning speeds e.g. 10 °C/min do not detect these transitions. Three replicates were conducted for each sample.

2.3. Fast protein liquid chromatrography (FPLC)

Protein chromatography was conducted on an AKTA 100 (GE Healthcare) using a Superdex 200 size exclusion column (GE Healthcare) with a molecular weight cut off of 600–10 kDa. Samples were solubilised in a buffer 0.02 mM phosphate buffer (pH 7) containing 0.1 wt% sodium dodecyl sulphate to disrupt hydrophobic bonding and 0.1 wt% NaCl to minimise interaction of the protein with the column. 50–100 μL was loaded onto the column which was eluted with 35 mL at 0.2 mL/min of the same buffer.

2.4. Synchrotron fourier transform infrared

Fourier transform infrared analysis of all protein fractions was performed at the Australian Synchrotron in Melbourne. Spatially resolved spectra were collected by placing particles of protein between diamond cells and compressing them to avoid saturation of the spectra. At least three maps of 7 × 8 spots were conducted for each material.

The spectra were collected using a Bruker Hyperion 3000 with an MCT collector and an XY stage. All data capture was conducted in Opus 6.5 (Bruker Optik GmbH). For each spot of 5 μm, 32 spectra were collected between 3900 and 700 cm^{-1} at a resolution of 4 cm^{-1} and averaged.

The data for each spot/grid point was exported from Opus and analysed using Matlab. All spectra were normalized to the highest point in the Amide I region (1625-1627 cm^{-1}). Spatially resolved data required screening to identify low protein regions which gave insufficient signal for secondary structure determination. These spots were identified by integrating the area under the amide III region (1180-1330 cm^{-1}). Points which fell below the 95% confidence interval, based upon the composition for that map, were excluded from further analysis.

The inverted second derivative method was used with a Savitzky Golay filter, consisting of a third order polynomial through nine data points. Assignment of peaks in the second derivative were conducted using the conventional limits: α-helices (1295-1330 cm^{-1}), β-turns (1270-1295 cm^{-1}) and random coils (1250-1270 cm^{-1}) and finally β-sheets (1220-1250 cm^{-1}) [24]. Borderline peaks (± 2 cm^{-1} of a boundary) were assessed for their proximity to peaks in the regions either side using Matlab. An average peak height for all peaks in the four regions associated with α-helices, β-turns, random coils and β-sheets were calculated and used to determine the fractional composition of the material [5,24].

2.5. X-ray diffraction

Powder X-ray diffraction was conducted using a Panalytical Empyrean XRD machine. X-rays were generated by a copper X-ray tube

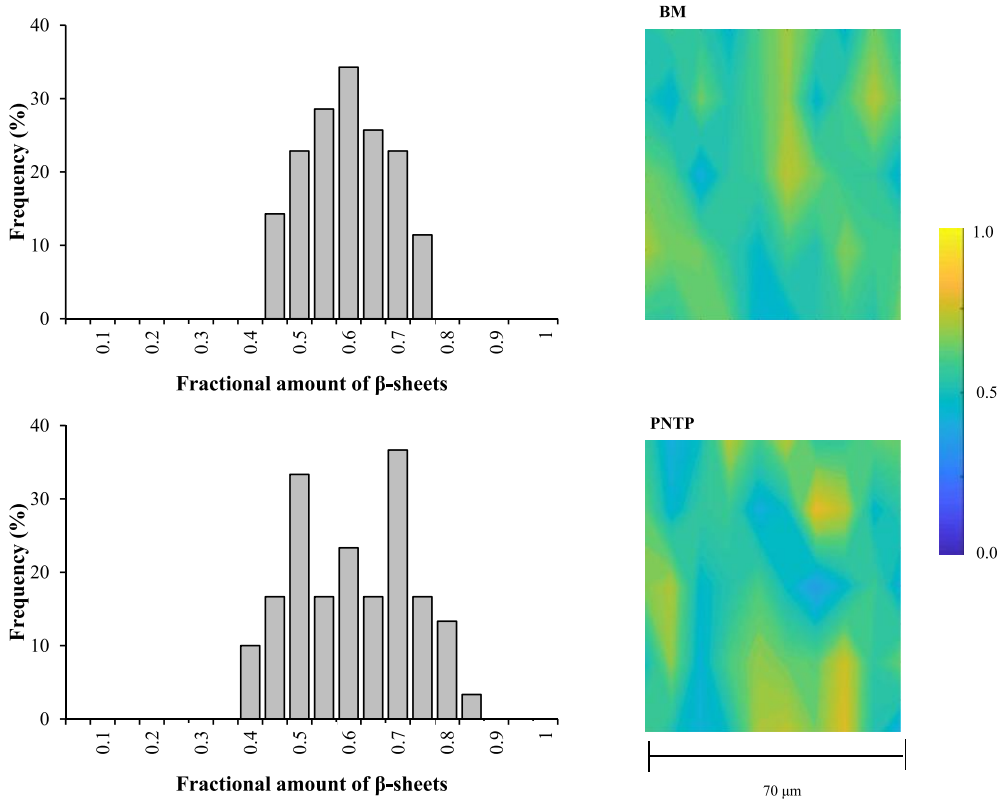

Fig. 2. Spatial distribution and histogram of β-sheet content in BM and PNTP.

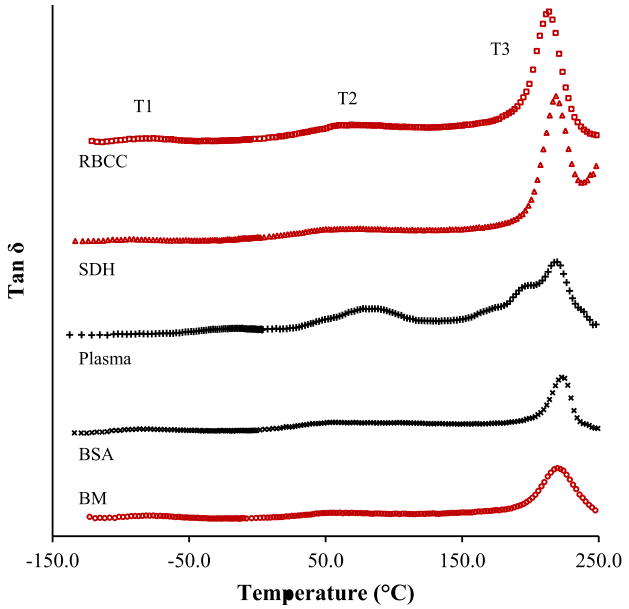

Fig. 3. Dynamic mechanical analysis conducted in powder pocket. Tan δ vs. temperature for each protein fraction and blood meal shown at the representative 1 Hz frequency. Haem containing fractions are displayed in red for clarity.

(k1 and k2 of 1.54) operating at 45 kV and 40 mA. Samples were analysed in triplicate on a spinning stage rotating at one revolution per second for 2 theta angles between 4° and 60°. The incident beam passed through a 10 mm mask, an automatic programmable divergent slit, and a 0.04 rad soller slit. The diffracted beam passed through a fixed 7.5 mm anti-scatter slit, a 0.04 rad soller slit, and a nickel filter before the intensity was measured by a PIXCel three-dimensional detector. A step size of 0.0268° was used with a time per step of 90 s.

Table 3
Secondary structure of blood meal and pre-processed material.

	α-helices	β-turns	Random coils	β-sheets
BM	17.50% (4.30)	12.20% (4.10)	13.50% (5.70)	56.70% (8.20)
PNTP	19.90% (5.10)	10.50% (4.20)	12.80% (11.40)	56.80% (12.30)

The amount of ordered structures was determined by baseline correcting the diffractogram between 4° and the minimum between 35 and 40°. A Gaussian curve was fitted to the amorphous fraction and subtracted. A further five Gaussian peaks were fitted to model the ordered fraction by minimizing the sum of squared errors. Total crystallinity was determined as the area ratio of the crystalline peaks to the combined area under the curve between 4 and 35°.

X-ray diffraction analysis was also performed on coagulated blood in a wet condition (40% moisture), dried after 72 h at 70 °C and following freeze drying. Thermal experiments in a controlled humidity environment were conducted on BSA and SDH. Scanned at room temperature, heated to above 75 °C and scanned again upon cooling.

3. Results

3.1. Blood meal and Novatein

DMA is one of the most sensitive thermal techniques to detect differences in thermal behaviour for dehydrated proteins. Dried proteins typically have a T_g between 120 and 250 °C [1]. Blood meal only displayed one T_g at 225 °C, while the incorporation of processing aids and

Table 4
Corresponding transition temperatures at 1 Hz for main transitions identified left to right. Corresponding activation energies (E_a) have been calculated when the fit to an Arrhenius relationship was greater than 0.90.

	Transition 1 (T1)			Transition 2 (T2)			Transition 3 (T3)		
	Temperature (°C)	Ea (kJ/mol)	R^2	Temperature (°C)	Ea (kJ/mol)	R^2	Temperature (°C)	Ea (kJ/mol)	R^2
RBCC	−81.7	63.1	0.96	71.1	n/a	0.66	218.1	712.2	0.97
SDH	−87.8	48.4	0.98	77.4	n/a	0.50	221.1	692.3	0.99
Plasma	−14.5	106.9	0.98	83.9	n/a	0.55	219.4	876.6	0.98
							198.0	653.4	0.97
							174.1	681.9	0.76
BSA	−82.0	91.7	0.97	61.4	n/a	0.84	216.1	1562.0	0.94
BM	−78.8	64.9	0.99	62.6	n/a	0.69	225.1	736.7	0.92

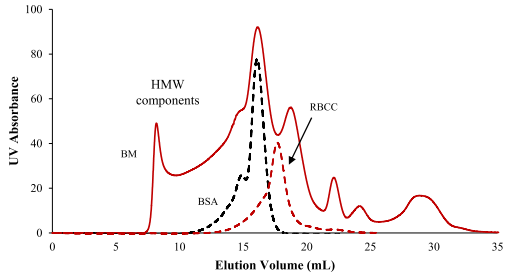

Fig. 4. FPLC analysis of protein fractions BSA and RBCC and blood meal. Blood meal demonstrates a high proportion of High Molecular Weight (HMW) components.

water resulted in multiple lower transitions (Fig. 1).

Consistent with earlier work, after extrusion, ENTP demonstrated two transitions, one at 40 °C and another transition at 110 °C which is broader in nature extending up to 150 °C. This may relate to observations during foaming of ENTP where foaming attempts at 120 °C failed, most likely associated with insufficient chain movement [33]. However, foaming above 150 °C was successful and also changed the chain conformation (protein secondary structure) of Novatein [32]. These thermal transitions in ENTP are better correlated with a protein rich phase at 110 °C, a protein-plasticiser phase at 40 °C and a plasticiser rich phase at −40 °C, dependent on the amount of water and plasticiser used which is in agreement with work recently presented by Uttio and Verbeek [21]. The extensive denaturation of blood meal is supported by the absence of a denaturing peak in DSC analysis, typically observed for

Table 5
Properties of the endothermic peak, standard deviation is shown in brackets.

	Temperature (°C)	Enthalpy (J/g)
SDH	77.87 (1.16)	3.31 (1.15)
RBCC	76.64 (1.69)	3.18 (0.48)
BSA	69.21 (6.40)	2.46 (0.19)
Plasma	75.21 (0.30)	1.66 (0.40)
BM	76.88 (1.28)	0.27 (0.24)

proteins in their native state [1,18]. In addition, many proteins also have an endothermic event, which for BM, PNTP and ENTP has been linked to crystallinity for samples with a similar degree of physical ageing [34]. Following PNTP production there is a reduction in crystallinity (as measured by XRD) from 25% ± 1.3 in blood meal to 21% ± 1.9 indicating an overall disruption of bonding within and between protein structures suggesting an associated change in secondary structure as well [34].

Secondary structure is important as aggregation restricts chain movement required for processing. Spatially resolved FT-IR analysis revealed that the average composition for blood meal and PNTP were similar, but the spatial variation was quite different, most notably, a bimodal distribution of β- Sheets within PNTP (Fig. 2). This arises from during PNTP production as some of the bonding is disrupted while highly aggregated regions are not accessible to processing additives and remain unaffected.

Based on previous work and the results presented here, there is no clear relationship which predicts foaming ability based on secondary structure alone. Through the application of knowledge from

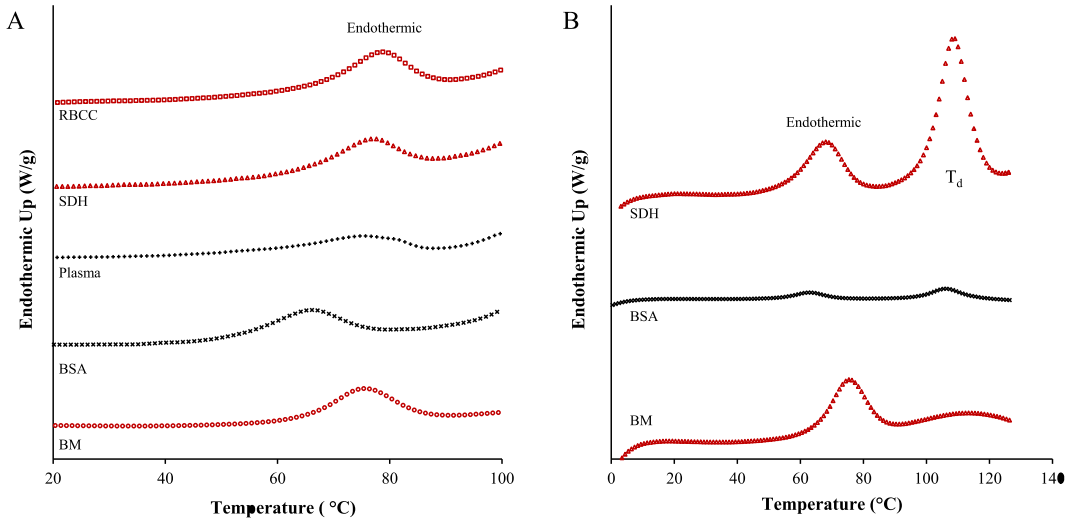

Fig. 5. DSC of protein fractions A. shows the endothermic peak and B. the denaturing peak.

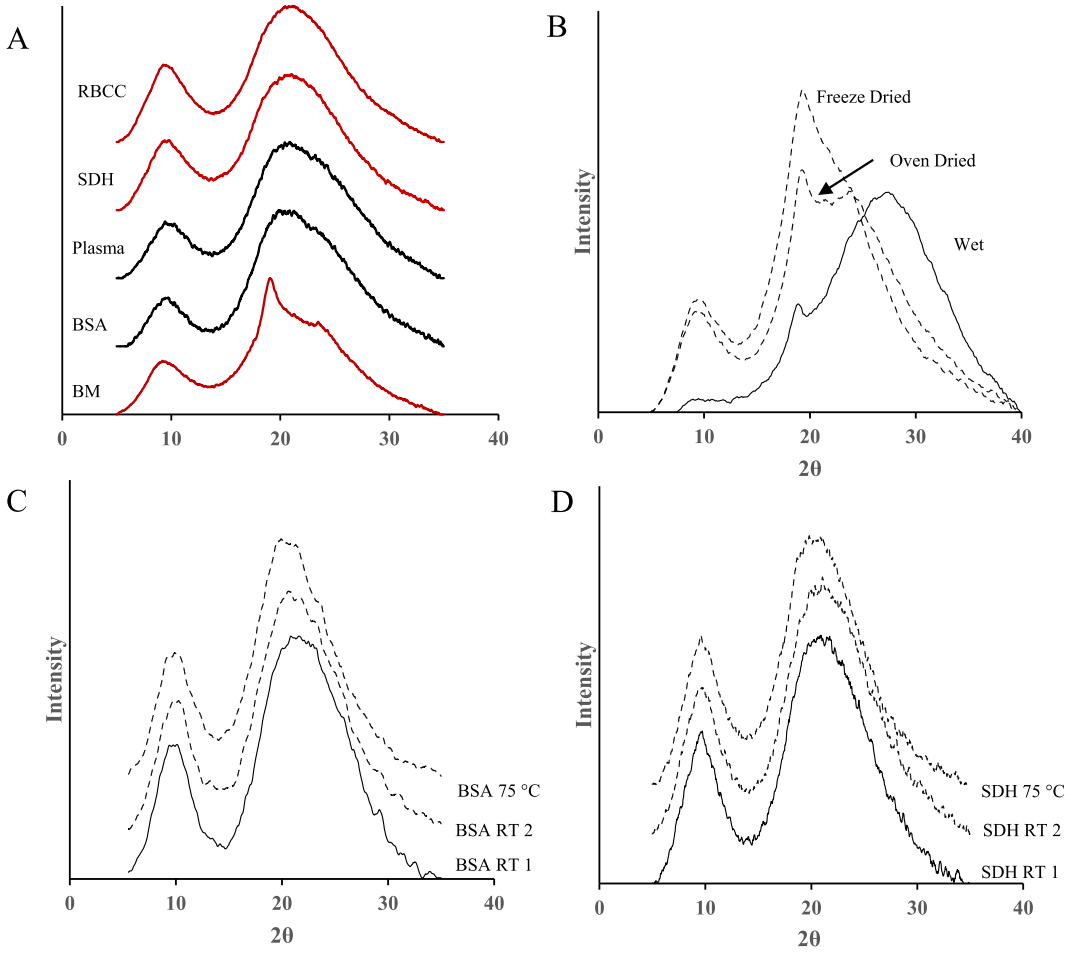

Fig. 6. A. XRD curves for blood meal and each of the blood fractions. B. The last graph is the behaviour of coagulated blood, oven dried and freeze dried samples. C. Heat treatment of BSA and D. Heat treatment of SDH. Three XRD scans are shown. Room temperature (RT 1) before heating, XRD at 75 °C and room temperature scan after (RT 2).

conventional polymer processing it could be expected that a more amorphous material would be preferred, as amorphous regions interacts more efficiently with the blowing agents [35]. As discussed blood meal is highly ordered, and PNTP is less so, which may impact foaming. It is also interesting to consider whether the increase in ordered structures arises from the native protein conformation or processing conditions.

3.2. Blood protein fractions

Dried red blood cells (RBCC), spray dried haemoglobin (SDH), plasma and bovine serum albumin (BSA) have a large highest transition in a similar range to blood meal (BM) (Fig. 3). The highest transition has been identified as a T_g despite demonstrating linear behaviour on an Arrhenius plot (ln frequency vs. 1/T). A T_g is usually identified as a non-linear α-relaxation however, when the temperature is sufficiently high large scale motion becomes unconstrained resulting in Arrhenius behaviour [1]. The activation energy was between typically between 700 and 900 kJ/mol, with the exception of BSA (Table 3). For plasma, three overlapping transitions were observed in the 190–225 °C region and all had similar activation energies and was designated as α-transitions.

The transition between 60 and 80 °C was initially thought to be a β-transition as it is close to 0.75 of the T_g temperature on a Kelvin temperature scale. A β-transition would indicate local chain movement, and on an Arrhenius plot should also demonstrate a linear relationship. The frequency dependence of this peak in all samples was non-linear and so it is suspected that this increase in chain movement may be associated with some other mechanism, similar to ageing as described by DSC (discussed later).

Minor differences between RBCC and SDH were observed with the first transition appearing narrower for SDH and 3 °C higher. Plasma and BSA both had a transition temperature at approximately 218 °C Table 4. This is consistent with the T_g of freeze dried BSA reported in literature to be 216 °C [36]. Plasma had additional transitions at 174 and 198 °C. This is likely due to onset of molecular motion for the other proteins present in plasma, namely α-, β- and γ-globulins and fibrinogen.

Although blood meal's T_g was similar to the individual fractions, the broadness of the transition could be explained by the molecular weight distribution of blood meal. FPLC analysis was conducted on the protein fractions which are completely soluble and partially soluble blood meal. RBCC demonstrated a single peak at an elution volume of 18 mL which correlates to the 16 kDa molecular weight of the haemoglobin molecule. BSA presents two peaks which can be attributed to the monomer (66.5 kDa, 16 mL) and dimer forms (132 kDa, 14 mL).

A clear increase was observed in the molecular weight distribution, with BM showing a large proportion of high molecular weight components (HMW) (Fig. 4). This means that even in the soluble fraction the protein component of blood meal was significantly cross linked. However, there are also some shorter fragments (approximately

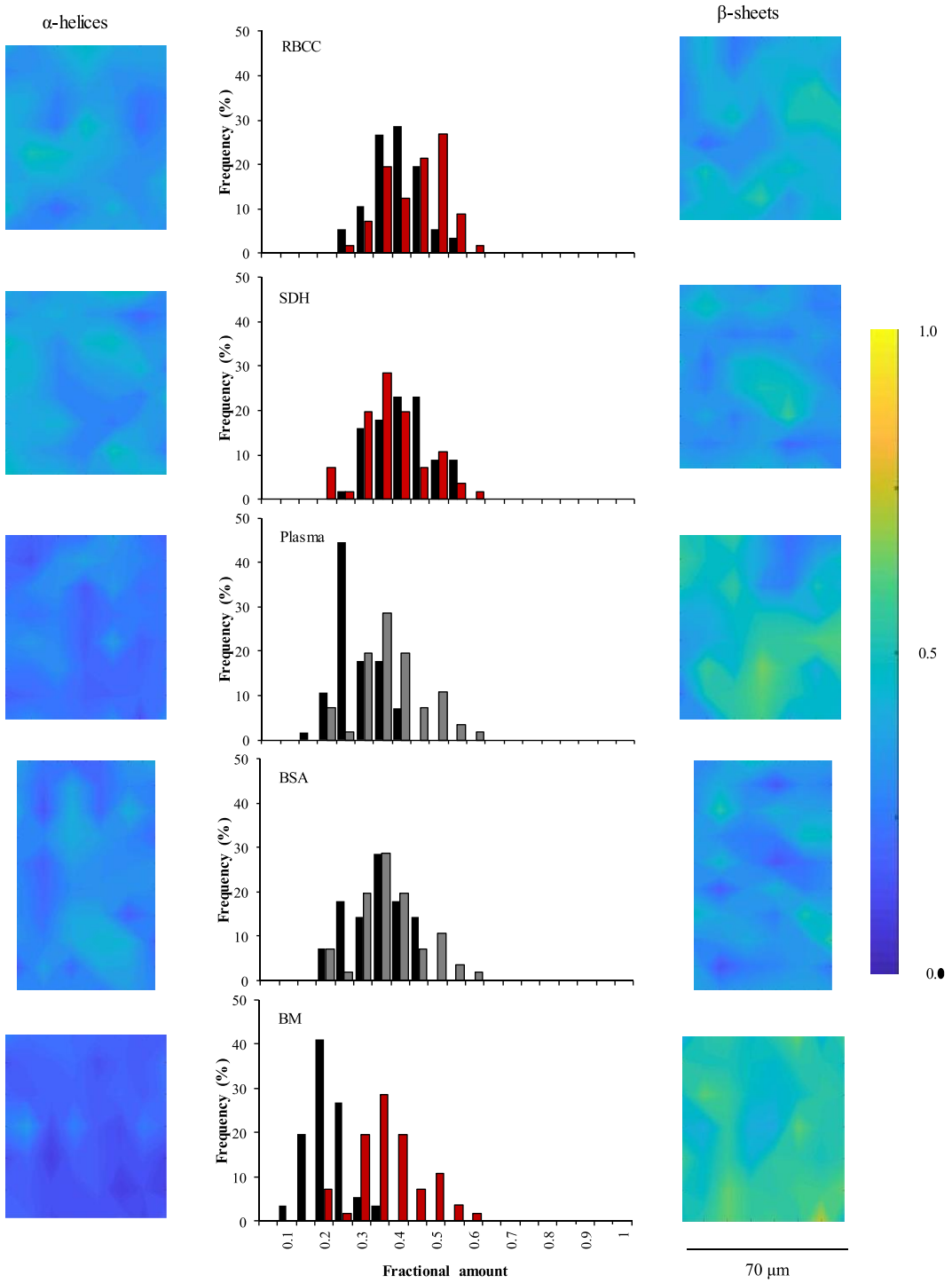

Fig. 7. Spatially resolved maps α-helical distribution (LHS) and β-sheet structure (RHS). Histograms of each distribution are shown in the centre for RBC, SDH, Plasma, BSA, and BM top to bottom. α-helical distribution shown in black, β-sheets structures shown in grey (for non-haem containing fractions) and red (for haem containing fractions).

12 kDa) that may influence processing of a bioplastic produced from BM (For example, the molecular weight distribution of polystyrene has been shown to affect cell size depending upon whether it is narrow or broad [37]). Finally the peaks at 22 mL and higher relate to SDS micelles and salt, respectively [10].

DSC revealed a denaturing peak around 115 °C in SDH and BSA, which was absent in BM, indicating that BM was highly denatured during drying. The curvature observed in Fig. 5 has been concluded to be an artefact of the DSC and is not a true denaturing peak. In addition, all proteins exhibited an endothermic event between 60 and 80 °C which was absent in the second scan (Fig. 5) and is associated with chain packing. It was hypothesized that the drying method would

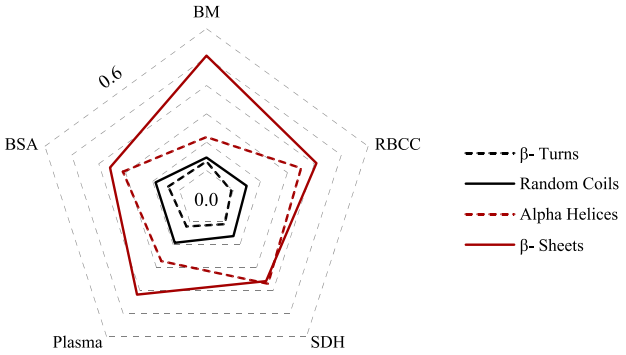

Fig. 8. Secondary fractional composition of blood meal and protein samples.

influence the relative magnitude of this event (ΔH, J/g), as some methods may cause the chains to become more constrained, as the chains pack more tightly. Blood meal had the lowest ΔH of 0.27 J/g, indicating it is the most constrained system (Table 5). The lack of chain mobility can be attributed to steam coagulation which thermally disrupts the native protein structure exposing hydrophobic regions. These regions aggregate together to form a more tightly bonded structure which excludes water. After dewatering, blood meal coagulate has a solids content of approximately 60% compared to conventional sludges which contain 20–30% solids. In comparison the protein fractions have had less thermally destructive treatments retaining their native structures to some extent and retaining more free volume than BM making them more soluble. Hence the need for SDS and urea to disrupt hydrophobic interactions and sodium sulphite to disrupt disulphide bonds/crosslinks in BM during Novatein processing.

RBCC and SDH demonstrated similar crystallinities to bovine serum albumin (approximately 30%). Of the protein fractions, plasma showed the lowest crystallinity and blood meal had a total crystallinity of 27%. The diffractogram of blood meal showed a pronounced peak at 18°, which is only present in this thermally dried protein and suggests higher crystallinity (Fig. 6A). However, there was also a reduction in the area of the peak at 8° relative to the purified fractions. The first peak corresponds to a d-spacing of 10 Å, which has been attributed to either inter-helix or inter-sheet structures in proteins. The peak at higher angles corresponds to a d-spacing of 4–5 Å and is associated with the repeating distance within these structures. The more pronounced peak at 18° in BM would suggest a greater proportion of tightly bonded structures (a smaller packing distance) at the expense of inter-structure packing, suggesting that BM has a higher proportion of ordered secondary structures. It is interesting, however, that none of the protein fractions demonstrated this peak.

To further explore protein chain spacing behaviour, BSA and SDH were heated to above 75 °C before analysis (Fig. 6C and D). The rearrangement of protein chains is limited in these materials as they were insufficiently plasticised and prevented the formation of the peak at 18°. However, this peak was observed in wet coagulate (60% water) and became more pronounced after oven or freeze drying (Fig. 6B). A lower peak intensity is also observed at 10° suggesting that the inter-structure distance became less upon the removal of water.

DSC and XRD both show that blood meal is a more constrained system suggesting some change in protein secondary structure. To study chain conformation, spatially resolved synchrotron based FT-IR analysis was conducted (Fig. 7). BM is highly aggregated, as seen by its high β-sheet content, followed by plasma, which had a much wider distribution of β-sheets (Fig. 7). This higher β-sheet content is due to aggregation during steam coagulation and drying where temperatures exceed 120 °C. This also comes at the expense of the α-helical content, similar to the results of thermal analysis for BSA [7] and porcine red blood cells [25].

Overall it was shown that the secondary structure of RBCC and SDH were very similar with a matching proportion of α-helices (Fig. 8). Of the two samples, RBCC had a slightly higher β-sheet content then SDH, while SDH had a slightly higher proportion of β-turns. Similar results were observed for plasma and BSA which were significantly different to the haem containing fractions. There was a good agreement between the two samples, however plasma was slightly higher in β-sheets than BSA. This could be due to the salts within the plasma fraction which may alter the conformation or due to the globulin and fibrinogen components which are removed in purified BSA.

Although all samples demonstrated a fraction of β-sheets greater than 30% this is lower than the content in BM. FPLC analysis uses surfactants to disrupt inter-chain bonding and BSA and RBCC demonstrated molecular weights corresponding to their monomer or dimer forms. Higher molecular weight components were observed in blood meal suggesting that some β-sheets may exist between protein chains not just within individual proteins. It is this bonding which is most likely disrupted during the production of PNTP creating a wider distribution of amorphous structures. Some β-sheets remain and will be dispersed throughout the material. The preservation of some of these structures is supported by the presence of the crystalline peak at 19° in XRD remaining in PNTP samples [38] although it is lower in intensity.

This suggests that blood meal should be considered as its own unique polymer. None of the techniques applied showed that the protein fractions influenced the behaviour of dried BM. This establishes that Novatein cannot be considered as the sum of its protein components unlike other thermoplastics which are influenced by their sub fractions. Most importantly, the protein secondary structure has implications during processing for materials like Novatein. As these structures have been shown not to melt during extrusion and injection moulding knowledge of their proportions, especially random coils, may facilitate the design of a material and enable minimisation of cycle times during injection moulding.

4. Conclusions

Blood meal is best considered as a biopolymer rather than the sum of its individual fractions as a result of how it is processed.

FPLC shows that the soluble fraction of blood meal has a significantly higher molecular weight than its two common fractions, RBCC and BSA. DSC analysis eluded to this difference which was supported by XRD through a clear crystalline peak at 18°. Together these techniques suggested a very different molecular arrangement which was very tightly packed. FTIR analysis of the amide III (1180-1330 cm^{-1}) confirmed this with BM consisting of at least 10% higher in β-sheet content than the blood fractions. The unique peak observed in XRD of blood meal was attributed to chain rearrangement in a hydrated state and dried BSA and SDH fractions did not display this feature upon heat treatment. Largely, they were resistant to change. Blood meal's behaviour can be explained by the disruption of the native protein structure during steam coagulation and extensive aggregation occurring through hydrophobic interactions between protein chains.

From a processing perspective the changes in BM during thermoplastic processing are more important than the behaviour of any of the individual proteins in blood meal. DMA has shown that the transitions in Novatein will effect processing and foaming behaviour with PNTP production disrupting the protein secondary structure from a highly aggregated state. It is therefore this behaviour that should be evaluated while investigating the foaming behaviour of this material rather than viewing blood meal as the sum of a series of low molecular weight components.

Overall this study added to the limited literature for the analysis of solid state proteins for bioplastics production and this knowledge may also be applied in the food, medical and animal feed industries.

Data availability

Data is available upon request.

Acknowledgements

The authors wish to acknowledge Rohit Giridhar for his assistance with the blood coagulate experiment. For the protein structure analysis (FT-IR) this research was undertaken on the Infrared Microspectroscopy (IRM) beamline at the Australian Synchrotron, part of ANSTO.

References

[1] J.M. Bier, C.J. Verbeek, M.C. Lay, Thermal transitions and structural relaxations in protein-based thermoplastics, Macromol. Mater. Eng. 299 (5) (2014) 524–539.
[2] L. Di Gioia, B. Cuq, S. Guilbert, Thermal properties of corn gluten meal and its proteic components, Int. J. Biol. Macromol. 24 (4) (1999) 341–350.
[3] A. Morales, J.L. Kokini, Glass transition of soy globulins using differential scanning calorimetry and mechanical spectrometry, Biotechnol. Prog. 13 (5) (1997) 624–629.
[4] T.R. Noel, R. Parker, S.G. Ring, A.S. Tatham, The glass-transition behaviour of wheat gluten proteins, Int. J. Biol. Macromol. 17 (2) (1995) 81–85.
[5] T. Hicks, C.J. Verbeek, M.C. Lay, J.M. Bier, Effect of oxidative treatment on the secondary structure of decoloured bloodmeal, RSC Adv. 4 (59) (2014) 31201–31209.
[6] C. Marrazzo, E. Di Maio, S. Iannace, Foaming of synthetic and natural biodegradable polymers, J. Cell. Plast. 43 (2) (2007) 123–133.
[7] K. Murayama, M. Tomida, Heat-induced secondary structure and conformation change of bovine serum albumin investigated by fourier transform infrared spectroscopy, Am. Chem. Soc. 43 (36) (2004) 11526–11532.
[8] M. Oliviero, E. Di Maio, S. Iannace, Effect of molecular structure on film blowing ability of thermoplastic zein, J. Appl. Polym. Sci. 115 (1) (2010) 277–287.
[9] J.T. Pelton, L.R. McLean, Spectroscopic methods for analysis of protein secondary structure, Anal. Biochem. 277 (2) (2000) 167–176.
[10] T.M. Hicks, C.J.R. Verbeek, M.C. Lay, M. Manley-Harris, Changes to amino acid composition of bloodmeal after chemical oxidation, RSC Adv. 5 (81) (2015) 66451–66463.
[11] G. Muschiolik, S. Draeger, Confectionery Gels with Whey Protein Concentrate 44 (1993), p. 227.
[12] J.M. Bier, C.J.R. Verbeek, M.C. Lay, Identifying transition temperatures in bloodmeal-based thermoplastics using material pocket DMTA, J. Therm. Anal. Calorim. 112 (3) (2013) 1303–1315.
[13] C.J.R. Verbeek, L.E. van den Berg, Extrusion processing and properties of protein-based thermoplastics, Macromol. Mater. Eng. 295 (1) (2010) 10–21.
[14] R. Liao, W. Yu, C. Zhou, Rheological control in foaming polymeric materials: II. Semi-crystalline polymers, Polymers 51 (2010) 6334–6345.
[15] R.T. Duarte, M.C. Carvalho Simões, V.C. Sgarbieri, Bovine blood Components: fractionation, composition, and nutritive value, J. Agric. Food Chem. 47 (1) (1999) 231–236.
[16] C.S. Bah, A.E.D.A. Bekhit, A. Carne, M.A. McConnell, Slaughterhouse blood: an emerging source of bioactive compounds, Compr. Rev. Food Sci. Food Saf. 12 (3) (2013) 314–331.
[17] E.J. Cohn, L.E. Strong, W. Hughes, D. Mulford, J. Ashworth, M.e. Melin, H. Taylor, Preparation and properties of serum and plasma proteins. IV. A system for the separation into fractions of the protein and lipoprotein components of biological tissues and Fluids1a, b, c, d, J. Am. Chem. Soc. 68 (3) (1946) 459–475.
[18] A. Farahnaky, F. Badii, I.A. Farhat, J.R. Mitchell, S.E. Hill, Enthalpy relaxation of bovine serum albumin and implications for its storage in the glassy state, Biopolymers 78 (2) (2005) 69–77.
[19] L. Ricci, E. Umiltà, M.C. Righetti, T. Messina, C. Zurlini, A. Montanari, S. Bronco, M. Bertoldo, On the thermal behavior of protein isolated from different legumes investigated by DSC and TGA analyses, J. Sci. Food Agric. 98 (14) (2018).
[20] C. Bengoechea, A. Arrachid, A. Guerrero, S.E. Hill, J.R. Mitchell, Relationship between the glass transition temperature and the melt flow behavior for gluten, casein and soya, J. Cereal Sci. 45 (3) (2007) 275–284.
[21] J.M. Uitto, C.J.R. Verbeek, The role of phase separation in determining the glass transition behaviour of thermally aggregated protein-based thermoplastics, Polym. Test. 76 (2019).
[22] J. Rault, Origin of the Vogel–Fulcher–Tammann law in glass-forming materials: the α–β bifurcation, J. Non-Cryst. Solids 271 (3) (2000) 177–217.
[23] G. Damian, V. Canpean, Conformational changes of bovine hemoglobin at different pH values, studied by ATR FT-IR spectroscopy, Rom. J. Biophys. 15 (1–4) (2005) 67–72.
[24] J.M. Bier, C.J.R. Verbeek, M.C. Lay, Using synchrotron FTIR spectroscopy to determine secondary structure changes and distribution in thermoplastic protein, J. Appl. Polym. Sci. 130 (1) (2013) 359–369.
[25] W.F. Wolkers, H. Oldenhof, In situ FTIR studies on mammalian cells, J. Spectro. 24 (5) (2010) 525–534.
[26] P. Belton, Mini review: on the elasticity of wheat gluten, J. Cereal Sci. 29 (2) (1999) 103–107.
[27] N. Wellner, E.C. Mills, G. Brownsey, R.H. Wilson, N. Brown, J. Freeman, N.G. Halford, P.R. Shewry, P.S. Belton, Changes in protein secondary structure during gluten deformation studied by dynamic Fourier transform infrared spectroscopy, Biomacromolecules 6 (1) (2005) 255–261.
[28] M. Levitt, J. Greer, Automatic identification of secondary structure in globular proteins, J. Mol. Biol. 114 (2) (1977) 181–239.
[29] A. Dong, P. Huang, W.S. Caughey, Protein secondary structures in water from second-derivative amide I infrared spectra, Biochemistry 29 (13) (1990) 3303–3308.
[30] K. Abrosimova, O. Shulenina, S. Paston, FTIR study of secondary structure of bovine serum albumin and ovalbumin, Journal of Physics: Conference Series, IOP Publishing, 2016, p. 012016.
[31] H.R. Costantino, K. Griebenow, P. Mishra, R. Langer, A.M. Klibanov, Fourier-transform infrared spectroscopic investigation of protein stability in the lyophilized form, Biochim. Biophys. Acta Protein Struct. Mol. Enzymol. 1253 (1) (1995) 69–74.
[32] C. Gavin, C.J.R. Verbeek, M.C. Lay, Morphology and compressive behaviour of foams produced from thermoplastic protein, J. Mater. Sci. 53 (22) (2018) 15703–15716.
[33] C. Gavin, M.C. Lay, C.J. Verbeek, Extrusion foaming of protein-based thermoplastic and polyethylene blends, PROCEEDINGS OF PPS-31: The 31st International Conference of the Polymer Processing Society–Conference Papers, AIP Publishing, 2016, p. 100003.
[34] C. Gavin, M.C. Lay, C.J.R. Verbeek, Conformational changes after foaming in a protein-based thermoplastic, J. Appl. Polym. Sci. 135(13) 46005.
[35] A.V. Nawaby, Z. Zhang, Solubility and diffusivity, in: R. Gendron (Ed.), Thermoplastic Foam Processing: Principles and Development, CRC Press, Boca Raton, 2004.
[36] J. Carpenter, D. Katayama, L. Liu, W. Chonkaew, K. Menard, Measurement of T g in lyophilized protein and protein excipient mixtures by dynamic mechanical analysis, J. Therm. Anal. Calorim. 95 (3) (2009) 881.
[37] C.M. Stafford, T.P. Russell, T.J. McCarthy, Expansion of polystyrene using supercritical carbon dioxide: effects of molecular weight, polydispersity, and low molecular weight components, Macromolecules 32 (22) (1999) 7610–7616.
[38] J.M. Bier, C.J.R. Verbeek, M.C. Lay, Thermal and mechanical properties of bloodmeal-based thermoplastics plasticized with tri(ethylene glycol), Macromol. Mater. Eng. 299 (1) (2013) 85–95.

7

Conformational Changes after Foaming in a Protein-Based Thermoplastic

A journal article

by

C. Gavin, C.J.R Verbeek and M.C. Lay

Published in

The Journal of Applied Polymer Science

Overview:

Novatein can be successfully foamed and the purpose of this chapter is to evaluate what changes have occurred within the material. This chapter applies dynamic mechanical analysis, differential scanning calorimetry, X-ray diffraction and Fourier transform Infrared (FT-IR) to establish this. The behaviour of blood meal, pre-processed NTP (PNTP) and extruded NTP (ENTP) have been previously studied but are included to establish relative changes in a foaming context and to overcome variability in the protein feed stock.

This work relates to objective three by examining chain architecture and plasticiser distribution near a bubble surface.

Contribution:

As first author for this publication the PhD candidate conducted all experimental work, data analysis and prepared the first draft of this manuscript. Under guidance from the supervisors the manuscript was revised and edited.

JOURNAL OF Applied Polymer SCIENCE

Conformational changes after foaming in a protein-based thermoplastic

Chanelle Gavin, Mark C. Lay, Casparus J. R. Verbeek
School of Engineering, Faculty of Science and Engineering, University of Waikato, Hamilton, New Zealand
Correspondence to: C. Gavin (E-mail: chanellegavin@gmail.com)

ABSTRACT: Novatein is a biopolymer produced from blood meal and can be foamed for use as a packaging material. The effect of foaming on protein ordered structures such as α-helices and β-sheets was investigated using synchrotron Fourier transform infrared (FTIR). Foaming caused a reduction in ordered structures due to an increase in random coils. FTIR also revealed a higher proportion of plasticizer (triethylene glycol, TEG) and β-sheets toward the surface of enclosed bubbles. Increased TEG will assist foaming with greater plasticization aiding nucleation, while β-sheets contribute to bubble stabilization. These structural changes occur as foaming takes place close to the degradation temperature of Novatein, and coincide with melting of α-helices and/or β-sheets. A more amorphous polymer is therefore produced which is subsequently easier to foam due to its increased elasticity. © 2017 Wiley Periodicals, Inc. J. Appl. Polym. Sci. **2018**, *135*, 46005.

KEYWORDS: biodegradable; biopolymers and renewable polymers; foams; proteins; thermoplastics

Received 10 August 2017; accepted 2 November 2017
DOI: 10.1002/app.46005

INTRODUCTION

Foaming polymeric materials provides a method of reducing part cost and/or weight, making it ideal for producing packaging materials. Foaming is achieved by either batch processing, foam extrusion or foam injection molding using materials such as polystyrene (PS), polypropylene (PP), polyethylene (PE), and poly(vinyl chloride). These materials are often selected for resistance to chemicals, ultraviolet, and moisture; properties which later prevent these materials from readily breaking down. Consequently, the need for similar products from biobased or biodegradable materials is increasing. Fortunately, starch, poly(lactic acid), poly(hydroxyalkanoates), bio-derived thermoplastics like bio-polyethylene terephthalate (Bio-PET), and thermoplastic proteins are becoming feasible alternatives for foamed materials.[1–5] Protein plastics are particularly interesting as they have the potential to be both bio-derived and biodegradable, making them ideal for limited life applications such as packaging foam.

Despite the large number of possible protein feedstocks from plant and animals, only a few of these have been used to make thermoplastics. To date, thermoplastic proteins have only been successfully produced from blood,[6,7] gelatin,[8,9] keratin,[10,11] soy,[4,12–14] kafirin,[15] and zein.[9,15–18] However, their subsequent commercialization and application in foaming is even more limited, and fewer still have been foamed without blending. Of these, only thermoplastic gelatin and zein has been foamed using CO_2 and N_2 in a batch system[9] and soy protein isolate has been foamed with a chemical blowing agent through a continuous FEX system.[19]

In general, when working with protein plastics the upper processing limit is determined by the temperature at which degradation and crosslinking of the protein occurs. For foaming, this is difficult to balance with the semicrystalline nature of the material, which demands higher processing temperatures.

Proteins have amorphous regions and crystalline domains in the form of regular structures (α-helices and β-sheets). These structures are analogous to lamella and spherulites in traditional polymers, are similar in size, and act to restrict protein chain movement. The presence of these structures in traditional foaming systems has both advantages and disadvantages. It is widely agreed that the uptake of a gas into the polymer matrix will occur only in the amorphous phase and the crystalline regions do not participate in any absorption and actively inhibit diffusion.[20] Consequently, the solubility of a gas within a semicrystalline material is lower than that of a purely amorphous counterpart and the foaming ability is reduced. To overcome this foaming should occur above the melt temperature of the polymer such that these structures are fully disrupted to achieve a truly homogenous polymer/gas melt, particularly for microcellular foaming.[20] If not fully melted the presence of crystalline regions of more than a few micron can lower the activation energy for gas bubble nucleation and increase the nucleation rate by providing a surface for the bubble to form on.[20–22]

Foaming is also affected by the viscosity of the polymer or polymer/gas mixture. Low shear viscosity will initially promote foaming by aiding nucleation. Appropriate extensional viscosity is then

required to enable growth. However, if the shear viscosity is too low, the foam will collapse during stabilization. Polymers which strain harden are therefore most suitable for foaming. For example, it was shown that zein which had a higher β-sheet content in its native state resulted in a collapsed foam as the material was unable to withstand elongational deformation while zein with a lower β-sheet content produced a fine-celled foam.[23]

The presence of impurities or solid additives can also promote fined-celled foams by acting as nucleating agents. The disadvantage of this is that it is difficult to achieve homogenous distribution of these particles within the material. Consequently, nucleation is non-uniform, resulting in irregular cell growth and difficulty in controlling cell morphology.

The impact of the semicrystalline nature of protein thermoplastics on foaming has primarily been focused on processing conditions and altering morphology.[4,8,9,19,24] An aspect not considered is that if crystalline regions (α-helices and β-sheets) in protein thermoplastics do not fully melt,[25] they may act as nucleation sites, similar to solid additives.

Novatein is a relatively new thermoplastic protein manufactured from blood meal, a byproduct of the meat processing industry. It has been extensively studied in terms of processing conditions, additives, and moisture content on protein secondary structure and mechanical properties for unfoamed materials. This study will investigate the effect of foaming Novatein on changes in both the thermal behavior of the bulk material and protein secondary structure.

EXPERIMENTAL

Thermoplastic Preparation

Pre-extruded Novatein (PNTP) was prepared by blending sieved blood meal (particle size < 710 μm, supplied by Wallace Corporation Limited, Waitoa, New Zealand) with additives and plasticizers in a bench scale Labtech high speed mixer at 1400 RPM. Three parts per hundred blood meal (pph) sodium sulfite and 3 pph sodium dodecyl sulfate from Merck (Germany), 10 pph agricultural grade urea from Ballance Agri-nutrients (NZ) was dissolved in 40 pph distilled water. This denaturing solution was added to the blood meal and well mixed in a bench scale Labtech high speed mixer at 1400 RPM before the plasticizer component (20 pph triethylene glycol (Merck) was added to produce PNTP. The material was sealed in two ziplock bags and stored overnight at 4 °C before extrusion. A Labtech Scientific twin-screw extruder with an *L*/*D* ratio of 44 and 20 mm diameter screws was used with a temperature profile of 70, 100–100, 110, 120 °C feeder to die (10 mm) to extrude the PNTP at a constant torque of 55%–60%. The material was then granulated by a tri-blade granulator (Castin Machinery Manufacturing Limited, New Zealand) through a 4 mm screen to produce extruded Novatein (ENTP).

Foaming Method

Foamed Novatein (FNTP) was produced using a single screw Boy 35A injection molder with a 24 mm diameter screw and an *L*/*D* ratio of 22. The machine was operated by withholding the nozzle from the mold to enable free expansion of the material as it exited the die. The Boy 35A has five temperature zones which can be independently controlled between the feeder and die. There are three large heating zones (zones 1–3) followed by plinth heating (zone 4) and finally nozzle heating (zone 5). During these trials the temperature of zone 1 was kept constant at 100 °C to prevent bridging in the feeder. The remaining temperatures were set to 160 °C. A pressure drop of 180 MPa occurred at the die, with an injection speed of 48 mm/s.

Analysis

Changes in ordered structure and thermo-mechanical behavior of blood meal, PNTP, ENTP, and powdered (less than 710 μm) foamed material was investigated using wide angle X-ray scattering analysis, dynamic mechanical analysis (DMA), differential scanning calorimetry (DSC), and thermogravimetric analysis (TGA).

Thermal Analysis. Powder pocket DMA analysis was conducted in a single cantilever configuration using a PerkinElmer DMA 8000 equipped with a temperature controlled furnace which was regulated by Pyris software. Samples (∼50 mg) were crimped in stainless steel powder pockets, cooled to 80 °C (193 K) and allowed to equilibrate. The temperature was then increased at a rate of 2 °C/min up to 150 °C (423 K). Multi-frequency data was collected at 0.1, 0.3, 1.0, 3.0, 10.0, and 30.0 Hz from −70 °C (203 K) with a dynamic displacement of 0.05 mm.

For DSC analysis, 5–8 mg of powdered samples were analyzed in sealed aluminum pans (PerkinElmer), in a PerkinElmer DSC 8500 with a Peak Scientific nitrogen generator connected to a compressed air supply. The nitrogen gas was supplied to the DSC at 100 psi through a PerkinElmer Intercooler 2 (–100 °C). Samples were cooled from room temperature to −80 °C and held isothermally for 5 min to equilibrate. Samples were heated at a rate of 10 °C/min to 180 °C. The scan was repeated after cooling to −80 °C at the same rate. During this procedure the DSC was purged constantly with nitrogen at 20 mL/min. Three replicates were conducted for each sample type.

TGA was conducted on powdered samples (6–10 mg in mass) using alumina pans in a TA Instruments SDT 2960. Samples were heated from room temperature to 800 °C at a rate of 10 °C/min, while being purged with dry air at a rate of 150 mL/min. Moisture content was determined by the mass loss up to 120 °C. An average moisture content was determined based upon three samples.

X-ray Analysis. The total amount of ordered structures was determined by powder X-ray diffraction (XRD) using a Panalytical Empyrean XRD machine. X-rays were generated by a copper X-ray tube operating at 45 kV and 40 mA ($\lambda 1 \approx \lambda 2 \approx 1.54$). Samples were analyzed on a spinner stage rotating at one revolution per second for 2 theta angles between 4° and 60° with a step size of 0.026°. A 10 mm mask, an automatic programmable divergent slit, and a 0.04 rad soller slit were configured on the incident beam. The diffracted beam passed through a fixed 7.5 mm anti-scatter slit, a 0.04 rad soller slit, and a nickel filter before the intensity was measured by a PIXcel three-dimensional detector. The amount of ordered structures (an average of three samples) was determined by baseline correcting the spectra between 4° and 35°. A Gaussian curve was fitted to the amorphous fraction and subtracted. A further five Gaussian peaks were fitted to model the ordered fraction by minimizing the sum of squared errors. The fitted peaks were

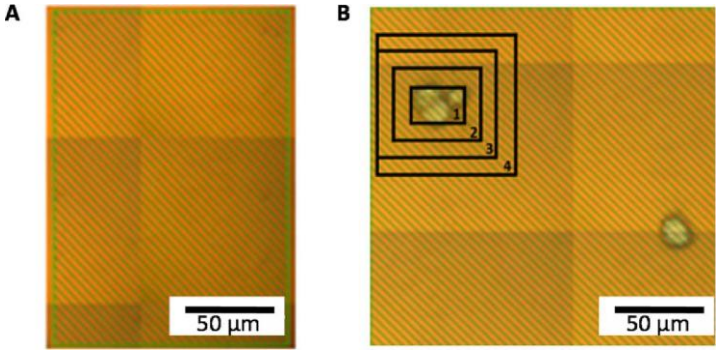

Figure 1. Samples analyzed by synchrotron FTIR. (A) Wall structure/bulk material. (B) Wall structure with observable bubbles (regions 1–4 annotated). [Color figure can be viewed at wileyonlinelibrary.com]

defined with respect to height, width, the calculated height to width ratio, and peak area. The corresponding *d*-spacing was calculated according to Bragg's Law.

Synchrotron Fourier Transform Infrared. FNTP samples were analyzed using the infrared micro-spectroscopy beamline at the Australian Synchrotron. Prior to analysis, samples were freeze dried for 48 h using a bench scale 2.5L Freezone freeze drier (Labconco Corporation, Kansas City), operating at −50 °C and <56 Pa. For analysis, the samples were flattened between two diamond slides. Fourier transform infrared (FTIR) spectra were collected in transmission mode on a Bruker Hyperion 3000 using an XY stage and MCT collector. Large maps of more than 299 spots were collected. The spectra were taken at 10 μm intervals with a spot size of ~7 μm. Spectra were collected for wavenumbers between 3800 and 800 cm^{-1} at a resolution of 4 cm^{-1}.

Two samples were analyzed: the first was a piece of the bulk material (wall structures); and the second contained encapsulated microbubbles which were stabilized when the material solidified upon cooling (Figure 1). The first sample was analyzed for changes in the bulk material composition following foaming, while the second sample was studied for changes in these structures and plasticization near the bubble surface. These changes were examined by first identifying the scans that were taken over the bubble surface (region 1). Further regions (2–4) were defined as one scan out from the previous region until the composition of the final region (region 4) matched the composition of the bulk material.

Analysis of the spectra was conducted using OPUS 7.0 software from Bruker Optik GmbH, Germany, and was used to determine the protein secondary structure and the plasticizer distribution. The distribution of α-helices, β-turns, random coils, and β-sheets was determined after the spectra have been screened for saturation in the amide III region (1180–1330 cm^{-1}). The area directly over the bubble in sample two was saturated (absorbance exceed 1.3) in the regions of interest [amide III and triethylene glycol (TEG) peaks]. This area (region 1) was therefore ignored for subsequent analysis.

To determine the composition, the area of each peak was integrated and the area ratios of α-helices, β-turns, and random coils to β-sheets calculated according to the method presented by Bier *et al.* and Hicks *et al.*[26,27] The integration limits were redefined as the minima were shifted toward lower wavenumbers and some peaks were broader in nature (Table I). The shift toward lower wavenumbers was ~5 cm^{-1}.

$$\beta = \frac{1}{\frac{A''_\alpha}{A''_\beta} + \frac{A''_t}{A''_\beta} + \frac{A''_r}{A''_\beta} + 1} \quad (1)$$

$$\alpha = \beta \frac{A''_\alpha}{A''_\beta} \quad (2)$$

$$t = \beta \frac{A''_t}{A''_\beta} \quad (3)$$

$$r = \beta \frac{A''_r}{A''_\beta} \quad (4)$$

$$\alpha + \beta + t + r = 1 \quad (5)$$

TEG was also examined using the primary alcohol group (C—O—H bond) between 1040 and 1095 cm^{-1} and the aliphatic ether group of C—O—C bonding around 1095–1150 cm^{-1}.

RESULTS AND DISCUSSION

X-ray Diffraction

Small changes in the total amount of ordered structures were detected between blood meal, pre-processed, ENTP, and FNTP. Three peaks characteristic of bonding within and between protein structures were observed (Table II) in all samples (Figure 2). Peak position did not change indicating no change in the average *d*-spacing within or between these structures. A slight decrease in peak 1

Table I. FTIR Wavenumber Assignments within the Amide III Region for Each Structure

Structure	Normal limits[26,27]	Redefined limits
α-Helices	1295-1330	1295-1335
β-Turns	1270-1295	1265-1295
Random coils	1250-1270	1235-1265
β-Sheets	1220-1250	1220-1235

Normal limits as defined in literature were redefined due to the shape of the second derivative.

Table II. Characteristic Protein Peaks in XRD Analysis

Peak	Angle	*d*-spacing (Å)	
1	9.7°	9.1	Spacing between structures e.g., β-sheets and α-helices.
2	19.1°	4.6	Corresponds to the distance between adjacent β-sheet or the hydrogen bonding distance within the α-helical backbone
3	20.7°	4.3	

area was noted while the combined area of peaks 2 and 3 increased when ENTP was foamed (Figure 3). Similarly, peak width for the first peak (which is associated with the spacing between crystalline structures) remained mostly constant with only a small amount of broadening for ENTP and FNTP samples. This indicated a wider variation in distance between these structures. Simultaneously, the width of peak 2 narrowed, suggesting increased regularity in this spacing. Peak 3, also associated with the distance between adjacent β-sheets or the hydrogen bonding distance within the α-helical backbone, remained constant (Figure 3). Peaks 4 and 5 are defined as the residual, an artifact of fitting a Gaussian amorphous halo, and do not correlate to any physical properties.

Overall, structural order in PNTP decreased compared to blood meal due to fewer intermolecular bonds. Extrusion of PNTP resulted in a slight increase in order due to protein aggregation and crosslinking, while foaming resulted in a small (Figure 3) but statistically significant reduction in order (P-value = 0.03).

Thermal Analysis

DSC analysis indicated that rearrangement of the protein chains was occurring during Novatein production and foaming and suggested that the amount of ordered structures changed as well. This was determined by examining the sub-T_g endothermic peak (Figure 3) which occurs in Novatein between 55 and 63 °C. This is associated with the energy required to reverse short-range and rotational rearrangements in protein chains, which occur over time toward an equilibrium conformation. This peak is associated with chain mobility, which is greatest in the amorphous fraction. ΔH is the energy required to recover lost free volume, therefore a greater value is correlated with more reorganization of the amorphous chains.[27,28] Producing PNTP resulted in an initial decrease in the temperature at which this peak occurred due to hydration and plasticization of the blood meal (Figure 3), but it was expected that subsequent processing would increase this temperature due to moisture loss. This did not occur as the peak position was the same for PNTP, ENTP, and FNTP (55 °C) (Figure 3), implying that there must be a mechanism to counteract this shift.

ΔH increased following PNTP production, due to the plasticizers and denaturants resulting in greater chain mobility, allowing the protein chains to relax to a smaller packed volume. ΔH decreased after extrusion due to an increase in ordered

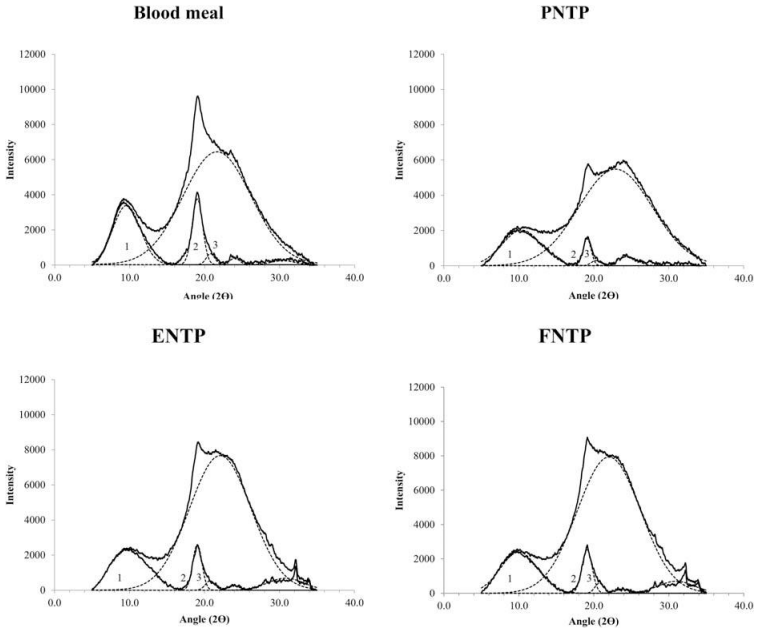

Figure 2. Baseline corrected XRD curves with amorphous halo and deconvoluted peaks shown.

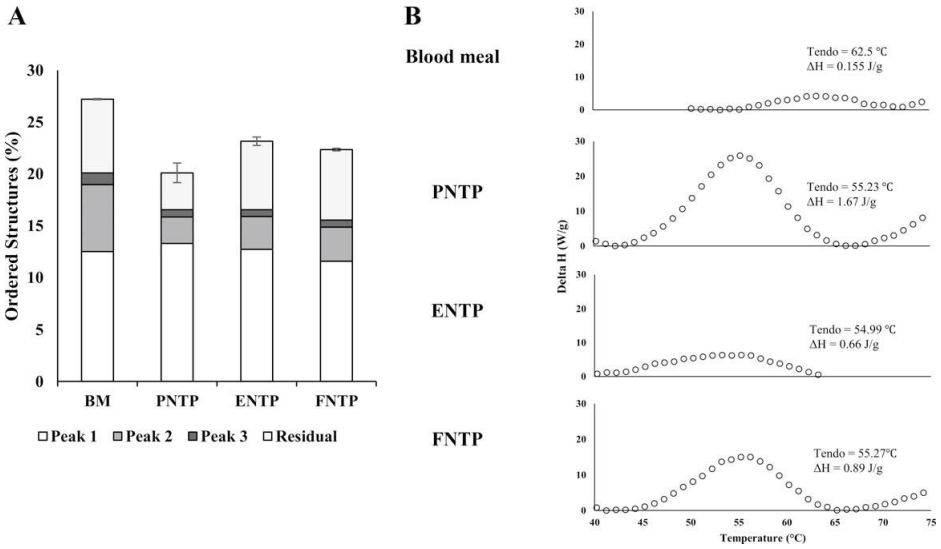

Figure 3. (A) Total ordered structures as determined by XRD reported as a percentage, relative peak areas also indicated. (B) Comparison of sub-T_g endothermic peak observed by DSC during the second heating scan.

structures, for example β-sheets, which has been observed previously using FTIR for NTP,[28] i.e., the amorphous fraction is more constrained and cannot relax to the same extent. However, following foaming ΔH increased, possibly due to the rapid expansion of the material as it exits the nozzle, disrupting the ordered structures[27] and producing shorter chains due to chain scission/hydrolysis. A drop in temperature at which the sub-T_g endothermic peak occurred for FNTP should also be observed if chain scission occurred, but a slight increase occurred and this is likely due to loss of plasticizer and moisture due to volatilization during foaming.

DMA indicated very little to no change in the position of the α-transition between ENTP and FTNP (Table III), associated with the glass transition (44 °C), but a reduction in the temperature at which the β-transitions occurred from −43 to −53 °C (Figure 4). Foaming of traditional polymers typically results in no changes in the DMA behavior for PP and PE,[29] therefore Novatein is consistent with this behavior. However, the absence of a shift in the glass transition temperature does not correlate with the reduction in moisture content of the material during foaming (Table IV) as determined by TGA. This suggests that foaming has suppressed the shift in glass transition. Furthermore, TGA analysis of this material determined no change in thermal stability with the production of volatiles and protein degradation occurring around 170 °C.

Table III. Thermal Transitions by Processing Stage as Determined by Tan δ Peak in DMA Analysis and Comparison to Previously Reported Values

BM	Ref.	Ti	Tii	Tiii
PNTP		−92	65	>150
ENTP		−73	−31	>150
FNTP		−43	44-54	112
BM		−53	44	115
BM	30	−91	63	220
PNTP	30	−82	32	126

All values reported in degrees Celsius.

Secondary Structure

The secondary structure was spatially resolved using synchrotron FTIR for two foamed NTP samples. The first was a part of the foam wall while the second contained observable bubble structures. The amide III region was used for analysis, as the amide I region experiences interference from urea peaks between 1600 and 1700 cm^{-1}. This region is also not commonly saturated using synchrotron light although some saturation was observed over the bubbles in the second sample (Figure 5).

To establish the composition of the bulk material all spectra from sample 1 were considered while data within four points of the bubble in sample 2 were excluded. Overall, both samples demonstrated the same composition and FNTP was found to have a lower α-helical (0.11–0.13) and β-sheet content (0.31–0.29), and higher levels of disordered structures, random coils, and β-turns (0.57–0.58) (Table V). The fractional composition changes of Novatein during processing (Table VI) has been reported previously by Bier *et al.*[26]

Foamed samples of Novatein had higher β-sheet content than the fraction observed for PNTP but lower than that for ENTP. This was unexpected as thermal treatment is known to promote the formation of β-sheets due to protein aggregation at the expense of α-helices. Consequently, the amount of disordered structures is higher in foamed samples. This increased level of

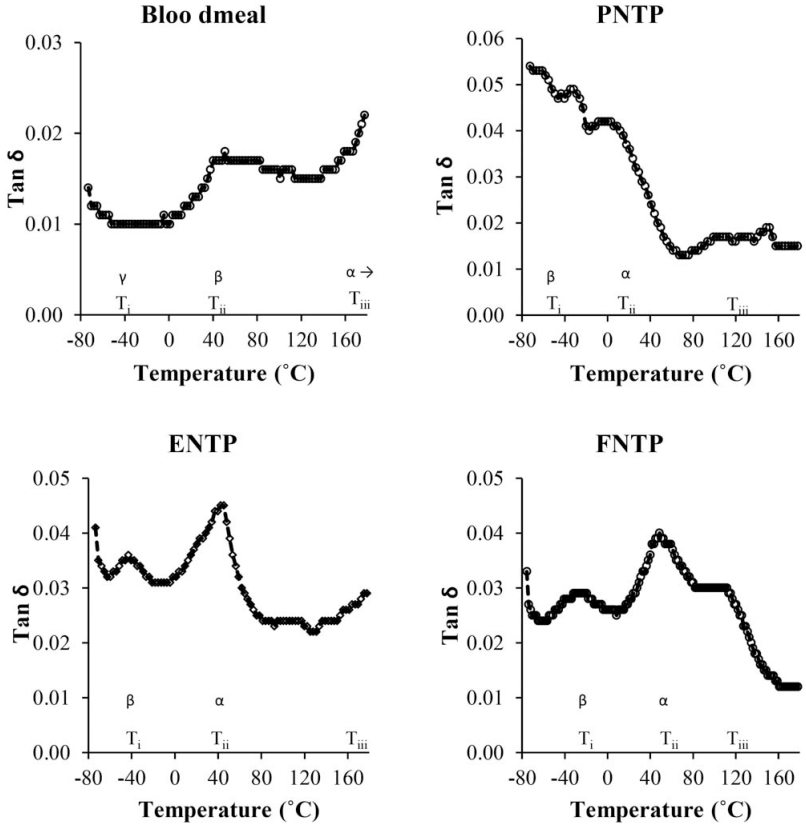

Figure 4. Thermal transitions identified by powder pocket DMA. Data shown is a representative frequency of 1 Hz.

Table IV. Moisture Content of Blood Meal, PNTP, ENTP, and FNTP.

Sample	Moisture content
Blood Meal	6.5% ± 0.3%
PNTP	23.2% ± 0.96%
ENTP	11.9% ± 2.14%
FNTP	8.5% ± 0.13%

Data presented as the average of three repeats with standard deviation.

Table V. Secondary Structure Composition of Foamed NTP Samples

	Sample 1		Sample 2	
Structure	Mean	SD	Mean	SD
α-helices	0.11	0.03	0.13	0.02
β-turns and random coils	0.57	0.04	0.59	0.04
β-sheets	0.31	0.04	0.29	0.04

disordered structures is consistent with the reduction in order observed by XRD and the changes in ΔH by DSC analysis, as these structures contribute to the amorphous fraction. This increase suggests that the reduction in ordered structure may be induced either by foaming or that foaming occurs in regions where there is a greater proportion of disordered structures due to their elasticity. Given that the foaming temperature is close to the melt temperature of α-helices and β-sheets (∼155–175 °C),[30] changes in secondary structure may be due to

Table VI. Previously Reported Composition of NTP by Processing Stage—Blood Meal (BM), Pre-extruded (PNTP), and Extruded (ENTP)[26]

	BM		PNTP		ENTP	
Structure	Mean	SD	Mean	SD	Mean	SD
α-helices	0.24	0.06	0.20	0.07	0.15	0.03
β-turns and random coils	0.41	0.09	0.52	0.08	0.48	0.04
β-sheets	0.35	0.09	0.28	0.07	0.36	0.04

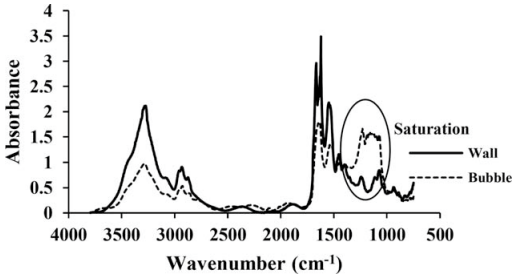

Figure 5. Representative spectra from FTIR analysis of the wall structure and bubble.

disruption of these structures and would explain the reduction in β-sheets.

The secondary structures around the bubble in sample 2 were spatially resolved. The spectra was saturated in the amide III region over the bubble surface possibly due to bending of infrared light through the bubble (Figure 5). Rectangles of one spot size close to the bubble were used to see if any gradient effects were present relative to the average (Figure 6). Ignoring region 1, the saturated bubble, region 3 was always higher or lower than region 2 (closer to the bubble) and region 4 (closer to bulk material). There was also a slight increase in β-sheet content closer to the bubble at the expense of random coils

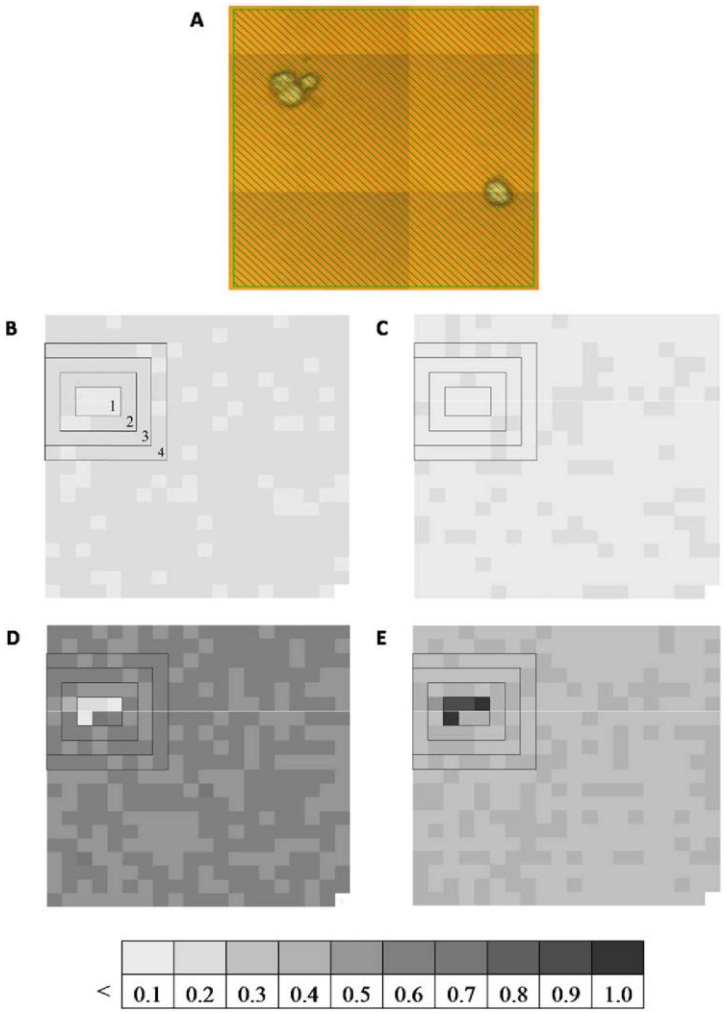

Figure 6. FTIR analysis of an NTP foam wall sample with bubbles. Region 1 is the bubble surface, region 2 is one spot removed, region 3 is two spots removed, and region 4 is three spots removed (bulk material). (A) The mapped area, (B) the distribution of α-helices, (C) the distribution of β-turns, (D) the distribution of random coils, and (E) the distribution of β-sheets within the sample. [Color figure can be viewed at wileyonlinelibrary.com]

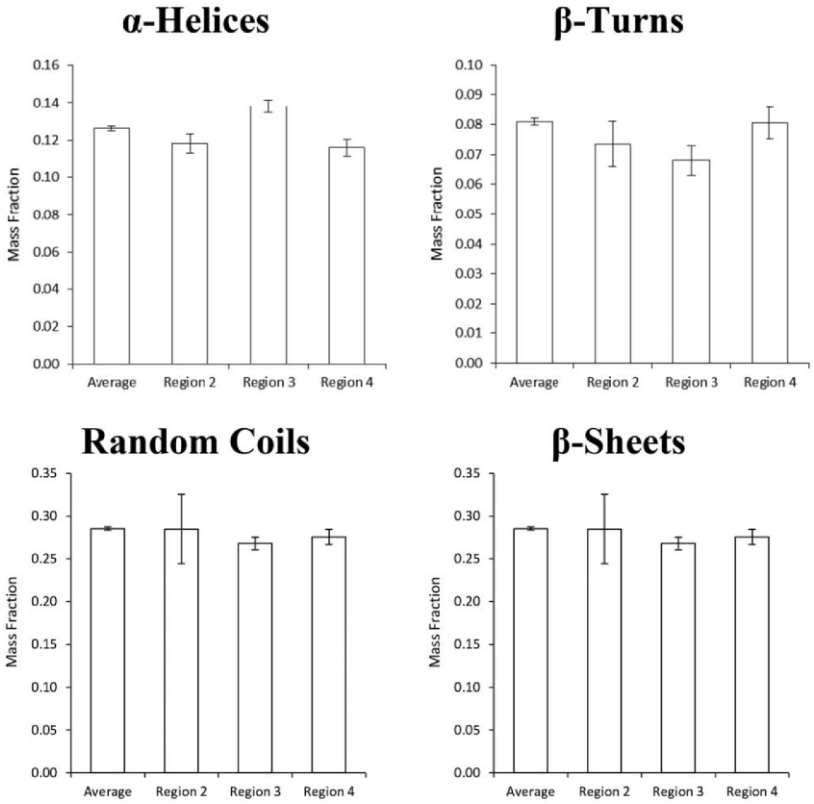

Figure 7. Fractional composition of secondary structures by region surrounding enclosed bubbles. Region 1—the bubble surface excluded due to saturation of spectra.

(Figure 7). It has previously been discussed in literature that these ordered structures may play a role in the elongational viscosity of protein thermoplastics and therefore affect bubble stabilization.[23]

A higher concentration of β-sheet structures near the bubble surface could be explained by a bubble nucleating near or on a β-sheet aggregate. A bubble will push the bulk material away until it is constrained by β-sheets resulting in an accumulation of β-sheets at the bubble surface. This highlights the role of β-sheets in bubble stabilization. It is also possible that the forces exerted by bubble growth may straighten protein chains, causing alignment, which could enable β-sheet formation. However, a lower fraction of β-sheets is observed within this material suggesting that

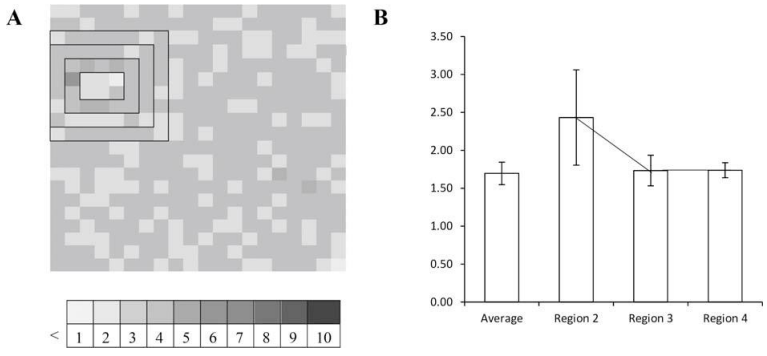

Figure 8. (A) TEG to amide III ratio for sample 2 a wall particle with bubble, (B) TEG to amide III ratio by region.

foaming overall disrupts these structures. Either way, the result is a series of ordered sheets around a stable bubble.

In region 3 α-helices increased and β-turns decreased (Figure 7), but this did not correlate with TEG distribution across the wall. It is possible that internal stresses within the cell wall produced by the presence of a stable bubble may have caused this slight variation in secondary structure.

Statistical analysis of the above changes by one way ANOVAs revealed that despite the increasing β-sheet and decrease in random coils toward the bubble surface neither trend was statistically significant with a P value of 0.35 and 0.34 respectively. Despite not being statistically significant, which is most likely due to a larger variation and lower rate of sampling near the bubble surface, the changes in random coils and β-sheets appeared linked. There was an increasing concentration of TEG toward the bubble surface. Increasing the plasticizer content would reduce surface tension during processing and by classical nucleation theory, aid nucleation by lowering the activation energy for bubble formation. The average TEG to amide III ratio, excluding points which bordered cells, was 2.11 ± 0.22 (Figure 8). This ratio is much higher than the ratios presented by Bier *et al.*[26] for ENTP and other processed NTP products. Near the bubble the wall structure has a greater proportion of plasticizer to protein. This would suggest that TEG is not lost during processing and that bubbles form in regions of high plasticization. Additionally, the increase in plasticization may also explain some of the reduction in ordered secondary structures and therefore the increase in the fraction of random coils. It is therefore proposed that a bubble could begin to form in an initially highly plasticized region which could occur due to greater interactions between water and TEG than TEG and protein. As the pressure is released following heating loss of the most volatile component, water, occurs. The result is the retention of TEG in an initially already highly plasticized region and the increase in the TEG to amide III ratio.

CONCLUSIONS

FTIR analysis was used to examine the change in secondary structure across a cell wall and around bubble structures. Overall, the foamed material demonstrated a higher proportion of random coil (amorphous) structures and simultaneously a higher TEG to protein ratio indicating that this material was more plasticized. These results are supported by a reduction in ordered structures (as measured by XRD) and DMA and DSC results. The increase in randomly coiled structures occurred due to disruption or melting of the secondary structures during processing. This facilitated foaming by contributing to the amorphous fraction. The production of ordered β-sheets near the surface of bubbles indicates that these structures may act to stabilize bubbles.

Overall it is believed that, like traditional polymers, the amorphous fraction is more active during foaming, participating in adsorption and diffusion of the blowing agent and dictating solubility. Therefore it is not until these crystalline regions are disrupted at higher temperature and the evolution of gaseous products occurs that foaming of Novatein is possible.

ACKNOWLEDGMENTS

The authors would like to acknowledge the contributions of the Biopolymer Network Ltd. (BPN), Aduro Biopolymers (Novatein commercialization), and the funding received from the New Zealand Ministry of Business, Innovation and Employment (BPLY1302 contract). This research was undertaken on the infrared micro spectroscopy beamline at the Australian Synchrotron, Victoria, Australia. Proposal number AS162/IRM/10935. The authors would also like to acknowledge the beamline scientists especially Dr. Danielle Martin and Dr. Mark Tobin for all of their assistance and lastly Dr. Jim Bier and Dr. Talia Hicks for collection of the spectra.

REFERENCES

1. Glenn, G. M.; Orts, W. J. *Ind. Crops Prod.* **2001**, *13*, 135.
2. Kaisangsri, N.; Kerdchoechuen, O.; Laohakunjit, N. *Ind. Crops Prod.* **2012**, *37*, 542.
3. Nabar, Y.; Narayan, R.; Schindler, M. *Polym. Eng. Sci.* **2006**, *46*, 438.
4. Liu, B.; Jiang, L.; Zhang, J. *Macromol. Mater. Eng.* **2011**, *296*, 835.
5. Zhang, J.-F.; Sun, X. *J. Appl. Polym. Sci.* **2007**, *106*, 857.
6. Verbeek, C. J. R.; van den Berg, L. E. *Macromol. Mater. Eng.* **2010**, *295*, 10.
7. Bier, J. M.; Verbeek, C. J. R.; Lay, M. C. *Macromol. Mater. Eng.* **2014**, *299*, 85.
8. Oliviero, M.; Sorrentino, L.; Cafiero, L.; Galzerano, B.; Sorrentino, A.; Iannace, S. *J. Appl. Polym. Sci.* **2015**, *132*, 1.
9. Salerno, A.; Oliviero, M.; Di Maio, E.; Iannace, S. *Int. Polym. Process.* **2007**, *22*, 480.
10. Barone, J. R.; Schmidt, W. F.; Gregoire, N. *J. Appl. Polym. Sci.* **2006**, *100*, 1432.
11. Barone, J. R.; Schmidt, W. F.; Liebner, C. F. *J. Appl. Polym. Sci.* **2005**, *97*, 1644.
12. Guerrero, P.; de la Caba, K. *J. Food Eng.* **2010**, *100*, 261.
13. Jane, J. L.; Wang, S. U.S. Pat. 5,523,293 (**1996**).
14. Zhang, J.; Mungara, P.; Jane, J. *Polymer* **2001**, *42*, 2569.
15. Di Maio, E.; Mali, R.; Iannace, S. *J. Polym. Environ.* **2010**, *18*, 626.
16. Sessa, D. J.; Selling, G. W.; Willett, J. L.; Palmquist, D. E. *Ind. Crops Prod.* **2006**, *23*, 15.
17. Verdolotti, L.; Oliviero, M.; Lavorgna, M.; Iozzino, V.; Larobina, D.; Iannace, S. *J. Cell. Plast.* **2015**, *51*, 75.
18. Trujillo-de Santiago, G.; Rojas-de Gante, C.; García-Lara, S.; Verdolotti, L.; Di Maio, E.; Iannace, S. *J. Polym. Environ.* **2015**, *23*, 72.
19. Mungara, P.; Zhang, J. W.; Jane, J. *Polym. Prepr.* **1998**, *39*, 148.
20. Doroudiani, S.; Park, C. B.; Kortschot, M. T. *Polym. Eng. Sci.* **1996**, *36*, 2645.
21. Baldwin, D. F.; Park, C. B.; Suh, N. P. *Polym. Eng. Sci.* **1996**, *36*, 1437.
22. Taki, K.; Kitano, D.; Ohshima, M. *Ind. Eng. Chem. Res.* **2011**, *50*, 3247.

23. Marrazzo, C.; Di Maio, E.; Iannace, S. *J. Cell. Plast.* **2007**, *43*, 123.
24. Filli, M.; Sjoqvist, M.; Ohgren, C.; Stading, M.; Rigdahl, M. *Annu. Trans. NRS* **2011**, *19*, 1.
25. Bier, J. M.; Verbeek, C. J.; Lay, M. C. *Macromol. Mater. Eng.* **2014**, *299*, 524.
26. Bier, J. M.; Verbeek, C. J. R.; Lay, M. C. *J. Appl. Polym. Sci.* **2013**, *130*, 359.
27. Hicks, T.; Verbeek, C. J.; Lay, M. C.; Bier, J. M. *RSC Adv.* **2014**, *4*, 31201.
28. Bier, J. M.; Verbeek, C. J. R.; Lay, M. C. *J. Therm. Anal. Calorim.* **2014**, *115*, 433.
29. Rodríguez-Pérez, M.; Rodríguez-Llorente, S.; De Saja, J. *Polym. Eng. Sci.* **1997**, *37*, 959.
30. Bier, J. M.; Verbeek, C. J. R.; Lay, M. C. *J. Therm. Anal. Calorim.* **2013**, *112*, 1303.

8

Formation of Secondary Structures in Protein Foams as Detected by Synchrotron FTIR

A journal article

by

C. Gavin, C.J.R Verbeek and M.C. Lay

Published in

The Journal of Polymer Testing

Overview:

Foam expansion is usually temperature dependent which will result in changes in chain conformation. The purpose of Chapter 8 is to explore these changes for Novatein foamed at different temperatures and to establish what changes occur in secondary structure and plasticiser distribution. This study uses synchrotron light in Attenuated Total Reflectance mode.

This work continues work on objective three and builds on the results from the previous publication to understand the role of protein secondary structure during foaming

Contribution:

As first author for this publication the PhD candidate conducted all experimental work, data analysis and prepared the first draft of this manuscript. Under guidance from the supervisors the manuscript was revised and edited.

Permission:

Reproduced from Formation of Secondary Structures in Protein Foams as Detected by Synchrotron FT-IR. Previously published in the Journal of Polymer Testing.

Polymer Testing 73 (2019) 82–86

Contents lists available at ScienceDirect

Polymer Testing

journal homepage: www.elsevier.com/locate/polytest

Formation of secondary structures in protein foams as detected by synchrotron FT-IR

Chanelle Gavin*, Casparus J.R. Verbeek, Mark C. Lay

School of Engineering, Faculty of Science and Engineering, University of Waikato, Knighton Road, Hamilton, New Zealand

ARTICLE INFO

Keywords:
Foaming thermoplastic protein
Structure
Plasticiser distribution

ABSTRACT

FT-IR analysis was used to study the effect of temperature on foaming Novatein, a semi-crystalline thermoplastic biopolymer based on blood meal. Foaming was caused by rapid expansion of steam, ammonia and CO_2 from urea hydrolysis, leading to expansion ratios between 3.8 and 5.6. Plasticisers were more concentrated near the bubble surface, suggesting some tri-ethylene glycol accumulation. The β-sheet fraction in Novatein was not influenced by foaming or thermal treatment, but their distribution was influenced by bubble growth. β-sheets agglomerated near the bubble surface and was more pronounced at higher temperatures.

1. Introduction

Fourier-transform infrared spectroscopy (FT-IR) can detect changes in bond structure and bonding environments and is used to assess grafting [1], curing [2], compatibility [3], plasticisation [4] and degradation [5] in materials. It is also applied for determining secondary structure of proteins [6]. FT-IR provides a method for direct assessment of the relative amounts of each ordered and disordered structure within proteins and protein-based plastics (e.g zein [7], gluten [8], soy protein isolate [9] and blood meal [10]) which cannot be achieved through differential scanning calorimetry (DSC) or X-ray diffraction analysis. Although DSC can be used to determine the crystallinity of conventional polymers this is more challenging for proteins as they often demonstrate more than one transition associated with multiple proteins or peptides present within the sample [11]. Powder X-ray diffraction is also limited, as despite changes in protein secondary structure being correlated to changes in inter- and intra-molecular spacing, this method can only be used to infer relative changes [12].

Protein secondary structure is influenced by plasticisation, by interrupting intramolecular hydrogen bonds to create new bonds between the plasticiser and the protein [13]. Some plasticisers increased α-helices in cast zein [4] and wheat protein isolate films [14] and changes in secondary structure have been linked to the ability of these materials to undergo thermoplastic processing. For example, zein plasticised with 25 wt% PEG400 showed an increase in disordered structures and successful production of blown films was influenced by the ratio of α-helices to β-sheets [7]. Analogous results have been seen in foaming systems where a high β-sheet content led to a collapsed foam structure [15].

Novatein is produced from blood meal using sodium sulphite, sodium dodecyl sulphate and urea as denaturants as well as water and triethylene glycol as plasticisers [16,17]. For Novatein, previous studies observed an increase in β-sheet content after injection moulding [10], but an increase in disordered structures upon foaming [18]. Foamed Novatein is both bio-derived *and* biodegradable and is most suitable for short term applications including packing or for reducing weight in moulded parts. An understanding of the structural changes which occur during foaming, in particular those related to foaming temperature, will inform processing leading to improved foam quality.

This study considers changes in secondary structure and plasticisation before and after foaming Novatein using FT-IR. The effect of temperature on changes in secondary structure is assessed using spatially resolved FT-IR in the vicinity of bubbles.

2. Materials and methods

Novatein is produced by combining dried protein (blood meal, BM) with 40 parts per hundred bloodmeal (pph) of water, 3 pph sodium sulphite, 3 pph sodium dodecyl sulphate, 10 pph urea and 20 pph triethylene glycol (TEG), and is produced by Aduro Biopolymers [17]. Blending all the ingredients creates a pre-extruded material (PNTP) which becomes a consolidated thermoplastic (ENTP) following extrusion. Previous work developed a suitable foaming method for Novatein which was used here to produce FNTP at 155, 160 and 165 °C under free expansion [13]. Previous scoping experiments showed Novatein can only be foamed between 150 and 170 °C.

* Corresponding author.
E-mail addresses: chanelle.gavin@waikato.ac.nz (C. Gavin), johan.verbeek@waikato.ac.nz (C.J.R. Verbeek), mark.lay@waikato.ac.nz (M.C. Lay).

https://doi.org/10.1016/j.polymertesting.2018.10.043
Received 15 August 2018; Received in revised form 5 October 2018; Accepted 27 October 2018
Available online 28 October 2018

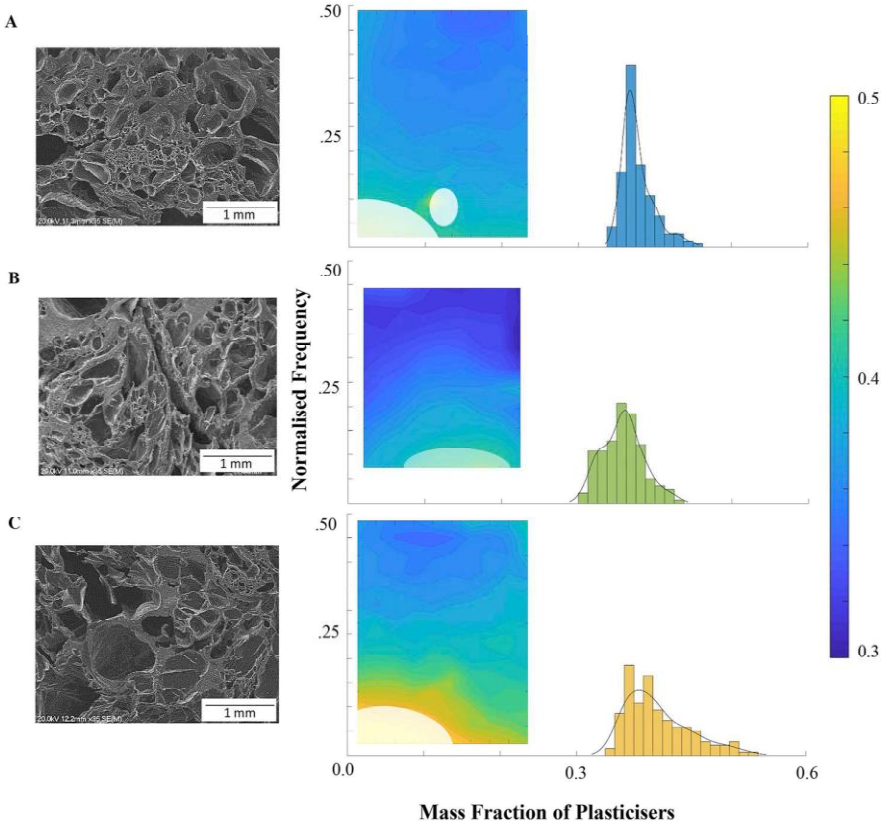

Fig. 1. SEM images of foamed samples with their associated spatial maps and histograms for total plasticiser content. Bubbles shown as white areas. **A**. T = 155 °C, **B**. T = 160 °C, **C.** T = 165 °C. Map sizes shown are 10 × 14 spots (A & C) and 10 × 9 spots (B).

The secondary structure of the bulk materials (BM, PNTP, ENTP and FNTP) was determined using FT-IR. For the foamed samples, the spatial distribution of these structures was also examined. All samples were freeze dried for 48 h (Freezone®, Labconco Corporation) at −50 °C and < 56 Pa to minimise the interference of water.

2.1. Foam characterisation

Foam density was calculated gravimetrically [13] and the expansion ratio was calculated using an unfoamed density of 1.2 g/cm^3 divided by the foam density. Moisture content (mass loss prior to 120 °C) was measured using Thermogravimetric Analysis (TGA). Powdered samples of approximately 10 mg were heated in alumina crucibles from room temperature to 800 °C, at a rate of 10 °C/min, using a Texas Instruments SDT 2960 analyser purged with 150 mL/min dry air. Scanning electron microscope images were produced from platinum sputter-coated samples using a Hitachi S-4700 SEM with an acceleration voltage of 20 kV.

2.2. Fourier transform infrared spectroscopy

Bulk composition of freeze dried powders was measured using a Bruker Platinum ATR equipped with a diamond crystal. Each sample was analysed three times using the average of 16 scans to produce a single spectra. The spectra was collected at a resolution of 4 cm^{-1} across a range of 3800 and 800 cm^{-1}.

Spatially resolved composition was examined using Synchrotron FT-IR in Macro ATR mode. Thin sections (5–10 μm thick) were microtomed and fixed to the sample stage using Kapton tape and analysed using a 250 μm germanium crystal. X–Y spatial resolution was achieved by moving the beam within the crystal to create maps of more than 80 spots (collected at 3 μm intervals with a spot size of approximately 3 μm). An average of 16 scans were collected per point using the Bruker Hyperion 3000 using an MCT collector at a resolution of 4 cm^{-1}.

2.3. FT-IR data analysis

All spectra were normalised to the highest point in the Amide I region (1625-1627 cm^{-1}). Spatially resolved data required screening to identify voids. These areas were identified as regions were the Amide I area was below the 95% confidence interval, based on the average composition for that map.

2.3.1. Plasticiser content and distribution

Urea absorbs in both the Amide I and TEG bonding regions (1040-1150 cm^{-1}), therefore protein content and the combination of urea and TEG (total plasticiszer) was determined using the area under the Amide III peaks, (1180-1330 cm^{-1}), (A_{III}), as a fraction of the combined Amide III and TEG region (A_{TEG}), Equation (1). The fraction of total plasticiser (urea and TEG combined) is therefore $x_{plasticiser} = 1 - x_{protein}$. All areas were calculated by integrating the spectra between these limits relative to a zero baseline.

$$x_{protein} = \frac{A_{III}}{A_{III} + A_{TEG}} \quad (1)$$

2.3.2. Secondary structure

The inverted second derivative method was used with a Savitzky Golay filter, consisting of a third order polynomial through nine data points. Assignment of peaks in the second derivative were conducted using the conventional limits [10], with borderline peaks assessed for

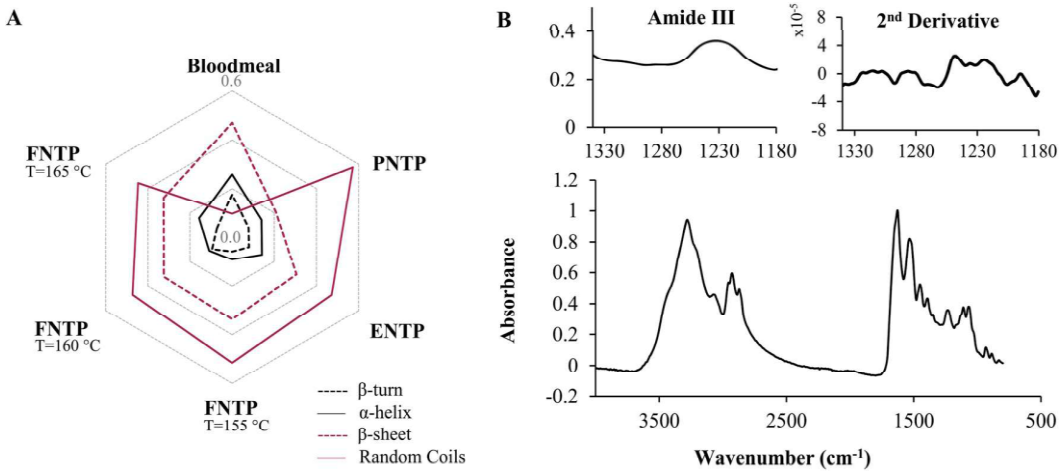

Fig. 2. Globar ATR results. **A.** Fractional composition for BM, PNTP, ENTP and FNTP at 155, 160 and 165 °C. **B.** Representative spectra of FNTP, insert shows the region of interest the Amide III (left) and the corresponding second derivative (right).

their proximity to peaks in the regions either side. An average peak height for all peaks in the four regions associated with α-helices ($A_\alpha^{'}$), β-turns ($A_t^{'}$), random coils ($A_r^{'}$) and β-sheets ($A_\beta^{'}$) were calculated and used to determine the fractional composition of the material according to Equations (2)–(6) [10,19].

$$\beta = \frac{1}{\frac{A_\alpha^{'}}{A_\beta^{'}} + \frac{A_t^{'}}{A_\beta^{'}} + \frac{A_r^{'}}{A_\beta^{'}} + 1} \quad (2)$$

$$\alpha = \beta\frac{A_\alpha^{'}}{A_\beta^{'}} \quad (3)$$

$$t = \beta\frac{A_t^{'}}{A_\beta^{'}} \quad (4)$$

$$r = \beta\frac{A_r^{'}}{A_\beta^{'}} \quad (5)$$

$$\alpha + \beta + t + r = 1 \quad (6)$$

3. Results

Increasing temperature led to an increase in expansion ratio from 3.8 to 5.6 along with an increase in cell size (Fig. 1). Expansion was attributed to water flashing due to a rapid pressure drop at the nozzle. However, triethylene glycol and urea may also participate as a blowing agents. FT-IR analysis of the bulk material showed that the mass fraction of plasticiser (urea and triethylene glycol) remained constant between all the processing stages, including foaming. While analysis of the bulk material provides an average composition for each sample, it cannot identify the distribution of the plasticisers.

The distribution of plasticiser (Fig. 1) was caused by an accumulation at the bubble surface. In the presence of water and heat, urea decomposes to ammonia and carbon dioxide [20]. This is consistent with an ammonia-like smell and the production of brittle foams during processing (loss of urea and water as plasticiszers). During foaming, cell growth will apply pressure to the surrounding material pushing outward. This pressure also thins the material, resulting in a highly plasticised or a concentrated region at the bubble surface, as the plasticiser does not diffuse back into the bulk material. This effect was more pronounced at high temperature and may also result in variances in secondary structure near the bubble surface.

Urea is a well-known protein denaturant [21] which is added to protein plastics to reduce hydrogen bonding and hydrophobic interactions [8] thereby enabling the protein chain to unfold. It has been used to enable thermoplastic processing of many proteins including wheat gluten [8], soy protein isolate [11], and blood meal [16] in non-foaming systems including sheet extrusion and injection moulding. The role of urea during foaming is still debatable with the potential for urea to undergo thermal decomposition, hydrolysis [20] or to participate in the carbamylation of lysine [22] and available cysteine [23].

Regardless of which reaction proceeds, urea is likely to be consumed and therefore the concentration gradient of plasticiser is most likely due to TEG, as it is very unlikely that significant amounts of TEG evaporated during foaming, based on its lower vapour pressure compared to water. Increased expansion with temperature was linked to an increase in the rate of urea hydrolysis [20], and a decrease in vapour density for water, ammonia and carbon dioxide, rather than TEG evaporation. This is consistent with the observed moisture content after foaming of 10.8% ± 0.6 as determined by thermogravimetric analysis (TGA). This suggests greater chain mobility due to higher plasticiser content at the bubble surface.

3.1. Secondary structure

Blood meal contained the highest β-sheet fraction and lowest α-helix fraction, while a reduction in β-sheets was observed along with the formation of random coils in PNTP (Fig. 2A). Thermal processing led to the reformation of β-sheets at the expense of random coils (ENTP). Changes in the other structures were insignificant in comparison, except for the foamed samples, where a slight reduction in random coils was observed with increasing foaming temperature. This meant that foaming affected the amorphous fraction but had little effect on bulk chain morphology. This does not mean that there were no changes in the distribution of these structures within the material which could be caused by plasticiser accumulation or due to alignment of protein chains under extension during bubble growth.

Spatially resolved data revealed that secondary structures were not uniformly dispersed and that their localisation was influenced by the presence of bubbles. Bubbles were observed in samples in areas high in β-sheets, while random coils were mainly observed in the high protein areas. The localisation of these protein motifs is highlighted in Fig. 3 by the bimodal distribution of the β-sheets structures. This was most pronounced at higher foaming temperatures where the material would have been more fluid enabling more chain alignment to occur, although this was not directly measured. The distribution of these structures did not correlate with plasticiser distribution (Fig. 1) and implies that there

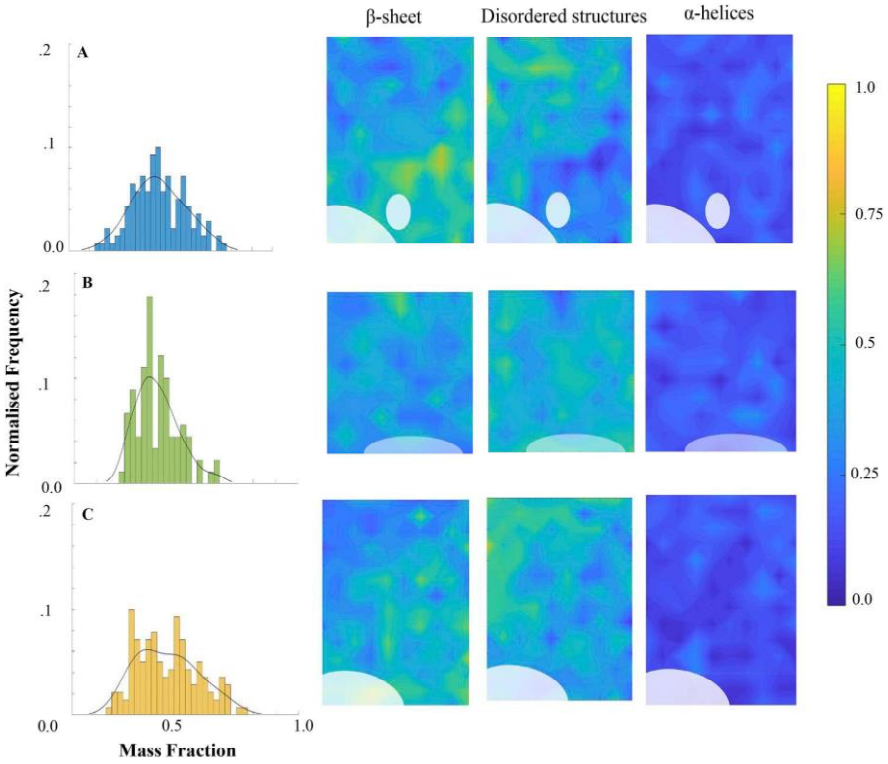

Fig. 3. Histogram of the distribution of β-sheets (left) and the corresponding spatially resolved maps of β-sheets, total disordered structures and α-helices. **A.** T = 155 °C, **B.** T = 160 °C, **C.** T = 165 °C.

was no link between these structures and the plasticiser content, rather that the secondary structure was influenced by cell growth. A greater amount of β-sheets could be observed near the bubble surface because of two possible mechanisms. Either the bubble nucleates on or near a β-sheet surface and grows until it is constrained by surrounding β-sheets, or the extensional forces caused by a growing bubble could cause alignment of the protein chains leading to β-sheet formation, as has been observed during deformation of gluten [24]. Ultimately it can be concluded that Novatein can be foamed irrespective of the fact that it is high in β-sheet content and its semi-crystalline nature.

4. Conclusions

Foaming was caused by rapid expansion of steam, ammonia and CO_2 from urea. This resulted in plasticiser being pushed out from the bubble causing an increased TEG concentration around the bubble surface. The overall β-sheet content was not influenced by foaming or thermal treatment. Instead, the distribution of these structures was influenced by bubble growth as seen by β-sheet agglomeration near the bubble surface. Ultimately, increased temperatures led to plasticiser accumulation and a bimodal distribution of β-sheets.

Acknowledgements

Biopolymer Network Ltd (BPN); Aduro Biopolymers; New Zealand Ministry of Business, Innovation and Employment (BPLY1302 contract); Australian Synchrotron (AS163/IRM/11405).

References

[1] M. Sclavons, P. Franquinet, V. Carlier, G. Verfaillie, I. Fallais, R. Legras, M. Laurent, F.C. Thyrion, Quantification of the maleic anhydride grafted onto polypropylene by chemical and viscosimetric titrations, and FTIR spectroscopy, Polymer 41 (6) (2000) 1989–1999.
[2] M.G. González, J.C. Cabanelas, J. Baselga, Applications of FTIR on Epoxy Resins-identification, Monitoring the Curing Process, Phase Separation and Water Uptake, Infrared Spectroscopy-materials Science, Engineering and Technology, InTech, 2012.
[3] M.J. Smith, C.J. Verbeek, Structural changes and energy absorption mechanisms during fracture of thermoplastic protein blends using synchrotron FTIR, Polym. Eng. Sci. 58 (51) (2018).
[4] T. Gillgren, S.A. Barker, P.S. Belton, D.M.R. Georget, M. Stading, Plasticization of zein: a thermomechanical, FTIR, and dielectric study, Biomacromolecules 10 (5) (2009) 1135–1139.
[5] G.W. Selling, The effect of extrusion processing on Zein, Polym. Degrad. Stabil. 95 (12) (2010) 2241–2249.
[6] J. Kong, S. Yu, Fourier transform infrared spectroscopic analysis of protein secondary structures, Acta biochim. et biophys. Sinica 39 (8) (2007) 549–559.
[7] M. Oliviero, E. Di Maio, S. Iannace, Effect of molecular structure on film blowing ability of thermoplastic zein, ýJ. Appl. Polym. Sci. 115 (1) (2010) 277–287.
[8] H. Türe, M. Gällstedt, R. Kuktaite, E. Johansson, M.S. Hedenqvist, Protein network structure and properties of wheat gluten extrudates using a novel solvent-free approach with urea as a combined denaturant and plasticiser, Soft Matter 7 (19) (2011) 9416–9423.
[9] Z. Wang, Y. Li, L. Jiang, B. Qi, L. Zhou, Relationship between secondary structure and surface hydrophobicity of soybean protein isolate subjected to heat treatment, J. Chem. 2014 (2014).
[10] J.M. Bier, C.J.R. Verbeek, M.C. Lay, Using synchrotron FTIR spectroscopy to determine secondary structure changes and distribution in thermoplastic protein, J. Appl. Polym. Sci. 130 (1) (2013) 359–369.
[11] X. Mo, X. Sun, Thermal and mechanical properties of plastics molded from urea-modified soy protein isolates, J. Am. Oil Chem. Soc. 78 (8) (2001) 867–872.
[12] W.M. Elshemey, A.A. Elfiky, W.A. Gawad, Correlation to protein conformation of wide-angle X-ray scatter parameters, Protein J. 29 (8) (2010) 545–550.
[13] C. Gavin, C.J.R. Verbeek, M.C. Lay, Morphology and compressive behaviour of foams produced from thermoplastic protein, J. Mater. Sci. 53 (22) (2018) 15703–15716.
[14] D. Jagadeesh, B. Prem Kumar, P. Sudhakara, C. Venkata Prasad, A. Varada Rajulu, J.I. Song, Preparation and properties of propylene glycol plasticized wheat protein isolate novel green films, J. Polym. Environ. 21 (4) (2013) 930–936.
[15] M. Oliviero, L. Sorrentino, L. Cafiero, B. Galzerano, A. Sorrentino, S. Iannace, Foaming behavior of biobased blends based on thermoplastic gelatin and poly (butylene succinate), J. Appl. Polym. Sci. 132 (48) (2015) 1–9.
[16] C.J.R. Verbeek, L.E. van den Berg, Development of proteinous bioplastics using bloodmeal, J. Polym. Environ. 19 (1) (2011) 1–10.
[17] K.L. Pickering, C.J.R. Verbeek, C. Viljoen, L.E. Van Den Berg, Plastics Material,

Novatein Limited, USA, 2012.
[18] C. Gavin, M.C. Lay, C.J.R. Verbeek, Conformational changes after foaming in a protein-based thermoplastic, J. Appl. Polym. Sci. 135(13) 46005.
[19] T. Hicks, C.J. Verbeek, M.C. Lay, J.M. Bier, Effect of oxidative treatment on the secondary structure of decoloured bloodmeal, RSC Adv. 4 (59) (2014) 31201–31209.
[20] J.N. Sahu, K. Mahalik, A.V. Patwardhan, B.C. Meikap, Equilibrium and kinetic studies on the hydrolysis of urea for ammonia generation in a semibatch reactor, Ind. Eng. Chem. Res. 47 (14) (2008) 4689–4696.
[21] M.C. Stumpe, H. Grubmüller, Interaction of urea with amino Acids: implications for urea-induced protein denaturation, J. Am. Chem. Soc. 129 (51) (2007) 16126–16131.
[22] D.B. Volkin, H. Mach, C.R. Middaugh, Degradative covalent reactions important to protein stability, Mol. Biotechnol. 8 (2) (1997) 105–122.
[23] J. Lippincott, I. Apostol, Carbamylation of cysteine: a potential artifact in peptide mapping of hemoglobins in the presence of urea, Anal. Biochem. 267 (1) (1999) 57–64.
[24] N. Wellner, E.C. Mills, G. Brownsey, R.H. Wilson, N. Brown, J. Freeman, N.G. Halford, P.R. Shewry, P.S. Belton, Changes in protein secondary structure during gluten deformation studied by dynamic Fourier transform infrared spectroscopy, Biomacromolecules 6 (1) (2005) 255–261.

9

The Role of Plasticizers during Protein Thermoplastic Foaming.

A journal article

by

C. Gavin, C.J.R Verbeek and M.C. Lay

Published in

The Journal of Applied Polymer Science

Overview:

Protein thermoplastics require denaturants and plasticisers to enable foaming. Plasticisers impact the behaviour of conventional polymers during thermoplastic processing. It is therefore expected that these additives and their amount will influence foam processing. This study examines the effect of water, urea and tri-ethylene glycol on Novatein's rheology, softening point and foaming ability.

The work relates to objective 4 mainly as it establishes a link between blend shear and extensional rheology and foaming ability. Some FT-IR data is presented so the study also contributes to objective 3 by understanding changes in protein secondary structure.

Contribution:

As first author for this publication the PhD candidate conducted all experimental work, data analysis and prepared the first draft of this manuscript. Under guidance from the supervisors the manuscript was revised and edited.

Permission:

JOURNAL OF Applied Polymer SCIENCE

The role of plasticizers during protein thermoplastic foaming

Chanelle Gavin, Casparus J. R. Verbeek, Mark C. Lay
School of Engineering, Faculty of Science and Engineering, University of Waikato, Knighton Road, Hamilton 3240, New Zealand
Correspondence to: C. Gavin (E-mail: chanelle.gavin@waikato.ac.nz)

ABSTRACT: Protein thermoplastics, like Novatein, typically comprise a polymer, additives, and plasticizers. During foaming, the plasticizers performed different functions; triethylene glycol (TEG) affected the T_g of the polymer, while water altered the shear viscosity and urea the extensional viscosity. Water and urea also functioned as blowing agents; increasing urea increased the expansion ratio, while an increase in TEG and water decreased it. It was concluded that at this level of plasticization, phase separation occurred and that the plasticizers are most influential during late bubble growth and stabilization. Contrary to previous thought, increasing water had no effect on the T_g, but did lower the shear viscosity, while increasing TEG had the opposite effect. This enables the properties of protein thermoplastics to be tailored during development. During foaming, lower viscosity allows more time for gases to diffuse before the viscosity in the surrounding polymer increases, restricting bubble growth. At higher TEG content, the material is processed further above its T_g, slowing down stabilization and decreasing expansion. This study clarified the role of plasticizers during foaming and showed a decrease in random coils and β-turns (measured by FT-IR) with increasing expansion ratio. Knowledge of these mechanisms enables tailoring properties of protein thermoplastics foams during development. © 2019 Wiley Periodicals, Inc. J. Appl. Polym. Sci. **2019**, *136*, 47781.

Received 11 December 2018; accepted 10 March 2019
DOI: 10.1002/app.47781

INTRODUCTION

Bioplastics are gaining popularity as more environmentally friendly alternatives are available to replace petrochemical-based plastics. As naturally occurring biopolymers, many proteins have been utilized to produce bioplastics; soy,[1,2] zein,[3] collagen,[4] gelatin, wheat gluten,[5] and blood meal[6] have all be investigated as bioplastics. Some of these reported successful extrusion,[2,4] injection molding, film blowing,[3] and sheet production[5]; however, fewer have reported successful foaming.[7,8]

To produce a thermoplastic protein, various additives are used in combination with water to enable extrusion, for example, compounds to reduce hydrophobic interactions (sodium dodecyl sulfate), crosslinking (sodium sulfite), and hydrogen bonding (urea). Additionally, polyol-based plasticizers (*e.g.* glycerol) are commonly used to further lower the glass transition temperature (T_g) of the material. Proteins are linear chains and their chain conformation is described by residual secondary structures (α-helices, β- sheets, random coils, and β- turns) making these materials semi-crystalline. However, unlike regular polymers, most protein-based thermoplastics do not melt, and the softening point is critical for processes such as extrusion and foaming.

Thermoplastic foaming takes place in three stages: nucleation, bubble growth, and stabilization. During foaming, the viscosity of the polymer is not constant.[9] Initially, a low viscosity aids nucleation and bubble growth; however, later a higher viscosity assists with stabilization of the foam. The change from low to high viscosity is attributed to the loss of gas (blowing agent) from the bubble surroundings. As the gas concentration decreases, the polymer becomes less plasticized and the viscosity increases where the rate of change in bubble radius is inversely proportional to viscosity.[10] Viscosity is temperature dependent and a lower viscosity at higher temperatures is preferred during bubble nucleation. This also allows for foam stabilization by lowering the temperature during the last stage of foaming to below the glass transition temperature.

The incorporation of a physical blowing agent also decreases viscosity (as well as the T_g), enabling the polymer to be foamed near the T_g of the neat polymer.[11] This has been observed when CO_2 was used as blowing agent in polystyrene, low-density polyethylene, and high-melt strength polypropylene (HMS-PP).[12] These materials, which are commonly used in foam extrusion, are shear thinning and the viscosity also decreases with increasing gas content. This occurs irrespective of whether the polymer is amorphous or semicrystalline leading to chain rearrangement in the amorphous phase.[13]

The role of chain conformation is important for foaming and will influence the final foam morphology.[9] During foaming, the inability of the molecular structure to disentangle quickly assists with preventing cell rupture.[11] This effect has been well documented for polypropylene (PP) where linear PP is more difficult to foam[14,15] as opposed to branched PP, which is strain hardening.[16] Proteins are linear chains but have a complicated secondary structure and the ability to crosslink, which may aid in preventing cell collapse.

However, many proteins, similar to linear PP[17] and PE,[18] demonstrate tension thinning behavior or a decrease in extensional viscosity with extensional strain rate, for example, plasticized kafirin, zein, gluten thermoplastic collagen, and hard wheat flour dough.[4,19,20] Most work regarding protein foaming is on baking, where the protein is cooked slowly and foaming is due to CO_2 evolution from fermentation. Water, as plasticizer, is continuously lost from the matrix leading to gradual cell stabilization. While tension thinning may assist with bubble growth, it will hinder stabilization in protein thermoplastics thereby requiring rapid loss of plasticizer to raise the T_g. The foaming ability of these is therefore also influenced by how far above the T_g processing is done as well as its initial viscosity.

The rheological and thermal behavior of protein thermoplastics is primarily studied in an extrusion context during the initial production of the material and although rheology is crucial to foaming. This combination has not been focused on for protein thermoplastics. Generally, increasing water and/or polyol content reduces viscosity.[4,21] However, the extent depends upon the protein and whether single or multiple plasticizers are used in combination. The shear and extensional viscosity of thermoplastic collagen can both be decreased by almost an order of magnitude when the water content alone was increased from 30 to 60%.[4] Incorporating glycerol was shown to have a negligible in the presence of water for this system; however, adding glycerol to sunflower protein isolate blends containing 50 pph water was shown to influence viscosity in another study.[21] Other recent work in the field has shown that in some cases a large amount of plasticizer can also lead to phase separation of these materials creating protein-rich and plasticizer-rich regions,[22] which may influence foaming of these materials.

Novatein is a protein-based bioplastic, an extrudable material produced from blood meal,[23] which is capable of injection molding and sheet formation. More recently, it was shown that it can also be foamed through free expansion. Novatein contains water and urea, which acts as plasticizers during low-temperature processing (extrusion and injection molding). Plasticizers influence the shear and extensional viscosity via a complex mechanism of interaction with the protein, water, and with itself. During foaming, (at high temperature and pressure), water and the products of urea hydrolysis (CO_2 and NH_3) also act as blowing agents, suggesting that foaming to be a complex process driven by rheology and plasticization. This article examines the effect of plasticizer content on foaming by considering changes in rheological behavior, blowing agent evolution, and macromolecular arrangement in Novatein.

EXPERIMENTAL

Materials

Blood meal was supplied by Wallace Corporation Limited, Waitoa, New Zealand. Urea (commercial grade) was purchased from Ballance Agri-Nutrients (New Zealand), and sodium sulfite, sodium dodecyl sulfate, and triethylene glycol (TEG) were obtained from Merck (Germany). Distilled water was manufactured on site from town supply.

Each formulation (Table I) was blended at 1400 RPM in a high-speed Labtech mixer using 1500 g of blood meal in a two-step process. First, a denaturing solution of all components, except TEG, was prepared by dissolving the components in water. Once this has been mixed into the dry blood meal, TEG was added to create a processable mixture.

These blends were extruded to form a consolidated thermoplastic in a Labtech Scientific twin-screw extruder with an L/D ratio of 44, using a temperature profile of 70, 100–100, 110, 120 C feeder to die (10 mm), at a constant torque of 55–60%. The material was then granulated by a tri-blade granulator (Castin Machinery Manufacturing Limited, New Zealand) through a 4 mm screen to produce extruded Novatein (ENTP).

Foamed Novatein (FNTP) was produced using a single screw Boy 35A injection molder with a 24-mm-diameter screw and an L/D ratio of 22. The machine was operated by withholding the nozzle from the mold to enable free expansion of the material as it exited the die. The temperature of the first heating zone was set to 100 C with the remaining zones and nozzle temperature set to 160 C. The injection pressure was set to 180 MPa with an injection speed of 48 mm/s.

Experimental Design

Shear and extensional rheology influence the foaming ability of polymers and can be changed by altering plasticizer content. In the case of Novatein, the amount of water, urea, and triethylene glycol in a formulation is important. As well as acting as plasticizers, these components could also act as blowing agents thereby affecting expansion. However, for a protein-plasticizer system, the plasticizer type and amount will also affect the thermal transitions/glass transition temperature.

Table I. Novatein Blend Composition Reported on a pph Blood Meal Basis. *Water 40 is also Referred to as Urea 10 and TEG 20

Sample	Abbreviation	Water (pph_{bm})	Urea (pph_{bm})	TEG (pph_{bm})	Sodium sulfite (pph_{bm})	Sodium dodecyl sulfate (pph_{bm})
1	Water 30	30	10	20	3	3
2	Water 40	40	10	20	3	3
3	Water 50	50	10	20	3	3
4	Urea 0	40	0	20	3	3
5	Urea 5	40	5	20	3	3
6	Urea 15	40	15	20	3	3
7	TEG 10	40	10	10	3	3
8	TEG 30	40	10	30	3	3

This complex behavior was investigated by eight blends, which were made to assess the effect of high and low water, urea, and triethylene glycol (TEG) contents. The formulations of Novatein (on the basis of 100 parts per hundred blood meal, pph_{bm}) are reported in Table I. A blend without any urea remains processable and has been included as reference; however, formulations without TEG or water are not processable as the blend is insufficiently plasticized.

Analysis

Expansion Ratio. Foams were cut into blocks approximately 25 × 25 × 20 mm to characterize density and expansion ratio. The average density was determined using 10 blocks. The volume of each block was measured using Vernier calipers, and each sample was weighed. The density (g/cm^3) was calculated, and the expansion ratio was based on the unfoamed density of Novatein, calculated from the density of protein 1.35 g/cm^3, urea 1.32 g/cm^3, TEG 1.1 g/cm^3, and water 1.0 g/cm^3 based on each individual formulation.

Cell morphology of the resulting foams was examined at both low and high magnification. Optical microscopy was used to observe the cellular structure at 6.4 and 16 times magnification, while scanning electron microscopy was used to observe higher magnifications of between 35 and 1000 times. Low-magnification images were taken using a Wild M38 microscope (Wild Heerburgg, Switzerland) equipped with image capture capabilities through a Nikon Digital Sight Camera. High-magnification images were taken after platinum sputter coating using a Hitachi S-4700 SEM with an acceleration voltage of 5 kV.

Fourier Transform Infrared Spectroscopy (FT-IR). Bulk composition of freeze dried powders was measured using a Bruker Platinum ATR equipped with a diamond crystal. Each sample was analyzed three times using the average of 16 scans to produce a single spectrum. The spectra were collected at a resolution of 4 cm^{-1} across a range of 3800 and 800 cm^{-1}.

Spatially resolved composition was examined using Synchrotron FT-IR in Macro ATR mode. Thin sections were microtomed and fixed to the sample stage using Kapton tape and analyzed using a 250 μm germanium crystal. X-Y spatial resolution was achieved by moving the beam within the crystal to create maps of more than 80 spots (collected at 3 μm intervals with a spot size of approximately 3 μm). An average of 16 scans was collected per point using the Bruker Hyperion 3000 using an MCT collector at a resolution of 4 cm^{-1}.

FT-IR data analysis. All spectra were normalized to the highest point in the Amide I region (1625–1627 cm^{-1}). Spatially resolved data required screening to identify voids. These areas were identified as regions were the Amide I area was below the 95% confidence interval, based on the average composition for that map.

Plasticizer content and distribution. Urea absorbs in both the Amide I and TEG-bonding regions (1040–1150 cm^{-1}), therefore protein content and the combination of urea and TEG (total plasticiszer) was determined using the area under the Amide III peaks, (1180–1330 cm^{-1}), (A_{III}), as a fraction of the combined Amide III and TEG region (A_{TEG}), Eq. (1).

The fraction of total plasticizer (urea and TEG combined) is therefore $x_{plasticiser} = 1 - x_{protein}$. All areas were calculated by integrating the spectra between these limits relative to a zero baseline.

$$x_{protein} = \frac{A_{III}}{A_{III} + A_{TEG}} \quad (1)$$

Secondary structure. The inverted second-derivative method was used with a Savitzky Golay filter, consisting of a third-order polynomial through nine data points. Assignment of peaks in the second derivative were conducted using the conventional limits,[24] with borderline peaks assessed for their proximity to peaks in the regions either side. The ratio of each peak to the highest point in either the β-sheet or randomly coiled region was calculated. The sum of these ratios in each region, α-helices (A''_α), β-turns (A''_t), random coils (A''_r) and β-sheets (A''_β) were calculated and used to determine the fractional composition of the material according to Equations 2–6.[24,25]

$$\beta = \frac{1}{\frac{A''_\alpha}{A''_\beta} + \frac{A''_t}{A''_\beta} + \frac{A''_r}{A''_\beta} + 1} \quad (2)$$

$$\alpha = \beta \frac{A''_\alpha}{A''_\beta} \quad (3)$$

$$t = \beta \frac{A''_t}{A''_\beta} \quad (4)$$

$$r = \beta \frac{A''_r}{A''_\beta} \quad (5)$$

$$\alpha + \beta + t + r = 1 \quad (6)$$

Rheology. The rheological behavior of each formulation was assessed using ENTP, prior to foaming. A dual-barrel Goettfert capillary rheometer, RG50 (Germany) was used to measure the rheology at four apparent shear rates (375, 600, 800, 1000 s^{-1}) in triplicate. One barrel was fitted with a 30-mm-long capillary and the other with an orifice of the same diameter but negligible length. Both dies had a 45 entrance angle to minimize the difference in entrance effects. The pressure was measured by pressure transducers located just above the dies in both barrels.

The rheometer provided apparent shear rate ($\dot{\gamma}_a$) and pressure readings for both barrels. P_1 corresponds to the pressure in the capillary, and in P_2 the orifice. The apparent shear stress (τ_a) was calculated according to Equation 7, where L is the length (30 mm) and R is the radius of the capillary (1 mm).

$$\tau_a = \frac{P_1}{2\left(\frac{L}{R}\right)} \quad (7)$$

The apparent viscosity (η_a) is then the ratio of the apparent shear stress to apparent shear rate[26] as presented in Equation 8:

$$\eta_a = \frac{\tau_w}{\dot{\gamma}_a} \quad (8)$$

Where, the corrected shear stress (τ_w) was then determined using the Bagley correction.[27]

$$\tau_w = \frac{P_1 - P_2}{2\left(\frac{L}{R}\right)} \quad (9)$$

The corrected shear rate requires a Rabinowitsch correction to account for the non-Newtonian behavior of the polymer. This correction is determined by the pseudo plasticity index (n), which

is determined by the power-law relationship of τ_w and $\dot{\gamma}_a$ (Equation 10).

$$\tau_w = k\dot{\gamma}_a{}^n \quad (10)$$

The index can therefore be determined using a double logarithmic plot of τ_w versus $\dot{\gamma}_a$, where n is the slope.

Applying the Rabinowitsch correction to the apparent shear rate values enables the calculation of the true shear rate ($\dot{\gamma}_w$) using the value of n determined from Equation 10.

$$\dot{\gamma}_w = \dot{\gamma}_a * \frac{3n+1}{4n} \quad (11)$$

The true viscosity is then determined by Equation 12:

$$\eta_w = \frac{\tau_w}{\dot{\gamma}_w} \quad (12)$$

The extensional viscosity of each blend was calculated using the Cogswell Equations, Equations 13, 14 and 15, using apparent data.[28]

$$\sigma_E = \frac{3}{8}(n+1)P_2 \quad (13)$$

Where, σ_E is the average extensional stress, n is the power-law index, P_2 is the pressure of the orifice, η is the shear viscosity, and $\dot{\gamma}$ is the apparent shear rate. The extensional strain ($\dot{\varepsilon}$) is used to calculate the extensional viscosity (η_e):

$$\dot{\varepsilon} = \frac{4}{3(n+1)P_2}\frac{\eta_a \dot{\gamma}_a{}^2}{} \quad (14)$$

$$\eta_e = \frac{\sigma_E}{\dot{\varepsilon}} \quad (15)$$

Dynamic Mechanical Analysis. Differences in position of thermal transitions and their activation energies due to plasticization were determined by analyzing samples of the extrudate using powder pocket DMA. The analysis was performed in a single cantilever configuration using a PerkinElmer DMA 8000 equipped with a temperature-controlled furnace, regulated by Pyris software.

Powdered samples (approximately 50 mg) were crimped in stainless steel pockets, heated to 25 C, and allowed to equilibrate. The temperature was then increased at a rate of 2 C/min up to 200 C. Multifrequency data were collected between 0.1 and 30.0 Hz with a dynamic displacement of 0.05 mm.

Statistical Analysis. An analysis of variance (ANOVA) was performed on the apparent shear rate and apparent shear viscosity data using Statistica software (produced by Dell). The contribution of each effect was determined by η^2 values, which were calculated for each effect as the sum of squares effect divided by sum of squares of all effects and error.

RESULTS AND DISCUSSION

Foam Morphology and Expansion

Free expansion using 40 pph water, 10 pph urea, and 20 pph TEG resulted in an expansion ratio of approximately four (Figure 1). Lowering the water or TEG content resulted in a slightly higher expansion ratio, while adding more decreased the expansion ratio. Optical microscopy (Figure 2) also showed a greater amount of unfoamed regions in the blends, which were highly plasticized (TEG 30 and Water 50, Table I) and a change in cell size distribution [Figure 1(b)]. Specifically, low-TEG blends produced high expansion ratio foams of 4.4, where the majority of cell were small between 50 and 100 μm in diameter and despite an increase in cell size in high TEG blends to 100–200 μm, overall the expansion ratio decreased. Similar results were observed for water, low levels resulted in smaller cells, while higher levels demonstrated a wider cell size distribution [Figure 1 (b)]. However, a decrease in expansion for the highly plasticized TEG 30 and Water 50 blends was observed overall due to large unfoamed regions.

Urea had the greatest effect on expansion. Low levels of urea (5 and 10 pph) had similar expansion, while increasing the urea content to 15 pph increased the expansion ratio to 4.5. This increased expansion was achieved through the production of more gaseous products. DMA indicated almost complete disruption of protein−protein interactions at this urea content, suggesting a more uniform morphology as of all the formulations this is the closest to an amorphous material.

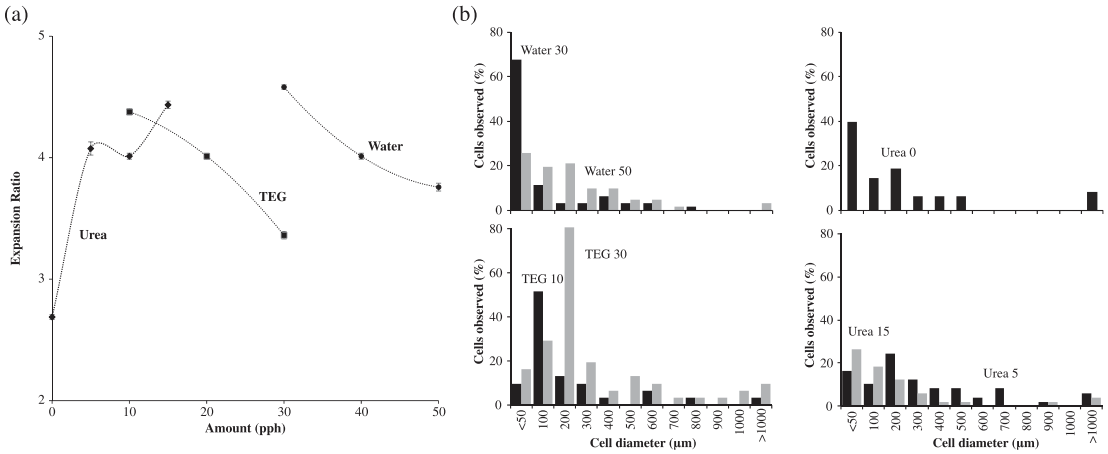

Figure 1. (a) Expansion ratio of each foamed product relative to plasticizer content. (b) Expansion ratio determined as expected density/measured foam density.

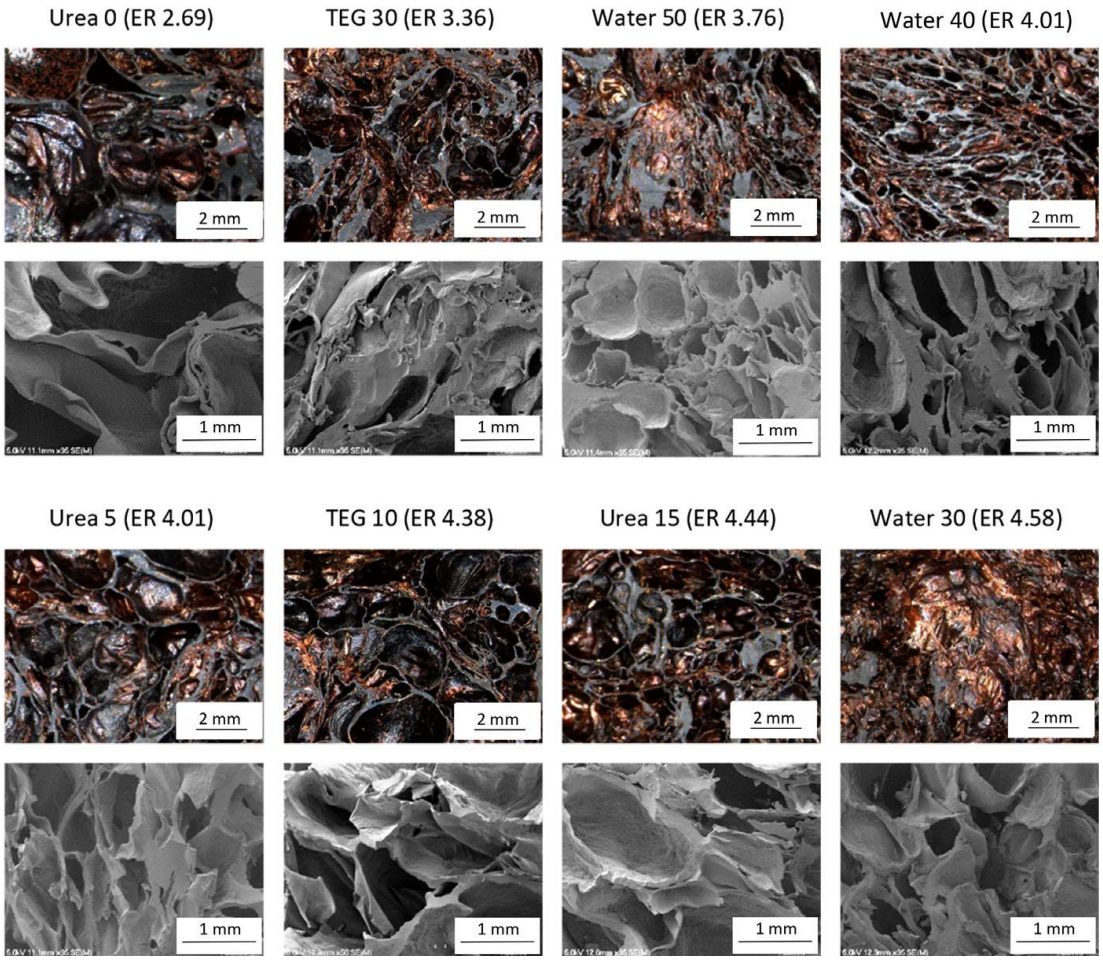

Figure 2. Cell structure of each foam using optical microscopy and SEM imaging. Images are arranged in order from lowest expansion ratio to highest. [Color figure can be viewed at wileyonlinelibrary.com]

However, the morphology looked very similar to the other formulations (Figure 2) and no distinction could be made for cell size distribution between foams containing 5, 10, and 15 pph urea [Figure 1 (b)]. Alternatively, the difference could be explained by the rheology (Figure 3).

Rheology

All formulations demonstrated shear thinning behavior as can be seen from their shear viscosity (Figure 3, Table II). Increasing the water content decreased the shear viscosity, which was also altered by the addition of 5–15 pph urea to a lesser extent, while TEG had no effect. This suggests differences in the way these plasticizers interact with the protein chains and may also be associated with changes in the thermal transition behavior of these blends. Consistent with previous work, water was a very effective plasticizer.[4,21,29–31] Plasticization occurs as water hydrates the protein chains, reducing the number of available hydrogen bonding sites for protein–protein interactions, increasing chain mobility. In the presence of polyols, plasticization behavior was altered. At low water content, primary plasticization occurs where the polyol binds with the protein chains, displacing water. However, at high water contents secondary plasticization takes place, where water and polyol hydrogen bond, resulting in phase separation (producing protein rich, protein–plasticizer, and plasticizer-rich regions).[22] This may explain the lack of a reduction in viscosity with TEG content as there was insufficient change in TEG content to promote a change in viscosity. While TEG has been shown to influence the shear viscosity in Novatein at under certain conditions,[31] its plasticizing effect is derived from its participation in secondary plasticization, where the following phase separation, the free volume theory is most applicable.[32] This effect was observed through dynamic mechanical analysis, and the 40 pph water and 10–30 pph TEG content may be sufficient for phase separation to

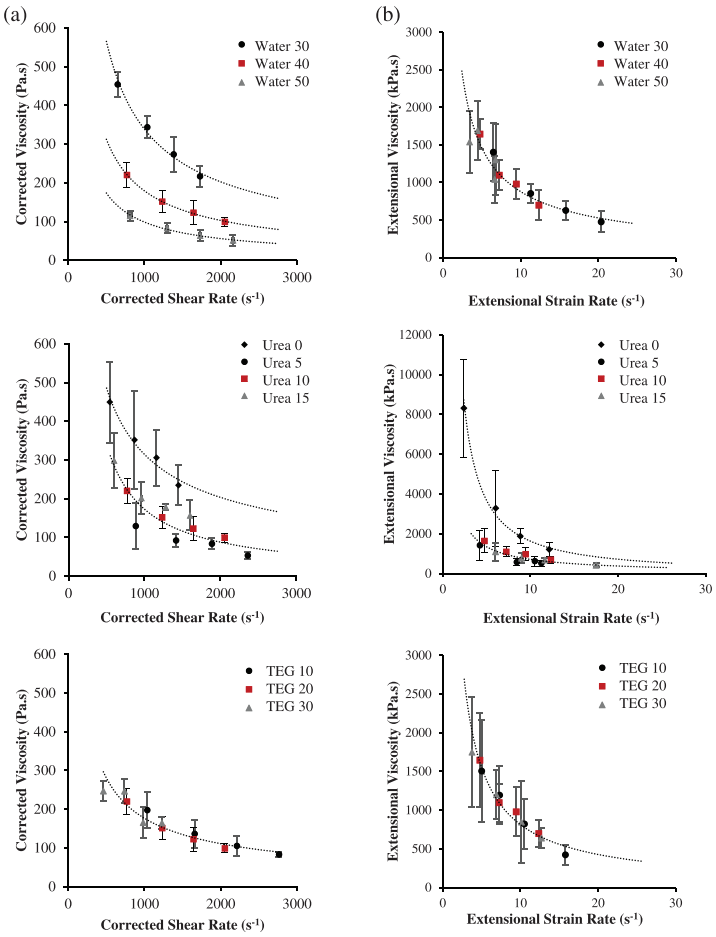

Figure 3. (a). Corrected shear viscosity and (b) extensional viscosity behavior for Novatein blends with variable water, urea, and triethylene glycol content, top to bottom. [Color figure can be viewed at wileyonlinelibrary.com]

occur. Therefore, these blends must be considered in conjunction with their thermal behavior, also observed by others.[4]

The difference in shear rheology between the urea-free and urea-containing blends is related to the ability of urea to hydrogen bond to the protein and facilitate chain unfolding. The reduction in intermolecular and intramolecular bonding creates more linear chains, which are more mobile and flow more readily. Also when urea binds to a protein, it frees three water molecules,[32] which could then participate in hydrogen bonding with other plasticizers.

A polymer's shear viscosity has strong implications for nucleation and stabilization. Prior to expansion, the material experiences very high shear rates (~45 000 s^{-1}) as it flows through the nozzle.

Table II. Effect of Blend Composition on Consistency Coefficient and Flow Behavior Index, $\eta = K\dot{\gamma}^{n-1}$

	Consistency coefficient (K)	Flow behavior index (n)	R^2
Water 40/Urea 10/TEG 20	45 754	0.198	0.99
Water 30	56 669	0.259	0.98
Water 50	28 008	0.182	0.99
Urea 0	24 139	0.372	0.96
Urea 5-Urea 10-Urea 15	151 121	0.019	0.74
TEG 10-TEG-20-TEG 30	18 001	0.331	0.93

Table III. Contributions of Each Effect as Calculated Using η^2 Values, as Determined from ANOVA

	F	*P*-value
Water	111.89	0.00
Urea	1.14	0.00
Shear rate	3.05	0.04
Triethylene glycol	Pooled factor	40
Water × shear rate	Pooled factor	40
Urea × shear rate	Pooled factor	40
Triethylene glycol × shear rate	Pooled factor	40

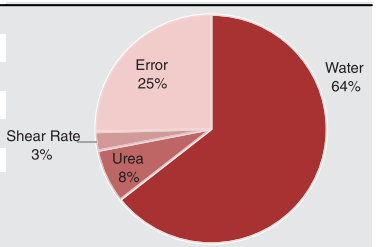

The shear thinning behavior observed indicates that the viscosity would quickly plateau at higher shear rates (Figure 3). Therefore during foaming, the behavior of all the blends with variable TEG content should be comparable and the absence of a change in viscosity resulting in no change in pressure drop across the nozzle. This means that any variations observed in the foam morphology of these blends is not due to the initial TEG content. For water and urea, differences in shear viscosity will still exist but the shear viscosity will be very low. For all of these blends, their tendency to phase separate will be important as foaming is more likely to occur in a protein-plasticizer rich regions than a protein–protein rich region. These effects are examined later by powder pocket dynamic mechanical analysis.

The more important factor in the foaming process is the loss of protein hydration and free volume, which occur as water and urea are lost as blowing agents. This will result in an increase in viscosity of the surrounding polymer and will subsequently constrain bubble growth, affecting foam morphology. The loss of these plasticizers will also affect the extensional viscosity, which is critical in foaming once the material leaves the nozzle and is no longer subjected to shear flow. This will also have implications for foam stabilization, which is either achieved through plasticizer loss, consequently increasing the T_g, or through cooling to below the T_g.

ANOVA was used to evaluate the effect of water, triethylene glycol, urea, shear rate, and their interactive effects. This analysis was conducted on apparent viscosity data as the corrected shear rates are different for each blend due to the application of the Rabinowitsch correction. This analysis also excluded the urea-free blend, which displayed significantly different behavior to the seven urea-containing blends, skewing the results. The effect of water, urea, and shear rate were all significant $P < 0.05$ (Table III) but TEG was not ($P > 0.06$). The contributions of each effect is shown in Table III, evaluated using η^2 values, which showed the effect of water was the most significant, accounting for 64% of the difference in apparent viscosity data while urea content accounted for only 8%.

Novatein demonstrated tension thinning behavior and despite the variation in shear viscosity, altering the plasticizer content had no effect on extensional viscosity. The addition of urea is an exception where the extensional viscosity did reduce. Although lower levels of urea correlate to higher K_E values, a single power-

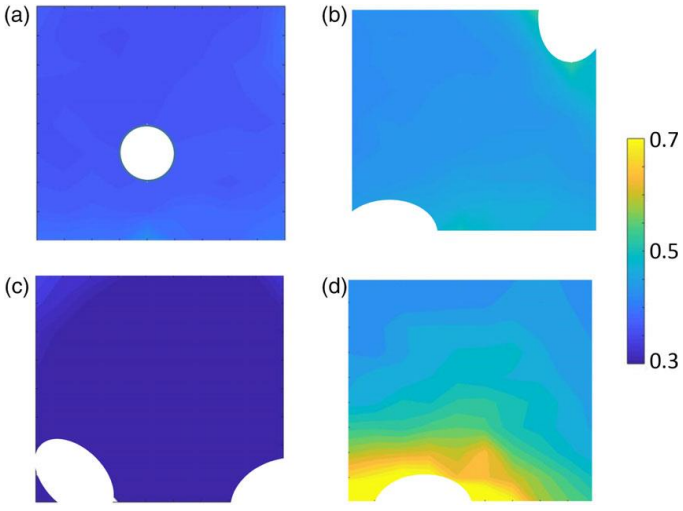

Figure 4. Plasticizer distribution for (a)TEG 10; (b) TEG 30; (c) Water 30; and (d) Water 50. [Color figure can be viewed at wileyonlinelibrary.com]

law fit is sufficient to describe the behavior of all urea-containing blends.

Tension thinning behavior is critical in bread production, and this behavior has been observed in doughs from hardened wheat flour, kafirin, and zein prolamins plasticized with water.[19] The observation of tension thinning behavior in Novatein is supportive of its foaming ability, and the dependence of extensional viscosity on the presence of urea suggests blends without urea will expand less.

The results here would lead to the conclusion that the major difference between these formulations was due to the change in shear viscosity, being most significant between the blend containing no urea and those that do. The foaming behavior of these blends may be further influenced by chain mobility (thermal transitions) and the temperature difference between these and the processing temperature.

A decrease in expansion was observed with increasing water content despite water being the primary blowing agent. Increasing water content did not change the softening point, as observed with TEG, but it did decrease the viscosity, which affects bubble growth. As water is depleted, viscosity will increase, which will constrain bubble growth. More blowing agent (water) usually increases expansion, but also will also delay the onset of viscosity increase. Without the viscosity increase water may be lost without participating in bubble growth.

TEG had no effect on shear or extensional viscosity and is also not a blowing agent, suggesting that the expansion of all the TEG formulations should have been similar. However, increasing TEG content decreased expansion and a greater amount of unfoamed regions and smaller cells were observed. The only difference between these blends was their softening behavior where the 30 pph TEG formulation had an 80 C difference between the processing temperature and the softening point (Figure 5). Increased plasticization must therefore impede bubble stabilization. With a lower T_g more water and urea must be removed to increase the T_g and stabilize the foam. Without this mechanism, the foam will remain above its softening point for longer and as it cools this can reduce the expansion of the foam as the gaseous products condense.

TEG has been observed to accumulate at bubble surfaces in previous work and has also been demonstrated using FT-IR in this study (Figure 4). The formulations, which were low in total plasticizer did not demonstrate a large amount of TEG accumulating at the bubble surface. However, a clear accumulation of TEG was observed for those samples with higher plasticizer [Figure 4(b,d)], being more pronounced when more water was present. This could occur through two possible mechanisms; either a bubble has nucleated in a water-plasticizer region or as the water diffuses into the bubble a TEG-rich region is formed. Irrespective of which mechanism is occurring, the viscosity of the region highly plasticized with TEG will be substantially different to any formulation tested. Without water, the protein network will also become quite constrained, stopping bubble growth.

Dynamic Mechanical Analysis

The shear viscosity of a polymer is dependent on how far above the T_g or T_m (or softening point) the material is processed. Each formulation of Novatein displayed different thermal transitions when analyzed through powder pocket DMA (Figure 5). The presence of three distinct peaks suggested phase separation and the formation of protein-rich, protein-plasticizer, and plasticizer-rich regions, similar to other work.[33]

In this work, focus was on the two main transitions typically observed around 110 and 20 C (Figure 3). As a plasticizer, water

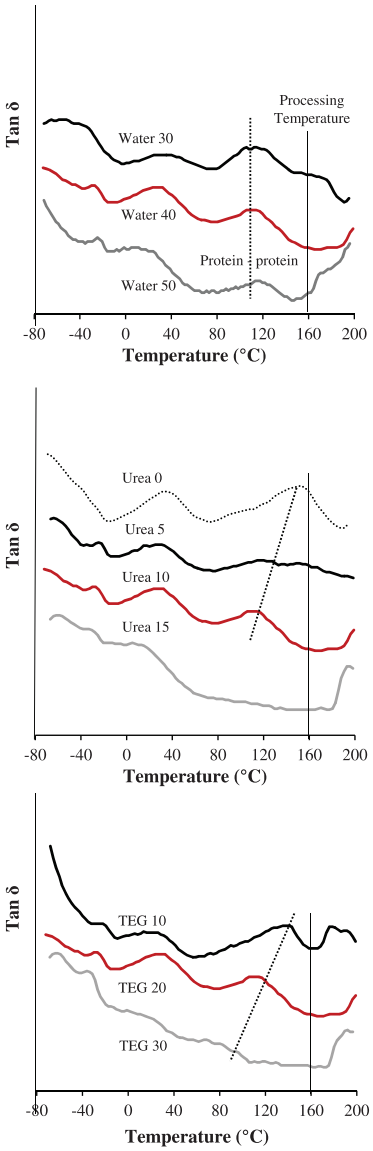

Figure 5. Transition behavior of extruded Novatein thermoplastic (ENTP). A total of 30 Hz of data are shown for water, urea, and triethylene glycol content. The base formulation is reported as Water 40, Urea 10, and TEG 20 and is shown in each graph for reference as a solid red line. [Color figure can be viewed at wileyonlinelibrary.com]

Table IV. Secondary Structure of ENTP, the Material Prior to Foaming, and FNTP, the Material after Foaming

Extruded novatein (ENTP)					
Sample	Expansion ratio	α-helices	β-turns	Random coils	β-sheets
Water 20	4.01	0.23	0.05	0.45	0.26
Water 30	4.58	0.18	0.05	0.049	0.27
Water 50	3.76	0.17	0.06	0.36	0.41
Urea 0	2.69	0.14	0.04	0.52	0.29
Urea 5	4.08	0.18	0.04	0.44	0.34
Urea 15	4.44	0.14	0.06	0.49	0.31
TEG 10	4.38	0.17	0.07	0.33	0.44
TEG 30	3.36	0.10	0.07	0.54	0.28
Foamed novatein (FNTP)					
Sample	Expansion ratio	α-helices	β-turns	Random coils	β-sheets
Water 20	4.01	0.14	0.14	0.37	0.36
Water 30	4.58	0.11	0.09	0.40	0.38
Water 50	3.76	0.19	0.10	0.43	0.28
Urea 0	2.69	0.28	0.02	0.36	0.33
Urea 5	4.08	0.13	0.09	0.40	0.38
Urea 15	4.44	0.14	0.08	0.43	0.35
TEG 10	4.38	0.16	0.12	0.31	0.41
TEG 30	3.36	0.10	0.08	0.48	0.34

did not appear to affect the transition temperature of the protein-rich phase; however, it did decrease the transition temperature (thereby increasing the difference between the softening point and the processing temperature) of the intermediate phase as well as changing the relative magnitude of these two peaks. This could either suggest that water did not reduce the intermolecular bonding in the protein-rich phase, or that the amount of water in the protein-rich phase remained constant and the increased peak in tan δ is due to increased phase separation. Either way a greater proportion of the material participates in the earlier transition and led to a reduction in viscosity.

In comparison, varying TEG had a minimal effect on the intermediate phase but did shift the transition of the protein-rich phase. Using a higher amount of TEG (30 pph) shifted the two peaks to lower temperatures and the magnitude of the higher transition was less. At low TEG levels (10 pph), two transitions associated with the protein-rich phase were observed. One below 140 C and the other above the processing temperature of 160 C, which is most likely associated with a more constrained protein network. This did not influence the shear rheology of the blend but could have influenced the potential for chain rearrangement during foaming and affect the protein secondary structure.

Adding urea had the most significant effect on these transitions. In the absence of urea, the major transition was at 155 C, just below the foaming temperature and would therefore have an excessively high shear viscosity. By adding urea to the blend, there was a reduction in the temperature of the protein-rich transition until the peak completely disappeared at 15 pph urea. The absence of a transition associated with the protein phase would suggest that a urea content

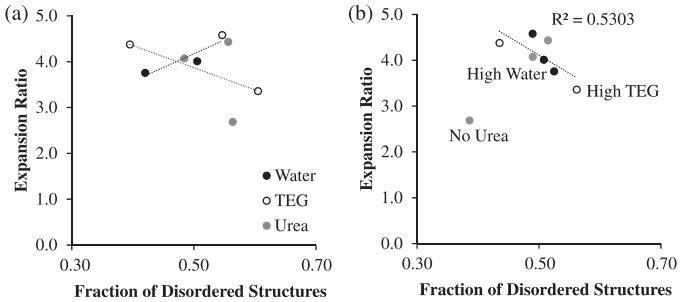

Figure 6. Correlation between expansion ratio and secondary structure. Disordered structures (random coils and β-turns) (a) before foaming. (b) after foaming. No urea data point in (b) has been excluded from correlation.

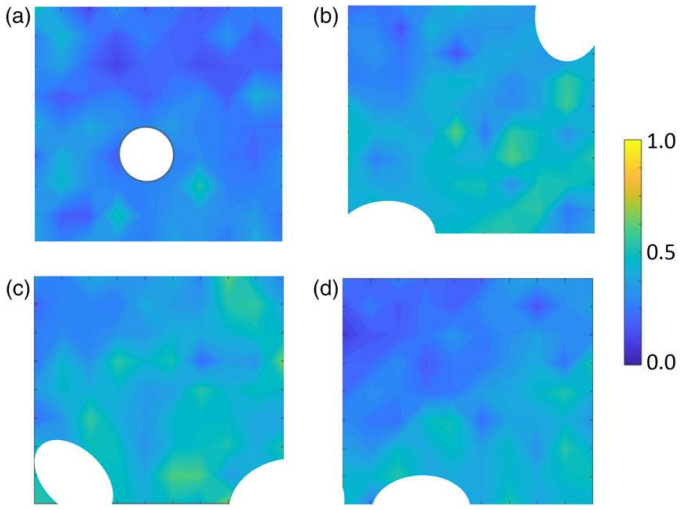

Figure 7. Distribution of β-Sheet structures for (a) 10 pph triethylene glycol; (b) 30 pph triethylene glycol; (c) 30 pph water; and (d) 50 pph water. [Color figure can be viewed at wileyonlinelibrary.com]

of 15 pph is sufficient to disrupt the hydrogen bonding between protein chains. The intermediate phase transition is also shifted to lower temperatures, becoming greater in magnitude and broader. The complete disruption of the protein-rich phase suggest that the material will be more amorphous and should flow more easily due to a lack of protein–protein interactions.

The work here would suggest that the amount of plasticizer (water and TEG) should be carefully controlled as both influence the rheology (increasing water) or chain mobility (increasing TEG). Reduced viscosity is desirable for processing, but excess blowing agent or over plasticization led to a lower expansion. Urea is therefore a critical component for foaming as it assists with both of these mechanisms, allowing for foaming at lower water and TEG content. However, another aspect, not considered yet, is the effect of these additives on protein chain conformation.

Chain Conformation

The secondary structure of each formulation was affected by the addition of water, urea, and TEG (Table IV). Increased water content reduced random coils and favored formation of β-sheets in ENTP, while TEG encouraged the formation of random coils (Table IV). The different trends for water and TEG are not unexpected when considered with DMA and rheology results. Foaming further affected the secondary structure, which is consistent with previous studies.[34,35] Typically, a reduction in random-coiled structures was observed in conjunction with an increase in β-sheets compared to ENTP.

The level of disordered structures (random coils + β-turns) in ENTP did not correlate with the final expansion ratio of the foam, therefore, secondary structure alone is not sufficient to predict foaming ability (Figure 6). However, after foaming, a lower level of disordered structures was observed for more expanded foams Figure 6. Following foaming, the material also had a large β-sheet content observed near the surface of bubbles (Figure 7). It is possible that the formation of these more constrained structures play a role in foam stabilization similar to strain hardening effects in traditional polymers.

CONCLUSIONS

Foaming protein thermoplastics is more complicated than that of traditional polymers due to protein plasticizer and plasticizer-plasticizer interactions, and the role of three common plasticizers (water, triethylene glycol, and urea) was investigated in this study. Urea acts as more than a blowing agent and was effective at reducing the extensional viscosity of Novatein. Additional water lowered the viscosity of the blend but not the softening point, while TEG lowered the softening point but not the viscosity. In both cases, a blend with more plasticizer lead to decreased expansion. For water, this was attributed to a lower viscosity allowing more time for gases to diffuse before viscosity increased to control bubble growth. Using higher amounts TEG, the material is further elevated above its softening point therefore stabilization will take longer to achieve.

ACKNOWLEDGMENTS

The authors wish to acknowledge the Biopolymer Network Ltd (BPN), Aduro Biopolymers, and the Australian Synchrotron beamline proposal (AS163/IRM/11405).

REFERENCES

1. Mo, X.; Sun, X. *J. Am. Oil Chem. Soc.* **2001**, *78*, 867.
2. Ralston, B. E.; Osswald, T. A. *J. Polym. Environ.* **2008**, *16*, 169.
3. Oliviero, M.; Di Maio, E.; Iannace, S. *J. Appl. Polym. Sci.* **2010**, *115*, 277.
4. Klüver, E.; Meyer, M. *J. Appl. Polym. Sci.* **2012**, *128*, 4201.
5. Türe, H.; Gällstedt, M.; Kuktaite, R.; Johansson, E.; Hedenqvist, M. S. *Soft Matter.* **2011**, *7*, 9416.

6. Verbeek, C. J. R.; van den Berg, L. E. *J. Polym. Environ.* **2011**, *19*, 1.
7. Marrazzo, C.; Di Maio, E.; Iannace, S. *J. Cell. Plast.* **2007**, *43*, 123.
8. Salerno, A.; Oliviero, M.; Di Maio, E.; Iannace, S. *Int. Polym. Proc.* **2007**, *22*, 480.
9. Liao, R.; Yu, W.; Zhou, C. *Polym.* **2010**, *51*, 568.
10. Shafi, M. A.; Flumerfelt, R. W. *Chem. Eng. Sci.* **1997**, *52*, 627.
11. Gendron, R. Thermoplastic Foam Processing: Principles and Development; CRC Press: Boca Raton, FL, **2005**.
12. Michaeli, W.; Kropp, D.; Heinz, R.; Schumacher, H. In Polymeric Foams: Technology and Developments in Regulation, Process and Products; Lee, S. T.; Scholz, D., Eds., CRC Press: Boca Raton, FL, **2009**.
13. Lee, S.-T.; Park, C. B.; Ramesh, N. S. Polymeric Foams: Science and Technology; CRC press: Boca Raton, **2006**.
14. Spitael, P.; Macosko, C. W. *Polym. Eng. Sci.* **2004**, *44*, 2090.
15. Park, C. B.; Cheung, L. K. *Polym. Eng. Sci.* **1997**, *37*, 1.
16. Nam, G.; Yoo, J.; Lee, J. *J. Appl. Polym. Sci.* **2005**, *96*, 1793.
17. Wang, Q.-J.; Huang, H.-X. *Polym. Test.* **2013**, *32*, 1400.
18. Wei, X.; Collier, J. R.; Petrovan, S. *J. Appl. Polym. Sci.* **2007**, *104*, 1184.
19. Oom, A.; Pettersson, A.; Taylor, J. R.; Stading, M. *J. Cereal Sci.* **2008**, *47*, 109.
20. Arabo, E. Y. M. *J. Food Eng.* **2011**, *103*, 294.
21. Orliac, O.; Silvestre, F.; Rouilly, A.; Rigal, L. *Am. Chem. Soc.* **2003**, *42*, 1674.
22. Uitto, J. M.; Verbeek, C. J. *Adv. Polym Tech.* **2018**, *37*, 2922.
23. Pickering, K. L.; Verbeek, C. J. R.; Viljoen, C.; Van Den Berg, L. E. U.S. Pat. US-20100234515-A1 (**2012**).
24. Bier, J. M.; Verbeek, C. J. R.; Lay, M. C. *J. Appl. Polym. Sci.* **2013**, *130*, 359.
25. Hicks, T.; Verbeek, C. J.; Lay, M. C.; Bier, J. M. *RSC Adv.* **2014**, *4*, 31201.
26. Huang, J. C.; Leong, K. S. *J. Appl. Polym. Sci.* **2002**, *84*, 1269.
27. Bagley, E. *J. Appl. Phys.* **1957**, *28*, 624.
28. Cogswell, F. *Tran. Soc. Rheo.* **1972**, *16*, 383.
29. Bengoechea, C.; Arrachid, A.; Guerrero, A.; Hill, S. E.; Mitchell, J. R. *J. Cereal Sci.* **2007**, *45*, 275.
30. Walia, P.; Lawton, J.; Shogren, R.; Felker, F. *Polym.* **2000**, *41*, 8083.
31. Mohan, V. B.; Verbeek, C. J. R. *AIMS Mater. Sci.* **2015**, *2*, 1.
32. Stumpe, M. C.; Grubmüller, H. *J. Am. Chem. Soc.* **2007**, *129*, 16126.
33. Chen, P.; Zhang, L. *Macromol. Biosci.* **2005**, *5*, 237.
34. Gavin, C.; Lay, M. C.; Verbeek, C. J. R. *J. Appl. Polym. Sci.* **2018**, *135*, 46005.
35. Gavin, C.; Verbeek, C. J.; Lay, M. C. *Polym. Test.* **2018**, *73*, 82.

10

Foaming Novatein Thermoplastic Protein

A concluding discussion

Foaming Novatein Thermoplastic Protein

Novatein Thermoplastic Protein (NTP) is a commercialised bioplastic which can be used to produce injection moulded parts and extruded sheets. Foaming extends its use to a loose fill packing material and reducing weight in moulded parts. The purpose of this work was to develop a foaming method for Novatein® and to investigate the principles which govern foaming for protein thermoplastics.

Initial scoping attempted to foam Novatein via extrusion, however, it was observed that the material was very rigid and easily broke i.e. the material had a low melt strength. Novatein was blended with linear low density polyethylene (LLDPE) compatibilised with maleic anhydride grafted polyethylene (PE-g-MAH) to reduce viscosity and increase melt strength. Water (physical blowing agent) or water and sodium bicarbonate (chemical blowing agent) were used as foaming agents. The best expansion ratio (1.85 times) was achieved using 50% Novatein blended with 40% LLDPE and 10% PE-g-MAH, using only the water present in Novatein as a blowing agent. Adding sodium bicarbonate produced very fine cells without large regions of unfoamed material, however the foam expansion did not improve. Despite the shear thinning behaviour of both these components, at the shear rates experienced during extrusion, the viscosity would still be high, hindering foaming. Gas loss also occurred through the feed hopper preventing a well-mixed, gas filled melt.

To further improve foam expansion it was concluded that Novatein could either be further plasticised, or the shear rate could be increased. However, extra plasticisers would increase resin costs, with no guarantee of improved foaming. An injection moulder operating semi-continuously at high speed was used to increase shear rate, and the nozzle was withheld from the mould to enable free expansion and maximise pressure drop. The expansion ratio of the Novatein:LLDPE blends increased from 1.85 to 2.5 and by substitution of LLDPE for low density polyethylene (LDPE) the expansion ratio was further increased to 3.0 because strain hardening stabilised the bubbles. However, pure Novatein had the highest expansion ratio of 4.4, because it had more

water available to act as a blowing agent compared to blends with PE. This formed the basis for further work.

This material has a narrow foaming window between 150°C, where no foaming occurs, and 170°C, where the protein degraded. Within this range the expansion ratio of the foam was improved to five, and foam density could be varied between 0.25-0.5 g/cm^3. Compressive strength and moduli were density dependent, between 200 and 600 kPa and 2.2 and 8 MPa, respectively. The density dependence of the mechanical properties has also been observed with conventional foams, but Novatein has a much higher density. The energy absorbing mechanism varied with low density foams being more elastomeric, while denser foams behaved more like plastic foams.

Foam morphology was chaotic with highly foamed and unfoamed regions and a mixture of open and closed cells. This was because Novatein is semi-crystalline (arising from residual protein secondary structure), which cannot be completely disrupted during foaming as the temperature required would degrade the protein. Another possible cause of the foam morphology is phase separation which may occur in this highly plasticised system.

Blood meal, from which Novatein is made, is a mixture of red blood cells and plasma containing; haemoglobin, bovine serum albumin, globulins, and fibrinogen. This is extensively aggregated during steam coagulation resulting in a high proportion of β-sheets and a heavily cross-linked material. This makes it very difficult to thermally disrupt without denaturants (urea) and plasticisers (tri-ethylene glycol and water). For the rest of the thesis blood meal was therefore treated as a highly aggregated polymer with its own unique properties. The high proportion of β-sheets in blood meal may explain why it was difficult to foam Novatein. Previous work has shown that production of PNTP disrupted β-sheet structures and that some reform during extrusion (ENTP).

The behaviour of water, urea and triethylene glycol as plasticisers and/or blowing agents was not known, although it was observed that blends without urea struggled to foam. Urea reduces extensional viscosity by disrupting

hydrogen bonding and hydrophobic interactions, facilitating chain unfolding making it critical for successful foaming of this material. But, urea may also contributes along-side water as a blowing agent. An ammonia smell was detected during foaming indicating urea thermally decomposes to produce NH_3 and CO_2 gases. Throughout this work the alternative roles for urea have also been identified. There is the potential for urea to hydrolyse in the presence of water or to have participated in carbamylation of lysine residues. Therefore, the exact amount of free urea in each blend is unknown but its presence is critical for foaming.

Increasing water lowered the shear viscosity of Novatein, but did not lower the softening point and did not increase foam expansion. This was attributed to the role of viscosity during late bubble growth where a higher viscosity is desirable to control bubble growth and prevent cell rupture before stabilisation. As there is more water available, the viscosity increase will occur more slowly and is not sufficient to counteract the loss of water vapour and to constrain bubble growth in that late phase. In comparison TEG also lowered the softening point such that the blend was further away from its glass transition temperature. As a result, the material did not solidify until either a greater amount plasticiser was lost from the blend increasing the T_g or the temperature was lowered. Either way, the result was that foam expansion with increasing TEG also decreased.

The above results were counter intuitive as firstly, the addition of more water was expected to increase foam expansion by increasing blowing agent availability and secondly, this highlights that the previous option of improving foam expansion by increasing plasticisation during extrusion may not have worked.

FT-IR showed TEG and possibly urea accumulated near the bubble surface. Initially it was thought that foaming occurred in these highly plasticised regions. There was also the possibly of plasticiser accumulating at the bubble surface as the bubble grew outwards and water migrated into the bubble as a blowing agent. Water and TEG are known to hydrogen bond and so the

accumulation is logical. It was also established that this accumulation occurred more in highly plasticised blends and could be linked to phase separation into protein rich, protein-plasticiser, and plasticiser rich regions as observed by other researchers. Irrespective of the mechanism the accumulation of plasticisers at the bubble surface would act to lower the viscosity in that localised area while a viscosity increase is desirable for bubble stabilisation.

For traditional polymers the inability of chains to slip past one another quickly assists with constraining bubble growth through strain hardening. This is not the case for linear polymers which is why PP is notoriously difficult to foam. Proteins are predominantly linear chains and branching is only achieved by crosslinking. Protein secondary structures may also contribute to the same mechanism as structures like β-sheets are quite rigid and act as physical crosslinks.

During foaming, bubble growth places pressure on the surrounding polymer and this causes chain alignment. In proteins, this offers the opportunity for hydrogen bonding between chains. i.e. the formation of β-sheets. In this work β-sheets have been observed at the bubble surface and it is expected that these are caused by this mechanism, although it is also possible that a bubble nucleates on or near a β-sheet and grows until it is constrained by encountering more of these rigid structures. Either way, evidence suggests β-sheets contribute to bubble stabilization (Figure 1).

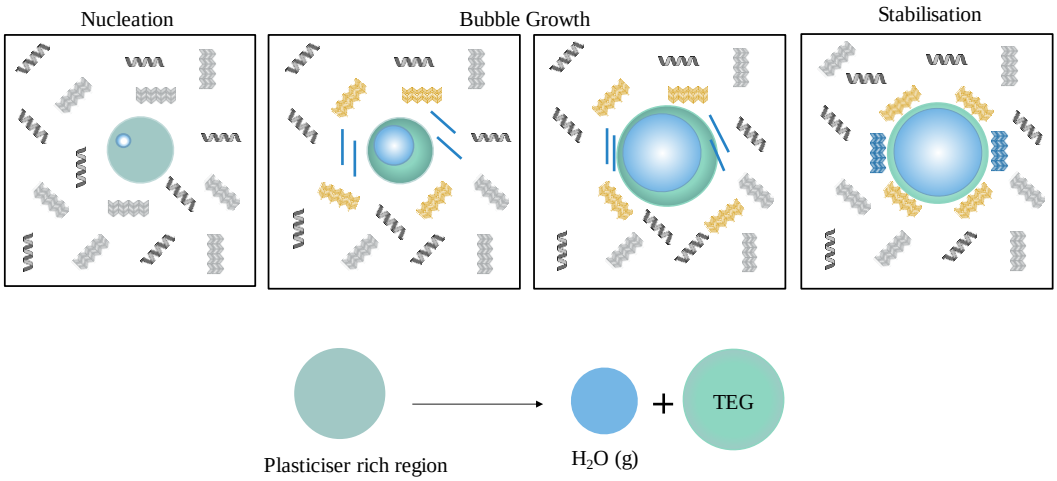

Figure 1: Role of plasticisers and protein secondary structure in foaming of Novatein, a protein thermoplastic.

In conclusion, a method for foaming Novatein has been established, despite its high β-sheet content. Foaming requires the extensional viscosity to be lowered, which is achieved in this work through adding urea. Alone, this is not sufficient to enable foaming in a low shear, low pressure system and foaming is only achieved in a high shear environment through the use of a rapid pressure drop rate and free expansion. The expansion for Novatein was increased from 1.85 to typically 4-5 through manipulation of the processing conditions and composition. In this study, the fundamental stages of bubble nucleation, growth and stabilisation have been investigated and shown to be highly complex depending upon rheology, glass transition temperature and conformation of the protein chains.

Recommendations for future work

This work has identified many areas for further investigation:

Producing a foam injection moulded article – Application of current principles to form a moulded article with a foamed interior for weight reduction in moulded parts.

Material development - Investigate different additives (primarily surfactants) to reduce viscosity, surface tension and promote nucleation. This may enable foaming via extrusion if the rheology of the system is appropriately controlled.

Assess the application of these findings to other proteins or protein blends – Potential feed stocks could be decoloured blood meal or bovine plasma. Either of these should demonstrate similar behaviour to Novatein (if plasma is thermally dried) but may be more appropriate in colour and odour.

Further investigation of an alternative foaming mechanism - If the protein thermoplastic is overly plasticised it may be possible to produce a foam through spinodal decomposition rather than nucleation mechanisms. A study of the outcome of the two nucleation mechanisms may provide an interesting comparison.

Investigation of secondary structure determination – Using FT-IR to assess conformational changes in bioplastics is still an emerging field. A comparison of protein conformation changes through both Amide I and Amide III for these materials and model proteins would provide an interesting comparison. In order to overcome the insufficient signal to noise ratio from globar source a synchrotron light source would be required. Saturation of the Amide I could be avoided through application of Attenuated Total Reflectance (ATR) or through careful sample preparation in transmission.

Appendix

THE UNIVERSITY OF WAIKATO
Te Whare Wānanga o Waikato

Co-Authorship Form

Postgraduate Studies Office
Student and Academic Services Division
Wahanga Ratonga Matauranga Akonga
The University of Waikato
Private Bag 3105
Hamilton 3240, New Zealand
Phone +64 7 838 4439
Website:
http://www.waikato.ac.nz/sased/postgraduat

This form is to accompany the submission of any PhD that contains research reported in published or unpublished co-authored work. **Please include one copy of this form for each co-authored work.** Completed forms should be included in your appendices for all the copies of your thesis submitted for examination and library deposit (including digital deposit).

Please indicate the chapter/section/pages of this thesis that are extracted from a co-authored work and give the title and publication details or details of submission of the co-authored work.

Chapter 2: Protein Plastic Foams – Advances in Physiochemical Properties of Biopolymers, Part 2.

Nature of contribution by PhD candidate	As first author for this publication the PhD candidate prepared the first draft of the manuscript, excluding the batch foaming section. Under the supervisors' guidance and with the assistance of the co-authors the manuscript was revised and edited.
Extent of contribution by PhD candidate (%)	55%

CO-AUTHORS

Name	Nature of Contribution
Mark Lay	Guidance during manuscript preparation, revision and editing.
Johan Verbeek	Guidance during manuscript preparation, revision and editing.
Anuradha Walallavita	25% - Preparation of the first draft of the batch foaming section, assistance with revision and editing the manuscript.

Certification by Co-Authors

The undersigned hereby certify that:

- the above statement correctly reflects the nature and extent of the PhD candidate's contribution to this work, and the nature of the contribution of each of the co-authors.

Name	Signature	Date
Mark Lay		12/12/18
Johan Verbeek		12/12/18
Anuradha Walallavita	AWalallavita	13.11.18

July 2015

THE UNIVERSITY OF WAIKATO
Te Whare Wānanga o Waikato

Co-Authorship Form

Postgraduate Studies Office
Student and Academic Services Division
Wahanga Ratonga Matauranga Akonga
The University of Waikato
Private Bag 3105
Hamilton 3240, New Zealand
Phone +64 7 838 4439
Website: http://www.waikato.ac.nz/sasd/postgraduate/

This form is to accompany the submission of any PhD that contains research reported in published or unpublished co-authored work. **Please include one copy of this form for each co-authored work.** Completed forms should be included in your appendices for all the copies of your thesis submitted for examination and library deposit (including digital deposit).

Please indicate the chapter/section/pages of this thesis that are extracted from a co-authored work and give the title and publication details or details of submission of the co-authored work.

Chapter 3: Extrusion foaming of protein-based thermoplastic and polyethylene blends– Published in AIP Conference Proceedings, https://doi.org/10.1063/1.4942308.

Nature of contribution by PhD candidate	As first author for this publication the PhD candidate conducted all experimental work, data analysis and prepared the first draft of this manuscript. Under guidance from the supervisors the manuscript was revised and edited. Both supervisors have been acknowledged as co-authors.
Extent of contribution by PhD candidate (%)	80%

CO-AUTHORS

Name	Nature of Contribution
Mark Lay	Guidance during manuscript preparation, revision and editing.
Johan Verbeek	Guidance during manuscript preparation, revision and editing.

Certification by Co-Authors

The undersigned hereby certify that:

- the above statement correctly reflects the nature and extent of the PhD candidate's contribution to this work, and the nature of the contribution of each of the co-authors.

Name	Signature	Date
Mark Lay		12/12/18
Johan Verbeek		12/12/18

July 2015

THE UNIVERSITY OF WAIKATO
Te Whare Wānanga o Waikato

Co-Authorship Form

Postgraduate Studies Office
Student and Academic Services Division
Wahanga Ratonga Mataurange Akonga
The University of Waikato
Private Bag 3105
Hamilton 3240, New Zealand
Phone +64 7 838 4439
Website: http://www.waikato.ac.nz/sasd/postgraduate/

This form is to accompany the submission of any PhD that contains research reported in published or unpublished co-authored work. **Please include one copy of this form for each co-authored work.** Completed forms should be included in your appendices for all the copies of your thesis submitted for examination and library deposit (including digital deposit).

Please indicate the chapter/section/pages of this thesis that are extracted from a co-authored work and give the title and publication details or details of submission of the co-authored work.

Chapter 3: Foaming behaviour of Novatein and blends with polyethylene compatibilised by maleic anhydride– Published in AIP Conference Proceedings, https://doi.org/10.1063/1.5016722.

Nature of contribution by PhD candidate	As first author for this publication the PhD candidate conducted all experimental work, data analysis and prepared the first draft of this manuscript. Under guidance from the supervisors the manuscript was revised and edited. Both supervisors have been acknowledged as co-authors.
Extent of contribution by PhD candidate (%)	80%

CO-AUTHORS

Name	Nature of Contribution
Mark Lay	Guidance during manuscript preparation, revision and editing.
Johan Verbeek	Guidance during manuscript preparation, revision and editing.

Certification by Co-Authors

The undersigned hereby certify that:

- the above statement correctly reflects the nature and extent of the PhD candidate's contribution to this work, and the nature of the contribution of each of the co-authors.

Name	Signature	Date
Mark Lay		12/12/18
Johan Verbeek		12/12/18.

July 2015

THE UNIVERSITY OF WAIKATO
Te Whare Wānanga o Waikato

Co-Authorship Form

Postgraduate Studies Office
Student and Academic Services Division
Wahanga Ratonga Matauranga Akonga
The University of Waikato
Private Bag 3105
Hamilton 3240, New Zealand
Phone +64 7 838 4439
Website: http://www.waikato.ac.nz/sasd/postgraduate/

This form is to accompany the submission of any PhD that contains research reported in published or unpublished co-authored work. **Please include one copy of this form for each co-authored work.** Completed forms should be included in your appendices for all the copies of your thesis submitted for examination and library deposit (including digital deposit).

Please indicate the chapter/section/pages of this thesis that are extracted from a co-authored work and give the title and publication details or details of submission of the co-authored work.

Chapter 4: Morphology and compressive behaviour of foams produced from thermoplastic protein– Published in the Journal of Materials Science, https://doi.org/10.1007/s10853-018-2714-5.

Nature of contribution by PhD candidate	As first author for this publication the PhD candidate conducted all experimental work, data analysis and prepared the first draft of this manuscript. Under guidance from the supervisors the manuscript was revised and edited. Both supervisors have been acknowledged as co-authors.
Extent of contribution by PhD candidate (%)	80%

CO-AUTHORS

Name	Nature of Contribution
Johan Verbeek	Guidance during manuscript preparation, revision and editing.
Mark Lay	Guidance during manuscript preparation, revision and editing.

Certification by Co-Authors

The undersigned hereby certify that:

- the above statement correctly reflects the nature and extent of the PhD candidate's contribution to this work, and the nature of the contribution of each of the co-authors.

Name	Signature	Date
Johan Verbeek		12/12/18
Mark Lay		12/12/18

July 2015

THE UNIVERSITY OF WAIKATO
Te Whare Wānanga o Waikato

Co-Authorship Form

Postgraduate Studies Office
Student and Academic Services Division
Waharanga Ratonga Matauranga Akonga
The University of Waikato
Private Bag 3105
Hamilton 3240, New Zealand
Phone +64 7 838 4439
Website: http://www.waikato.ac.nz/sasd/postgraduate/

This form is to accompany the submission of any PhD that contains research reported in published or unpublished co-authored work. **Please include one copy of this form for each co-authored work.** Completed forms should be included in your appendices for all the copies of your thesis submitted for examination and library deposit (including digital deposit).

Please indicate the chapter/section/pages of this thesis that are extracted from a co-authored work and give the title and publication details or details of submission of the co-authored work.

Chapter 6: Thermal Analysis and Secondary Structure of Protein Fractions in a Highly Aggregated Protein Material

Nature of contribution by PhD candidate	For this publication the PhD candidate prepared the first draft of this manuscript. Experimental work was conducted in collaboration with the co-authors but analyzed and formatted by the PhD candidate. The PhD candidate also assisted with the collection of the spectra at the Australian Synchrotron. Under guidance from the supervisors and the co-authors the manuscript was revised and edited.
Extent of contribution by PhD candidate (%)	50%

CO-AUTHORS

Name	Nature of Contribution
Johan Verbeek	Guidance during manuscript preparation, revision and editing.
Mark Lay	Guidance during manuscript preparation, revision and editing.
Jim Bier	Experimental work specifically dynamic mechanical analysis (DMA) and X-ray diffraction (XRD). Jim was a co-proposer for the Australian synchrotron application for the FTIR beam line where the spectra were collected and assisted with manuscript revision and editing.
Talia Hicks	Experimental work specifically the differential scanning calorimetry (DSC) analysis and fast protein liquid chromatography. Talia also assisted with [redacted] manuscript revision and editing.

Certification by Co-Authors

The undersigned hereby certify that:

- the above statement correctly reflects the nature and extent of the PhD candidate's contribution to this work, and the nature of the contribution of each of the co-authors.

Name	Signature	Date
Johan Verbeek		13/12/18
Mark Lay		13/12/18
Jim Bier		13/12/18
Talia Hicks	on behalf of Talia	13/12/18

July 2015

THE UNIVERSITY OF WAIKATO
Te Whare Wānanga o Waikato

Co-Authorship Form

Postgraduate Studies Office
Student and Academic Services Division
Wahanga Ratonga Matauranga Akonga
The University of Waikato
Private Bag 3105
Hamilton 3240, New Zealand
Phone +64 7 838 4439
Website: http://www.waikato.ac.nz/sasd/postgraduate/

This form is to accompany the submission of any PhD that contains research reported in published or unpublished co-authored work. **Please include one copy of this form for each co-authored work.** Completed forms should be included in your appendices for all the copies of your thesis submitted for examination and library deposit (including digital deposit).

Please indicate the chapter/section/pages of this thesis that are extracted from a co-authored work and give the title and publication details or details of submission of the co-authored work.

Chapter 7: Conformational changes after foaming in a protein based thermoplastic– Published in the Journal of Applied Polymer Science, https://doi.org/10.1002/app.46005.

Nature of contribution by PhD candidate	As first author for this publication the PhD candidate conducted all experimental work, data analysis and prepared the first draft of this manuscript. Under guidance from the supervisors the manuscript was revised and edited. Both supervisors have been acknowledged as co-authors.
Extent of contribution by PhD candidate (%)	80%

CO-AUTHORS

Name	Nature of Contribution
Mark Lay	Guidance during manuscript preparation, revision and editing.
Johan Verbeek	Guidance during manuscript preparation, revision and editing.

Certification by Co-Authors

The undersigned hereby certify that:

- the above statement correctly reflects the nature and extent of the PhD candidate's contribution to this work, and the nature of the contribution of each of the co-authors.

Name	Signature	Date
Mark Lay		12/12/18
J Verbeek		12/12/18

July 2015

THE UNIVERSITY OF WAIKATO
Te Whare Wānanga o Waikato

Co-Authorship Form

Postgraduate Studies Office
Student and Academic Services Division
Wahanga Ratonga Matauranga Akonga
The University of Waikato
Private Bag 3105
Hamilton 3240, New Zealand
Phone +64 7 838 4439
Website: http://www.waikato.ac.nz/sasd/postgraduate/

This form is to accompany the submission of any PhD that contains research reported in published or unpublished co-authored work. **Please include one copy of this form for each co-authored work.** Completed forms should be included in your appendices for all the copies of your thesis submitted for examination and library deposit (including digital deposit).

Please indicate the chapter/section/pages of this thesis that are extracted from a co-authored work and give the title and publication details or details of submission of the co-authored work.

Chapter 8: Formation of secondary structures in protein foams as detected by synchrotron FT-IR – Published in the Journal of Polymer Testing, https://doi.org/10.1016/j.polymertesting.2018.10.043.

Nature of contribution by PhD candidate	As first author for this publication the PhD candidate conducted all experimental work, data analysis and prepared the first draft of this manuscript. Under guidance from the supervisors the manuscript was revised and edited. Both supervisors have been acknowledged as co-authors.
Extent of contribution by PhD candidate (%)	80%

CO-AUTHORS

Name	Nature of Contribution
Johan Verbeek	Guidance during manuscript preparation, revision and editing.
Mark Lay	Guidance during manuscript preparation, revision and editing.

Certification by Co-Authors

The undersigned hereby certify that:

- the above statement correctly reflects the nature and extent of the PhD candidate's contribution to this work, and the nature of the contribution of each of the co-authors.

Name	Signature	Date
Johan Verbeek		12/12/18
Mark Lay		12/12/18

July 2015

THE UNIVERSITY OF WAIKATO
Te Whare Wānanga o Waikato

Co-Authorship Form

Postgraduate Studies Office
Student and Academic Services Division
Wahanga Ratonga Matauranga Akonga
The University of Waikato
Private Bag 3105
Hamilton 3240, New Zealand
Phone +64 7 838 4439
Website: http://www.waikato.ac.nz/sasd/postgraduate/

This form is to accompany the submission of any PhD that contains research reported in published or unpublished co-authored work. **Please include one copy of this form for each co-authored work.** Completed forms should be included in your appendices for all the copies of your thesis submitted for examination and library deposit (including digital deposit).

Please indicate the chapter/section/pages of this thesis that are extracted from a co-authored work and give the title and publication details or details of submission of the co-authored work.

Chapter 9: The role of Plasticizers during Protein Thermoplastic Foaming

Nature of contribution by PhD candidate	As first author for this publication the PhD candidate conducted all experimental work, data analysis and prepared the first draft of this manuscript. Under guidance from the supervisors the manuscript was revised and edited. Both supervisors have been acknowledged as co-authors.
Extent of contribution by PhD candidate (%)	80%

CO-AUTHORS

Name	Nature of Contribution
Johan Verbeek	Guidance during manuscript preparation, revision and editing.
Mark Lay	Guidance during manuscript preparation, revision and editing.

Certification by Co-Authors

The undersigned hereby certify that:

- the above statement correctly reflects the nature and extent of the PhD candidate's contribution to this work, and the nature of the contribution of each of the co-authors.

Name	Signature	Date
Johan Verbeek		12/12/14
Mark Lay		12/12/14

July 2015